Large scale processing of dielectric electroactive polymers

Vudayagiri, Sindhu

Publication date:
2014

Document Version
Publisher's PDF, also known as Version of record

Large scale processing of dielectric electroactive polymers

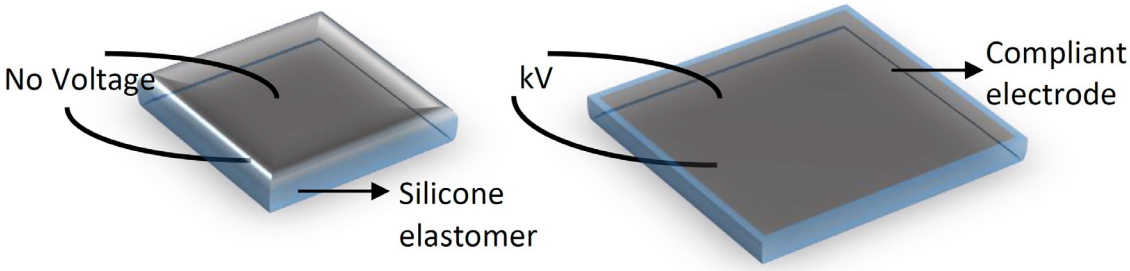

Sindhu Vudayagiri
Ph.D. Thesis
July 2014

DTU Chemical Engineering
Department of Chemical and Biochemical Engineering

Large scale processing of dielectric electroactive polymers

Sindhu Vudayagiri

July 2014

Supervisor: Anne Ladegaard Skov

PhD Thesis

Danish Polymer Centre, DTU, Kgs.Lyngby

DTU Chemical Engineering
Department of Chemical and Biochemical Engineering

Address: The Danish Polymer Centre
Department of Chemical and Biochemical Engineering
Technical University of Denmark
Building 227
DK-2800 Kgs. Lyngby
Denmark
Phone: +45 4525 6801
Web: www.dpc.kt.dtu.dk

Print: J&R Frydenberg A/S
København
October 2014

ISBN: 978-87-93054-45-5

PREFACE

The thesis is written in partial fulfilment of the requirements for obtaining a PhD degree. The work has been carried out at the Danish Polymer Centre (DPC), Department of Chemical and Biochemical Engineering at the Technical University of Denmark (DTU) from August 1 2011 to July 31 2014. The PhD study has been funded by Danish National Advanced Technology Foundation.

I would like to thank almighty GOD for the wonderful way SHE/HE has led me up to now.

I convey my sincere gratitude to my supervisor Anne Ladegaard Skov for her unstinted cooperation, encouragement and patience for the successful completion of this work.

Words are not enough to thank my intellectual and hardworking colleague Liyun Yu who has been very supportive and has a profound influence on my PhD study.

I am grateful to my fellow colleagues Frederikke Bahrt, Suzan Sager Hassouneh, Irakli Javakhishvili and Kaustav Goswami for the wonderful research environment and for their insightful thoughts and comments. A special thanks to Benslimane Mohamed Yahia, Hansen Ulrik, Hans-Erik Kiil and Yde Jens Juul of Danfoss PolyPower A/S for the guidance and for the coordination of this project.

I dedicate this thesis to my parents and husband.

Finally I thank the country of Denmark which has truly been a home away from home and has given me the happiest days of my life so far.

Sindhu Vudayagiri

July, 2014

Research is creating new knowledge- ***Neil Armstrong***

Contents

ABSTRACT

Efficient processing techniques are vital to the success of any manufacturing industry. The processing techniques determine the quality of the products and thus to a large extent the performance and reliability of the products that are manufactured. The dielectric electroactive polymer (DEAP) technology is relatively new and is in the initial stages of development with no established large scale manufacturing techniques. Danfoss Polypower A/S has set up a large scale manufacture process to make thin film DEAP transducers. The DEAP transducers developed by Danfoss Polypower consist of microstructured elastomer surfaces on which the compliant metallic electrodes are sputtered thus enabling large strains of non-stretchable metal electrode. Thin microstructured polydimethlysiloxane (PDMS) films are quintessential in DEAP technology due to scaling of their actuation strain with the reciprocal of square of films' thickness. Production of thin elastomer films with microstructures on one or both surfaces is therefore the crucial step in the manufacturing. The manufacture process is still not perfect and further optimization is required. Smart processing techniques are required at Danfoss Polypower to solve production issues in DEAP film manufacture. The primary issue in the processing is the release of thin PDMS films from a corrugated substrate on which the films are cured. The films are weak owing to their small thickness and low Young's modulus. The process of peeling the films from the substrate either induces pre strain or tears the films leading to a total shut down of the manufacturing. Further problem arises in the lamination step of the manufacturing process. The thin films manufactured in the industry with the current process have only one microstructured surface. The complaint electrode is sputtered on the microstructured surface of the film. Two such films are laminated to make a single DEAP laminate with two microstructured surfaces. The lamination process introduces two problems: 1) it may entrap air bubbles and dust at the interface which will cause the films to breakdown at the operating voltages and 2) after lamination the thickness of the elastomer is double that of the single film and as thickness of the elastomer between the electrodes increases, higher voltages are required to produce a desired strain.

The objective of this research work is to find suitable solutions to the above discussed technical hitches. To facilitate easy release of the films from substrates, following three approaches are investigated: 1) chemical modification of the elastomer film by adding surface active block copolymers to reduce its surface energy, 2) use of surfactants as release agents and 3) compounding a silicone resin with the elastomer matrix. An alternate process of making microstructured films by hot embossing has been established in this research. From our experiments it has been learnt that addition curing PDMS elastomer has the unique property to retain an imprint made on it at gel point. With hot embossing technique the microstructures can be imprinted directly on the films at gel point. Thus, films can be made on a flat substrate and embossed instead of making the films on a corrugated substrate. Releasing the films from a flat substrate is easier compared to the corrugated substrate. To address the lamination problem, bilaterally microstructured films can be made by combining the hot embossing method with the existing manufacturing process eliminating the lamination step. The bilaterally corrugated monolithic films have lower thickness than the laminated films made with conventional manufacture process. This new technique developed on a lab scale is quick, economical, easy and can be implemented on a large scale. The results of all our experiments and the hot embossing technique have been discussed.

RESUME PÅ DANSK

Effektive processeringsteknikker er vitale for succes af enhver produktionsvirksomhed. Processerings-teknikken bestemmer kvaliteten af produkterne og dermed også i stor udstrækning deres ydeevne samt pålidelighed. Dielektrisk elektroaktive polymer (DEAP) teknologien er relativ ny og er i opstartsfasen uden veletablerede produktionsanlæg. Danfoss PolyPower A/S har fremstillet et produktionsanlæg til at fremstille DEAP film. Disse film består af mikro-strukturerede elastomer-overflader hvorpå der sputteres kompatible elektroder. Denne teknik bevirker, at uelastiske metalliske elektroder kan strækkes. Tynde, mikrostrukturerede film af polydimethylsiloxan (PDMS) er strengt nødvendige for DEAP teknologien, da filmenes aktuering afhænger af filmtykkelsen i potensen -2. Den eksisterende produktionsteknologi er langt fra perfekt og videre optimering er krævet. Det primære problem er at løsne de tynde PDMS film fra det korrugerede substrat, hvorpå PDMS'en er hærdet. Filmene er svage pga deres tynde geomtri og deres lave Youngs modul. Afpilnings-processen introducerer præstræk i filmene og sommetider forårsager den også irreversible brud, som bevirker at produktionsprocessen må startes om med stort materialespild som resultat. Videre problemer opstår i lamineringsprocessen, hvor to ensidede korrugede film lamineres sammen på deres u-korrugerede sider. Lamineringsprocessen introducerer to problemer, nemlig 1) at både luftbobler og støvpartikler kan fanges mellem de to film og forårsage reduceret elektrisk sammenbrudsstyrke og 2) at tykkelsen fordobles ved lamineringen og dermed sænkes aktueringen med en faktor 4.

Formålet med dette arbejde er at finde egnede løsninger til de tekniske udfodringer skitseret ovenfor. For at facilitere nem afpilning er 3 metoder afprøvet, nemlig 1) kemisk modifikation af elastomeren ved at addere overfladeaktive copolymerer til reduktion af dens overfladeenergi, 2) brug af overfladeaktive kemikalier til at reducere kontakten til substratet og 3) formulering af en elastomer med resin. Endvidere er en alternativ proces til at fremstille mikrostrukturerede film blevet udviklet i dette projekt. Det er vist, at PDMS elastomerer kan bibeholde sin form ved geleringspunktet. Dette kan benyttes til at varmepræge PDMS film, der på forhånd er reageret til at være omkring geleringspunktet, med den krævede processeringshastighed. En fordel ved teknikken er, at filmene laves på et fladt substrat med væsentligt mindre overfladeareal. Dette bevirker væsentligt mindre kræfter krævet for afpilning. En yderlige fordel er, at dobbeltsidet mikrostrukturede film kan fremstilles ved kombination af varmeprægning med den eksisterende proces og dermed eliminere lamineringsprocessen. Disse dobbeltsidet korrugerede film har fordelen af mindre tykkelse end laminaterne. Den i laboratoriet udviklede proces er hurtig, nem, økonomisk og kan implementeres på stor skala.

1.Introduction

A transducer is a device that converts a signal from one form of energy to another form of energy. Electroactive polymer (EAP) transducers respond to an electrical stimulation by showing a significant change in their size and shape, thus converting the electrical energy into mechanical energy. [1] EAPs are classified as electronic and ionic as shown in Table 1.

Table 1.1: Types of EAPs [1]

Electronic EAP	**Ionic EAP**
Liquid crystal elastomers	Ionic polymer gels
Electro viscoelastic elastomers	Electro rheological fluids
Electrostrictive paper	Conductive polymers
Electrostrictive graft elastomers	Ionic polymer metallic composite
Ferroelectric polymers	-
Dielectric elastomer	-

The ionic EAPs respond to the electric field due to mobility of ions generated in the material. They have some advantages over electronic EAPs such as low driving voltage. [1] The disadvantages are that they require an electrolyte and hence encapsulation becomes mandatory for practical applications. [1] In addition, ionic EAPs also have slow response and low electro-mechanical coupling efficiency. In comparison, the electronic EAPs respond to an electric field due to the development of Maxwell forces in the material. [1] They have advantages like high mechanical energy density and relatively large actuation forces. They can operate for a long time in room conditions, exhibit rapid response in the order of few milliseconds and can hold strain under DC. Their only disadvantage compared to ionic EAPs are that they require high voltages. Actuation displacement of EAPs is generally more than 10 % while SMA have a displacement of less than 8 % and have a short fatigue life. Electroactive ceramics (EAC) are capable of displacements only in the range of 0.1-0.3 %. EAPs are lighter with an average density of 1-2.5 g/cc, compared to SMA ~ 5-6 g/cc and EAC ~ 6-8 g/cc. [2] The response time of EAPs is in the order of microseconds whereas for SMA it ranges from seconds to minutes. EAP materials can be easily formed in any desired shape and can be used to build micro-electro-mechanical-type mechanisms (actuators and sensors). [2] EAPs can be used to make mechanical devices without the need for traditional components like gears and bearings, which are responsible for the high costs, weight and premature failures of electromagnetic technology. [2]

The topic of our research is dielectric elastomers. In the following sections, the working principle of dielectric elastomer EAPs, their applications and manufacture process will be discussed.

1.1.Dielectric electro active polymers (DEAP)

DEAPs are dielectric elastomers which exhibit large strains when sandwiched between two compliant electrodes and subjected to a high voltage. DEAPs are very unique and functional since they combine large active deformations, high energy densities, good efficiencies and fast response compared to other EAPs. [3] They are soft, flexible, normally incompressible and highly resilient so that a high strain level can be achieved. [1] Acrylics, polyurethanes and PDMS are some of the most commonly used DEAP elastomers.

1.1.1.Working principle:

When a dielectric electro active elastomer sandwiched between compliant electrodes on both sides is subjected to a high voltage, Maxwell stress is generated in the elastomer which is an electrostatic field induced mechanical stress causing the electrodes to come closer by squeezing the elastomer film resulting in lateral expansion as shown in Figure 1.1.

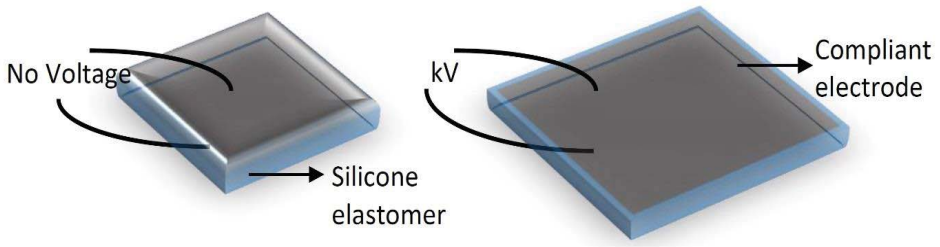

Figure 1.1: Working principle of a DEAP actuator

The film reverts back to its original shape when the high voltage is ceased. The working principle of DEAP resembles a capacitor and the DEAP actuator is also considered as a variable capacitance device. The capacitance, *C*, of a DEAP is illustrated with an electrical model. [1, 4]

$$C = \varepsilon_r \varepsilon_o \frac{A}{t} \tag{1.1}$$

where A is area of film, t is film thickness, ε_r is relative dielectric permittivity, $\varepsilon_0 = 8.85\times10^{-12}$ F/m is permittivity of free space. The DEAP transducers can function as actuators, generators and sensors and their working mechanism is explained as follows.

Actuator: When a voltage is applied to the compliant electrodes of a DEAP, electrostatic forces will squeeze the dielectric elastomer material between the electrodes causing an expansion in area. The electrostatic model developed by Pelrine *et al* [5] gives the compressive stress and strain output of the elastomer as shown in equations (1.2) and (1.3).

$$p = \varepsilon_r \varepsilon_0 \left(\frac{V}{d}\right)^2 \tag{1.2}$$

$$s_z = -\varepsilon_r \varepsilon_0 \frac{(V/d)^2}{Y} \tag{1.3}$$

In equation (1.2) and (1.3) p is compressive stress, V is the applied voltage, d is thickness of the film, s_z is thickness strain and Y is Young's modulus.

Sensor: Consider a DEAP sandwiched between two compliant electrodes through which a constant current is flowing. When a pressure or shear deforms the DEAP, the capacitance of the DEAP changes. The change in capacitance will be proportional to amount of deformation and can be measured. The change in capacitance can thus be used to sense pressure and the set up can function as a sensor. Carpi *et al* [6] relate the capacitance change to the square of the strain ratio as shown in equation (1.4).

$$C = C_o\lambda^2 \tag{1.4}$$

In equation (1.4) C is the instantaneous capacitance, C_o is the initial capacitance and λ is the material strain.

Generator: When a DEAP under tension at constant charge mode is allowed to relax, its capacitance decreases and voltage increases accordingly. The working principle is inverse of that of an actuator. A conversion of mechanical energy to electrical energy is possible and the set up acts like an electrical energy generator.

***Advantages and applications*:** DEAP transducers - due to their small size, flexibility and noiseless operation - are good candidates for being used as actuators in fields such as medical, haptic, aerospace, entertainment and robotics. Dielectric elastomer actuators have been known for their unique properties. They can show a maximum elongation strain of 120–380 % [7], large stresses of up to 3.2 MPa [7], high specific elastic energy density of up to 3.4 J/g [8], high speed of response of the order of microseconds, and high peak strain rates of up to 34,000 %/sec. [9, 10] The other actuator technologies like electromagnetic coil show a maximum strain of 50 % and for a piezo electric it is 0.1-1.7 %. [11] DEAP transducers operate with high power density and do not encounter friction problems at low speeds, for example a DEAP rotary motor has greater power density efficiency at lower operational speeds since gearing is eliminated and gives continuous output when compared to electromagnetic, pneumatic and hydraulic motors. [12,3] The material and production costs of DEAP actuators are estimated to be lower than electromagnetic actuators and DEAP actuators come in greater size and shape variations. [3] The high voltage requirement of DEAP can be easily tackled with by using low input voltage and high output voltage bidirectional converters. [13]

At a research level many different versatile devices have been developed using DEAP technology. The actuation mechanism of these materials resembles the movement of muscles in living organisms which opens up new possibilities in medical sciences for making life like prosthetics. They find applications in biomedical sciences as 'artificial muscles'. In the field of robotics soft DEAP actuators are favored because the physical properties of traditional transducers like the electromagnetic motors is very different from that of animal muscles and the robots built with them have restricted motion and give no flexibility to the robotic skeletons. [1,14] As consumer electronics, DEAP speakers, valves, sensors, motors and pumps have been developed and can soon become commercially available. DEAP generators are successfully used for wave energy harvesting. DEAP actuators are used for making haptic gaming accessories and speakers, which take virtual entertainment to an all new level enabling users to feel the sound. DEAPs have a huge potential in aerospace applications where miniature actuators that are light, compact with low power consumption are required for telerobotic devices, release mechanisms, antenna and

instrument deployment, positioning devices, aperture opening and closing devices, and real-time compensation for thermal expansion in space structures. [1,2]

Although the DEAP transducers have many advantages over the traditional transducers, there are concerns over the stability and durability of DEAPs. The full potential of the DEAP technology cannot be realized unless the large scale processing techniques as well as the material properties of DEAP elastomers are optimized. [1, 15, 16, 17]

1.2.Industrial manufacture process

For making the DEAP technology commercial, a scalable industrial manufacture process has been established by Danfoss PolyPower A/S (DPP). [15]

DEAP technology of DPP: A unique specialized DEAP design which is optimized to give the maximum strain output has been developed by DPP. [17-22] A thin film DEAP produced by DPP is shown in Figure 1.2. It consists of two corrugated thin PDMS elastomer films laminated back to back to form a single unit of thickness ~ 80 μm which forms the basic building block of the transducers. The compliant silver electrodes of thickness ~ 100 nm are sputtered on the film's microstructured surface. [15] When a high voltage is applied on the electrodes the elastomer film in between expands in a direction perpendicular to the length of the corrugation lines.

The microscale corrugations which have a sinusoidal profile serve two main functions 1) they protect the metallic electrode from high strains endured by the elastomer when used as transducers, since the local strain on the corrugations are very small compared to the overall strain and 2) the corrugations render the DEAP laminate anisotropic, directing the expansion in a single direction and restricting the movement in other directions. [15, 16] Compliant metal electrodes have advantages such as high conductivity and low electrical losses, and these properties do not deteriorate significantly with strain. [16] The wave depth and wave period of the sinusoidal corrugations depend on the type of the carrier web on which the films are made on.

In DPP a roll to roll coating process is used to manufacture thin microstructured PDMS films as shown in Figure 1.3. The process is elucidated in the following 7 simple steps. [15] The process explained here is of the initial scalable process of DPP and now a full scale process is employed. The entire process is performed in a clean room environment in order to minimize defects in the fabricated elastomer films, which may manifest themselves as breakdown voltage failures.

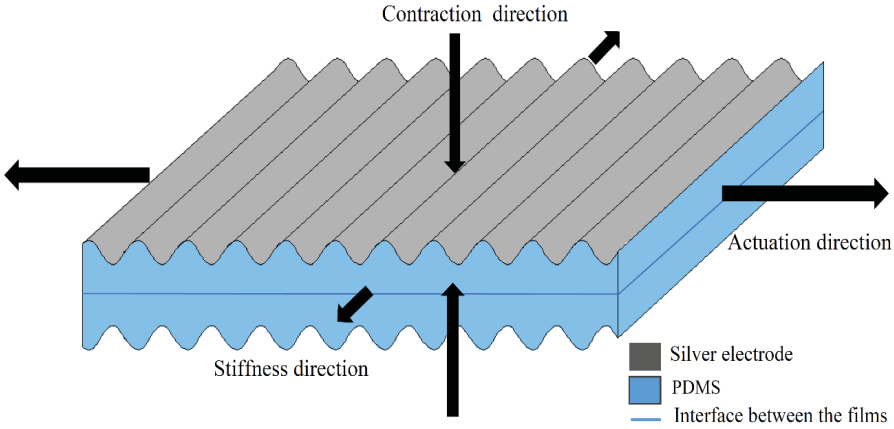

Figure 1.2: Two films adhered to produce a thin film DEAP

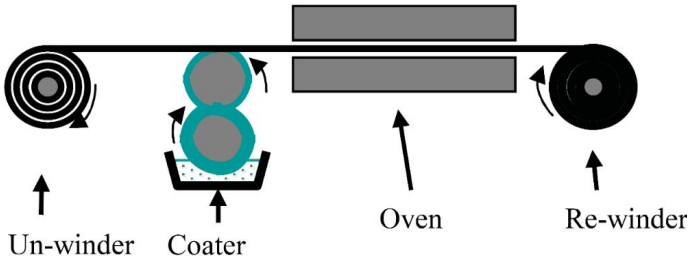

Figure 1.3: Schematic of the industrial manufacture process [15]

1.2.1.Mixing

A uniform mixture of the addition curing polydimethylsiloxane elastomer is made using speed mixer and a roll mill. The mixture consists of vinyl terminated PDMS, a hydride crosslinker, platinum catalyst, desired fillers, a suitable inhibitor and solvent. The amount of solvent used is different for every mixture and depends on the type of silicone and the percentage of filler used. The solvent ensures uniform dispersion of filler. In order to minimize energy expended while mixing the formulations and spreading them on carrier web to make films, it is preferable to set the viscosity of the elastomer mixtures below 40 kPa·s in the manufacturing process.

1.2.2.Coating

The elastomer mixture is then cast on a 'carrier web' substrate using a gravure coating process to form a thin, uniform, continuous coating of well-defined thickness of ~ 40 µm. The silicone elastomer mixture is coated on the carrier web at a speed of ~ 120 m/h.

Carrier web: Carrier webs are specially designed substrates which transfer the corrugated microstructure onto the films. The carrier webs are made of temperature stabilized polyethylene terephthalate band (0.2 mm) coated with methyl acrylate UV resin, which have the microstructured surface as shown in Figure 1.4. They have a sinusoidal corrugation profile. Depending on the

dimensions of the waves the webs can be classified as follows. One type of carrier web is defined by a wave depth of 5 µm and a period of 10 µm, which allows for a film strain of 33 % with no electrode breakage. Another type of carrier web has a depth and period of 7 µm, and films with this corrugation pattern work well up to about 100 % strain. Carrier webs with slightly different wave dimensions are also used for producing certain films. Based on the direction of the corrugation lines with respect to the length of the web there are two types of webs. The corrugation lines along the length of the carrier web are referred to as 'down-web', and when corrugation lines are perpendicular to the length of the web, the pattern is called 'cross-web'. [15, 16] Carrier web is a crucial part of the manufacture process as it imparts the corrugated profile to the film. The carrier web is in the form of a roll as shown in Figure 1.4. In the current process, using the carrier web, kilometers of microstructured film can be manufactured. The corrugations on the current carrier web have width of 20 cm (active area) and the total width of carrier web is ~ 30 cm leaving enough passive area for handling the film as shown in Figure 1.5.

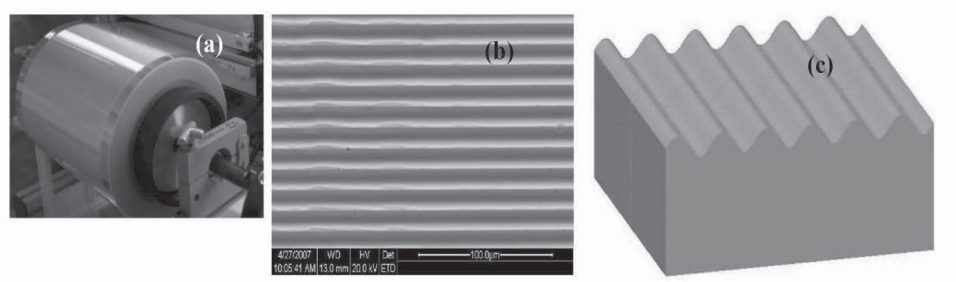

Figure 1.4: The carrier web used for manufacturing corrugated thin PDMS films **a)** carrier web roll, **b)** microscope image of surface of carrier web and **c)** 3D cross-sectional schematic of carrier web [15]

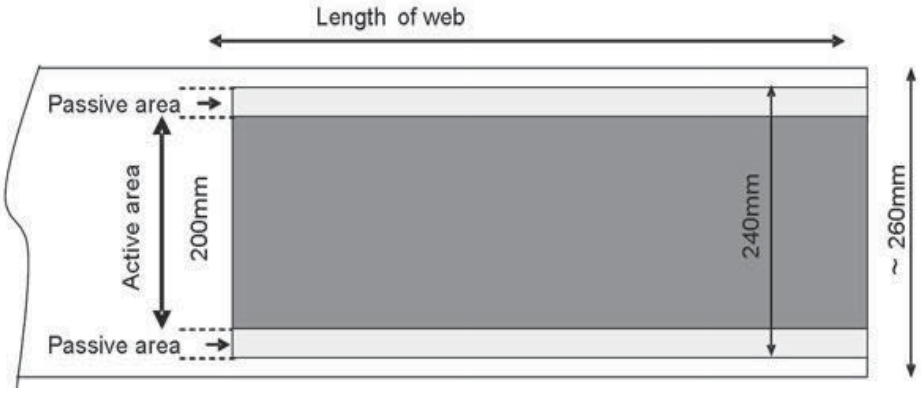

Figure 1.5: Carrier web layout [23]

1.2.3.Curing

The elastomer coating on the carrier web is then cured in an oven at 100 ºC. The dimensions of the oven and the speed of the carrier web are adjusted so that the residence time of the film in the oven is ~2 min. The PDMS elastomer mixture crosslinks by hydrosilylation reaction as shown in Figure 1.6.

1.2.4.Peeling

The cured films are then peeled off the carrier web using an automated delamination equipment, shown in Figure 1.7, at a constant speed and with controlled force. The flat surface of the peeled film is transferred onto a backing material with the corrugated surface facing upwards and wound onto a roll. The speed of delamination is ~120 m/h.

1.2.5.Electrode deposition

The corrugated side of the elastomer film is plasma treated and then sputtered with a thin and uniform layer of a conductive metal such as silver, gold, nickel and alloys under vacuum. The thickness of the deposited metal is ~100 nm. The speed of metallization is ~36 m/h.

1.2.6.Lamination

The metallized films are then laminated mechanically in a 'back to back' configuration so that the flat sides of the films are in contact. The lamination equipment has two symmetric arms each of which transfers a metallized film so that the two films are laminated at the contact area to form one monolithic structure with corrugated/electrode surfaces on both sides. The thickness of the laminated film is ~ 80 μm. The speed of lamination is ~ 120 m/h.

1.2.7.Final assembly

The laminated films are then stacked or rolled to make different types of transducers.

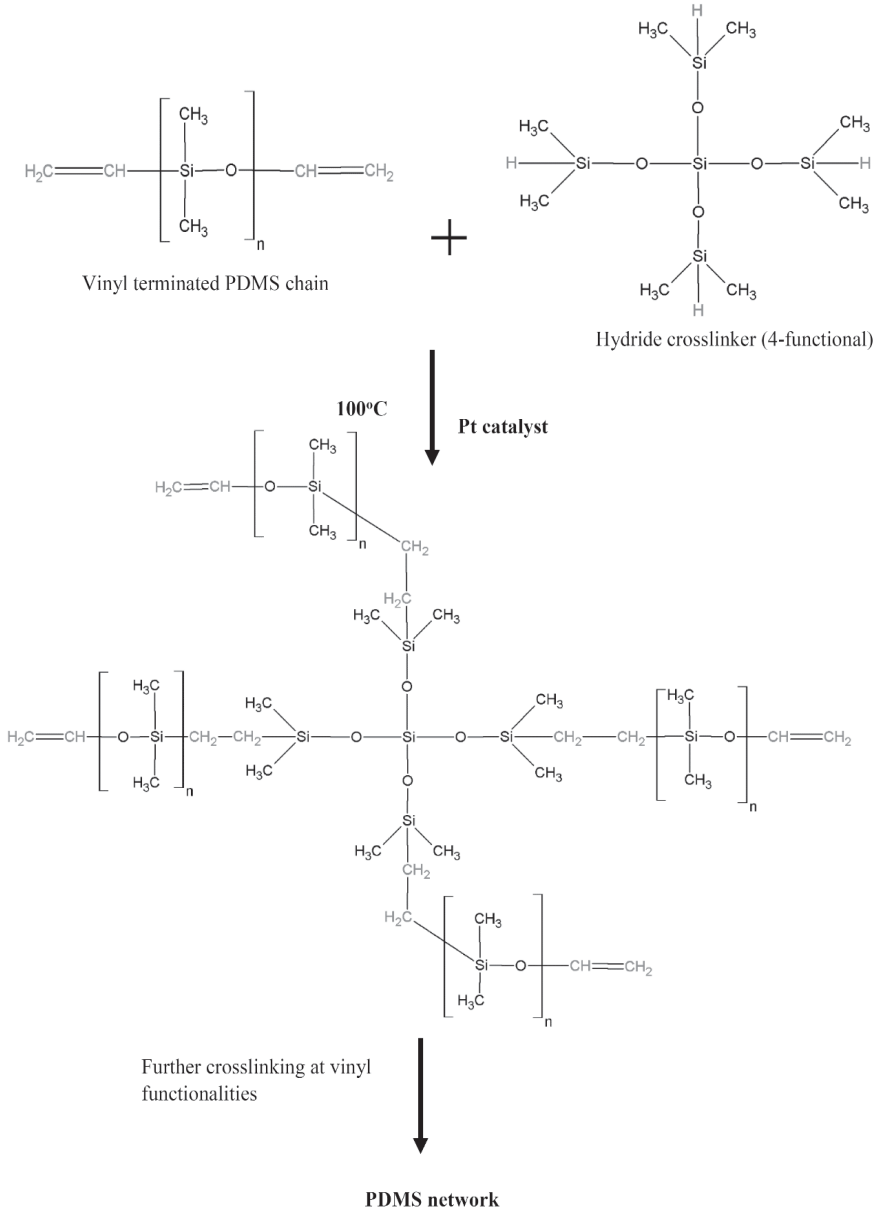

Figure 1.6: Hydrosilylation reaction illustrated with a 4-functional crosslinker

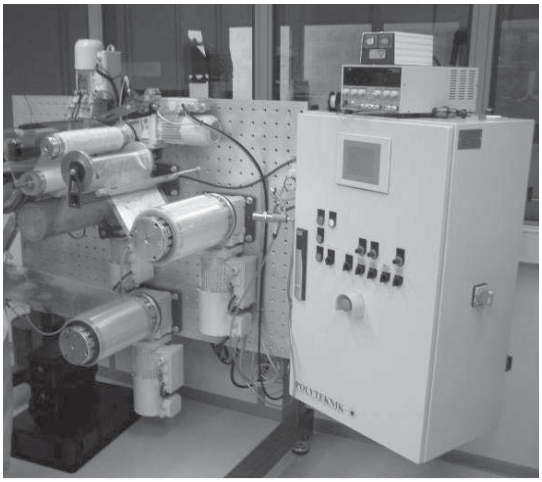

Figure 1.7: Delamination equipment showing the peeling of the cured film from carrier web [15]

1.3.Types of silicone elastomers

DPP uses different types of silicone elastomers for making the corrugated films for DEAP transducers. A brief explanation of these different silicone systems is as follows. Silicone formulations based on curing temperatures are classified as 1) high-temperature vulcanisable (HTV) and 2) room-temperature vulcanisable (RTVs) rubbers. The HTV rubbers can be classified further as 1) liquid silicone rubbers (LSRs) and 2) millable silicone rubbers, depending on the degree of polymerization. [24] LSRs are low-viscosity silicone (low molecular weight), with a viscosity of 100,000 to 8,000,000 cPs, and they are based on platinum catalysed curing, which offers curing times of a few seconds to minutes at elevated temperatures. [24] Millable silicone rubbers, also known as 'high consistency rubbers' (HCRs), are high molecular weight polydimethylsiloxanes with viscosities of 1,000,000 to 50,000,000 cPs and are peroxide cured, which makes their 90 % curing (t90) time two or three times slower than LSRs. [24] LSRs require lower pressure than millable silicon rubbers for injection moulding, due to their low viscosity, though they cure to form an elastomer of Y similar to millable silicon rubbers. [24] LSR premixes are more viscous than RTVs, and in general the cured elastomer has a much higher Y than RTVs. [25, 26] End-linked linear polydimethylsiloxane (PDMS) polymers, crosslinked with low-functional [27] or even high-functional crosslinkers [28] without any fillers, have poor mechanical properties, so silicone networks used in DEAP technology are therefore reinforced with silica fillers for mechanical strength. [29] The extent to which the fillers influence the elastomer properties depends on filler size, filler treatment, how well the fillers are dispersed in the elastomer matrix and the interfacial interaction between the matrix and fillers. [30]

1.4.Issues in large scale manufacture process

The manufacturing process explained in section 1.2. has some setbacks in the peeling and the lamination steps. These steps induce some defects in the PDMS films, which are explained below.

1.4.1.Peeling and release

The thin uniform coating of PDMS mixture that is cast on the carrier web is cured at high temperature by hydrosilylation reaction, where the vinyl terminated PDMS chains are crosslinked by a hydride crosslinker in the presence of a platinum catalyst (Figure 1.6). The cured film is then peeled from the carrier web substrate using a delamination equipment with controlled force and speed. The process of releasing the film from the substrate is not as smooth as it desired and it induces considerable prestrain and defects in the film, which affects the performance of the films as actuators. [31] The low thickness of the films and their low Young's modulus makes the films very weak. As thickness of the film decreases, the peel force required to peel the film increases. [32] Though the surface energy of PDMS is only 19–21 mJ/m^2 [33], which is comparable to polytetrafluoroethylene (Teflon), the films establish good contact with the carrier webs since the films have low Young's modulus. The cohesive forces developed between the film and substrate thus contributes to the high peel force requirement during peeling. Furthermore, since the surface of the carrier web consists of microscale corrugations, the actual surface area is ~ 2.4 m^2 per m^2 of carrier web (calculated for a 100 % cross-web). Hence the required peel force/m^2 increases and often exceeds the tear strength of the films. [31]

1.4.2.Lamination

The metallized films are laminated mechanically in a 'back to back' configuration using a constant load such that the flat sides of the films are in contact. This step is essential as it produces the DEAP laminate with corrugated surfaces on both sides. The DEAP laminate has certain drawbacks compared to a monolithic film for two main reasons: 1) minute air bubbles or dust particles at may get trapped at the interface between the films and 2) the thickness of the dielectric material between the electrodes is doubled. The dielectric breakdown strength of air is 3 V/µm [34], which is very low compared to the operating voltages of the DEAP laminates [14, 35, 36]. The trapped air bubbles at the interface will easily break down at the high operating voltages of DEAP laminates making them more susceptible to failure. In theory, lamination serves to decrease the probability of the thin film actuator to breakdown under high voltage, as it would require two defects at the same spot on both films. However, this advantage would be rendered futile if the lamination process introduced air gaps at the interface. The thickness of a single film manufactured in DPP is ~ 40 µm [23], making the laminated film thickness ~ 80 µm.

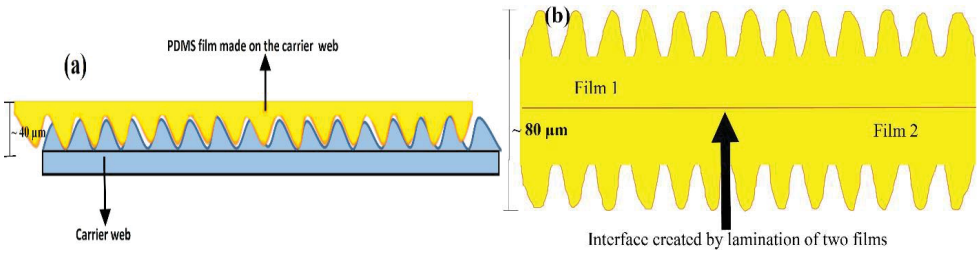

Figure 1.8: Schematic of **a)** Single film and **b)** Laminated film (Not to scale)

Equations (1.2) and (1.3) from Pelrine *et al's* model [5] show that the compressive stress and strain outputs of the DEAP films decrease as the thickness of the films increase. Since the laminates have higher thickness than the single films their performances are not optimal. In the current manufacture process production of thinner films (< 40 μm) is challenged by the release problem. Figure 1.8 shows a schematic representation of a laminated film.

1.4.3.Economics of the process

This process is expensive, as it requires miles of carrier web to make the films. The carrier web is specifically designed for this manufacture process. Modifying or replacing the carrier web is not an option right now due to the commercial unavailability of such substrates in large quantities. Therefore an alternative process to make thin, corrugated elastomer films is required to make the DEAP technology economically competitive with other actuator, generator and sensor technologies. The targeted speed is ~ 600 m/h for a profitable process. The process needs to be optimized to reach the target speeds.

1.5.Current research in EAP/DEAP technology

Many companies and research groups have been developing DEAP transducers on micro and macro scale. Each of these groups has a unique specialized design for their transducers aimed at specific applications. Knowledge of the various DEAP technologies gives valuable insights into the current trends and provides us an extensive view. As examples of production scenarios of thin film DEAP transducers, a very limited selection of different production technologies are discussed without undermining the prominence of other research groups which have not been discussed below.

1.5.1.Industry

Artificial Muscle, Inc. of Sunnyvale, California, [37] is a subsidiary of Bayer Material Science LLC and a spinoff of SRI international. Their EAP technology consists of a thin layer of dielectric polymer film sandwiched between compliant electrodes. Their focus is on producing small DEAP actuators of about a millimeter thick and in cm scale with compliant metal electrodes, which can be form-fitted into a wide array of end-products, integrating their DEAP technology seamlessly so that actuation can augment a broad spectrum of end-user experiences.

The most famous commercial products from AMI is the Vivitouch [38] that has transformed mobile gaming by immersing players with a new dimension of tactile feedback. This haptic technology gives the feel of what one sees and hears in a video game such as explosions, crashes etc. Vivitouch can be augmented with smart phones, tablets, handheld consoles etc. Vivitouch consists of a DEAP actuator panel. The audio signals from the phone, PC or speakers are given as the input to the tiny actuator panel which are instantly converted into vibrations that resonate with the audio signals. The Vivitouch 4D speaker utilizes the same technology in a speaker which recreates the sensation of a live pulsating music with a sub-woofer base feel. On a reseach level AMI is collaborating with a wide-range of partners to develop DEAP technology for medical, aviation, aerospace, consumer products. Overall, their DEAP technology is small scale (cm scale) with high performance.

1.5.2.Research groups

The research group of Prof. Smela (Laboratory for Micro technologies) [39] develops EAP technology on a microscale. They make conjugated polymer actuators, dielectric elastomer actuators and nastic actuators. Prof. Smela's group is working on miniature DEAP actuators using conventional micro fabrication techniques and materials. [40] Their products include micro robotic arms and micro origami to name a few. Micro fabrication introduces new challenges such as making compatible compliant electrodes, finding an elastomer that does not require pre-strain, depositing and patterning the elastomer. Developing a successful surface micromachining process sequence and powering the small actuators are other challenges. This group makes compliant electrodes by mixing a platinum salt with the photo curable elastomer precursor and when this mixture is exposed, the salt is reduced and the elastomer material becomes a shiny gray conductive skin. This metal composite has the same Young's modulus as the original elastomer. Thus their electrodes can endure high strains with good conductivity. It is an interesting technique, as their electrodes have the conductivity of metal and the elasticity of elastomer. Carbon grease and carbon powder cannot be used in micro fabricated devices as these materials can rub off easily. An issue that must be addressed when miniaturizing a DEAP actuator is prestrain. Without prestrain, DEAPs do not actuate when a voltage is applied and/or they suffer failure due to pull-in. Prof. Smela's group uses special patterning techniques for the films and electrodes, with which they are able to achieve about 5 % strain without pre-strain. Spin coating is employed to make the thin PDMS films on a Si substrate. A new technique for etching these films that combines dry etching to achieve a high aspect ratio followed by wet etching to remove the final few microns of material without attacking the Si substrate has been invented by the group.

The research group of Prof. Schlaak [41] specializes in developing stacked multilayer DEAP actuators for tactile displays and peristaltic pumps. Their DEAP actuators are made of high elastic silicone elastomer films of 20 µm thickness with thin graphite powder electrodes. Despite the large strain of about 20 % that can be achieved by these actuators, the deflection of a single layer is not applicable. The idea behind using layered actuators is for increasing the absolute value of deflection without increasing the driving voltage. This multilayer principle is developed for the application in tactile displays as a high density of actuators is necessary for these displays. Working models of DEAP tactile feedback devices have been developed by Prof. Schlaak's group. [42, 43] In general, tactile displays are used to transmit information about a surface to user. This could be useful for applications in tele manipulating. A subgroup of tactile displays is braille displays. [42] Each Braille symbol is represented by an arrays of eight pins which can be sensed or hidden in the housing of the braille display as shown in Figure 1.9. [42] A PC-mouse with a DEAP pad resting against the users palm has also been developed. [43] The goal is to provide tactile feedback to four different areas inside the palm while surfing the computer. The pad has an overall diameter of 52 mm. It consists of 40 active layers with a layer thickness of 40 µm, made with spin coating process, resulting in an overall thickness of 1.6 mm. At 1 kV DC driving voltage, the deflection is about 180 µm. On one pad there are four single actuators to provide feedback for four directions. [43]

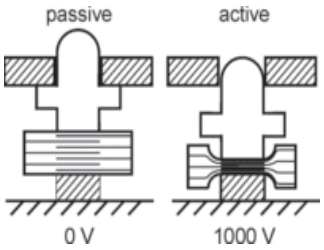

Figure 1.9: Schematic view of a braille display with dielectric actuators [42]

A miniaturized peristaltic fluid delivery system with electrostatic elastomer actuators has been developed by Prof. Schlaak's group. [44] A peristaltic pump is a positive displacement pump for transporting fluids conventionally made with tubing and rollers. The DEAP peristaltic pump is formed by contraction of the actuator elements in a cavity. The periodic actuation of the actuator elements makes this cavity migrate through the pump and thus transport the fluid. Living cells are often threatened by the high shear loads on rotating parts in conventional pumps. [44] DEAP peristaltic pumps are particularly suitable for transferring these kind of delicate liquids since this type of pump without valves, seals and rotating parts, manages to transport without the risk of high shear. [44] Prof. Schlaak's group has developed a novel scalable planar DEAP actuator capable of fast and large in-plane actuation which includes a post-buckled slender beam as a bistable element that improves static and dynamic performance of planar DEAP. [45] Generator modules and stiff supports have been investigated by Prof. Schlaak's group in order to find the optimal mechanical interconnection that produces maximum deformation on the elastomer generator during the energy harvesting cycle. To maximize the absolute energy harvested a generator module should have a stack of passive PDMS layers with the same thickness but decreasing Young's moduli from the outer to the inner layers. This provides a balance between a high capacitance of the generator modules and low reaction forces at the stiff support areas in the compressed state. [46]

The research group of Assoc. Prof. Shea develops highly reliable micro-electro-mechanical systems (MEMS) for use in spacecraft, as well as innovative polymer MEMS micro-actuators. The group develops miniaturized DEAP actuators for miniaturized artificial muscle actuators. [47] Their ongoing projects include devices to apply mechanical strain to biological cells, microfluidic pumps and valves, soft robotics, foldable robots, flexible DEAP rotary motors and tunable radio frequency (RF) devices. [47] The silicones used by the group for DEAP actuators are: 1) Sylgard 186 from Dow Corning, USA, 2) CF18-2186 from Nusil, USA and 3) CF19-2186 from Nusil, USA. [48] The compliant electrodes are made with two main technologies: 1) low energy metal ion implantation and 2) pad-printed carbon electrodes. [48] Implantation produces conductive electrodes, which can be patterned with a shadow mask or by a lift-off process. The main drawback of this method is that it is made in a vacuum chamber and is therefore very time-consuming. Pad printing technique consists of stamping a thin patterned layer of a carbon/silicone mixture on a silicone membrane. The electrode is subsequently crosslinked in an oven, which produces very resilient electrodes with a strong adhesion to the elastomeric membrane. [48]

A rotary micro motor made entirely of DEAP has been developed by Assoc. Prof. Shea's group. [49] The motor consists of a silicone membrane stretched on a frame. Three electrodes are patterned on the membrane and a rigid orbiter is placed at the center of the membrane. The Figure 1.10 b shows the activation sequence of the electrodes and the displacement of the orbiter caused

by the electrode expansion. [49] The group's more recent works include a novel DEAP device developed for cell mechanotransduction studies with notable advantages compared to the conventional techniques, namely its high optical transparency, its good electric field confinement (minimal stray electric field) and its compatibility with matrix configuration which would enable high screening throughput experiments. [50] An analytical model of the dielectric elastomer minimal energy structure in the case of a simple rectangular geometry which studies the influence of the main design parameters on the actuator's behavior has been developed by the group. [51]

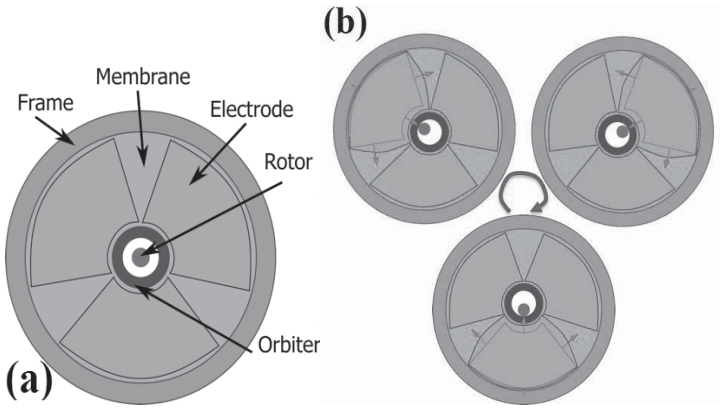

Figure 1.10: **a)** DEAP rotary motor scheme and **b)** activation [49]

The research group of Assoc. Prof. Anderson has a main focus on biomimetics using DEAP technology for applications such as wearable sensors and power generators. [52] Biomimetics involves drawing inspiration from nature to develop new technologies. The lab also develops and sells DEAP devices for sensing, control and energy harvesting. One of the recent publications of the group is on transferring electrical energy between two dielectric elastomer actuators. [53] DEAP transducers used for actuation and power generation are typically operated at kilovolt potential. Effective recovery of the electrical energy inherently stored during operation will greatly improve the efficiency of a DEAP devices. [53] The group has achieved 51% of energy transfer from one DEAP to another DEAP of similar size. Improved energy transfer is expected with lower electrode resistance. [53]

Prof. Pei's group develops DEAP actuators and generators using interpenetrating polymer networks as elastomers. [54] The group's projects include mechanical design, fabrication, and testing of polymer actuators and generators. The group has developed a number of electronic and electroactive polymers for applications in electro-optic and electro-mechanical devices, including light emitting diodes, polymer light emitting electrochemical cells, and biologically-inspired robots. [54] Research interests of the group span from material synthesis, processing, to design of functional devices. The group applies organic synthesis, polymer synthesis, solution-based processing and nanofabrication in the discovery of new polymers and multifunctional composites. One of the recent publication of the group is on interpenetrating polymer networks for high-performance electro elastomer artificial muscles. [55]

The research group of Prof. Suo at Harvard works extensively on producing giant deformations in DEAP actuators.[56] One of the recent works of this group deals with highly stretchable and

transparent ionogels as nonvolatile conductors for DEAP transducers. Creasing instability, creasing-wrinkling transitions in elastomer films and the factors affecting the crease shape and size has been extensively researched by the group. [56] One of the recent publication of the group is on highly deformable actuators made of dielectric elastomer membrane sandwiched between two soft conductors, rolled into a hollow tube, pre-stretched in the hoop direction, and fixed at the ends of the tube to two rigid rings. [57] Usually DEAP actuators that undergo large deformation in response to external stimuli are subject to instability that is usually undesirable. The group has demonstrated that large actuation strains without instability are achievable when the height-to-radius ratio of the tube is small and the hoop pre-stretch is large. [57]

Reader Carpi's group has main research focus on biomedical & bioinspired mechatronic devices made from DEAP transducers.[58] In particular, the activities of the group cover the design, prototyping and testing of new devices and applications. Two such successfully developed devices are bioinspired electrically tunable lenses and electrically refreshable braille cells. [58] The recent publication of the group is about plasticization of a soft silicone for dielectric elastomer actuation. [59] To enable large deformations, either using elastomers that suppress pull-in electromechanical instability or driving the actuator at the verge of instability while still preventing it is applied. Whenever these strategies are not applicable, softening the material using plasticizers remains the mechanical approach of choice to enable large deformations. Their work provides an understanding of the effects of plasticizer on properties other than Young's modulus which are of importance to actuator designers. [59]

Reader Rossiter, head of the Soft Robotics Group at Bristol Robotics Laboratory works on fabricating compliant technologies for robotic systems and medical applications using DEAP technology.[60] The group has developed new polymer-composite actuators involving principles of buckling and bi-stability and robots which are inspired by biomimetic study of swimming organisms, including bacteria and fish. One of the recent publication of the group is about biomimetic soft artificial cilia made with DEAP actuators. [61] The work explains the design and implementation of artificial cilia, based on a biomimetic planar DEAP actuator. [61]

Prof. Kovacs' group at EMPA works on developing devices such as shell-like DEAP actuator and fish-like propulsion of an airship based on DEAP transducers. [62] In addition, super-compliant metallic electrodes for DEAP actuators and electro-mechanical modeling of DEAP transducers with micro-structured electrodes are also being worked upon by the group. The recent work of the group is on measuring the bending of asymmetric planar EAP structures. [63] It is demonstrated that using a cantilever bending system with optical readout revealing a sub-micrometer resolution allows us to detect bending of rather conventional planar asymmetric, DEAP-structures applying voltages well below 10 V. [63] The apparatus will therefore become a powerful means to analyze and thereby improve low-voltage DEAP-structures to realize nanometer-thin layers for stack actuators to be incorporated into artificial sphincter systems for treating severe urinary and fecal incontinence. [63]

Kofod's current research is on new nano-composite materials for applications as linear DEAP transducers. The research involves understanding electrical, mechanical and dielectric properties of novel composite materials incorporating nanometer sized fillers. Another of the recent work of Kofod is on rotary motion achieved by new torsional dielectric elastomer actuators design. [64] The work reports a new way to produce a rotation motion actuated by dielectric elastomer

actuators. Two specific electrode designs have been developed and the rotation of the actuator centers has been demonstrated and measured. At low strains, the rotation shows a nearly quadratic dependence with the voltage. [64]

1.6.Objective and research outline

Our objective is to set up techniques for solving the issues discussed in section 1.4. Two different types of approaches are used to solve the drawbacks in the manufacturing process

1.6.1.Surface modification by chemical and physical methods

The films are chemically modified by adding low surface energy di-block copolymers like fluorinated ethers to bring down the surface energy of the films and thereby to ease the release of the films. Also, release agents like detergents and surfactants are used to ease the release and performance of the films are tested. [65] Furthermore, a silicone resin is compounded with the silicone matrix and the peel forces of the films are tested. Such a resin makes the films more hydrophobic and less sticky. [65] The methods used are required not to interfere with the Young's modulus and the breakdown strength in a negative way. Therefore the vital properties of the PDMS films such as breakdown strength and Young's modulus are measured to analyze if they are affected by the above mentioned techniques for easing the release.

1.6.2.Alternate manufacturing process

The published procedures for manufacturing microstructured thin PDMS films for DEAP purposes are designed for producing small units and not a continuous film and most often with microstructures only on one surface of the PDMS film. [66] Most of the techniques employed for replicating high aspect ratio microstructures on PDMS films involve the usage of sacrificial layers, which are either metallic or polymeric. [67-69] Although these methods are highly successful, they are neither suitable for producing a continuous film nor economically viable. A new technique for making thin PDMS films with one or both microstructured surfaces by 'hot embossing' has been established in our research. [70] From the experiments conducted in our lab, it is realized that addition curing PDMS elastomer can retain an imprint made on it at gel point (GP) which makes embossing possible. [70] Thus by hot embossing corrugated structure is imprinted on the addition curing film at GP using an embossing roll. The hot embossing is performed at elevated temperatures so that time taken by the elastomers to reach their GP is reduced to a few seconds and the process can be operated at an economic speed. [70] A nickel stamp with corrugation lines has been successfully used to emboss the films at GP. Since the corrugations are imprinted directly on films using an embossing roll, the need to make the films on a carrier web is eliminated. The films made on a flat substrate are easier to peel compared to the carrier web with a large surface area. The hot embossing process is quick, easy, fast and scalable and is economically competitive with other DEAP manufacturing processes. Hot embossing is possible with different types of silicone systems, namely room-temperature vulcanisable (RTV) silicone, LSR and LSR composites with additional permittivity-enhancing fillers. [70, 71] A combination of hot embossing with the existing manufacturing process can be used for producing bilaterally microstructured thin PDMS film. A monolithic film with corrugated surface on both sides does not have the drawbacks of a laminated film (Figure 1.11). Bilaterally corrugated films have been successfully manufactured on lab scale in this research work. With some fine tuning this process

can be scaled on to a large scale process. Also, the speed of hot embossing is ~ 403 m/h which is closer to the target speed aimed by the industry.

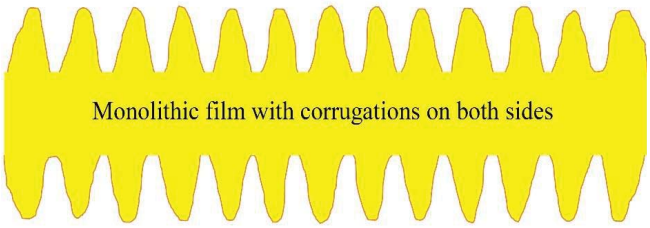

Figure 1.11: A schematic of a bilaterally corrugated thin PDMS film

2.Surface and release properties of thin PDMS films

In this chapter the surface properties of thin polydimethylsiloxane films and the factors affecting the release/peel forces of the films based on Kendall's thin film peeling theory are analyzed. The relationship between the adhesive energy, surface energy, Young's modulus, peel angle and peel force of the films is analyzed. Furthermore, the effects of the additional crosslinker, platinum catalyst and silicone oil on the peel forces of the films are investigated. The silicone matrix is doped with 1 wt. % of perfluoroether allylamide, a low surface energy block copolymer to lower the surface energy of the films and its effect on peel force is investigated. The results presented in this chapter have been published in Polymer journal, volume 45(8), pages 871-878 (2013) and is attached as Appendix I.

2.1.Surface energy

The carrier web substrate on which the PDMS films are made is a polyethylene terephthalate (PETE) sheet of thickness 0.2 mm coated with microscale corrugations of methyl acrylate resin. Poly methyl acrylate has a surface energy is ~ 35.1 mJ/m^2 [72] and the methyl acrylate resin is hydrophobic. The surface energy of PDMS is 19 ~ 21 mJ/m^2 and contact angle with water is ~ 110^o. [33] To understand the surface energy of any surface one should be familiar with the surface physics. The molecules in the bulk are bound in all directions by the neighboring molecules, whereas the molecules sitting on a free surface of the film will be bound by lesser molecules than those in the bulk as illustrated in Figure 2.1. The molecules on a free surface of the film will thus have lesser binding energy than those molecules in the bulk. [73] This missing (negative) binding energy can be viewed as a positive energy added to the free surface. External forces must perform positive work against internal surface forces to increase the area of a surface. [73] The surface energy is thus defined as the sum of all intermolecular forces that are on the surface of a material, the degree of attraction or repulsion force of the material surface exerted on another material. Surface energy is expressed as the normal force per unit area. Surface energy is present at all surfaces and interfaces. [73]

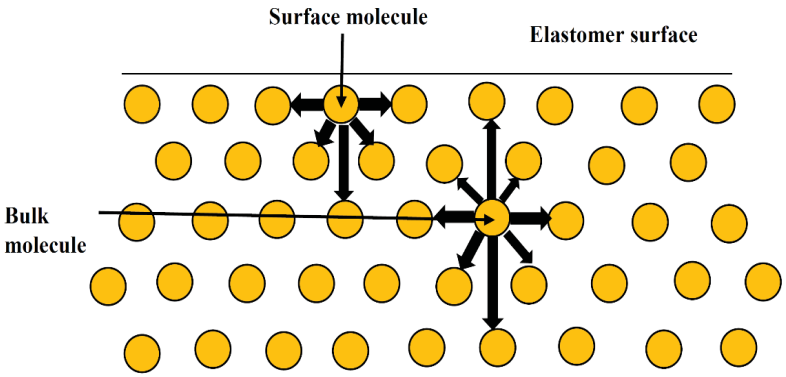

Figure 2.1: The binding energy of surface and bulk molecules

2.2.Peeling analysis

The peel force required to peel a film from a substrate is a complex function of geometry, the mechanical properties of the film and the substrate, thickness of the film, interfacial cohesive properties and also the friction between the surfaces. Figure 2.2 shows a PDMS films of thickness ~ 40 µm being peeled from a carrier web substrate manually. A detailed study and analysis of the peel test and the factors which govern the peel force has been presented by Thouless *et al*. [74] There are many theories to determine the peel force [74,75], adhesive fracture energy or the interfacial adhesion [76] when a film is being peeled from a substrate. Thin-film peeling theory by Kendall [77] which explains the peeling of a thin elastomer film from a rigid substrate is the most appropriate to analyze the peeling of our thin PDMS films from the carrier web.

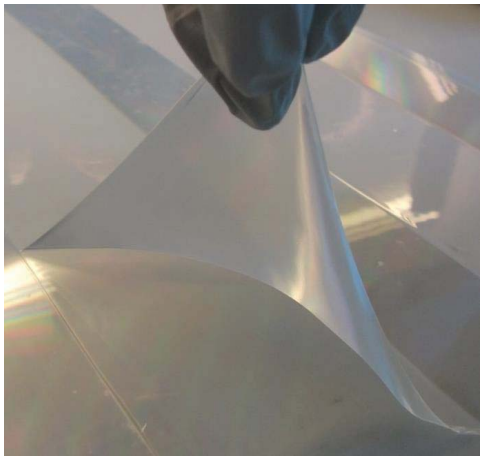

Figure 2.2: Peeling a PDMS film of thickness ~ 40µm from a carrier web substrate

Consider an elastomer film of thickness d which is being peeled from a rigid substrate at a peel angle θ with a force F (Figure 2.3). The elastomer has a Young's modulus E. The adhesive energy between the film and the glass substrate is R. Consider a unit length Δc of the film being peeled from the substrate between the points A and B. [77] The width of the film at any given point is b. The three contributions to the energy changes involved in the peeling process are

1) Surface energy - due to creation of new surfaces [$-bR\Delta c$]
2) Potential energy - due to the movement of the applied force $[F(1-cos\theta)]\,\Delta c$
3) Elastic energy - due to extension of the film in the direction of the applied force $\left[\frac{F^2\Delta c}{2bdE}\right]$

Adding up these contributions and assuming energy conservation the following equation is obtained. [64]

$$-bR\Delta c + F(1-cos\theta)\Delta c + \frac{F^2\Delta c}{2bdE} = 0 \qquad (2.1)$$

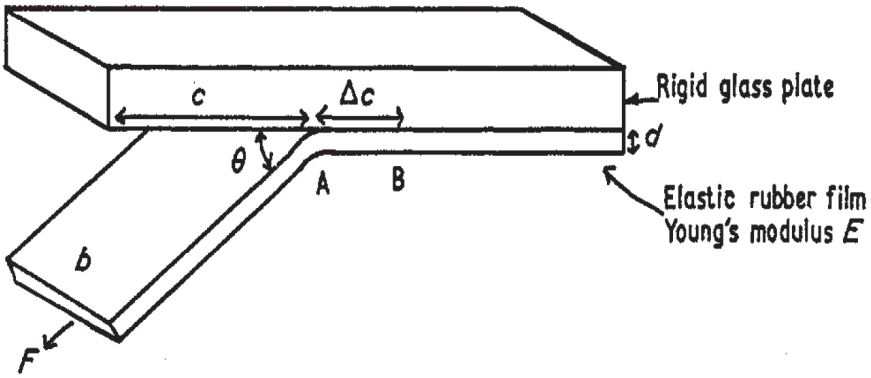

Figure 2.3: Peeling an elastomer film from a rigid substrate [77]

In our case, the corrugations on the surface of the carrier web make the release process all the more difficult as it increases the surface area (~ 2.4 m^2 per m^2 of carrier web) and hence larger force is needed to peel the film.

From the equation (2.1) the adhesive energy R can be calculated. R is different from surface energy, work of adhesion or any thermodynamic quantity and R gives an estimate of the adhesive force between the substrate and the film. If the R between the substrate and the elastomeric film is high, then the force F required to peel the film will also be high.

2.3.Simulation of Kendal's model

Rearranging equation (2.1) an expression for adhesive energy (R) is obtained,

$$\left(\frac{F}{b}\right)^2 \frac{1}{2dE} + \left(\frac{F}{b}\right)(1 - cos\theta) - R = 0 \qquad (2.2)$$

The solution for the quadratic equation above is used to solve for peel force (F)

$$\frac{F}{b} = (1 - cos\theta)dE \pm \sqrt{dE(2R + (1 - cos\theta))} \qquad (2.3)$$

Equation (2.2) and (2.3) are simulated using Matlab to analyze the relationship between adhesive energy, peel force, Young's modulus, peel angle and film thickness. The plots generated with certain input values are shown in Figure 2.4, 2.5, 2.6 and 2.7. Figure 2.4 shows that for a fixed peel force a film with low Young's modulus experiences more adhesive energy with the substrate compared to a film with higher Young's modulus. Kendal's model predicts that when the modulus of the film approaches zero the adhesive energy at the interface approaches infinity. From 0 to 0.5 MPa, the adhesive energy decreases rapidly with increasing Young's modulus. From 0.5 MPa to 1MPa the adhesive energy shows a gradual decrease of 10 to 7 N/m. Beyond 1 MPa the adhesive energy does not show much variation. From the plot in Figure 2.5 it is seen that as the peel angle increases from 0 to 180^o the adhesive energy between the film and the substrate increases from 10 to 23 N/m. From Figure 2.6 it is seen that the model predicts an increase in peel force with increase in adhesive energy. From Figure 2.7 it can be inferred that as the thickness of the film increases

from 20 to 150 µm the adhesive energy between the film and the substrate decreases from 16 to 8 N/m.

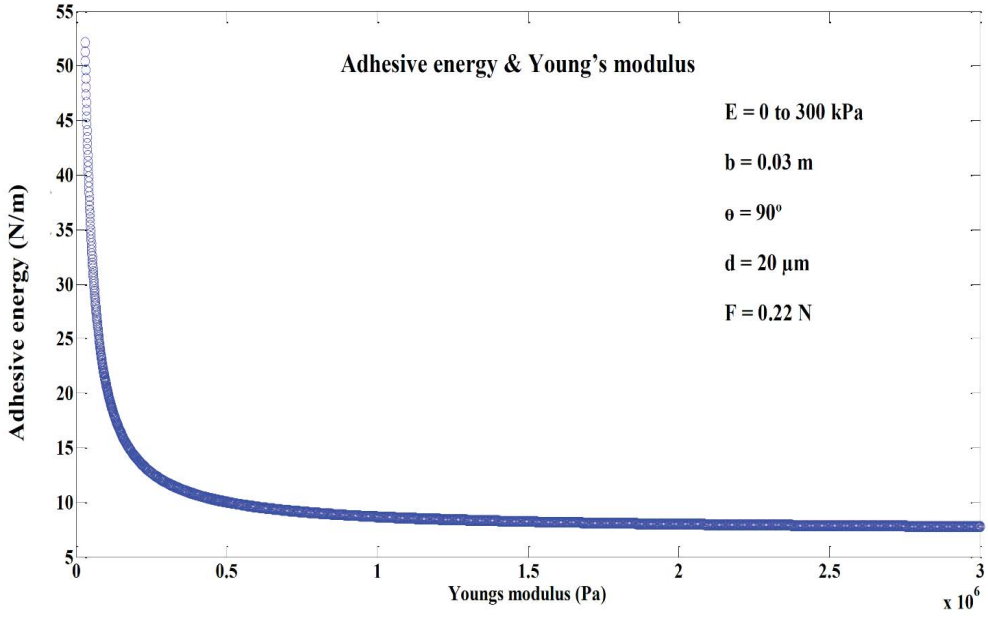

Figure 2.4: Variation of adhesive energy with Young's modulus

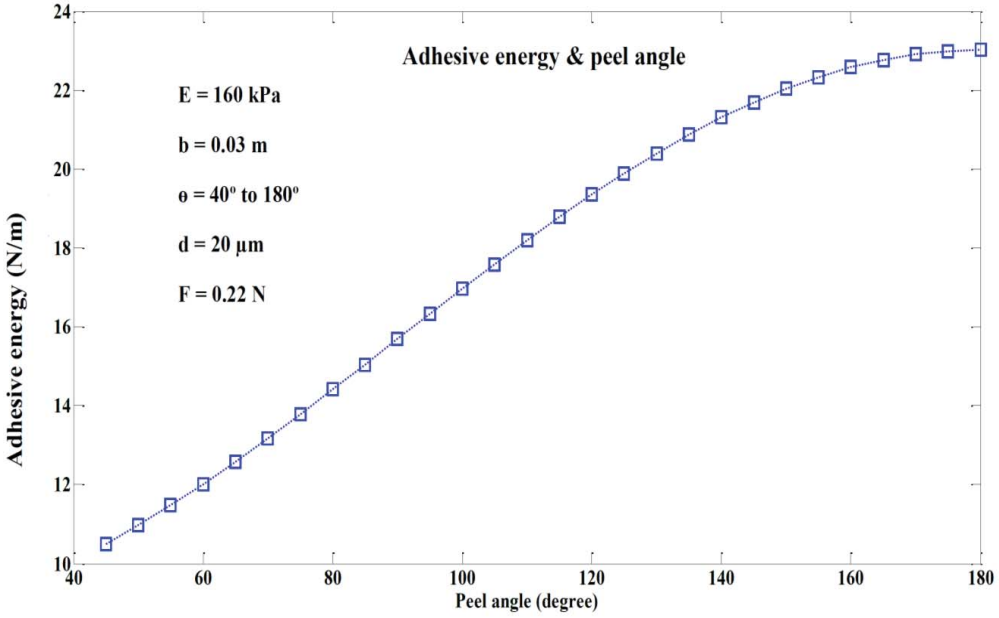

Figure 2.5: Variation of adhesive energy with peel angle

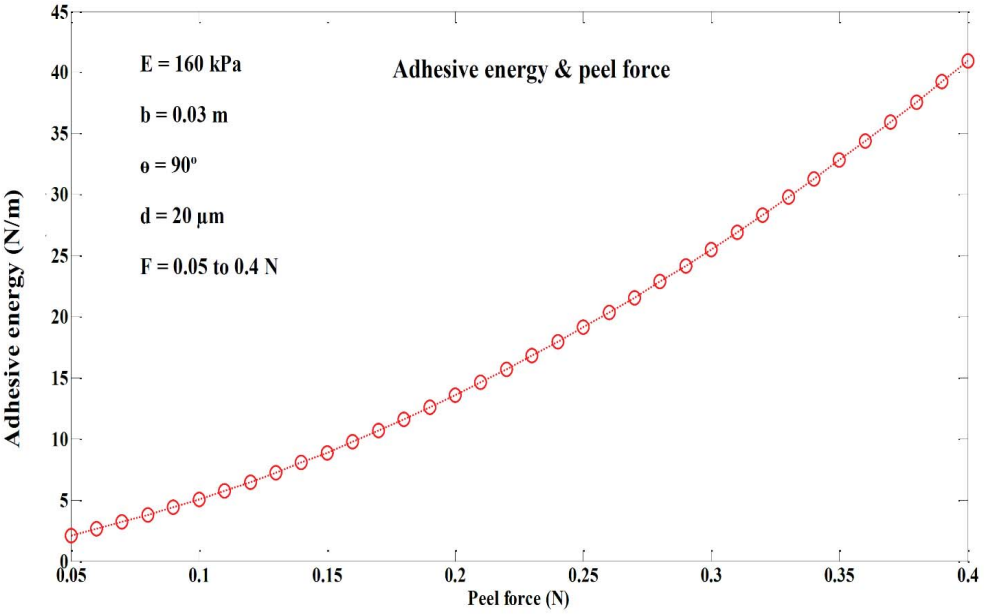

Figure 2.6: Variation of adhesive energy with peel force

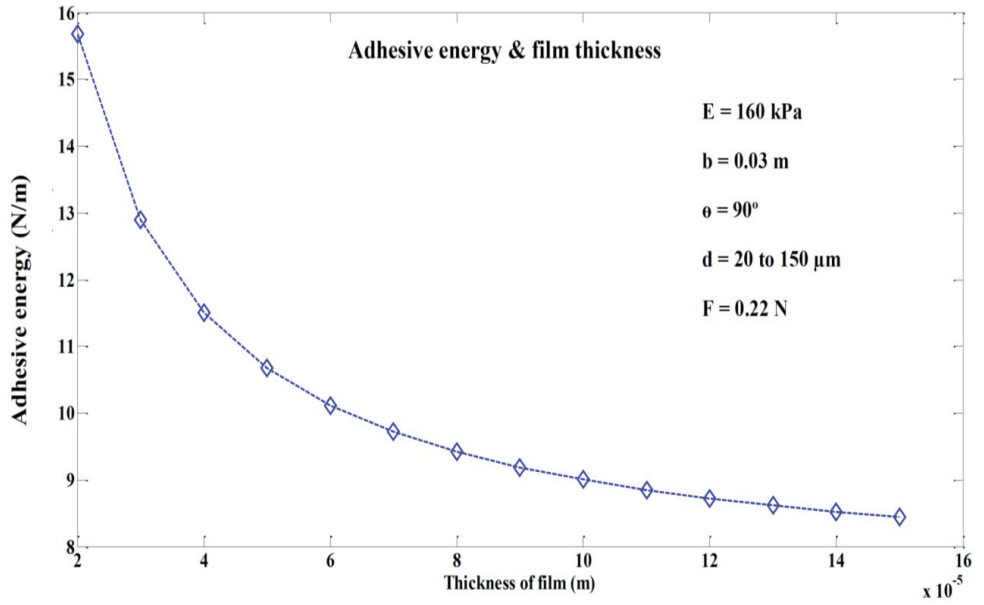

Figure 2.7: Variation of adhesive energy with film thickness

A lower peel angle (< 90°), higher Young's modulus (~ 1 MPa) and a thickness of above 40 µm will give an adhesive energy of ~ 10 to16 N/m which corresponds to a peel force of ~ 0.15 to 0.2 N per 30 mm width of the sample. The smaller the peel angle, the smaller will be the potential

energy contribution. Since, the standard peel tests are performed at $\theta = \pi/2$ or $\theta = \pi$, the peel angle modification and its effect on peel force is not tested. The delaminator used in the industry can vary the angle of peeling and hence the variation of peel force with peel angle can be tested in the industry. The elastomeric contribution to peel is governed by the Young's modulus which is a material property that cannot be modified for DEAP applications. The surface energy contribution to peel force can be lowered, if the surface energy can be brought down. This should preferably be done without affecting the bulk properties of the material (mechanical and dielectric) properties.

2.4.Surface modification of the PDMS films

Through the addition of suitable surface-active block copolymers, it has been shown that the surface energy can be decreased further or that the film can be made selectively non adhesive to a particular substrate. [78] A polymeric additive with a lower surface energy than its host matrix is known to adsorb preferentially at the free surface and consequently decrease the adhesion of that surface toward a particular substrate. [50] PDMS is doped with small quantities of a perfluoroether additive that contains low energy trifluoromethyl (CF_3) groups. [79] These low energy CF_3 groups will migrate to the two surfaces of the silicone film and will segregate. Because of the high density of the CF_3 groups in the perfluoroether, it is possible to obtain a silicone surface with very low surface energy simply by adding very small quantities of perfluoroether. Perfluoroether allylamide [$F(CFCF_3CF_2O)_7CFCF_3CONHCH_2CH{=}CH_2$, PFE] added to curing PDMS (0.3-1.5 weight %) lowered the surface energy of PDMS from 19 to 8 mJ/m^2. [33, 79] The PFE molecules added to the PDMS are chemically bonded to the silicone network by the platinum catalyzed hydrosilation reaction. [79] The PDMS films are doped with 1 wt. % PFE and the films are examined to determine whether they yield favorable results.

To investigate the influence of the PFE on the mechanical properties, the linear rheological properties of the pure PDMS and PDMS doped with PFE will be examined. Furthermore, to investigate the changes induced on the surface of the films by the PFE, contact angle measurements and peel tests on these surfaces have been performed. Dielectric permittivity tests are also conducted to investigate the influence of PFE on permittivity because an increase in the dielectric permittivity would be an advantage for DEAP films and would make it possible to address additional issues beyond process related problems. [80]

The allyl groups ($-CH{=}CH_2$) of PFE react with the hydride groups ($-Si-H$) of the crosslinker (methyl hydrogen siloxane) and compete with PDMS in the hydrosilation reaction, shown in Figure 2.8. To ensure proper bonding of the PFE to the silicone network and complete crosslinking of PDMS, sufficient crosslinker has to be added to the reaction mixture. The effects of the additional crosslinker and platinum catalyst in the reaction mixture are also investigated. Hence, various compositions of crosslinker and catalyst are used in the reaction mixture.

2.5.Experimental

The materials and instruments used in the experiments are listed below.

2.5.1.Materials

The PDMS elastomer, oil and inhibitor used for the following set of experiments are 1) Elastosil RT-625 (a commercially available RTV silicone), 2) Powersil Fluid TR50 and 3) Inhibitor PT 88 respectively, obtained from Wacker Chemie AG, Germany. The PFE (KDP-4645) is supplied by DuPont Krytox Performance Lubricants, USA.

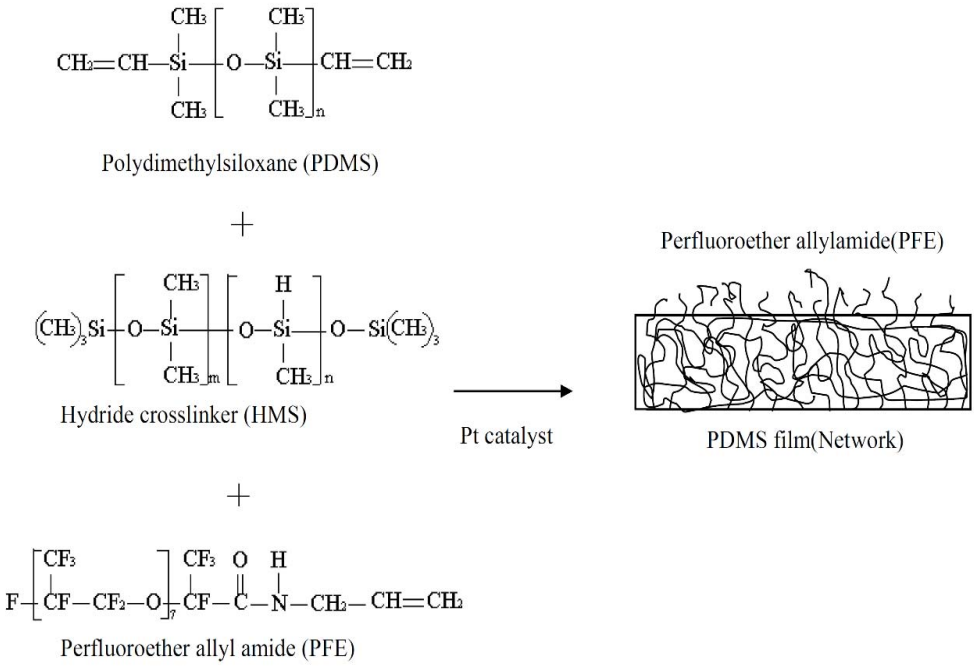

Figure 2.8: Modification of the PDMS network with PFE [79]

2.5.2.Instrumentation

Rheological experiments

Rheological measurements (time sweep and frequency sweep) on the silicone networks are performed with a controlled stress rheometer AR-2000 (TA instruments, USA).

Contact angle experiments

Contact angle experiments are performed using the Contact Angle system (OCA Data Physics, Germany). The probe liquids are water and hexadecane from Sigma-Aldrich, USA.

Peel experiments

Peel tests are performed in Danfoss PolyPower A/S using the Zwick/Roell (Zmart.pro, Germany) material tester.

Dielectric permittivity experiments

The dielectric permittivity tests on the samples are performed using Novocontrol Alpha-A (Novocontrol Technologies GmbH & Co. KG, Germany), a high performance frequency analyzer.

2.6.Procedure

The experimental procedure is explained in the following sections.

2.6.1.Preparing the addition curing PDMS mixture and films

Elastosil RT 625 is supplied as premixes A and B. Premix A is a mixture of vinyl terminated PDMS and crosslinker while Premix B is a mixture of vinyl terminated PDMS and catalyst amongst other components such as fillers. Premix A and premix B are mixed in the prescribed proportions (9:1), using the speed mixer DAC 150FVZ-K (Synergy Devices Ltd., UK) for 2 minutes at 1000 rpm. Similarly, samples with Elastosil RT-625 (9:1), PFE (1 wt. %), oil (15 wt. %) and inhibitor (0.8 wt. %) are also mixed.

Another set of samples are made with Elastosil RT 625 where the mixing ration of A and B are is 10:1, so that the resulting mixture has more crosslinker. The amount of PFE added to this mixture is also 1 wt. %. The crosslinker percentage is increased in the second set of samples so that the PFE has sufficient crosslinker to react with. Oil (15 wt. %) and inhibitor (0.8 wt. %) are also added to some elastomer samples of this set to investigate the influence of these constituents as well.

To examine the effects of additional catalyst, next set of samples are made, where Elastosil A and B are mixed in the ratio 9:1.1. PFE (1 wt. %), Oil (15 wt. %) and inhibitor (0.8 wt. %) are also added to these set of samples.

Mixing the premixes A and B of Elastosil will result in the hydrosilation reaction of the vinyl terminated polydimethylsiloxane (─CH═CH2) with the hydride crosslinker (─Si─H) in the presence of the platinum catalyst, resulting in a PDMS network. PFE also reacts with the crosslinker, when present in the mixture. In total 18 samples are made with varying compositions (Table 2.1), to investigate the effects of PFE, additional crosslinker and oil on the silicone films. The films are made by casting a coating of the addition curing mixture on a 30 % carrier web (Refer to section 1.2.2.) using a 3540 bird film applicator The segregation of PFE in the surface is the same in the film–air interface and the film–substrate interface. The PFE migrates to the surfaces/interfaces of the PDMS film uniformly. Fourier transform infrared spectroscopy curves showing the peaks with the same intensity for PFE on both the interfaces of the PDMS film are presented in Figures 2.9 and 2.10.

2.6.2.Rheological experiments

To investigate the effects of PFE, additional crosslinker and catalyst on the mechanical properties of Elastosil, rheological tests are performed. Time sweeps of the samples (Table 2.1) are performed at 2 % strain, at temperatures 23 ^{o}C and 80 ^{o}C and in a frequency of 1 Hz. The applied strain (2 %) is ensured to be within the linear regime of the material. Samples with inhibitor are cured at 80 ^{o}C, as the inhibitor inhibits the curing at room temperature. Samples without the inhibitor are cured at 23 ^{o}C. Mechanical characterization (frequency sweeps) of the samples is performed by LVE measurements. Films of thickness 1 mm (1000 microns) are prepared with the sample mixtures using 1 mm frames. After complete curing, the films are cut to make 25 mm diameter discs. LVE measurements on these samples are performed from a frequency of 100 Hz to 0.001 Hz with 2 % strain (which is ensured to be within the linear regime of the material based on an initial strain sweep) using the 25 mm aluminum parallel plate geometry at 25 ^{o}C. The normal force applied by the aluminum disc on the sample is 5-10 N.

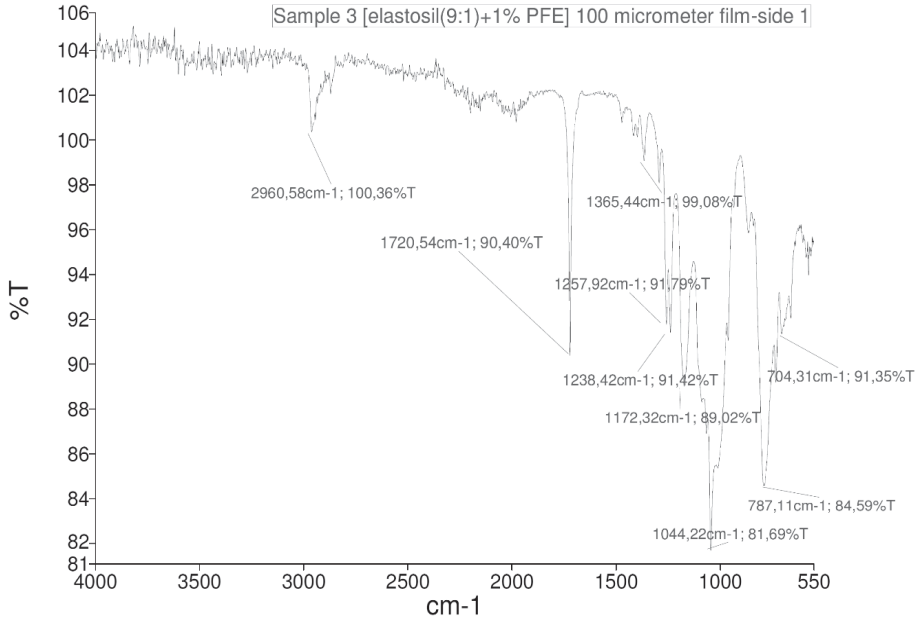

Figure 2.9: FTIR curve at the air-film interface showing a peak at 1720.54 cm^{-1} corresponding to the C=O stretch of PFE (90 %T)

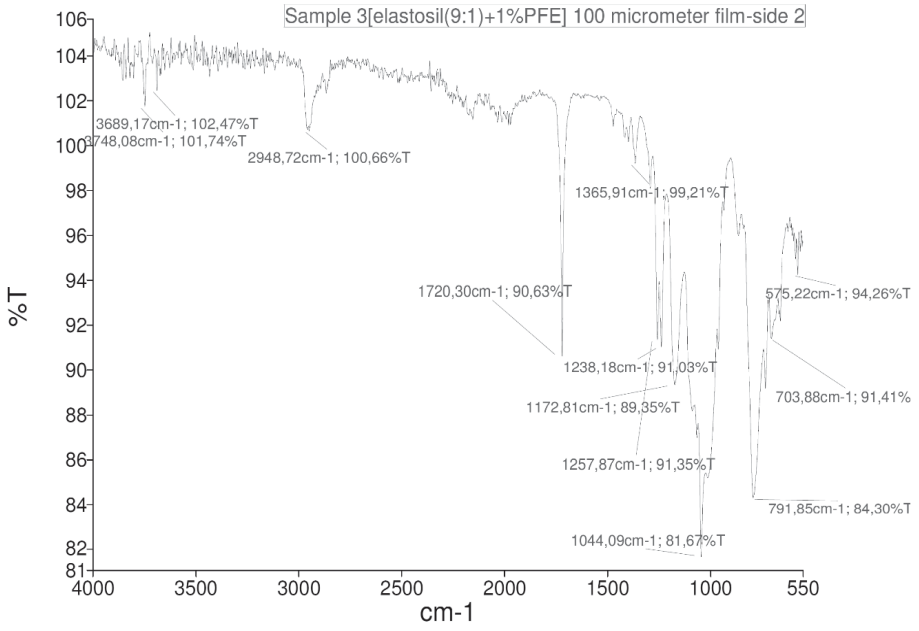

Figure 2.10: FTIR curve at the film-substrate interface showing a peak at 1720.30 cm^{-1} corresponding to the C=O stretch of PFE (90 %T)

2.6.3.Contact angle experiments

As described above, addition curing mixtures are prepared with the different compositions. Films of thickness 1 mm are made on a flat substrate. Once fully cured, the films are tested for contact angles. Advancing and receding contact angle experiments are performed on the samples using water as the probe liquid. For the advancing and receding contact angle a 6 µl drop is expanded by dispensing 30 µl liquid through a needle at a constant rate of 1 µl/sec. The pressure in the drop is built initially as the drop expands and when the drop reaches full size a reverse dispense through the needle is initiated and the drop reduces in size. The contact angle of expanding drop keeps increasing and reaches a constant value and the contact angle decreases for the receding drop. An average of the constant values from runs 20 to 40 is taken as the contact angle. Static contact angle measurements are made with hexadecane as the probe liquid. Since hexadecane swells the surface of the PDMS films, the contact angle measurements are made within 5 ~ 10 s of the drop coming into contact of the film.

2.6.4.Peel experiments

Peel tests are performed on the samples to estimate the peel force and the adhesive energy. Films of thickness 100 µm are made on the 30 % down web with the addition curing mixtures using a 3540 bird film applicator (Elcometer, Germany). The dimensions of the samples are 30×30 mm^2. Once the films are fully cured on the carrier web, they are tested for peel force with a peel angle of 90^o. A peel curve is obtained from plotting the peel force versus length of sample peeled.

2.6.5.Dielectric permittivity experiments

For the permittivity tests films of thickness 1 mm are made from the addition curing mixtures and once fully cured, discs of diameter 25 mm are cut of it. They are then tested for their dielectric permittivity.

2.7.Results and discussions

The results of the experiments are discussed below.

2.7.1.Rheological experiments

The time sweeps of sample 6 and sample 12 are shown in Figure 2.11. These samples show the greatest deviation because they contain the highest (1 wt. %) and lowest (0 wt. %) amounts of PFE, respectively. After the onset of the hydrosilation reaction, the PDMS network approaches chemical gelation. A crosslinking polymeric system is said to reach its gel point (GP) at a critical extent of the crosslinking reaction at which either the weight-average molecular weight diverges to infinity (infinite sample size) or the first macromolecular cluster extends across the entire sample (finite sample size). [81, 82]. The GP that is at the crossover between G' and G'' is an important processing parameter for DEAP materials. The addition of PFE to the Elastosil RT 625 does not modify the GP significantly. From the results, it can be concluded that the addition of 1 wt. % PFE does not lead to any changes in the process conditions for the RTV rubber, which is very favorable for the process. The frequency sweeps of samples 6 and 12 are compared in Figure 2.12. Again, these are the samples showing the most deviation because they contain 1 wt. % and 0 wt. % PFE, respectively. From the frequency sweeps (Figure 2.12), it is evident that the storage modulus G' of pure Elastosil RT 625 film is not greatly influenced by the addition of PFE. The addition of PFE lowers the elastic-modulus by a few percent, which is within the experimental

uncertainty of the measurements, but the increase in G" with the addition of PFE confirms that there is a small but still fairly insignificant decrease in the elasticity of the material with PFE. The deviation in G'' is much clearer because the magnitude of G'' is dominated by the very small sol fraction. In contrast, G' is dominated by the elastically active material. [83]

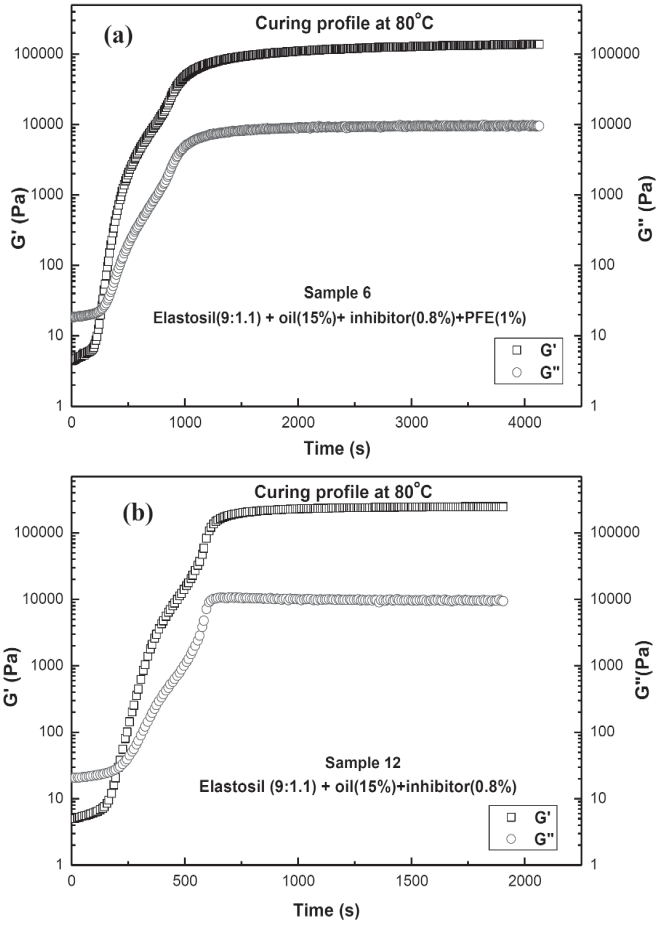

Figure 2.11: **a)** Curing profiles of sample 6 (Elastosil (9:1.1) + oil (15 wt. %) + inhibitor (0.8 wt. %) + PFE (1 wt. %)) and **b)** sample 12 (Elastosil (9:1.1) + oil (15 wt. %) + inhibitor (0.8 wt. %)) at 80 °C

In Table 2.1, the elastic moduli of all the samples G' ($\omega \rightarrow 0$) and other process related properties, such as the time for the material to obtain 97 % of its final strength (t_{97}) and the crossover point of G' and G", are tabulated. The t_{97} is also an important parameter for many processing considerations because it may be overly expensive to wait for the last 3 % of reaction, which proceeds very slowly, and in the case of fairly stoichiometric networks, does not influence the elasticity significantly.

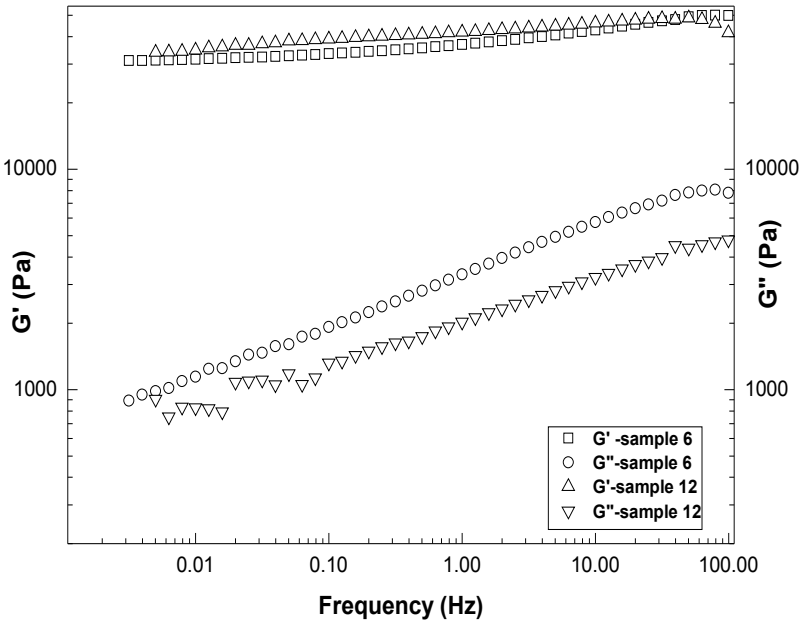

Figure 2.12: Frequency sweeps of sample 6 (Elastosil (9:1.1) + oil (15 wt. %) + inhibitor (0.8 wt. %) PFE (1 wt. %)) and sample 12 (Elastosil (9:1.1) + oil (15 wt. %) + inhibitor (0.8 wt. %)) at 23 °C

2.7.2.Contact angle and surface energy

Advancing and receding drop with water

The advancing and receding water contact angle experiments are performed on the samples. The Elastosil RT 625 samples without PFE have an average water contact angle of 110^o, which is characteristic of PDMS. [33] Samples with 1 wt. % PFE have an average water contact angle of 115^o as the, shown in Figure 2.13.

Static contact angle with n-hexadecane

The static contact angles measured with n-hexadecane are tabulated in Table 2.1.

Surface energy calculation

According to the Fowkes's method [84] the surface energy of a solid surface (S) can be calculated using the contact angle of a liquid (L) using a simple formula.

$$\frac{\sigma_L(cos\theta+1)}{2} = \sqrt{\sigma_S^P}\sqrt{\sigma_L^P} + \sqrt{\sigma_S^D}\sqrt{\sigma_L^D} \quad (2.4)$$

$$\sigma_L = \sigma_L^D + \sigma_L^P \quad (2.5)$$

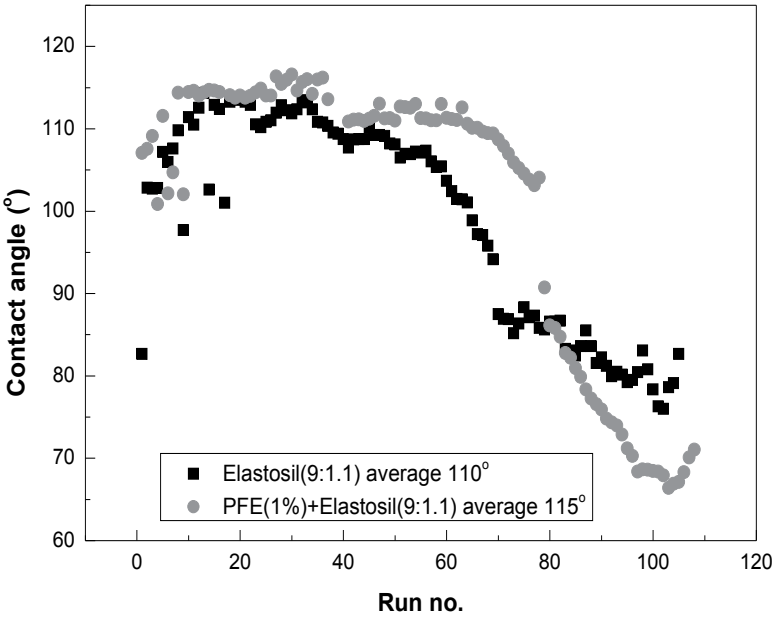

Figure 2.13: Advancing and receding drop experiment with water on pure Elastosil RT 625 (9:1.1) and Elastosil RT 625 doped with 1 wt. %PFE

In equations (2.4) and (2.3), σ is the surface energy (surface tension), P denotes the polar component of surface tension and D is dispersive component of surface tension.

When we use a liquid whose polar component is zero, the surface tension of the liquid will then be $\sigma_L = \sigma_L^D$. Hence equation (2.4) will become

$$\sigma_S^D = \frac{\sigma_L(cos\theta+1)^2}{4} \tag{2.6}$$

Thus, using the contact angles of a polar liquid like water and a non-polar liquid like n-hexadecane, one can estimate the surface energy of a solid using the equations (2.4) and (2.6). The results are tabulated in Table 2.1. The samples doped with PFE have a much lower surface energy than the pure Elastosil RT 625 samples, shown in Figure 2.14. Films with PFE have a higher contact angle with n-hexadecane and a lower surface energy, compared to the films without PFE. However samples 12, 13, 14 and 17 (20.3, 19.4, 20.8, 18.9 mN/m, respectively) have almost similar surface energy values of which samples 14 and 17 have PFE and samples 12, 13 do not have PFE.

2.7.3.Peel experiments

A peel curve obtained from the peel test of sample 3 is shown in Figure 2.15. The peel force F which is the force used in peeling a length of 1 mm of the sample is plotted against the length of the sample that is being peeled. From the peel curve we see that F increases to a maximum value

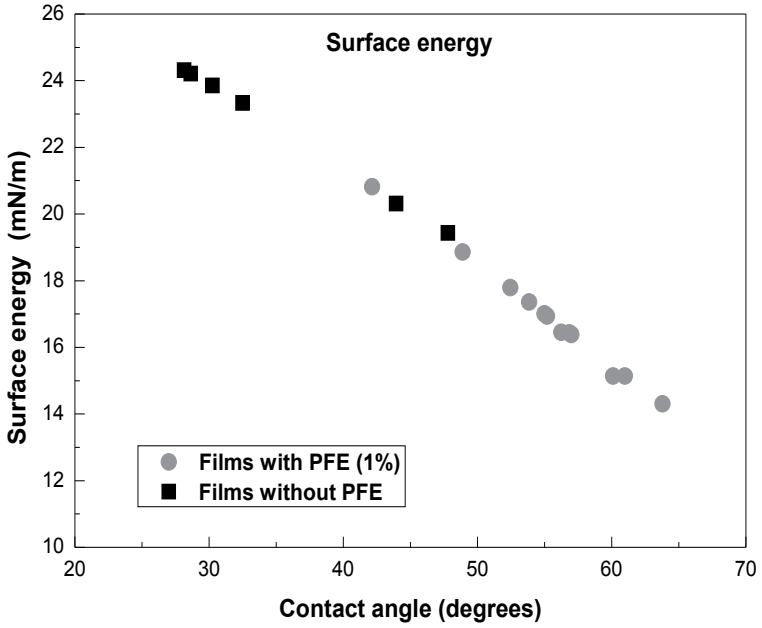

Figure 2.14: Surface energies calculated using Fowkes' method

and then falls to a low constant value. From examining the F of the samples, it is observed that samples 6 and 12 with 15 wt. % oil and 0.8 wt. % inhibitor have the maximum F values. Samples 5, 8, 10, 11, 15, 17 and 18 all of which contained 15 wt. % oil have low F values compared with the average of 0.0157 N/mm. In contrast, samples 7, 9 and 16, which contain 0.8 wt. % inhibitor (without oil), had higher F values than the average of 0.0157 N/mm. The presence of oil in the addition curing mixtures certainly makes the release easier, as it acts like a release agent. The values of maximum and constant peel force of all samples are tabulated in Table 2.1.

In the Figure 2.16 the surface energy and the F of the samples are plotted. It is observed that the samples with low surface energy and those with high surface energy both have similar patterns with F. The reduction of surface energy of the samples did not reduce or affect their F.

Using the peel equation (2.2) and equations (2.7) and (2.8) below, the adhesive energy R is calculated. [77]

$$E = 2G(1+\upsilon)' \tag{2.7}$$

$$\mathrm{G} = \mathrm{G}'(\omega \to 0)) \tag{2.8}$$

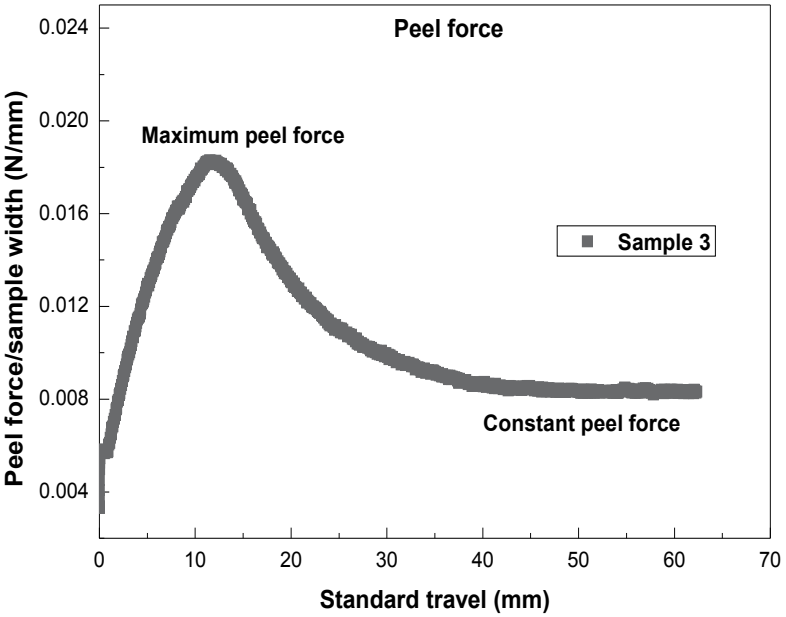

Figure 2.15: A peel curve

In equations (2.7) and (2.8) G is the static shear modulus and υ is the poisson ratio. The F is obtained from the peel tests and the *E* is calculated from equation (2.7). The value of G is calculated from equation (2.8) [85] and G' is obtained from the frequency sweeps (Table 2.1) of the rheological tests. The Poisson ratio (υ) for silicone elastomers is taken as the same as natural rubber (0.5), since silicone elastomers are very close to being incompressible. [86] The maximum value of *F* is used for all calculations in order to estimate the maximum *R* between the film and the substrate during the processing. A comparison of samples 2 and 12 clearly shows that as the *E* increased, the *R* decreased. *[Sample 2 has F= 0.016 N/mm, E=0.18 MPa, and the calculated R = 27 N/m. Sample 12 has F= 0.022 N/mm, E=0.10 MPa and the calculated R= 61.7 N/m.]*

From Figure 2.17 and 2.18 one can understand the relationship of the *E*, *R* and *F*. From Figure 2.17 it is observed that as the *F* increased the value of *R* also increased. To lower peel force, the adhesive energy needs to be lowered. From Figure 2.18 it is observed that *R* and *E* are related inversely, in accordance to equation (2.1) and an approximate assumption can be made that as the material's Young's modulus increases the film develops lesser adhesive energy at the interface. Although surface energy, *F* and *R* are related through the action of surface forces, the relation is not obvious. [87] The relationship of *F*, *R*, *E* and release can be understood further from the theory proposed by Johnson *et al*. [79] Every surface has a surface energy resulting from the action of surface forces. When two surfaces are in intimate contact, these surface forces act as attractive adhesive forces.

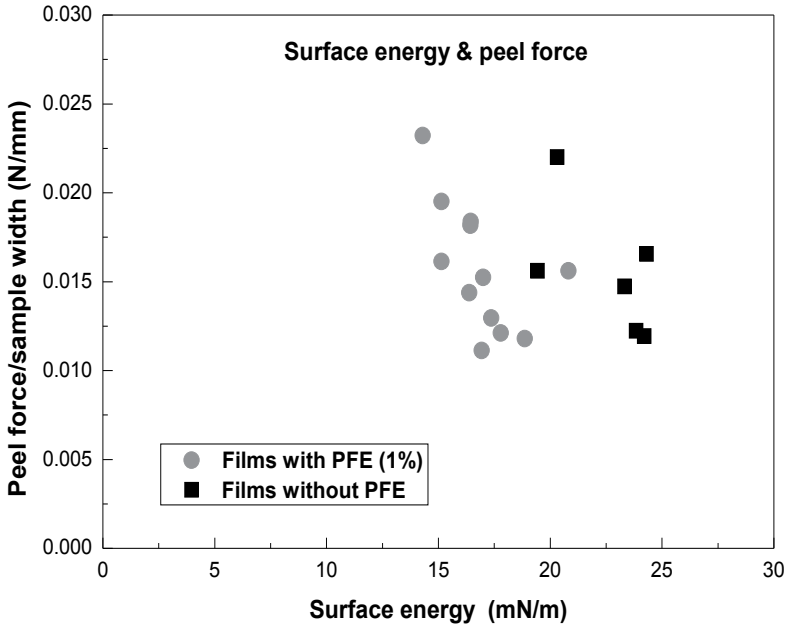

Figure 2.16: Comparison of the surface energies of the samples with peel force F

The strength of the attractive (adhesive) force between two surfaces depends on the contact surface area. [74] Interfacial gaps due to surface asperities or dust particles will strongly influence the adhesion between the surfaces because the attractive forces decrease rapidly with increasing separation. [74] Materials with low elastic modulus, will even out easily against a substrate and make very good contact. Therefore they are strongly adhered to the substrate. [74] Hence, to peel the film off, one needs to overcome the adhesive energy and apply a high *F*. To make the release easier, the contact at the interface needs to be reduced to prevent the surfaces from adhering strongly. Release agents if used would prevent the intimate contact at the interface and ease the release of a surface from another surface. In contrast, materials with high Young's modulus will not flatten out against another surface and cannot make an intimate contact and hence experience a lower adhesive energy.

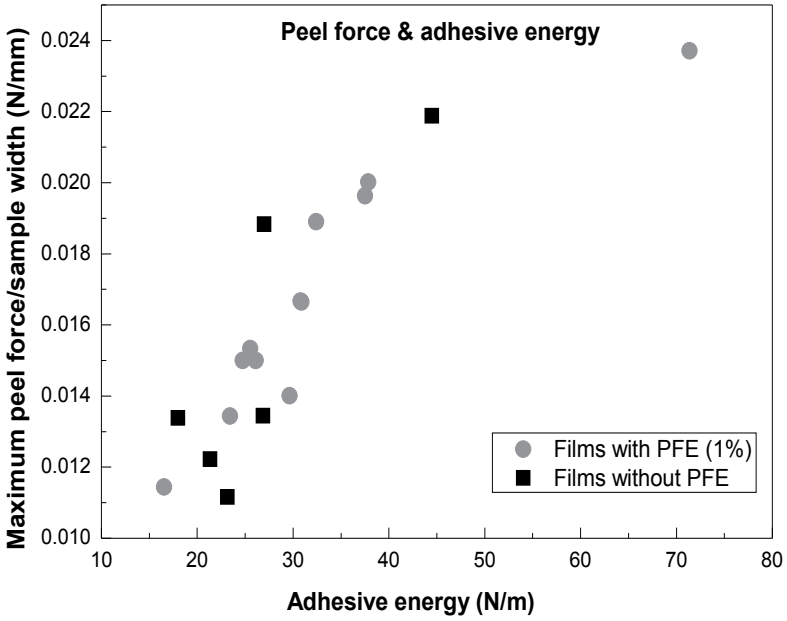

Figure 2.17: Relationship between the adhesive energy R and the peel force F

2.7.4.Dielectric permittivity

In Figure 2.19, dielectric permittivity (ε=ε'+iε") of samples 1, 3, 5, 13, 14 and 15 are shown. The dielectric constant is an essential piece of information when designing capacitors or in our case an actuator which operates with the same principle of a capacitor. The permittivity (ε) of PDMS films used in our experiment is usually around 3.2 [80]. The tests conducted confirmed that the ε of the samples are not influenced much by PFE addition and are well within the allowed limits. The ε' of samples vary in a range of 3.1 to 3.4 (Figure 2.19). In addition, the low variation in permittivity values can be attributed to the addition of oil and inhibitor.

2.8.Conclusions

PFE additive is ideal for decreasing surface energy of PDMS films without affecting the bulk properties though it failed to decrease the peel forces. The reason for this is because the elastic contribution to the peel force is much higher than the potential and the surface energy contribution. The addition of PFE to the Elastosil RT 625 did not influence the storage modulus G' much, as seen from the time sweeps. The dielectric permittivity of the samples is also not influenced by the addition of PFE. Elastosil RT 625 doped with PFE has high contact angle in the advancing drop and during the receding drop the surface behaves more hydrophilic than the pure Elastosil RT 625 films. This can be due to the presence of high energy moieties near the surface. The amide groups

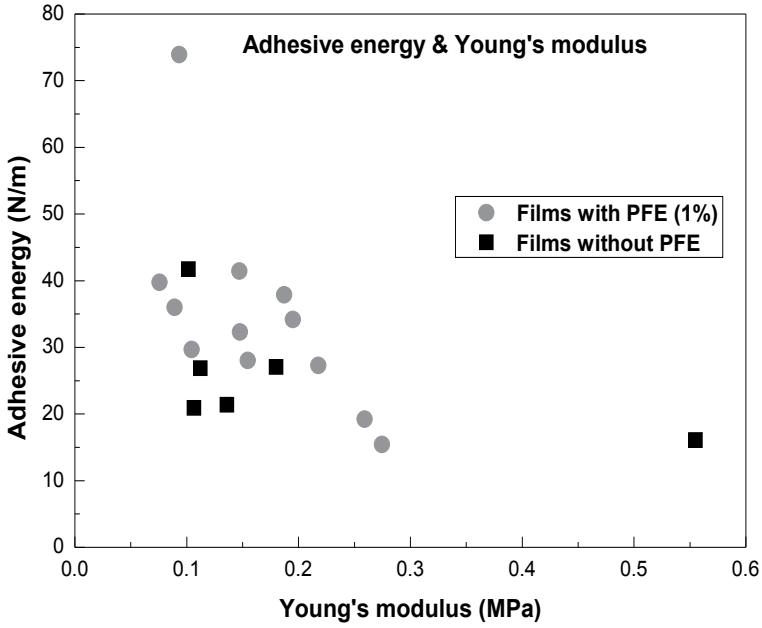

Figure 2.18: Relationship between the adhesive energy and Young's modulus

just beneath the surface are highly polar and hence get exposed when water (polar liquid) comes into contact with the surface. [79]

The Kendal's model predicts that an elastomer film with a Young's modulus ~ 1 MPa, thickness > 40 µm when peeled with an angle < 40^{o} gives a peel force of ~ 0.15 to 0.2 N for a sample width of 30 mm i.e., 0.005 N/mm to 0.007 N/mm which is lower than the samples tested (Refer Table 2.1). From the samples tested it has been shown that adhesive energy decreased with increasing Young's modulus. For the investigated elastomer films, the Young's moduli are low, which makes them even out against surfaces easily and establish good contact. This contact increases the adhesive/cohesive forces, making the release hard. Increasing the Young's modulus or film thickness is not an option for our films and hence other techniques for easing the release of the films will be investigated.

Table 2.1: Composition of the samples and their properties

Sample no.	Elastosil (A:B)	PFE (wt. %)	Inhibitor (wt. %)	Oil (wt. %)	Temperature (°C)	GP (minutes)	t_{97} (minutes)	G'(ω→0) (MPa)	E= 3G (MPa)	Contact angle with n-hexadecane	Surface energy (mN/m)	Max. peel force 'F' per mm (N/mm)	Average peel force per mm (N/mm)	Adhesive energy 'R'(N/m)
1	9:1	-	-	-	23	65.8	780	0.19	0.57	32.5	23.3	0.015	0.007	16.1
2	9:1.1	-	-	-	23	53.9	317	0.06	0.18	28.2	24.3	0.017	0.009	27.0
3	9:1	1	-	-	23	50.5	406	0.06	0.18	55.0	17.0	0.018	0.008	34.2
4	9:1.1	1	-	-	23	54.7	789	0.05	0.15	60.1	15.1	0.016	0.009	32.3
5	9:1	1	0.8	15	80	5.2	52.2	0.05	0.15	57.0	16.4	0.014	0.009	28.0
6	9:1.1	1	0.8	15	80	4.4	67.8	0.03	0.09	63.8	14.3	0.023	0.014	73.9
7	9:1	1	0.8	-	80	4.4	19.8	0.06	0.18	61.0	15.1	0.019	0.013	37.8
8	9:1	1	-	15	23	77.3	1012	0.025	0.08	55.2	16.9	0.011	0.007	39.7
9	9:1.1	1	0.8	-	80	5.5	42.6	0.05	0.15	56.3	16.5	0.018	0.010	41.4
10	9:1.1	1	-	15	23	80.3	826	0.09	0.28	52.5	17.8	0.012	0.007	15.4
11	9:1	-	0.8	15	80	4.7	37.5	0.04	0.12	28.7	24.2	0.012	0.006	20.9
12	9:1.1	-	0.8	15	80	3.4	30.3	0.034	0.10	44.0	20.3	0.022	0.013	61.7
13	10:1	-	-	-	23	45.9	454	0.04	0.12	47.8	19.4	0.016	0.010	26.9
14	10:1	1	-	-	23	51.5	1246	0.09	0.27	42.2	20.8	0.016	0.008	19.2
15	10:1	1	0.8	15	80	7.9	87.5	0.04	0.12	53.9	17.4	0.013	0.009	29.6
16	10:1	1	0.8		80	7.2	50.8	0.074	0.22	56.9	16.4	0.018	0.011	27.3
17	10:1	1	-	15	23	62	679	0.03	0.09	49.0	18.9	0.012	0.008	36.0
18	10:1	-	0.8	15	80	6.9	61	0.05	0.15	30.3	23.9	0.012	0.009	21.4

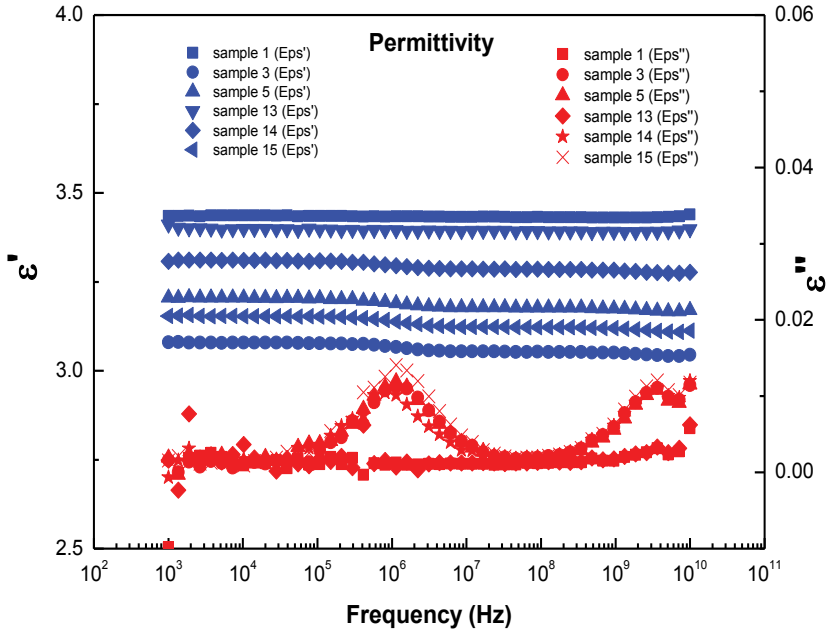

Figure 2.19: Dielectric permittivity test

3.Techniques for easing the release of PDMS films

From the simulations and experiments in the previous chapter it is concluded that peel force can be decreased by increasing the Young's modulus of the films or by increasing the thickness of the films. Increasing the film thickness is not a possibility as the current requirements in the actuator manufacturing put a strict limitation on the thickness of the elastomers, such that a maximum permissible thickness is around 40 μm. The relatively small Young's modulus for these elastomers (1 MPa for a metallized film [15]) is a requirement for actuation capabilities. Hence increasing the films thickness or the elastomer's Young's modulus is not an option. To ease the release of the films detergents (Akuta) and surfactants (Polysorbate-20, Triton X-100, Cetomacrogol-1000 and Tergitol) have been used as release agents and the peel forces are measured. Furthermore, an MQ-type silicone resin is compounded with the elastomer matrix and the peel forces of the films are measured. The methods used for easing the release are required not to interfere with the Young's modulus and breakdown strength of the films in a negative way. The results of the work presented in this chapter are published in Polymer Advanced Technologies, volume 25(3), pages 249-257 (2014) and is attached as Appendix II.

3.1.Surface energy and interfacial tension

Interfacial tension between two surfaces is somewhat similar to surface energy in which cohesive forces are also involved. The sign of the interfacial tension depends on the strength of the cohesive forces holding molecules of a material together compared with the strength of the adhesive forces between the opposing molecules of the interfacing materials. When the strength of the adhesive forces between opposing molecules at the interface is higher, the two materials tend to stick well with each other. If the interfacial energy between two liquids is negative, then a large amount of energy can be released by mixing them, and hence, the liquids get mixed instead of staying separate. Immiscible liquids such as oil and water have a positive interfacial energy density, which makes them seek a minimum interfacial area. The surface energy density associated with an interface between a solid or liquid and a gas is always positive because of the missing negative binding energy of surface molecules. Interfaces between solids and liquids or between solids and solids are not required to have positive interfacial energy density. Even if they have a negative interfacial energy density, they will not mix but this might lead to adhesion or the materials will stick too well at the interfaces. [73] The strength of the attractive (adhesive) force between two surfaces depends on the contact surface area. [87] Interfacial gaps due to surface asperities or dust particles will strongly influence the adhesion between the surfaces because the attractive forces decrease rapidly with increasing separation. [87]

3.2.Techniques for reducing the interfacial tension between the films and substrate

Decreasing the interfacial cohesive forces between the film and carrier web will help ease release of the films. Interfacial tension can be lowered by chemical or physical modification of the surfaces involved.

3.2.1.Addition / Grafting of surface active functionalities

The presence of strong adhesive forces between the films and substrates cannot be avoided in some practical applications which require soft (low Young's modulus) PDMS films. Addition of surface active block copolymers can make the film selectively non adhesive or adhesive to a particular substrate [78] and ease the release. Low surface energy additives will migrate to the films surfaces, without affecting the bulk properties and just influence the surface properties. One such examples is perfluoroether allylamide ($F(CFCF_3CF_2O)_7CFCF_3CONHCH_2CH=CH_2$, PFE) which when added in small quantities of 0.5 – 1.5 wt. % the surface energy of the PDMS films decreased from 19 mJ/m to 8 mJ/m, making the films more hydrophobic. [79] Similarly, grafting functionalities like bis(trifluoromethyl)phenyl into PDMS network via crosslinkers also made the films more hydrophobic as the water contact angle of PDMS films increased from 110^o to 116^o. [88] Increasing the hydrophobicity of films will make them poorly adhering to certain substrates and may help ease the release. All these methods of incorporating surface active functionalities are expensive and phenyl compounds are not environmentally friendly materials. These methods require advanced chemistry and will increase the price of the elastomer. Furthermore the migration of the covalently attached surface-active functionalities to the surfaces of the elastomers may be very unfavorable since the deposition of electrodes may become very difficult, and the electrodes may no more be well connected to the elastomer.

3.2.2.Teflon coating on the substrates

The substrates on which the films are made can be treated with PTFE (polytetrafluoroethylene) or ceramic non-stick coatings or can be metallized to make the release easy. The substrate in our case has microscale corrugation lines (5 μm-7 μm of wave height and 7-10 μm of wave period). [15, 16] Such coatings on a microstructured surface will interfere with the corrugation pattern, hence a very thin coating with 100 % coverage is required. These coatings may not be durable and one minor defect may destroy the film as the film can be easily torn apart. Also, these coatings are expensive considering the miles of carrier web being used for the manufacture process.

3.2.3.Surfactants

Surfactants are substances which reduce the surface tension of the liquid in which they are dissolved in. Surfactants also reduce the interfacial tension between two liquids. Surfactant molecules have a hydrophilic head and hydrophobic tail. The different types of surfactants are 1) non-ionic 2) anionic 3) cationic and 4) zwitterionic (amphoteric).

Surfactants in aqueous solution orient themselves to form micelles and the concentration at which the micelles appear is called critical micelle concentration (CMC). As the concentration of surfactant increases in the aqueous solution the surface tension drops progressively and at concentrations beyond the CMC the surface tension attains a constant value as shown in Figure 3.1. By application of surfactant solution on the carrier web (Figure 3.2) the adhesive forces at the interface between the film and carrier web can be reduced. By using a surfactant solution with concentrations more than CMC we ensure an effective coverage on the carrier wed and reduction of the interfacial tension. CMCs can be determined by various methods like fluorescence spectroscopy, UV absorption spectroscopy and the electrical conductivity method to name a few. [89-92]

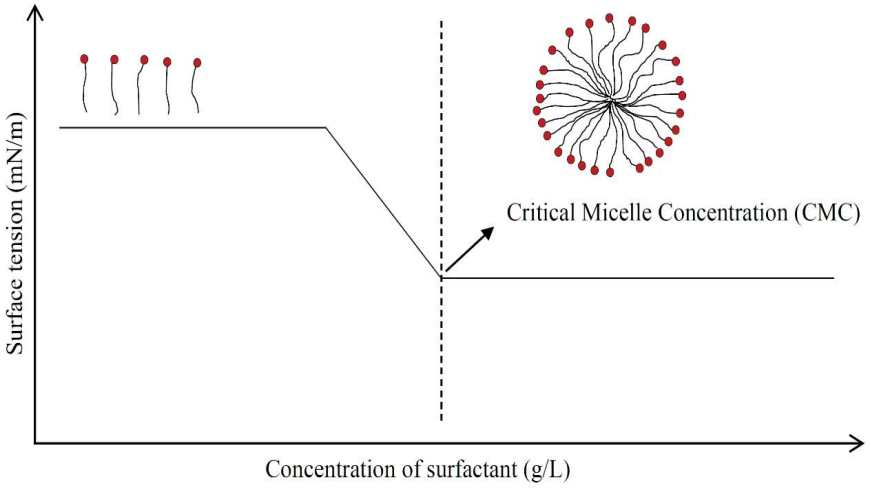

Figure 3.1: Critical micelle concentration of a surfactant

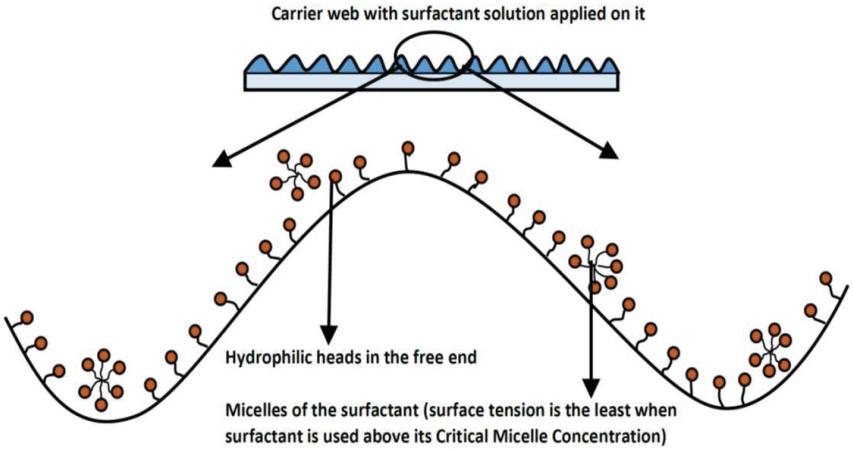

Figure 3.2: Surfactant on carrier web

3.3.Experimental

The materials and instruments used in the experiments are explained in the sections below.

3.3.1.Detergent and non-ionic surfactants

The detergent tested is Akuta dish washing machine cleaning liquid. The contents of this detergent are water, fatty alcohols, sodium cumenesulfonate, potassium cumene sulfonate, citric acid and trisodium citrate.

The non-ionic surfactants tested are as follows:

1. Polysorbate-20 (Polyoxyetheylene (20) sorbitan monolaurate) from Sigma-Aldrich, USA. The molecular mass of Polysorbate-20 is 1227.54 g/mol. The CMC of Polysorbate-20 is 0.06 mg/ml. [93]
2. Triton™ X-100 (Polyethyleneglycol tert-octylphenyl ether) from Sigma-Aldrich, USA. The molecular mass of Triton X-100 is 647g/mol. The CMC of Triton is 0.129- 0.582 mg/ml. [94]
3. Tergitol® solution (Nonylphenol Ethoxylate) NP-40s from Sigma-Aldrich, USA. The molecular mass of Tergitol is 1982.47 g/mol. The CMC of tergitol is 0.232 mg/ml. [95]
4. Cetomacrogol-1000 (Polyethylene glycol monocetylether) PO841 from Tokyo Chemical Industrial Co. Ltd, Japan. The molecular mass of cetomacrogol is 1123.5 g/mol. The CMC of cetomacrogol is 0.0063 mg/ml. [96]

Non-ionic surfactants are chosen in this case, in order to avoid ionization of the surfactant under electric field since the application of films as actuators requires use of high voltage. Figure 3.3 shows the chemical structures of the surfactants used.

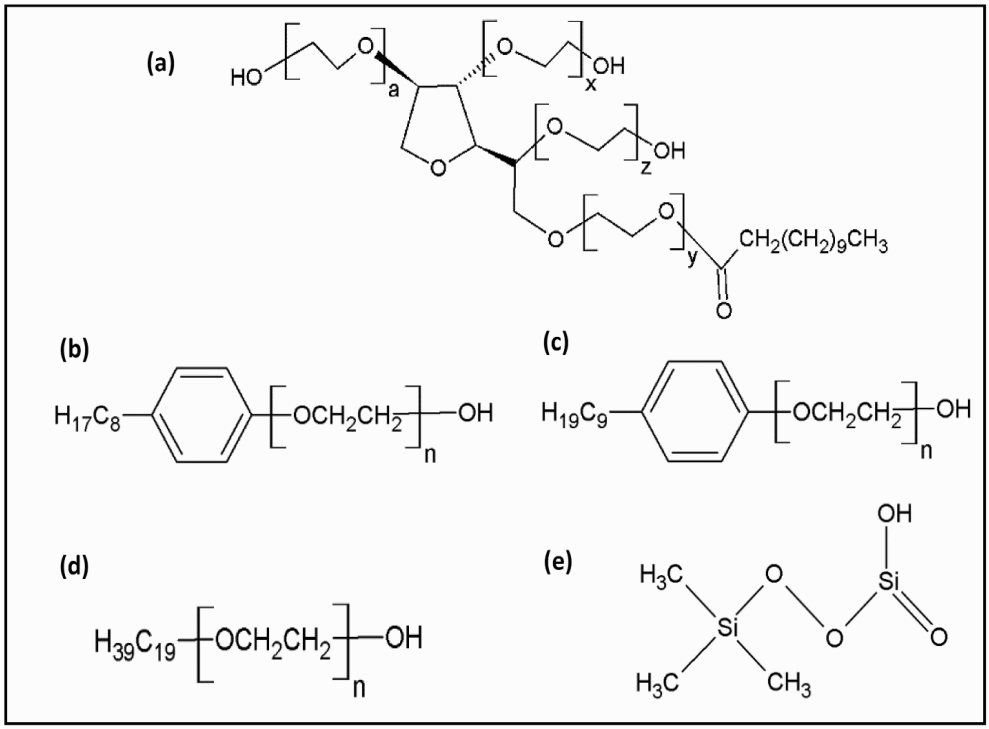

Figure 3.3: **a)** Polysorbate-20, **b**) Triton X-100, **c)** Tergitol NP40, **d)** Cetomacrogol-1000 and **e)** Belsil TMS 803

3.3.2.Silicone networks

Films made of the following three types of silicone formulations are tested for peel forces. With the advent of LSR composites as better materials for DEG [97] it is necessary to test the performance of surfactants on these films in addition to the conventional RTVs used in industry.

1. Elastosil RT 625, oil and inhibitor. (Refer to section 2.5.1. for product information)
2. Elastosil LR 3043 / 50, an LSR is obtained from Wacker Chemie AG, Germany. Elastosil LR 3043 / 50 is supplied as premixes, A and B. Premix A has PDMS and platinum catalyst and premix B has the PDMS crosslinker. OS-20, an ozone-safe volatile methylsiloxane (VMS) fluid is obtained from Dow Corning, USA. The mixing ratio of the Elastosil premixes (A and B) and OS-20 is 5:5:7 by mass.
3. POWERSIL XLR 630 A/B, a low viscosity LSR and Belsil® TMS 803, a resin are both obtained from Wacker Chemie AG, Germany. XLR630 is supplied as premixes A and B. The premix A has PDMS and platinum catalyst and premix B has the PDMS crosslinker. The mixing ratio of premixes A and B is 1:1. Belsil TMS 803 is an MQ type silicone resin commonly known as trimethylsiloxysilicate. It is a white powder with a particle size of 10 μm. It is also mixed in a ratio of 1, 3 and 5 wt. % with XLR 630.

3.3.3.Instrumentation

Rheological experiments

Refer to section 2.5.2.

Peel experiments

Refer to section 2.5.2.

Break down experiments

Electrical break down tests are performed in Danfoss PolyPower A/S on an in-house built device based on international standards (IEC 60243-1 (1998) and IEC 60243-2 (2001)).

3.4.Procedure

The experimental procedure is described as follows.

3.4.1.Coating surfactant on carrier web

The carrier web is coated with the detergent/surfactant solution with a soft paper. The webs coated with detergent/surfactant solution are then dried in the oven for 2 min at 80-100 ^{o}C. Elastomer mixtures are then coated on the dried webs. Akuta is not a viscous detergent and hence is not diluted with de-ionized water. Pure surfactants are very viscous fluids and they accumulate on the films as shown in Figure 3.4 (a, b). Therefore, the surfactants are diluted with de-ionized water with varying concentrations. The films made on carrier webs coated with aqueous solutions containing < 20 wt. % surfactant do not show much accumulation of surfactant as shown in Figure 3.4 (c, d). Hence, 2.5, 5, 7, 10 and 20 wt. % surfactant solutions are tested as release agents. The carrier webs used for the tests are 100 % down-web.

3.4.2.Preparing the addition curing mixtures and films

The silicone formulations are mixed using speed mixer DAC 150FVZ (Hauschild Co., Germany) in the proportions as stated below.

1. Elastosil RT 625 premixes are mixed in the prescribed proportions (9:1) along with inhibitor (0.8 wt. %) and silicone oil (15 wt. %) for 2 minutes at 1000 rpm.
2. Elastosil LR 3043/50 premixes along with OS-20 solvent in the ratio (5:5:7) are mixed for 5 minutes at 2000 rpm. This silicone formulation requires solvent for making it coatable. A solvent is used instead of oil to make it a relatively hard elastomer.
3. XLR 630 premixes are mixed in the ratio of 1:1 along with Belsil resin (1, 3 and 5 wt. %) for 2 minutes at 1000 rpm. The XLR is neither mixed with oil nor solvent.

Mixing the premixes initiates the hydrosilation reaction of the vinyl terminated polydimethylsiloxane (─CH═CH_2) with the hydride crosslinker (─Si─H) in the presence of the platinum catalyst, resulting in a PDMS network as shown in Figure 1.6.

The mixtures thus made are coated on the carrier web - Elastosil RT 625 and LR 3043/50 on surfactant treated carrier web and XLR 630 with Belsil on an untreated carrier web - using a 3540 bird film applicator, (Elcometer, Germany) with 100 µm blade. Films are cured in the oven for 2 minutes at 100 ºC.

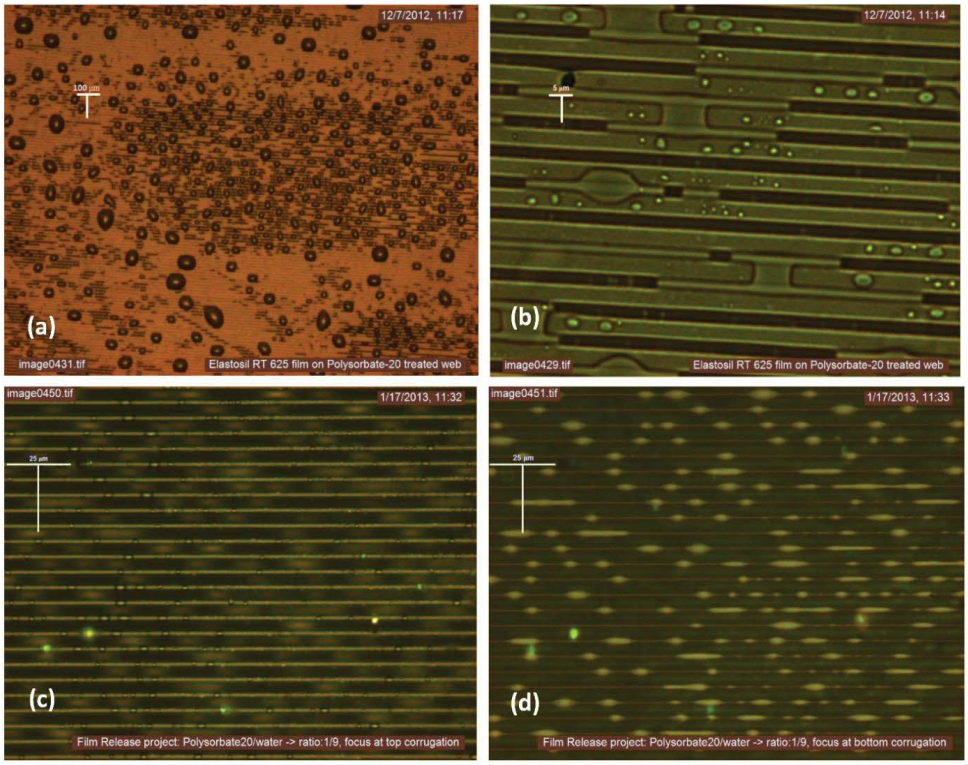

Figure 3.4: **a, b)** Elastosil RT 625 films made on the pure Polysorbate-20 treated carrier webs showing accumulated in the corrugations and **c, d)** Elastosil RT 625 films made on the treated carrier webs (Polysorbate-20: water = 1:9) showing reduced accumulation of Polysorbate-20 in the corrugations

3.4.3.Rheological experiements

Linear viscoelastic (LVE) measurements on the cured silicones films of thickness1 mm (made on 1 mm thick frames) and 25 mm diameter are performed from a frequency of 100 Hz to 0.001 Hz with 2 % strain (which is ensured to be within the linear regime of the material based on an initial

strain sweep) using the 25 mm aluminum parallel plate geometry at 25 ^{o}C. The normal force applied by the aluminum disc on the sample is 5-10 N.

3.4.4.Peel experiments

The Elastosil RT 625 and Elastosil LR 3043/50 films cured on the surfactant treated carrier webs and the XLR 630 with Belsil resin films cured on untreated carrier webs are tested for peel forces. The dimensions of the samples used for peel tests are 30×30 mm^2. Once the films are fully cured on the carrier web, they are tested for peel force with a peel angle of 90^{o}. A peel curve is obtained from plotting the peel force versus the length of the sample peeled. The maximum F from peel tests are used for all calculations in order to estimate the maximum R between the film and the substrate during the processing. The equations (2.1), (2.7) and (2.8) are used for calculating the adhesive energy.

3.4.5.Dielectric break down tests

The Elastosil RT 625 and LR 3403/50 films cured on surfactant treated webs will have the surfactant on their surfaces. It is necessary to test the influence of these surfactants on the break down strength of the films. The effect of Belsil resin on the breakdown strength of XLR 630 films are also tested. The film thicknesses are measured with microscopy of cross-sectional cuts and the distance between the spherical electrodes is set accordingly with a micrometer stage and gauge. An indent of less than 5 % of sample thickness is added to ensure that the spheres are in contact with the sample. The polymer film (30 -70 μm) is slid between the two spherical electrodes (radius of 20 mm) as shown in Figure 3.5 a, and a stepwise increasing voltage is applied (50 - 100 V/step) at a rate of 100 V/s. The average breakdown value is found using the Weibull distribution. [98] Each sample film is subjected to 10 breakdown measurements and an average of these values is indicated as the breakdown strength of the sample. In our experiments two samples in each type are tested.

3.5.Results and discussions

The results of the experiments are discussed below.

3.5.1.Rheological experiments

The E values are calculated according to equation 2.7 and 2.8 using the storage modulus values obtained from the LVEs and the values are as follows. 1) Elastosil LR3043/50 is 536 kPa, 2) Elastosil RT 625 is 107 kPa, 3) XLR 630 with 1 wt. % Belsil is 2550 kPa, 4) XLR 630 with 3 wt. % Belsil is 5860 kPa and 5) XLR 630 with 5 wt. % Belsil is 3630 kPa. The error margin in the readings is ± 5%.

3.5.2.Dielectric breakdown experiments

The methods used for easing the release should not lead to a decrease in the dielectric breakdown of the films. Akuta decreased the breakdown strength of the films (Figure 3.5 b) from 82 V/μm to 73 V/μm, which is a significant reduction leading to an overall reduction of Figure of merit by 20.7 %. [99] The Akuta detergent has sodium/potassium cumenesulfonate which are zwitterionic surfactants which have Na^{+}/K^{+} and O^{-} in the hydrophilic head. The detergent can easily percolate into the film and interfere with the breakdown strength of the films as the surfactants and salts in Akuta get ionized/charged under electric field. [100] Also, Akuta had a corrosive effect on films

as it is observed that the films became sticky over a period of time which makes them unusable. Such conductive films cannot be used for making actuators. Hence, usage of Akuta as a release agent is discarded. Further tests are conducted with non-ionic surfactants as they do not have conducting ions. Aqueous solutions with 10 wt. % non-ionic surfactants are tested for their effect on break down strength of the films. For both Elastosil RT 625 and LR 3043/50 films, Polysorbate-20 shows the least influence on breakdown strength, compared to other surfactants (Figures 3.5 b, c). Figure 3.5 d shows that the addition of resin depreciates the breakdown strength of the XLR 630 films, the maximum depreciation being 16 % for 5 wt. % resin. In Figure 3.5 d the error bars mark the difference in the measurements between two identical samples which is around 4-7% and hence the percentage depreciation of breakdown strength with increasing resin concentration is subject to error but the decreasing trend remains precise.

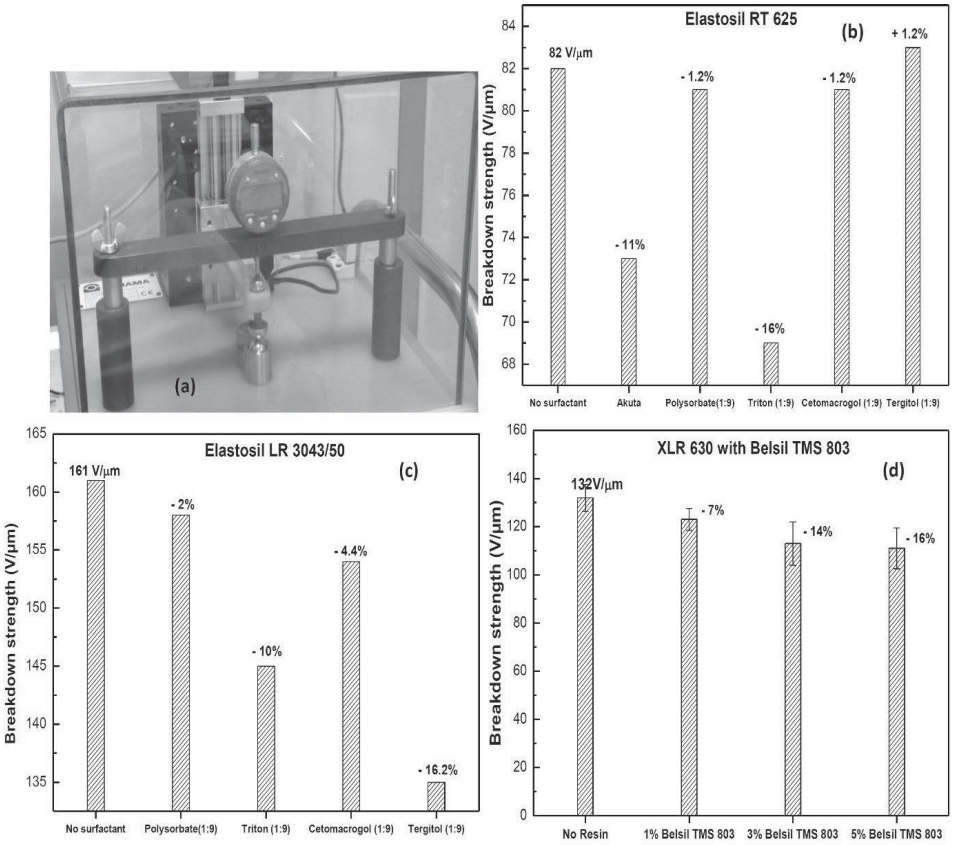

Figure 3.5: **a)** An electrical breakdown test being performed, **b)** Effect of surfactants on breakdown strength of Elastosil RT 625, **c)** Effect of surfactants on breakdown strength of Elastosil LR 3043/50 films and **d)** Effect of Belsil TMS 803 on breakdown strength

3.5.3.*Peel experiments*

The peel test results for the Elastosil RT 625 and LR 3043/50 films made on surfactant treated webs along with the calculated adhesive energy values are tabulated in Table 3.1 and the adhesive energy are plotted in Figure 3.6.

Table 3.1: Peel forces and adhesive energy of the PDMS films with various surfactants as release agents

No.	Surfactant	% of surfactant in aqueous solution	Material	Sample thickness (µm)	Max. peel force (N)	E= G'(ω→0) (k Pa)	Adhesive energy 'R'(N/m)
1	Polysorbate-20	0	Elastosil RT 625	58	0.33	106	20.9
			Elastosil LR 3043/50	41.7	1.6	536	116.4
		2.5	Elastosil RT 625	-	-	106	-
			Elastosil LR 3043/50	53	1.23	536	70.6
		5	Elastosil RT 625	-	-	106	-
			Elastosil LR 3043/50	46	1.2	536	70.4
		7.5	Elastosil RT 625	-	-	106	-
			Elastosil LR 3043/50	74.5	0.74	536	32.5
		10	Elastosil RT 625	52.7	0.22	106	12.2
			Elastosil LR 3043/50	52.7	0.08	536	2.8
		20	Elastosil RT 625	70	0.28	106	15.2
			Elastosil LR 3043/50	23.1	0.31	536	14.6
2	Cetomacrogol	0	Elastosil RT 625	58	0.33	106	20.9
			Elastosil LR 3043/50	41.7	1.6	536	116.4
		10	Elastosil RT 625	50.1	0.21	106	11.2
			Elastosil LR 3043/50	40	0.71	536	36.8
		20	Elastosil RT 625	38.8	0.20	106	11.5
			Elastosil LR 3043/50	44.2	0.54	536	24.9
3	Tergitol	0	Elastosil RT 625	58	0.33	106	20.9
			Elastosil LR 3043/50	41.7	1.6	536	116.4
		10	Elastosil RT 625	54.1	0.3	106	18.8
			Elastosil LR 3043/50	54.6	0.81	536	39.6
		20	Elastosil RT 625	42.1	0.27	106	18.2

			Elastosil LR 3043/50	24.5	0.79	536	52.9
4	Triton X-100	0	Elastosil RT 625	58	0.33	106	20.9
			Elastosil LR 3043/50	41.7	1.6	536	116.4
		10	Elastosil RT 625	90.9	0.25	106	11.7
			Elastosil LR 3043/50	41.1	0.76	536	39.5
		20	Elastosil RT 625	52.4	0.14	106	6.4
			Elastosil LR 3043/50	42.3	0.54	536	25.2

Akuta reduced the R between Elastosil RT 625 film and carrier web from 20.9 N/m to 14.9 N/m, but since Akuta lowered the breakdown strength of the films, its further use is however discarded. The results with non-ionic surfactants are plotted in Figures 3.6 a, b. The R values of XLR 630 film with varying percentages of Belsil resin are in Figure 3.6 c. For RT 625 films the value of R is reduced from 21 N/m to a lowest of 6.3 N/m with Triton X-100 (20 wt. % solution). RT 625 films show lower R values (20 N/m) than LR 3043/50 films overall. The low R values of RT 625 films can be attributed to the presence of 15 wt. % oil in the formulations which is a trend observed in the work by Vudayagiri *et al*. [31] Aqueous solutions with 2.5, 5 and 7.5 wt. % Polysorbate-20 gave very high R values for Elastosil LR 3043/50 films as the surfactant content is too low and does not reduce the R effectively. For LR 3043/50 films the value of R is reduced from 116.4 N/m to a lowest 2.8 N/m with a 10 wt. % Polysorbate-20 solution, which is a reduction of more than 98 %.

For XLR630 films the value of adhesive energy (R) reduced from 20.7 N/m to a lowest of 10.5 N/m with 3 wt. % with Belsil resin. From Figure 3.6 c it is seen that as Young's modulus of the films increase their peel force/adhesive energy decreases. [31] Belsil TMS 803 is a trimethylsiloxy silicate MQ type resin [101] which when compounded with PDMS networks makes them more hydrophobic (Figure 3.6 d). The resins can be incorporated with the reactive Si-H or Si-Vinyl groups so that they can bond with the elastomer matrix via the hydrosilylation reaction. [102] At 3 wt. % resin, the crosslinking density is optimum and a high Young's modulus is attained by the cured elastomer as seen from Figure 3.6 c. When the resin is increased to 5 wt. % the Young's modulus decreases which could be attributed to Belsil interfering negatively with the crosslinking of the elastomer matrix.

A 10 wt. % Polysorbate-20 solution is the optimum surfactant to be used as a release agent as it gave low peel forces and had negligible effect on the dielectric breakdown strength of the films. Polysorbate-20 caused the blackening of the silver electrode that is sputtered on it. Initially, the color change suggested oxidation of the silver electrode. On the contrary, Polysorbate-20 is a reducing agent and undergoes self-oxidation. Polysorbate-20 and 80 are used as reducing agents to reduce silver salts to silver metal nanoparticles. [103] The possibility of silver metal getting oxidized by Polysorbate-20 is therefore excluded and Polysorbate-20 may rather work as protective sacrificial layer. A 1 wt. % solution of Polysorbate-20 has an interfacial tension of 2 mJ/m^2 with oil and a surface tension of 34 mJ/m^2. [104] Polysorbate-20 is obtained from Sigma-Aldrich, USA for 397 DKK per kg. The amount of Polysorbate-20 required is 3.5 g/m^2 of the

surface area of carrier web (real surface area, including corrugations), which translates to 1.4 DKK/m^2. The calculations are made considering a 50 % wastage of the surfactant since there is a

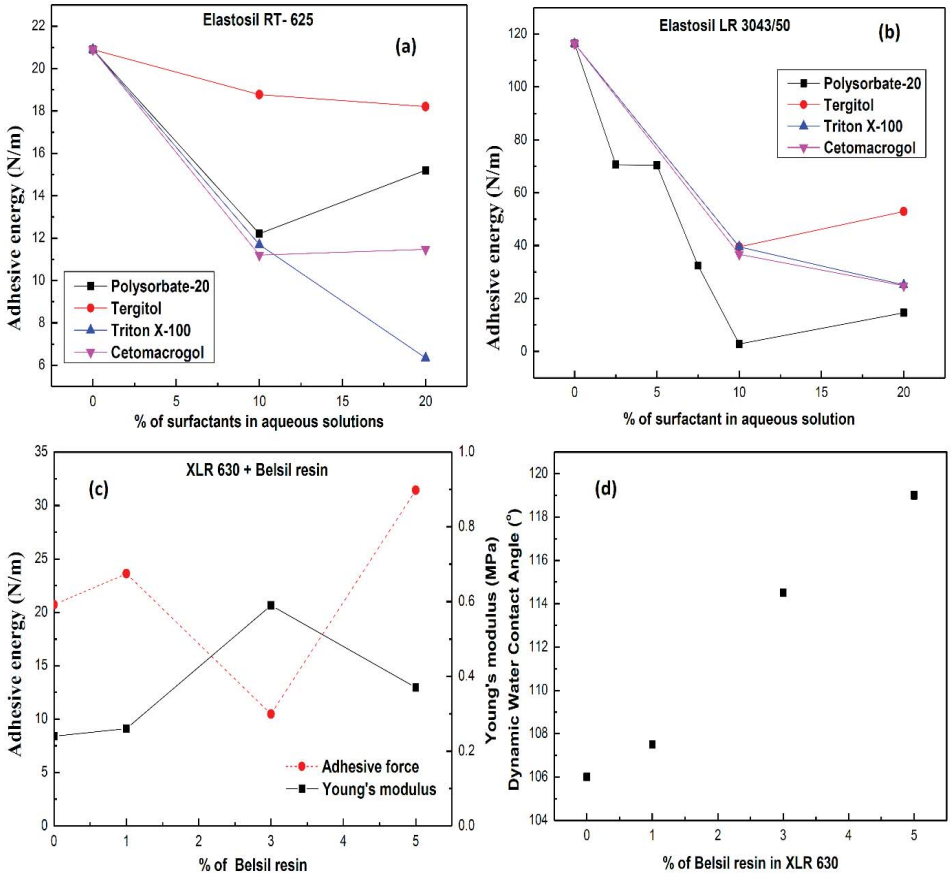

Figure 3.6: **a)** Adhesive energy between Elastosil RT 625 film and the carrier web coated with various surfactants, **b)** Adhesive energy between Elastosil LR3043/50 film and the carrier web coated with various surfactants, **c)** Adhesive energy between XLR 630 film with varying concentrations of Belsil resin and the carrier web and **d)** Effect of Belsil TMS 803 on the XLR 630 water contact angle

loss during the application and evaporation process. The use of Polysorbate-20 is therefore a cheap and environmentally friendly alternative as opposed to fluorinated elastomers and liners. In comparison to Belsil resin, Polysorbate-20 is a cheaper alternative and it doesn't interfere with the crosslinking reaction.

3.6.Conclusions

Akuta detergent reduced the adhesive energy to 14.9 N/m, but it had a corrosive effect on the films and decreased the breakdown strength of the films. It is therefore not suitable to be a release agent.

The Belsil resin at 3 wt. % concentration reduced the adhesive energy to 10.5 N/m and had a negative influence on the breakdown strength of the XLR630 films. Hence, this method will compromise the quality of the DEAP films.

The adhesive energy between the film and the carrier web is the lowest (2.8 N/m) with a 10 wt. % Polysorbate-20 solution. Also, Polysorbate-20 does not interfere with the breakdown of the films unlike Akuta or Belsil resin. Using Polysorbate-20 is the best and the most economical method for easy release of very thin polydimethylsiloxane films from microstructured carrier webs in the current manufacturing process set up.

4.Hot embossing as an alternate process for manufacturing microstructured thin PDMS films

In this chapter an alternate process for producing a micro corrugated PDMS film is explained. This alternate process uses hot embossing to impart the corrugation pattern to the films, eliminating the use of carrier web substrate and thereby decreasing the release problems. From the experiments conducted in our lab it is shown that vinyl terminated PDMS elastomers undergoing high temperature hydrosilylation reaction exhibit the unique property to retain an imprint made on them at the GP. This property is what makes hot embossing possible. To our knowledge no known technologies or processes are commercially available for embossing microstructures and sub-micron structures on elastomers like silicones in large scale production of films. The predominantly used technologies to make microscale components for micro fluidic devices and microstructures on PDMS elastomer is 1) reaction injection molding 2) UV lithography and 3) photolithography. Hot embossing is one of the simplest, most cost-effective and time saving methods for replicating structures. The work discussed in this chapter has been published in Journal of Elastomers and Plastics, volume 46(7), pages 623-643 (2014) and is attached as Appendix III. Further work is published in another paper in the same journal, doi: 10.1177/0095244314526743 (2014) and is attached as Appendix IV.

4.1.Hot embossing a silicone elastomer

Replication of components and structures in macro, micro, sub-micron and nano-scale is not new to the polymer industry. Mass-fabrication of a lot of components and products in the consumer industry has been made possible by replication technologies. Replication of macro-scale components and structures have been done for many years with well-established processes like the 1) injection molding 2) injection compression molding 3) compression molding 4) thermoforming and 5) blow molding or extrusion process for a variety of thermoplasts and thermosets. [105, 106] A large variety of polymers can be processed with these methods, comprising a wide range of thermal and mechanical properties. All of these methods are highly automated and optimized. With the already established macroscopic replication process, microscale replications can also be performed.

For replication of microstructures in thermoplasts, thermosets and UV-curable polymers the processes are 1) micro reaction injection molding 2) micro injection molding 3) micro injection compression molding 4) micro hot embossing 5) micro thermoforming and 6) nano-imprint lithography. The reaction injection molding process technology is available for a few elastomers apart from the thermosets and thermoplasts. It is being used to process LSRs which are two component pumpable silicone materials that are mixed and rapidly heat-cured to form elastomeric components. In this process, LSR is injected into the mixer at the prescribed amounts and mixed, which are then injected into the mold under pressure where the mix cures (at elevated temperatures) and gives the product of required shape and structure. Hot embossing and micro/nano printing undergo constant development depending on the requirements, materials and constraints of a particular product. [105, 107] Limitations such as structure size, molding area, complexity of structures, material properties and process times make the processes even more complex. The hot embossing process that is usually used in industry for thermoplasts is shown in Figure 4.1. The polymer in the form of a thin film is heated up to the melting range by conduction. Then the film is compressed to fill the micro cavities of the mold and then the polymer film is cooled and demolded. The force applied on the film into the mold is optimized, regulated and controlled. This serves an inspiration for the following experiments of embossing microstructures on addition curing PDMS films.

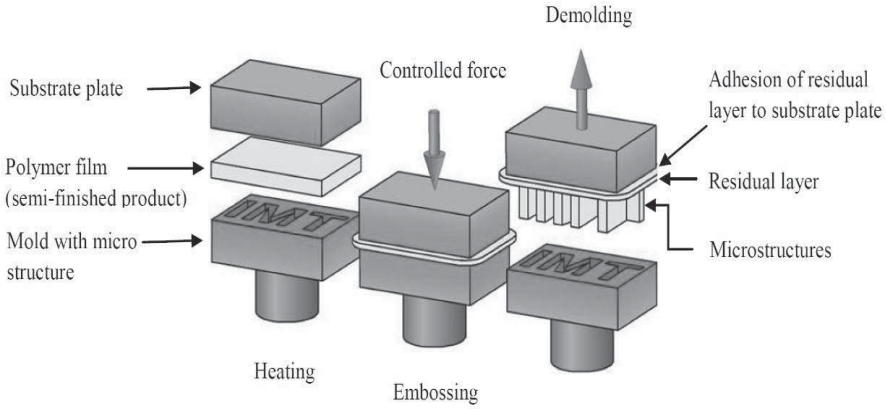

Figure 4.1: Schematic representation of a typical hot embossing process for thermoplasts [105]

4.2.Experimental

The materials and instruments used in the experiments have been listed below.

4.2.1.Materials

The silicone networks used for the hot embossing process are as follows.

1) DMS V35 (vinyl terminated PDMS) (M_w = 49500 g·mol^{-1}) from Gelest Inc, USA. + crosslinker, tetrakis(dimethylsiloxy)silane (SIT7278.0) (M_w = 328 g·mol^{-1}) for platinum cure of 2-component RTV from Gelest Inc, USA + catalyst, platinum cyclovinylmethyl-siloxane complex (511) is supplied by Hanse Chemie AG, Germany.

2) Elastosil RT 625, oil and inhibitor. (Refer to section 2.5.1. for product information)

3) Silastic LC-50-2004, an LSR and OS-20, an ozone-safe volatile methylsiloxane (VMS) fluid are obtained from Dow Corning, USA. It is supplied as premixes A and B. Silastic A contains the vinyl terminated PDMS and catalyst and Silastic B contains the vinyl terminated PDMS and crosslinker.

4.2.2.Instrumentation

Rheological experiments

Refer to section 2.5.2.

Aluminum roller

Initially, an embossing roller made of PVC (polyvinyl chloride) is used for embossing. A sheet of the carrier web with microstructure is fixed to the roller, which would impart the structure to the films. However, this roller could not be heated and hence embossing with a PVC roll is not possible. Later, an aluminum roller is employed as it could be heated (Figure 4.2). Since the roller is operated with hands, the force on the roller could not be controlled and it varied with every operation. The weight of the aluminum roller is 3 kg, to which an additional human pressure is also added on. So the exact pressure is unknown and dependent on the operator.

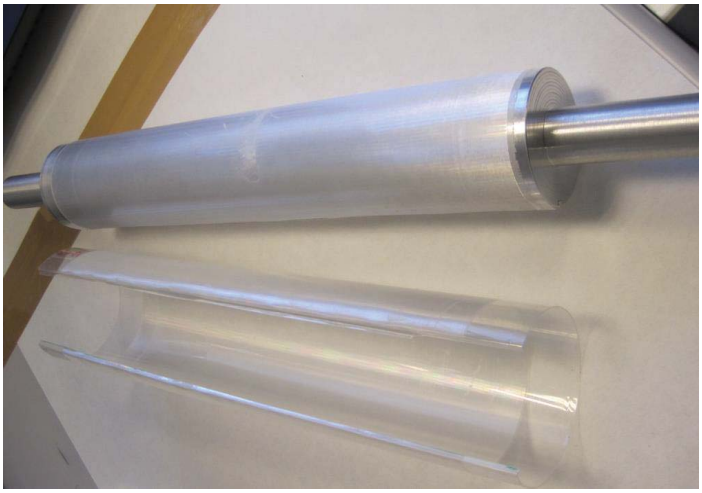

Figure 4.2: Aluminum embossing roller with a piece of the carrier web ready to be fixed

Gravure roll coater

In order to completely control the pressure and speed of the embossing an offset Gravure Lab Coater, 24" wide, Model#E-BC12POG3 (Euclid Coating Systems Inc., USA) is used for embossing (Figure 4.3). The diameter of the rolls is 6". With this instrument, the force applied and the speed of the rolls can be regulated. The coater is modified to suit the embossing process. To heat the rolls to a desired temperature, infra-red lamps are placed above the top roll and below the bottom roll. Each infra-red lamp has two bulbs. A laser gun thermometer is used to check the temperature of the rolls. When the rolls are heated up to the required temperature, one bulb in each lamp is switched off to maintain the temperature and to prevent the rolls from heating further. The top roll of the coater is fixed with a down-web (Refer to section 1.2.2. in chapter 1). It is to be noted that the period of corrugation peaks are 10 μm and the depth is 4 μm.

4.3.Procedure

A step by step procedure for the hot embossing process is illustrated below.

4.3.1.Preparation of the elastomer mixture

The procedure for making the addition curable PDMS network is different for each material used. In the following section the details of the different recipes are given.

DMS V35: Two premixes A and B are made by mixing half of the required amount of DMS-V35 with the crosslinker, and the other half of DMS-V35 with the platinum catalyst separately by using a Speed mixer DAC 150FVZ-K (Synergy Devices Ltd., UK). [107] The two parts are stored separately to avoid curing and are not mixed until the films have to be made. [107] When premixes A and B are mixed in the ratio 1:1 using speed mixer (2 min @ 2000rpm) the three components PDMS, catalyst and crosslinker are homogeneously distributed and the hydrosilation reaction

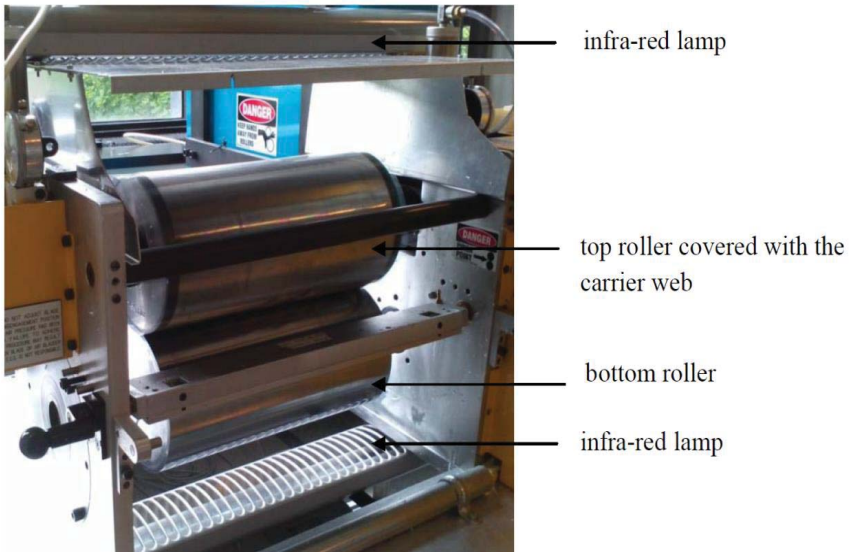

Figure 4.3: Gravure lab coater used for embossing

proceeds uniformly. The premixes are made such that in the final mixture, the ratio of the number of hydride groups in crosslinker (4 hydrides/molecule) is equal to the number of the vinyl groups in V35 (2 vinyl groups/molecule). The stoichiometric imbalance (*r*) is calculated from the equation (4.1) and for the applied mixture *r*=1. [108] However, usually slightly higher values of *r* give the strongest networks. [109] The crosslinking reaction taking place between the reactive groups of the linear vinyl-terminated PDMS and 4-functional (4*f*) crosslinkers (i.e. vinyl (─CH=CH_2) and hydride (─Si─H)) is presented in Figure 1.6.

$$r = \frac{f}{2} \times \frac{M_{PDMS}}{M_{crosslinker}} \times \frac{m_{crosslinker}}{m_{PDMS}} \tag{4.1}$$

In equation (4.1) f is the functionality of the crosslinker, M_{PDMS} is the molecular weight of PDMS, $M_{crosslinker}$ is the molecular weight of crosslinker, $m_{crosslinker}$ is the mass of crosslinker in our mixture, m_{PDMS} is the mass of PDMS polymer in our mixture.

Elastosil RT625: Refer to section 3.4.2. for the mixing procedure of Elastosil RT 625.

Silastic LC-50-2004: Silastic LC-50-2004 premixes A and B are mixed in the prescribed ratio of 1:1 using the speed mixer for 2 min at 2000 rpm. The solvent OS20 is mixed with Silastic in different proportions to reduce the viscosity and thereby ease the processing and initial coating of the films.

***4.3.2.Rheological measurements**:*

The GP of the silicone network should be investigated before proceeding to embossing process. The time and temperature required to reach GP determines the preheating conditions of the embossing process. The LVE measurements during the crosslinking of the stoichiometrically balanced samples 1) DMS V35 (*r*=1, Pt=1.6 ppm), 2) Elastosil (A:B=9:1) + 15 wt. % silicone oil

+ 0.8 wt. % inhibitor and 3) Silastic (A:B=1:1) + 10 wt. % of OS20, at temperatures 80 ^{o}C, 60 ^{o}C and 40 ^{o}C are performed at a controlled strain mode with 2 % strain which is within the linear regime of the material based on an initial strain sweep test and in a frequency range from 100 Hz to 0.01 Hz.

4.3.3.Film preparation

Once the elastomer mixtures are ready, films are made using a 3540 bird film applicator, (Elcometer, Germany) on a PETE (polyethylene terephthalate) substrate.

4.3.4.Preheating the film

The films made on the PETE substrate are preheated prior to the embossing till the addition curing proceeds to the GP. The time and temperature for preheating is fixed based on the GP estimated by rheological experiments. Pre-heating the films in oven rendered films with fully cured surfaces since free surfaces cured faster than the bulk of the film. Such films cannot be embossed. Therefore, preheating in an oven is ruled out. In contrast, a hot plate heats up the film from the bottom, and thereby the film cures from below and the free surface for embossing is still around GP. The hot plate used is an IKA*C.MAG HS7 (IKA, Germany). It is found that homogenous heat transfer is not possible with a hot plate as the substrate did not have good contact with hot plate. Later, the films on the PETE substrate are preheated on a hot steel roll with a smooth surface which gave sufficient contact area and hence large and homogeneous heat transfer. Hot steel roll is therefore used for preheating the films.

4.3.5.Embossing

With aluminum roller:

The films preheated to GP are immediately embossed with the aluminum roll which is covered with the carrier web (Figure 4.4). The aluminum roller is also heated in the oven prior to embossing. The force applied on the film by the roll imprints the corrugations lines on the film and the temperature of the roll ensures that the film cures and retains the microstructure. The temperature to which the embossing roll is heated depends on the material used.

With gravure roll coater:

The films which are preheated on a steel roller until they reach GP (Figure 4.5) are immediately embossed using the gravure lab coater. The top roll of the coater is covered with the 30 % down carrier web and hence the top roll acts as the embosser. Both the top and bottom rolls are heated using IR-lamps to a preferred temperature. The temperature of embossing depends on the type of PDMS used. The speed of the rollers and the pressure between the rollers (pressure on the film) is adjusted to give the best results.

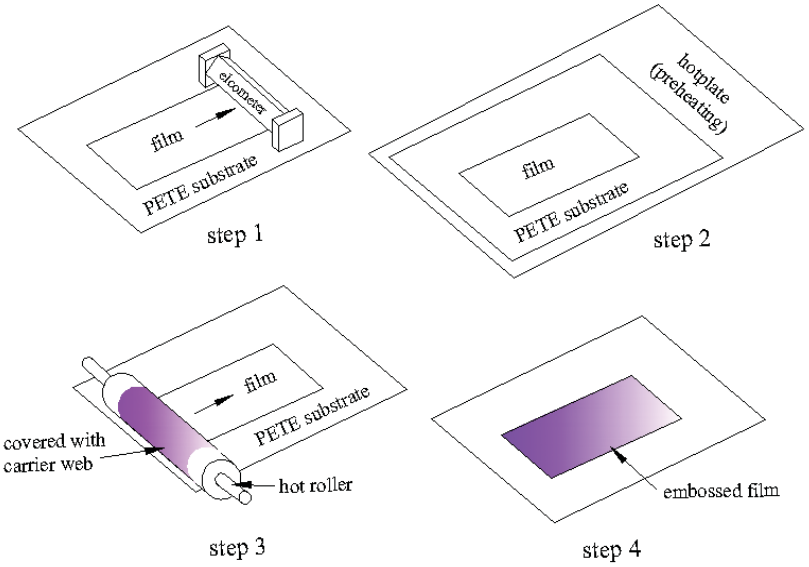

Figure 4.4: Schematic representation of the hot embossing process with the aluminum roller

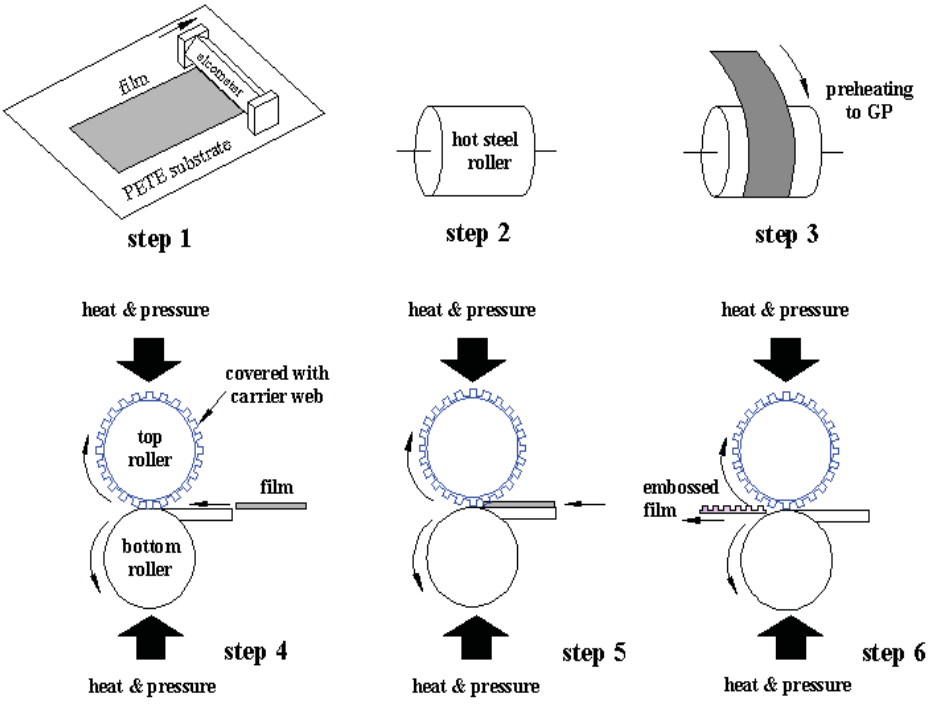

Figure 4.5: Schematic representation of hot embossing process with the gravure lab coater

4.3.6.Complete curing

The films which are embossed are left to cure completely upon heating in an oven. The temperature and time of curing depends on the material used.

4.4.Gel point, developing elasticity and onset of embossing

After the onset of the hydrosilation reaction, the PDMS network approaches chemical gelation, which is a phenomenon by which a crosslinking polymeric material undergoes a phase transition from liquid to solid state. [110] A crosslinking polymeric system is said to reach its GP at a critical extent of the crosslinking reaction at which either the weight average molecular weight diverges to infinity (infinite sample size) or the first macromolecular cluster extends across the entire sample (finite sample size). [110, 81] Thus at the GP, a thermosetting polymer system is transformed from a viscoelastic liquid to a viscoelastic solid by the introduction of chemical crosslinks creating a three dimensional network. There is a dispute as to whether the GP occurs at the crosspoint of the G' and G" in a LVE. [81, 82, 83] There is one class of polymers only for which the GP coincides with the crossover point. These are the polymers which have a power law relaxation upon reaching the GP ($G(t) \sim t^{-n}$), with a specific exponent value $n = \frac{1}{2}$. [82] Stoichiometrically balanced polymer networks or networks with excess crosslinker at temperatures much higher than their glass transition temperature show such behaviour and hence have a GP that coincides with crossover point of G' and G". [82] Though power law relaxation is the norm for polymers at GP, not all of them have the exponent value of $n = \frac{1}{2}$. The polymers which have an exponent value $n \neq \frac{1}{2}$ will have a crossover point either before the actual GP ($n < \frac{1}{2}$) or after the actual GP ($n > \frac{1}{2}$). So, the crossover point cannot be used to detect the GP in such cases. [82]

Since we study the LVE model of a stoichiometrically balanced V35 system, where gelation is caused by end-linking reaction of primary chains, the GP occurs at the crossover point of the storage (G') and loss modulii (G"). In the case of the commercial RTV silicone Elastosil RT-625 and the commercial LSR Silastic LC-50-2004 the crossover of G' and G" will be used as the GP, assuming that they are stoichiometrically balanced. Beyond the GP the elasticity increases steadily with increasing crosslinking density. Knowledge of the GP is essential to design the embossing experiments. The higher the temperature, the quicker is the transition from visco-elastic liquid to solid and the less time required to reach GP. The embossing should be started at the GP in hot embossing because the hydrosilation reaction is much faster at high temperatures and the window for embossing at GP is reduced to a few seconds. At room temperature the reaction rates are much slower and there is a space of 10-15 min after the GP, at which embossing can be done.

4.5.Results and discussion

The results of the experiments are discussed as follows.

4.5.1.Rheological measurements

In Figure 4.6 a, the curing profile of V35 at 40 ºC can be seen. The system doesn't contain fillers, so the crossover is very clear as G' << G'' in the beginning of the curing process. The same behavior is observed at 60 ºC and 80 ºC as well with the increase in reaction speed being the only difference. The curing profile for Elastosil at 80 ºC is shown in Figure 4.6 b. The crossover happens early in the curing process due to the presence of reinforcing particles in the commercial mixture. Curing profiles for Silastic at 80 ºC and 40 ºC can be seen in Figure 4.7. At 80 ºC Silastic shows

similar curing behavior as Elastosil. For the Silastic at 40 ºC, there are three crosspoints, which are completely reproducible crossovers. First crosspoint is 10 min, second is 69 min and third is 265 min. The three crosspoints are likely to arise due to the competing effect of reaction and solvent evaporation. The Silastic is highly viscous and just a small extent of reaction causes G' to increase. The first two crossovers are due to these competing phenomena and the third crossover is regarded as the true GP, which is further supported by $\frac{\partial G'}{dt}$ being strongest at this point. Table 4.1 shows the GPs of the three materials at 40 ºC, 60 ºC and 80 ºC. Figure 4.8 shows the storage and loss moduli G' and G" of V35, Elastosil and Silastic films as a function of the applied frequency at 23 °C. Silastic film has the highest modulus, which means it is harder than the other two films, with V35 being the softest.

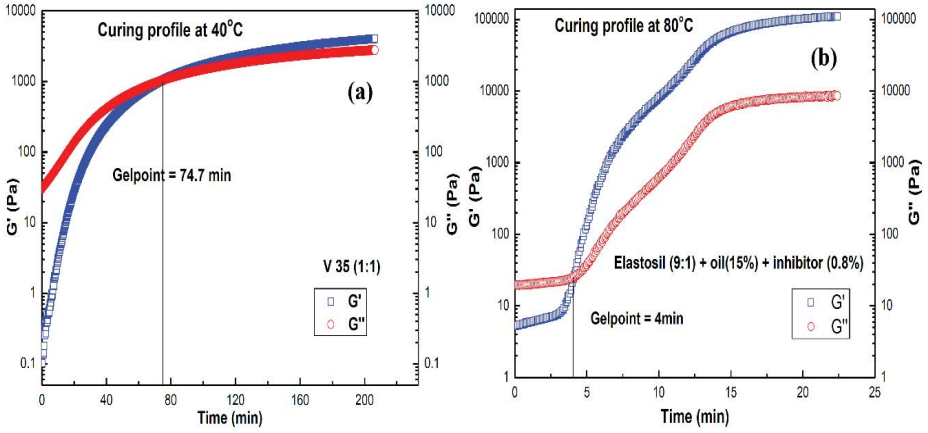

Figure 4.6: **a)** Curing profile of DMS V35 at 40 ºC shows GP at 74.7 min and **b)** Curing profile of Elastosil at 80 ºC shows GP is at 4.0 min

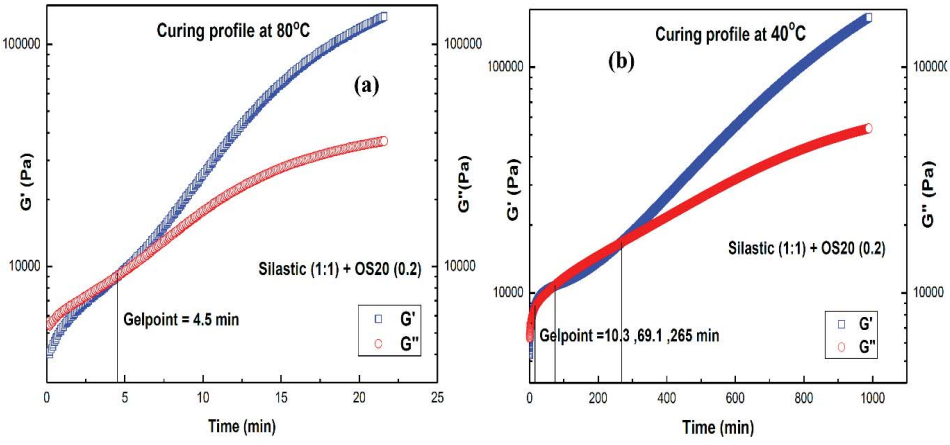

Figure 4.7: **a)** Curing profile of Silastic at 80 ºC shows GP is at 4.5 min and **b)** Curing profile of Silastic at 40 ºC shows GPs at 10.3, 69.1 and 265 min

Table 4.1: Gel points at various temperatures

No.	Temperature	V35	Elastosil	Silastic
1	40 ºC	74.7 min	192 min	10.3 min (first), 69.1 min (second) and 265 min (third)
2	60 ºC	16 min	30.2 min	5.9 min
3	80 ºC	15.8 min	4.0 min	4.5 min

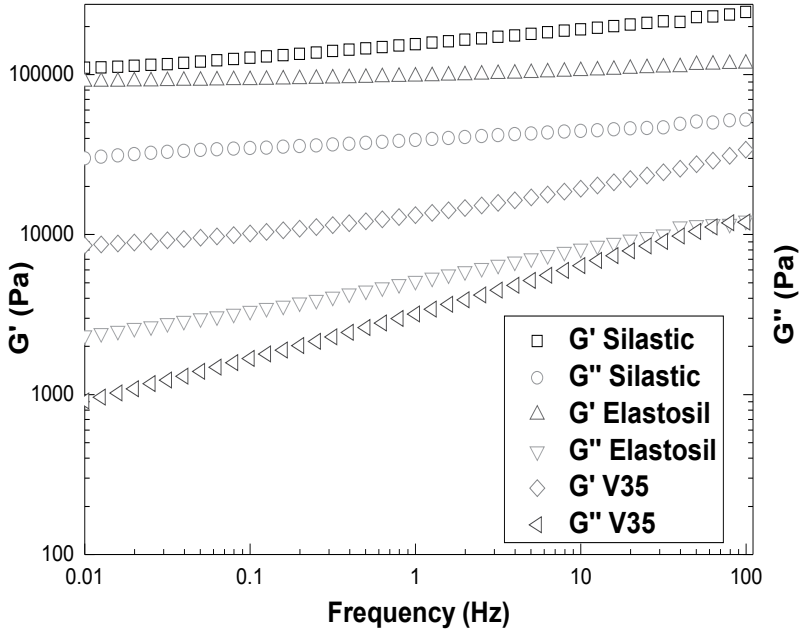

Figure 4.8: Comparison of the frequency sweeps of V35, Elastosil, and Silastic at 23 ºC

4.5.2. Requirements of the embossing process

From the many trials and errors of the embossing process, the most required conditions of embossing process can be established as shown in Figure 4.9.

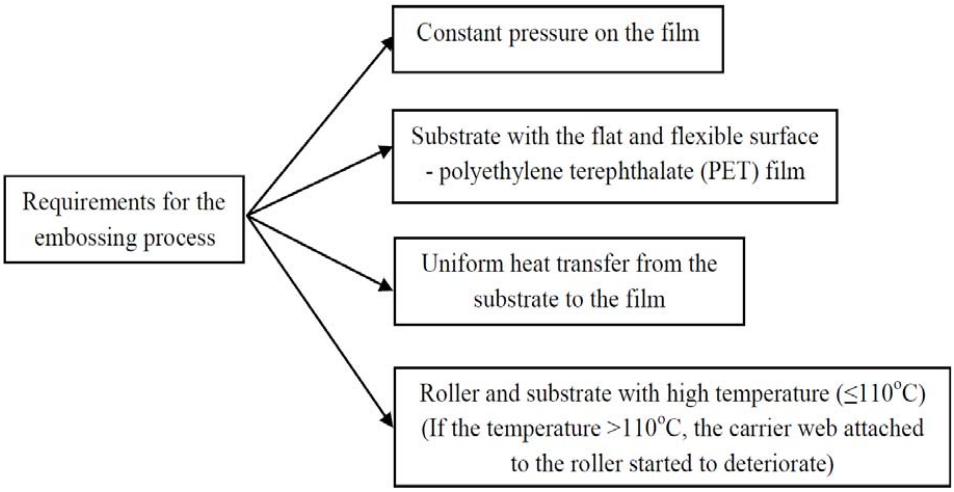

Figure 4.9: Requirements for the embossing process

4.5.3. Conditions of embossing process

The PVC embossing roller failed to work as it could not be heated. The optimum conditions for embossing by the two methods 1) using an aluminum roller and 2) using the Euclid coater are investigated. At 80 °C both Elastosil and Silastic have a GP around 4 min (Refer to Table 4.1). V35 has a GP around 16 min at 80 °C. Thus, to emboss the mixtures at 80 °C, the film still needs 5 minutes (for Elastosil and Silastic) and 16 min (for V35) to develop sufficient elasticity. To further decrease this 'development time' the temperature is increased. When preheated at 110 °C approximately 5-15 s is sufficient for Elastosil, Silastic and V35 to reach GP and embossing can be done on the films.

Aluminum roll method: The V35 film of 500 µm thickness embossed with aluminum roller at 110 °C (15 s to GP) gave the best embossing. The Elastosil film of 100 µm thickness embossed with aluminum roller at 110 °C (5 s to GP) gave best embossing. For the Silastic film of 50 µm thickness embossed with aluminum roller at 110 °C (10 s to GP) gave best embossing. The results are tabulated in Table 4.2.

Table 4.2: Embossing conditions for aluminum roll method

No.	Material	Thickness of the film (µm)	Preheating temperature & time
1	V35	500	Roller (110 °C), 15 s
2	Elastosil	100	Roller (110 °C), 5 s
3	SILASTIC LC-50-2004	50	Roller (110 °C), 10 s

Gravure roll coater method: The V35 film of 500 µm thickness embossed with coater at 110 ºC (15 s to GP) with a pressure of 30 psi and roller speed of 1.4 rpm gave the best results. Elastosil film of 100 µm thickness embossed with coater at 110 ºC (5 s to GP) with a pressure of 25 psi and roller speed of 1.4 rpm (0.0112 m/s) gave the best results. Silastic film of 100 µm thickness embossed with coater at 110 ºC (10-12 s to GP) with a pressure of 20 psi and roller speed of 1.4 rpm gave the best embossing. Table 4.3 briefs these conditions. Figures 4.10, 4.11 and 4.12 show the microscope pictures of the embossed V35, Elastosil and Silastic films with the best embossing results.

Figure 4.10 shows the microscope images of embossed V35 film of thickness 500 µm. It is embossed with a 30 % piece of down carrier web with period of 10 µm and height of 4 µm. The V35 film corrugations measured a period ~ 12.5 µm and height ~ 2.9 µm. This indicated that when the V35 film is peeled off, it did not recover its original shape, as it is highly viscoelastic. Assuming a 25 % strain from the period differences, one would expect reduction of height down to 3 µm. Even after waiting long enough time, it did not recover its original shape.

Figure 4.11 shows the microscope images of embossed Elastosil film of thickness 100 µm. It is embossed with a 30 % piece of down carrier web of period 10 µm and height 4 µm. The elastosil film corrugations measured a period ~ 9.8 µm and height ~ 3.5 µm, which is ~ 80 % replication of carrier web dimensions.

Figure 4.12 shows the microscope images of embossed Silastic film of thickness 100 µm. It is embossed with a 30 % piece of down carrier web of period 10 µm and height 4 µm. The Silastic film corrugations measured a period ~ 10 µm and height ~ 4 µm, which is ~ 100 % replication of carrier web dimensions. The results of the hot embossing by gravure lab coater are tabulated in Table 4.3.

Table 4.3: Embossing conditions for gravure roll coater method

No.	Material	Preheated on	Preheat temperature (ºC) & time of films	Film (µm)	Roller speed (rpm)	Roller pressure (psi)	Comments
1	V35	Steel roller	110 (15 s)	500	1.40	30	Films are at GP and are embossed fully.
2	Elastosil	Steel roller	110 (3 s)	100	1.40	25	Film did not reach GP and it stuck to the roller while embossing.
3	Elastosil	Steel roller	110 (5 s)	100	1.40	25	Films are at GP and are embossed fully.
4	Silastic	Hot plate	150 (10 s)	100	1.40	20	The methyl-acrylate coating (the layer carrying the microstructure) on carrier web bonded with Silastic, and came off with the film.

5	Silastic	Hot plate	110 (10 s)	100	1.40	20	Film did not reach GP and it stuck to the roller while embossing.
6	Silastic	Steel roller	110 (10 s)	100	1.40	20	Films are at GP and are embossed fully.
7	Silastic	Steel roller	110 (10 s)	100	1.40	25	Film did not reach GP and it stuck to the roller while embossing. 'Island formation' (Figure 4.15) is seen
7	Silastic	Steel roller	110 (10 s)	100	1.85	20	Corrugation is not deep enough on the embossed film.
8	Silastic	Steel roller	110 (10 s)	100	1.85	30	Due to high embossing pressure, film partly stuck on the web though it is at GP.

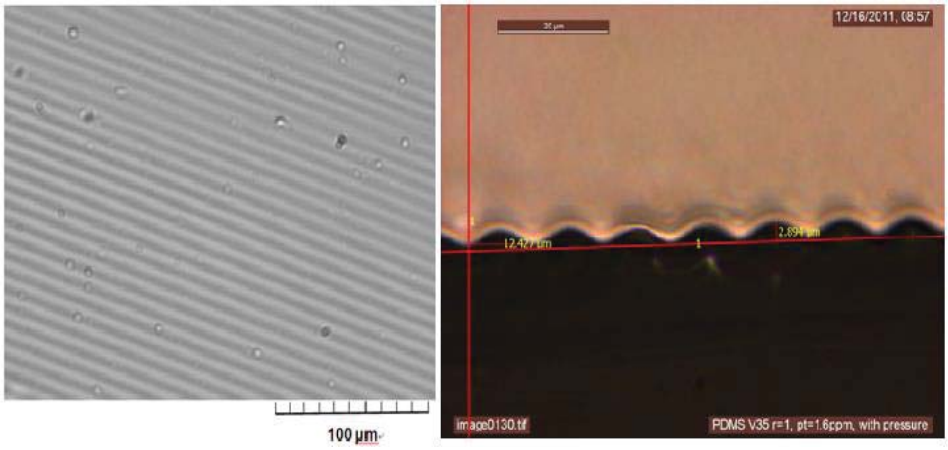

Figure 4.10: Microscopic images of embossed V35 film (No. 1 in Table 4.3)

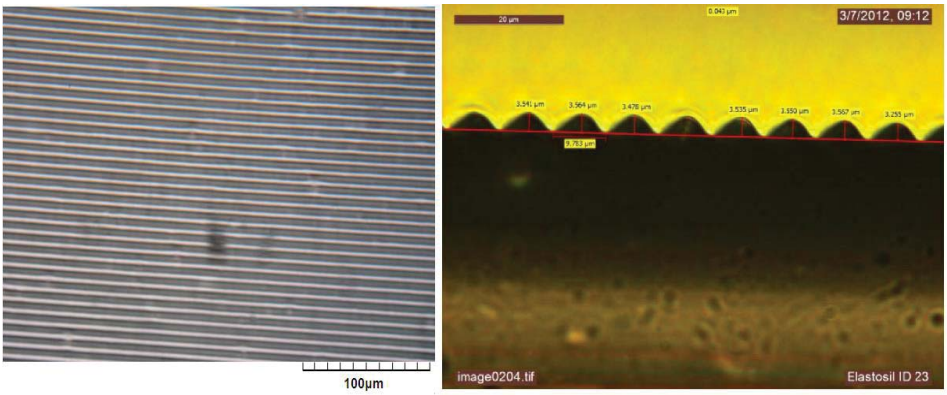

Figure 4.11: Microscopic images of embossed Elastosil film (No. 3 in Table 4.3)

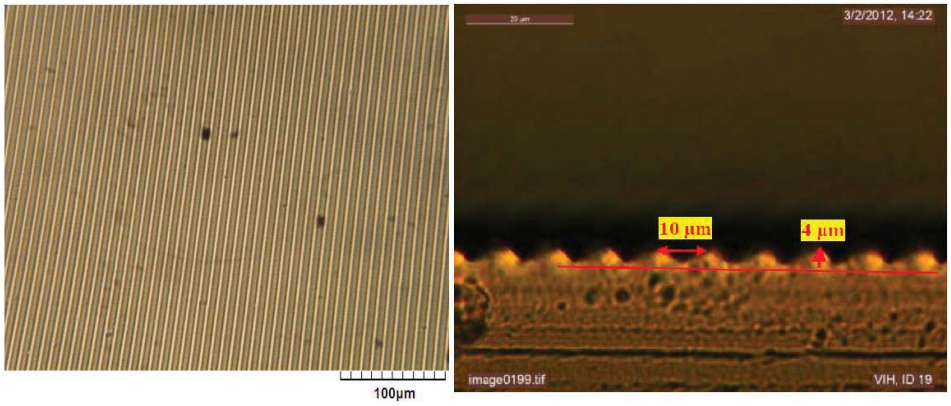

Figure 4.12: Microscopic images of embossed Silastic film (No. 6 in Table 4.3)

4.5.4. Time window for hot embossing

There are two vital factors for designing the embossing experiments

1) Time to reach GP
2) The time window (around GP) at which the embossing can be performed.

As the temperature of pre-heating and embossing increases (40 ºC, 60 ºC and 80 ºC), the time taken to reach GP and the time window for embossing decreases. At 80 ºC the time available for embossing is still around a few minutes after GP. To quicken the embossing process, time sweeps of the samples are performed at 110 ºC. At 110 ºC the time to reach GP and the time window for embossing is around a few seconds. For industrial processes smaller time windows are preferred, as the production is quicker. In Figure 4.13 the time window of the embossing process, using the Euclid gravure lab coater for all three materials at 110 ºC is shown. Figure 4.13 shows a plot of G'/G'(final) against the time at which preheating is started, followed by embossing. The ratio G'/G' (final) is used instead of G', in order to make the data comparable (Table 4.4). The pressure used varies with the material and is indicated in Figure 4.13 and the speed of the roller is 1.4 rpm. In Figure 4.14, the process window for embossing Elastosil RT 625 is shown.

Table 4.4: Time window for hot embossing at 110ºC

No.	Material	GP (s)	G'(@GP)/ G'(final)	G'(initial)/G'(final)	G'(final) in Pa
1	V35	15	0.089	0.013935	9049
2	Elastosil	5	0.0008	0.000056	213500
3	Silastic	10	0.047	0.0102	44570

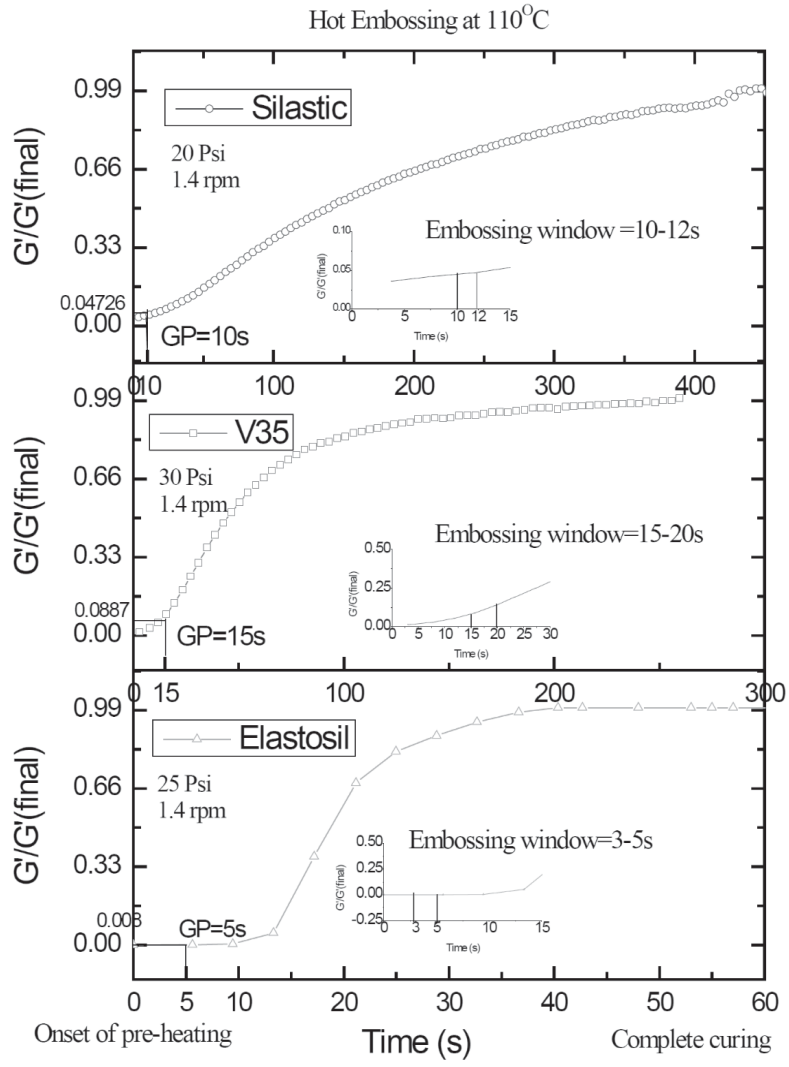

Figure 4.13: Time window for embossing at 110 ºC

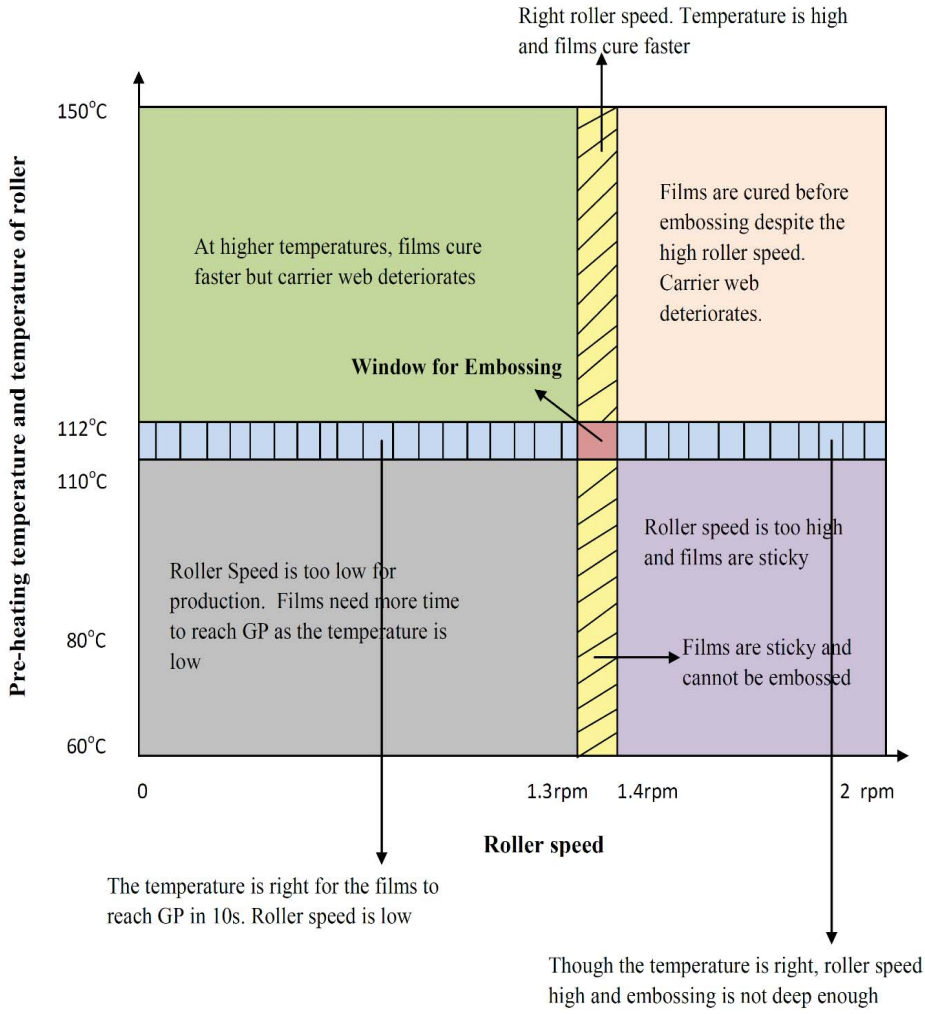

Figure 4.14: Process window for embossing Elastosil RT 625 at 25 psi roller pressure, preheated for 5 s

4.5.5.Problems with embossing

Pre-heating the polymer film made on the substrate is a very important step in the embossing process. The film needs to be pre-heated uniformly. To ensure uniform heating the film needs to be in good contact with the hot plate. The surface of the hot plate has to be very smooth and should be made of a metal which is a very good conductor and dissipater of heat like steel, copper or aluminum. If the film is not heated uniformly, three cases can happen.

1) Regions of the film which are not in contact with hot plate will not reach the GP,

2) Regions of the film which are in good contact would reach GP or,

3) Some regions of film would have cured completely due to prolonged preheating.

The uncured parts of the film stuck to the embossing roller and the fully cured regions of the film did not have any embossing on them as they have hardened fully. The regions which are at GP would have embossing. This results in island-like structures on the film (as seen in Figure 4.15).

Figure 4.15: Island formation during embossing process due to non-uniform heating

4.6.Hot embossing with nickel stamp on LSRs composites

Two modifications are now introduced to the above hot embossing process i.e., 1) a nickel stamp embosser and 2) LSR with fillers.

4.6.1.Nickel embosser

The primary focus is to make a metal mold with engraved corrugation pattern on it. The corrugation pattern from a 30 % carrier web is transferred on to a nickel plate by sputtering a thin layer of metal on carrier web and then plated with nickel electrochemically. It has been verified that the structures have been transferred to nickel by visual inspection (light diffraction on surface) and by confocal microscopy shown in Figure 4.16. The plate is made of a nickel-vanadium alloy (93 % Ni, 7 % V). The thickness of the plate is 237 μm (Figure 4.16). The nickel plate does not inhibit the addition curing of the films. Films cured on nickel plate are shown in Figure 4.17 which prove that nickel plate does not inhibit the curing of the elastomer films. The microstructured nickel plate is used as the embosser instead of a roll with carrier web wrapped on it. Hot embossing with nickel plate is performed on a simple device which can press under controlled pressure.

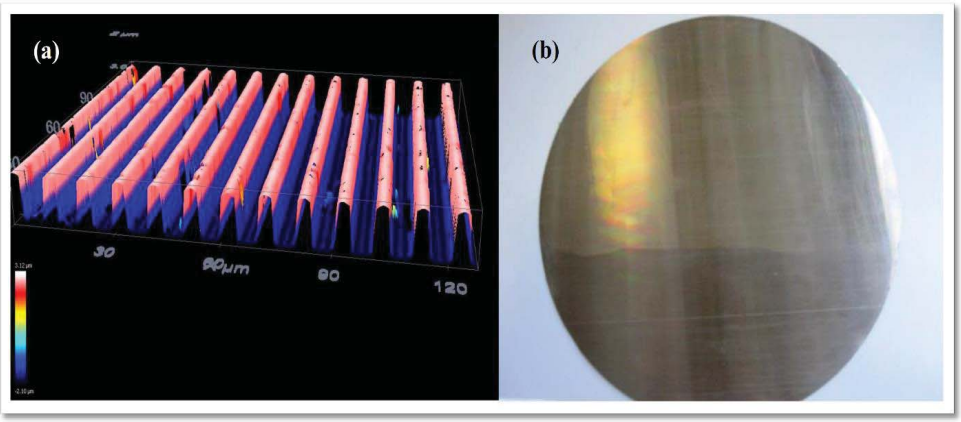

Figure 4.16: **a)** Confocal microscopic image of the corrugated nickel plate and **b)** Nickel plate (thickness = 237 µm) with microstructure (corrugation: period = 10 µm, depth = 5 µm) used for embossing

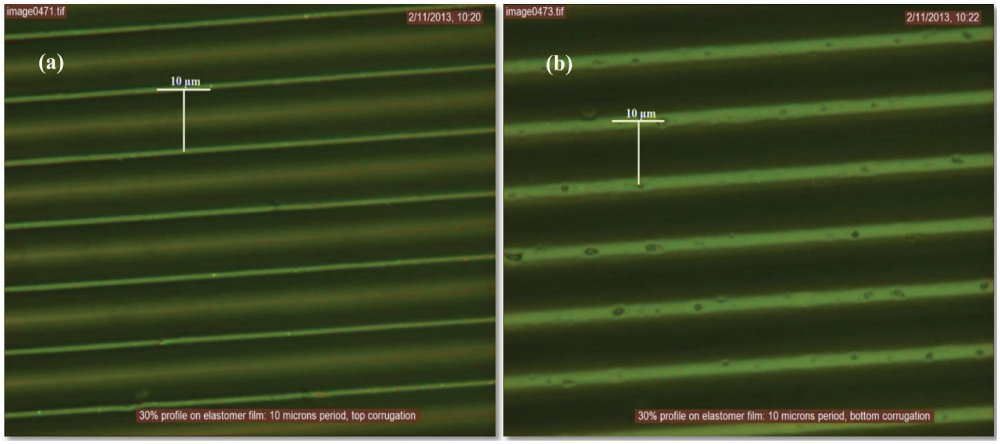

Figure 4.17: Microstructures replicated on the silicone film cured on nickel plate. **a)** top corrugation and **b)** bottom corrugation

4.6.2.LSR composites

LSR formulations with different proportions of the filler TiO_2 will be embossed, unlike the previous method where pure RTV silicones and LSRs are embossed. When combined with fillers, the viscosity of the LSR mixtures increases further. Producing thin films (20-40 µm) with highly viscous mixtures is difficult as it is hard to spread the viscous mixtures. In order to prevent the mixtures from getting too viscous and to disperse the fillers efficiently a solvent (OS20) is also used in LSR formulation. Viscosity studies are performed on the various formulations in order to examine if LSR formulations have viscosities permissible by the existing manufacturing constraints.

4.6.3.Material

POWERSIL XLR 630 A/B, a low viscosity LSR is obtained from Wacker Chemie AG, Germany. XLR630 is supplied as two parts A and B. The part A contains PDMS and platinum catalyst, and

part B contains PDMS and crosslinker. The mixing ratio of parts A and B is 1:1. Hydrophobic rutile TiO_2 (Hombitec RM130F) is obtained from Sachtleben Chemie Gmbh, Germany. The primary particle size is 21 ~ 25 nm. OS-20 solvent (an ozone-safe volatile methylsiloxane (VMS) fluid) is obtained from Dow Corning, USA.

4.6.4.Procedure

Varying amounts (0, 5, 10 and 15wt. %) of TiO_2 nanoparticles are mixed into the XLR630 part A and B with solvent OS20 using a Speed Mixer (DAC 150FVZ, Hauschild Co., Germany) at 3500 rpm for 2 min. The mixing is ensured to be homogenous by adding sufficient solvent to allow for higher mobility of the particle/silicone mixtures. The formulations of LSR mixtures are listed in Table 4.5. The uniform mixtures are cast on a temperature-stabilized polyethylene terephthalate (PETE) substrate with a thin film applicator 3540 bird film applicator, Elcometer, Germany. (See step 1 in Figure 4.18)

Table 4.5: Formulations of LSR mixtures

No.	XLR 630 A : XLR630 B : TiO_2 : OS20*
1	50 % : 50 % : 0 % : 0 (phr)
2	47.5 % : 47.5 % : 5 % : 10 (phr)
3	45 % : 45 % : 10 % : 15 (phr)
4	42.5 % : 42.5 % : 15 % : 20 (phr)

*Amounts of XLR 630 and TiO_2 are in mass ratio, OS20 in parts per hundred rubber

The films made on the PETE substrate are preheated prior to the embossing such that the addition curing elastomer proceeds to the GP. The time and temperature for preheating is fixed based on the GP estimated by rheological experiments. [70] (See step 2 in Figure 4.18)

The films that are preheated till they reach GP are immediately embossed with the nickel stamp in between the plates of pneumatic pressure device shown in Figure 4.19. The nickel plate is also heated prior to embossing so that it is around 100 ^oC at the time of embossing. The force applied on the film by the plate imprints the corrugations lines on the film and the temperature of the plate ensures that the film cures and retains the microstructure. The property of the silicone elastomers to retain an imprint made on it at the GP, enables the embossing of microstructures. The applied force between the nickel plate and film is adjusted by the pressure meter as shown in Figure 4.19. (See step 3 in Figure 4.18)

By reducing the pneumatic pressure the plates in the pressure device are separated as shown in Figure 4.18 step 4. The film that is embossed is left to cure completely in the oven at 100 ^oC for 2 min and then is demolded from nickel pate. The demolding step is not as tedious as the delamination process. When the film is peeled as in the conventional process, it is subjected to high peel forces. In demolding step, the film has the support of the substrate when the nickel plate is detached and also their contact time is less to develop any credible adhesive energy between the cured film and the nickel plate. In the continuous embossing roll method there is no demolding/delaminating step, as the film simply moves out continuously from in-between the

rolls. The contact time is very short between the embosser and film and complete wetting of the surface does not happen.

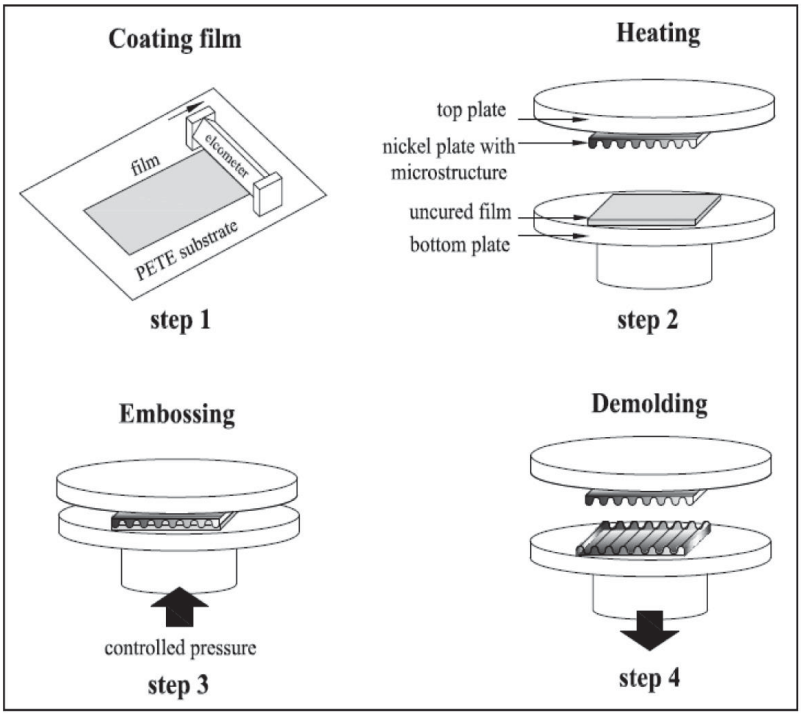

Figure 4.18: Schematic representation of hot embossing process with the corrugated nickel plate

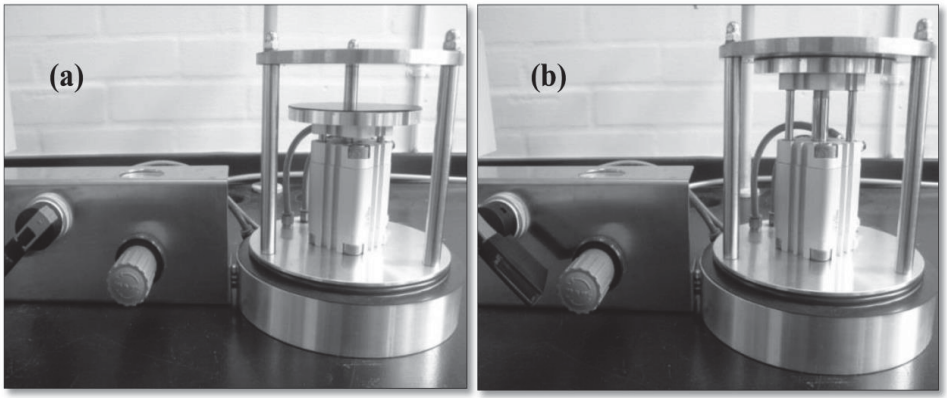

Figure 4.19: Pressure instrument used for embossing **a)** release and **b)** pressurization

4.6.5.Results

The curing profiles of LSR mixtures at 60 ºC and 80 ºC are shown in Figure 4.20. The crossover of storage modulus G' and loss modulus G'' is used as the GP assuming that the commercial elastomer is stoichiometrically balanced or has an excess crosslinker. [81, 82] In addition our elastomer is mixed with TiO_2 filler and the GP may not exactly coincide with the crossover point of G' and G''. However it is a good estimate of the optimal time for embossing, since the filled system has similar rheological behaviour at the GP as the unfilled system. For simplicity, a plot of tan δ = G''/G' is shown in Figure 4.20 and the point at which tan δ reaches the value of 1 indicates the GP (cross point of G' and G''). The GP may not be reached at tan δ = 1 for filled systems but the measure of tan δ = 1 still gives the optimal conditions for embossing. Since the platinum catalyzed hydrosilylation reaction rate increases with temperature, the time to reach GP decreases with the increase of temperate (60 ºC to 80 ºC). [111] The time to reach GP defined as tan δ = 1 also decreases with increasing filler amount (0-15 wt. %) due to hardening effect of the fillers. The curing profiles at 110 ºC are not presented here as the crosspoint (tan δ=1) occurs within a few seconds (15-40 s) and the rheometer takes 30 s to start up and take measurements by which time the material has already cured. The GPs of the mixtures at 110 ºC and the conditions for embossing are presented in Table 4.6.

Table 4.6: Embossing conditions of LSR-filler

No.	XLR 630 A : B : TiO_2 : OS20*	Preheat temperature (ºC)	Preheat time/time to reach GP (s)	Pressure (bar)
1	50 % : 50 %: 0 %: 0 phr	110	35	2
2	47.5 % : 47.5 % : 5 % : 10 phr	110	30	2
3	45 % : 45 % : 10 % : 15 phr	110	22	2
4	42.5 % : 42.5 % : 15 % : 20 phr	110	15	2

*Amounts of XLR 630 and TiO_2 are in mass ratio, OS20 in parts per hundred rubber

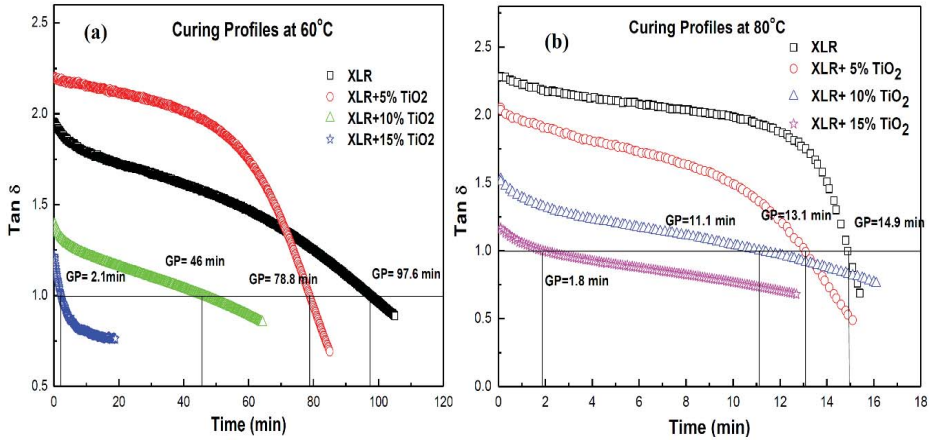

Figure 4.20: **a)** Curing profiles of LSR mixtures at 60 ºC and **b)** Curing profiles of LSR mixtures at 80 ºC

Figure 4.21 (a) shows the dynamic moduli (G' and G'') of the LSR films with TiO_2 nanoparticles as a function of the applied frequency at 23 °C. The storage modulus (G') value increases with increasing filler concentration of the mixtures and so does the loss modulus (G''), which indicates that the inorganic filler leads to the enhancement of the plasticity with reduction of elasticity. The dynamic viscosity curves of LSR formulations are shown in Figure 4.21 (b). The addition of fillers reinforces the mixture viscosity, which results in an increase of the elastic modulus. It is seen that XLR 630 with 15 wt. % TiO_2 and 20 pph OS20 has the highest viscosity of 10,000 Pa·s (0.01 s^{-1}), which is well below the permissible limit. A viscosity below 40,000 Pa·s is preferred in the film manufacture process in order to minimize the energy expenditure on mixing the formulations and spreading them on substrates to make films.

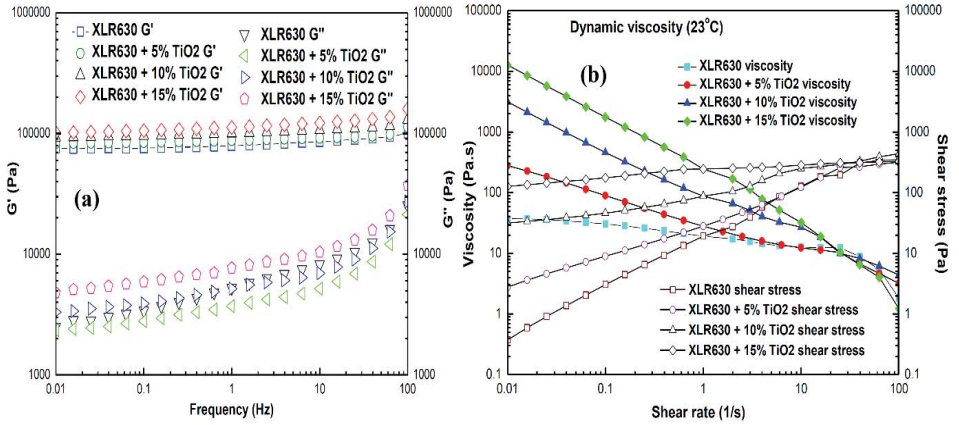

Figure 4.21: **a)** Frequency sweeps of LSR films at 23 ºC and **b)** Dynamic viscosity curves of the LSR mixtures at 23 ºC

Optical characterization of the embossed film is performed using an optical microscope (Leica DMLB, Germany) connected to a Highlight 2000 from Olympus, Tokyo. The microscopic images of cross-section and surface for the LSR films embossed by the nickel plate are shown in Figures 4.22 and 4.23. The corrugation morphologies are the same as the microstructure on the Nickel plate, which means the corrugations are replicated 100 %. Since the images are obtained from an optical microscope, the corrugations are not clearly seen and the dimensions may be subject to an error of ± 10%.

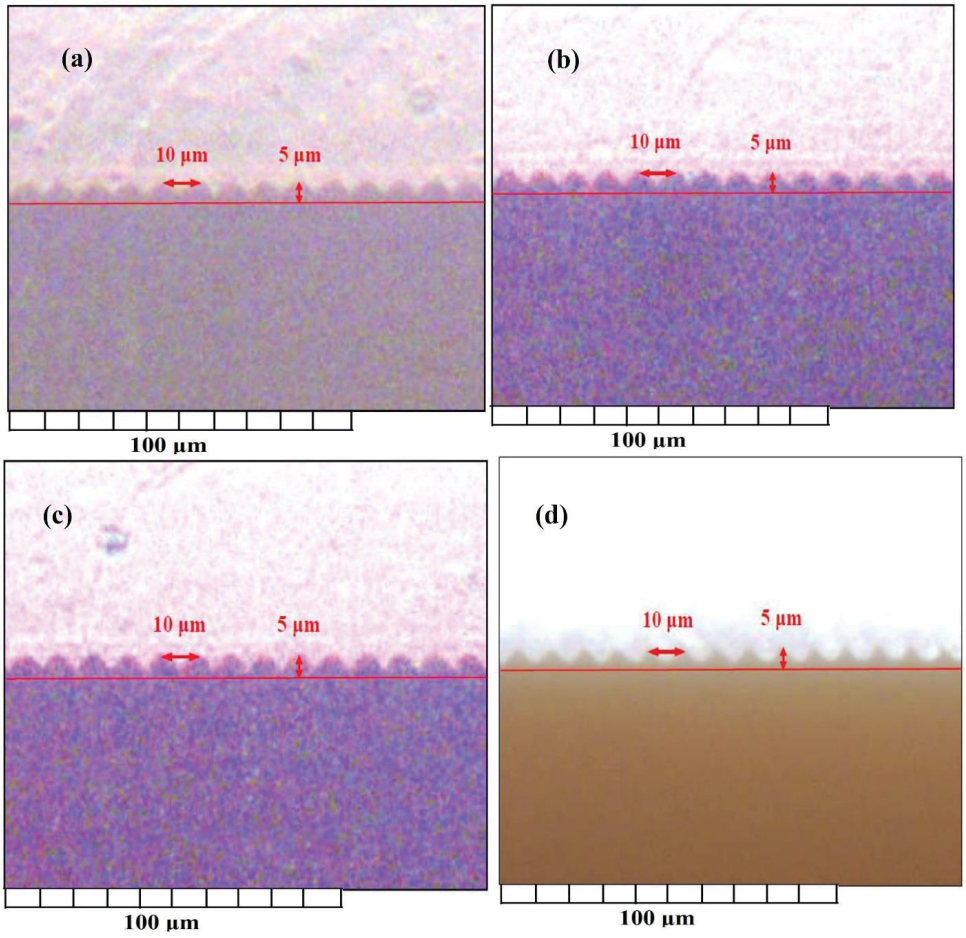

Figure 4.22: Cross-section morphologies of the embossed films **a)** XLR630, **b)** XLR630 + 5 wt. % TiO_2, **c)** XLR630 + 10 wt. % TiO_2, **d)** XLR630 + 15 wt. % TiO_2

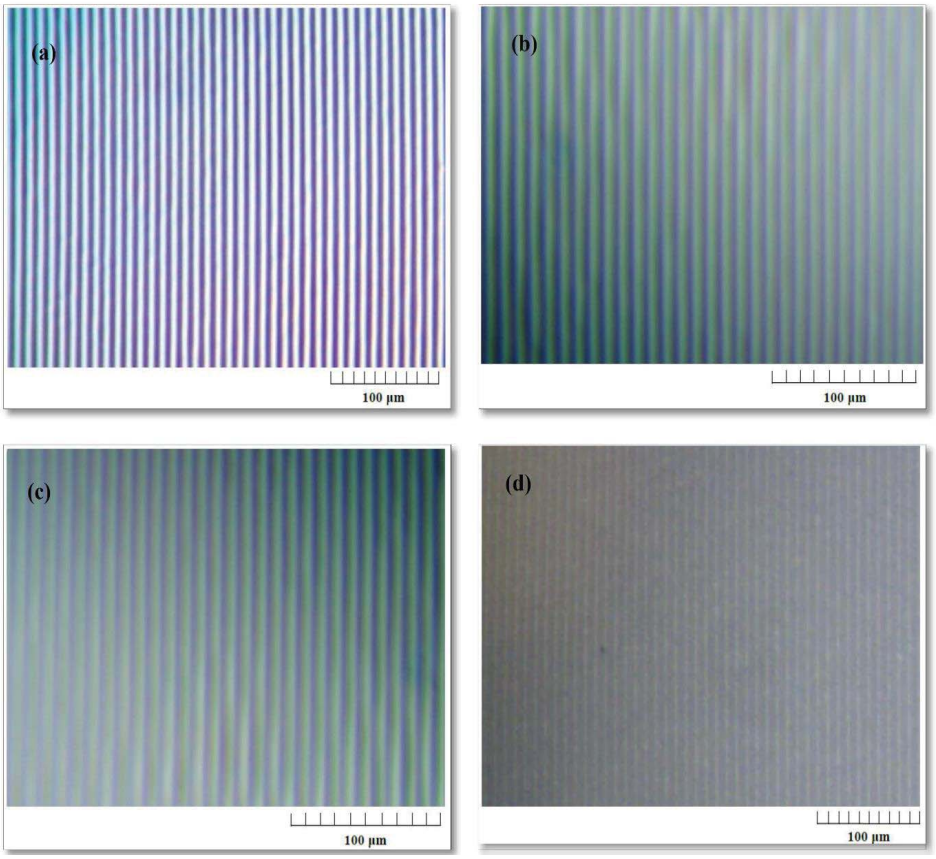

Figure 4.23: Surface morphologies of the embossed films a) XLR630, **b)** XLR630 + 5 wt. % TiO_2, **c)** XLR630 + 10 wt. % TiO_2, **d)** XLR630 + 15 wt. % TiO_2

4.7.Conclusions

Hot embossing of silicone elastomer is very different and difficult from embossing thermoplasts. The PDMS elastomer cures and hardens by hydrosilation reaction unlike the thermoplasts which can be melted and hardened by heating and cooling respectively.

Determining the GP of the silicone network is the main criteria to design the embossing experiment. Hot embossing of microscale corrugation lines on addition curing vinyl terminated polydimethyl siloxane films is successfully performed and the step by step embossing process has been established. The embossing is shown to be possible for systems with and without fillers with Young's moduli ranging from 27 KPa to 0.5 MPa, which indicates a great versatility of the process. It is also shown that a given embossing setup could be used for several materials by altering the preheating conditions, pressure and speed of the rollers.

Hot embossing using a nickel stamp has been employed successfully to imprint microstructures on thin addition curing LSR films with varying amounts of fillers. This further asserts that the process is very suitable for large scale industrial manufacture. It is envisioned that when the corrugated nickel plate is rolled onto a roll a continuous roll to roll embossing process can be

developed. Thus a process without carrier web can be established, eliminating release issues and making the process very economic. Hot embossing is cost effective, simple, and a quick method for imprinting microstructures on addition curing PDMS. It can be performed in batch or a continuous process.

5.Bilaterally microstructured PDMS film production using hot embossing

The current manufacturing process at DPP as explained in section 1.2. produces films with a one-sided microstructured surface only. Two such films are laminated back to back to make a DEAP laminate with corrugated surfaces on both sides. The lamination process has disadvantages (Refer to chapter 1, section 1.3.2.) and it would be advantageous to produce a thinner monolithic film with both surfaces corrugated as this increases the film's performance efficiency. The new technique introduced herein produces bilaterally microstructured film by combining hot embossing method with the existing manufacturing process. In employing the new technique, films with microstructures on both surfaces are successfully made with two different LSR formulations: 1) pure XLR630 and 2) XLR630 with titanium dioxide (TiO_2). The above silicone elastomer formulations are chosen based on the preferences of DPP. A paper on the results of the work presented in this chapter has been accepted by Polymer-Plastics Technology and Engineering and is attached as Appendix V.

5.1.Disadvantages of laminating two films

The disadvantages of laminating two PDMS films are 1) minute air gaps and dust particles entrapped at interface and 2) the thickness of dielectric material between the electrodes doubles. Refer to section 1.3.2. in chapter 1 for a detailed explanation.

The films are laminated mechanically in the industrial process. To ensure proper mechanical contact between the films without any air gaps the flat surfaces of the laminating films are air-plasma treated and their mechanical strength and breakdown strength is tested. From the studies conducted in our lab, it is established that films laminated by air-plasma treatment showed a decrease in breakdown strength compared to single films of the same thickness, even though they have the same mechanical properties as a single film. Hence, laminating two films mechanically or by air-plasma treatment only degrades the film's breakdown strength. Other proposed methods of adhering two PDMS films – using silicone oil and a crosslinker at the interface of two fully cured PDMS films, and adhering two partly cured films – are not suitable for the current manufacturing process. [112,113]

The thickness of a single film manufactured in the industrial process is ~ 40 µm, making the laminated film thickness ~ 80 µm. Equations (1.2) and (1.3) show that the compressive stress and strain outputs of the dielectric films decrease as the thickness of the films increases. [5] Hence it is ideal to have thinner films for an improved performance efficiency. The production of thinner films (< 40 µm) is challenged by the release problem in the current manufacturing process [31, 65]. This has been explained by numerical simulations and experimental results in chapter 2. Hence producing a single film with a thickness < 40 µm is not an option now.

The published procedures for manufacturing microstructured thin PDMS films are designed for producing small units, most often with microstructures only on one surface of the PDMS film [66]. Most of the techniques employed for replicating high aspect ratio microstructures on PDMS involve the usage of sacrificial layers, which are either metallic or polymeric [67-69]. Although these methods are highly successful, they are neither suitable for producing a continuous film nor economically viable. A novel, economical, fast, continuous and easy process for making bilaterally microstructured thinner PDMS films is therefore necessary to overcome the problems discussed above. In the new method described herein, a combination of hot embossing technique with the existing manufacturing process is used. Also, the films made with new technique in our lab are thinner than the DEAP laminate.

A comparison of the film thickness is shown in Figure 5.1. Embossing microstructures on thin PDMS films has been successfully demonstrated with different types of silicone systems. [70, 71]

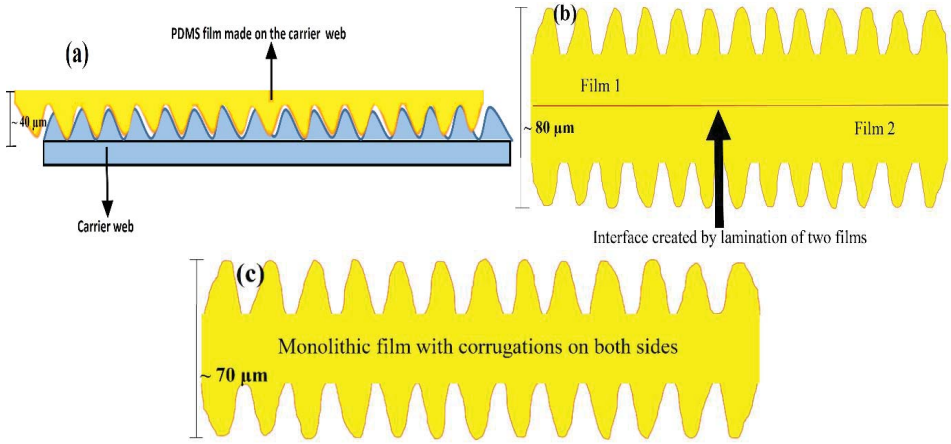

Figure 5.1: **a)** Film with one corrugated surface made in industry (~40 µm), **b)** a DEAP laminate (~ 80 µm) and **c)** monolithic film made in lab (~ 70 µm) (Not to scale)

5.2. Experimental

5.2.1.Materials

The elastomer, filler and solvent used are POWERSIL® XLR® 630 A/B, Hydrophobic rutile TiO_2 and OS-20 solvent respectively. (Refer to section 4.6.3. for product information)

5.3.1.Instrumentation

Gravure lab coater

Refer to section 4.2.2. in chapter 4 for coater description. The top roll of the coater is fixed with a cross-web of 7 µm corrugation profile, thus making it the embossing roll.

Rheological experiments

Refer to section 2.5.2.

Scanning electron microscope (SEM)

The morphology of the films is examined with scanning electron microscope (SEM) (FEI Inspect S, USA). The film sample is immersed in liquid nitrogen for a few minutes before cutting, in order to obtain a precise cross-section. The cut sample is deposited on a copper holder for the investigation of cross-section morphology. All samples are coated with gold under vacuum conditions before testing.

5.3.Procedure

Bilaterally corrugated films of two different elastomer formulations – pure XLR630 and XLR630 with TiO_2 – are made using the new process. An overview of the steps involved is shown in Figure 5.2.

5.3.1.Preparing mixtures and films

Formulations for the LSR mixtures, which are listed in Table 5.1, are mixed using a Speed Mixer (DAC 150FVZ, Hauschild Co., Germany) at 3500 rpm for 2 min. In formulation 2, the homogeneity of the TiO_2 particles in the silicone matrix is ensured by adding sufficient solvent. The uniform mixtures are cast onto a carrier web substrate with a 3540 bird film applicator (Elcometer, Germany) to produce a film of thickness ~ 70 µm (see step 1 in Figure 5).

Table 5.1: LSR mixture formulations

No.	XLR630 A : XLR630 B : TiO_2 : OS20 * (phr)
1	50 % : 50 % : 0 % : 0 (phr)
2	42 % : 42 % : 16 % : 20 (phr)

*Amounts of XLR630 and TiO_2 are in mass ratio, OS20 in parts per hundred rubber (phr)

5.3.2.Gel point and viscosity determination

The LSR mixtures are tested for GP on the rheometer set to a controlled strain mode with 2 % strain, which is ensured to be within the linear regime of the material based on an initial strain sweep test. The test is performed at a constant frequency of 1 Hz by applying parallel plate geometry of 25 mm in diameter and a gap of 0.5-1 mm at 60 ^{o}C and 80 ^{o}C. LVE data for the LSR films are measured with parallel plate geometry of 25 mm in diameter at 23 ^{o}C. The LVE diagrams are obtained from frequency sweeps, from 100 Hz to 0.01 Hz.

The viscosities of the mixtures are tested by flow sweep step with the shear rate from 10^{-2} s^{-1} to 100 s^{-1} at 23 ^{o}C using parallel plate geometry of 25 mm in diameter.

5.3.3.Preheating

The elastomer film cast on the carrier web is preheated on a hot steel roll (step 3 in Figure 5.2) prior to the embossing process, such that the hydrosilylation reaction proceeds to the GP. The time and temperature for preheating are fixed based on the GP estimated by rheological experiments. [70] The bottom surface of the elastomer films takes up the corrugation pattern from the carrier web substrate as it cures.

5.3.4.Embossing

The elastomer film at the GP on the carrier web is embossed by passing it through the rolls of a gravure coater. A piece of the carrier web is wound around the top roll, thus making it the embossing roll. This top roll imprints the corrugation pattern onto the surface of the film, and the temperature of the roll ensures that the film cures and retains the microstructure. The force applied between the rolls is 25 psi and the speed of the rolls is 1.4 rpm (see steps 4, 5 and 6 in Figure 5.2).

The diameter of the roll is 6" and its circumference is therefore 18.84". Thus, the speed of the roll is 0.0112 m/s.

5.3.5.Post curing

The embossed film is placed in the oven at 100 ^{o}C for 5 min, in order to cure completely. As the thickness of the bilaterally microstructured film (~ 70 µm) is higher than a single film (~ 40 µm), peeling away from the carrier web is not as tedious as in the conventional process. [12, 28]

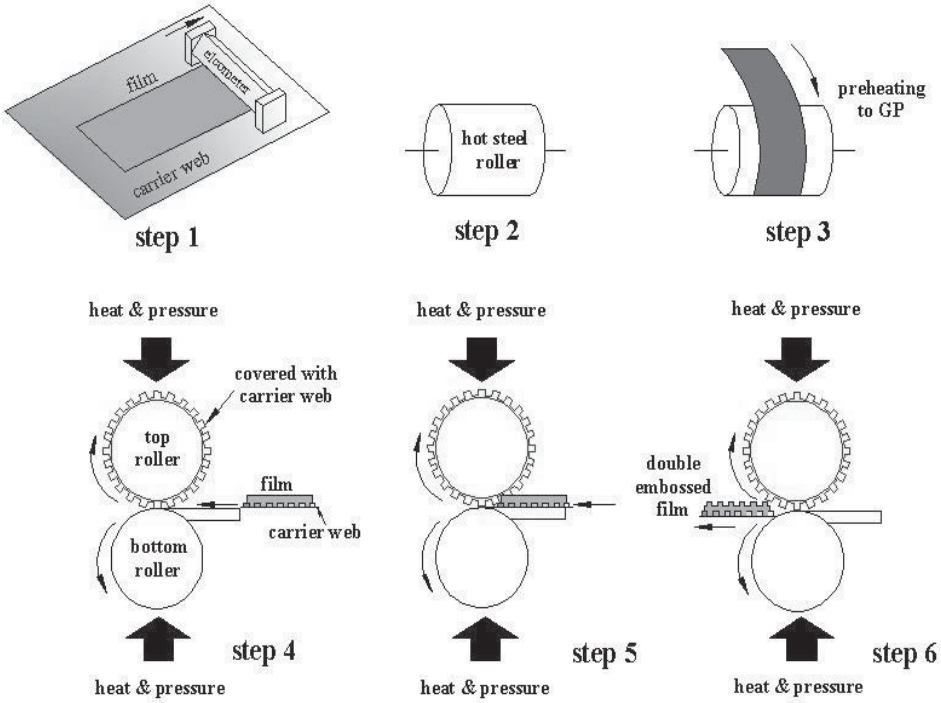

Figure 5.2: Schematic of the bilaterally microstructured thin film production

5.4.Results and discussion

5.4.1.Gel point determination

For stoichiometrically balanced networks and networks with excess crosslinkers, the GP coincides with the crossover point of storage modulus (G') and loss modulus (G'') in a LVE diagram. [82] In the case of the filled system – XLR630 with a TiO_2 filler – the GP may not exactly coincide with the crossover point for G' and G''. However it is a good estimate of the optimal time for embossing, since the filled system has similar rheological behaviour at the GP as the unfilled system. For the commercial LSR system, XLR630, the crossover point for G' and G'' in the LVE will be used as its GP, since we are most interested in the physical crossover rather than the true GP. At room temperature, the time it takes for our LSR systems to reach the GP is three days. As the temperature increases, the time it takes for the LSR systems to reach the GP decreases and the elastomers cure rapidly. Thus, the available time window for embossing at elevated temperatures is reduced to a few seconds, thereby making the process quick and efficient. At 60 ^{o}C the GP of

XLR630 is 97.6 min, which decreases almost six times by increasing the temperature to 80 °C (Figure 5.3). The curing reaction for the filled system proceeds to the GP much faster than pure XLR630. At 60 °C the time taken to reach the GP for the filled system is 3.6 min, which decreases by nine times at 80 °C to a mere 0.4 min (Figure 5.3). These timescales are still slow for a large-scale manufacturing process to operate at an economical speed. Hence, GPs at 110 °C are determined, though the crossover of G' and G'' could not be represented on an LVE, as the reaction hits the GP within 4 -7 s for both systems. The rheometer takes a minimum of 30 s to equilibrate before starting up the measurements, by which time the LSR system on the bottom plate has already cured and the measurements start after the GP. The conditions for embossing are listed in Table 5.2.

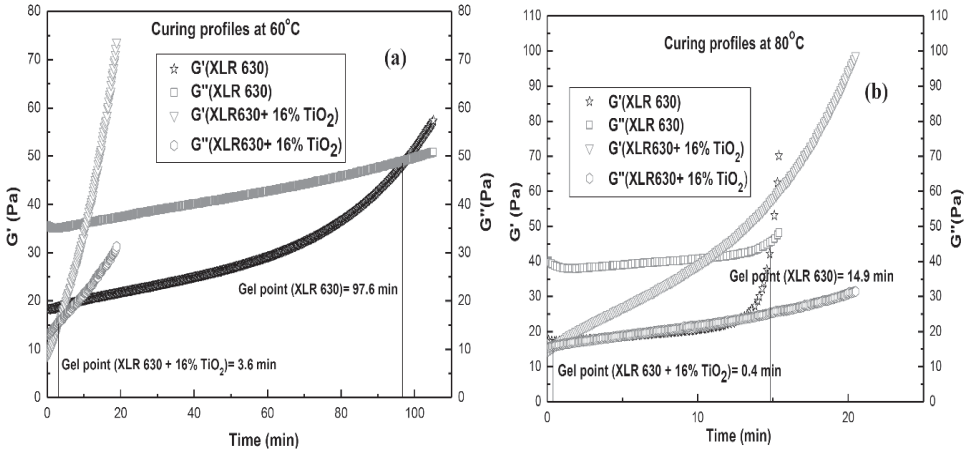

Figure 5.3: Curing profiles, **a)** GP estimation at 60 °C and **b)** GP estimation at 80 °C

5.4.2.Modulus and Viscosity

Frequency sweeps of the elastomer mixtures are shown in Figure 5.4 as a function of the applied frequency at 23 °C. The storage modulus (G') and loss modulus (G'') of the composite XLR630 are higher than that of pure XLR630, which indicates that the inorganic filler leads to the enhancement of plasticity along with reduction in elasticity. [71]

The viscosity of the elastomer increases with the addition of TiO_2 filler, and the viscosity of the XLR630 with TiO_2 filler is 1.4 kPa·s (0.01 s^{-1}). In order to minimise energy expended while mixing the formulations and spreading them on carrier web to make films, it is preferable to set the viscosity of the elastomers below 40 kPa·s in the manufacturing process and the LSRs used here fall well below this limit. [71]

5.4.3.SEM Images

The SEM images in Figure 5.5 and 5.6 show the cross-section morphology and top view of the bilaterally microstructured films. Figure 5.5 shows the pure XLR630 films and Figure 5.6 shows the XLR630 with TiO_2 films. Film thickness is ~ 70 µm, and no significant deviations in thickness are observed along either the length or the width of the sample. The images confirm the formation

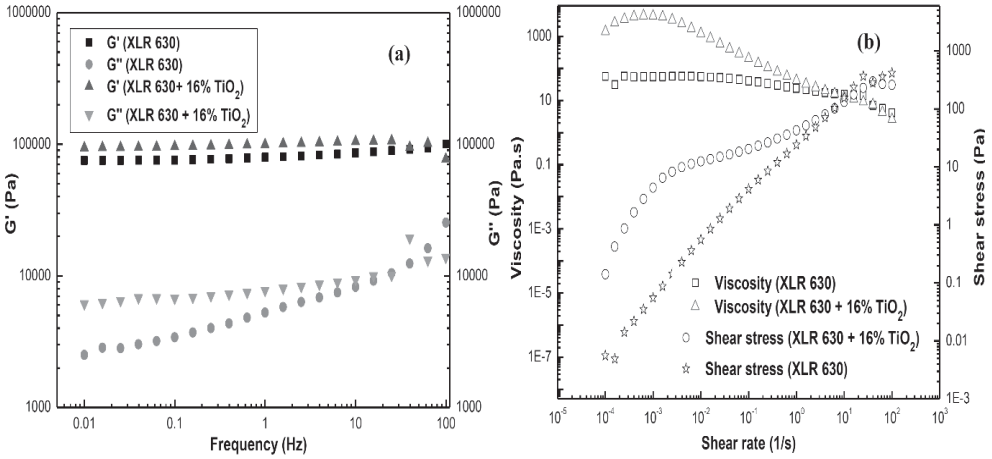

Figure 5.4: **a)** Storage and loss modulus and **b)** Dynamic viscosity and shear stress of the formulations

Table 5.2: Conditions for embossing the top surface of the film

No.	Temperature (°C)	Crossover of G' and G'' (GP)		Film thickness (μm)	Pressure (psi)	Roll speed (rpm)
		XLR630	XLR630 + 16% TiO_2 + OS20			
1	60	97.6 min	3.6 min	70	25	1.4
2	80	14.9 min	0.4 min	70	25	1.4
3	110	7 s	4 s	70	25	1.4

of corrugations on both sides of the film. In Figures 5.5 b and 5.6 b it is apparent that the embossed side of the film has corrugations with larger periods than those formed by the carrier web. The wave period on the embossed surface is exaggerated by almost twice the original profile. Furthermore, the embossed side of the film suffers from deformation and the corrugations never recover their original dimensions, perhaps because the LSR mixture is still flowing before complete curing is achieved. This could be corrected by fine-tuning the conditions of the embossing process further. The embossed side of the film also shows an accumulation of dust, which could be prevented by performing the experiment in a clean room facility.

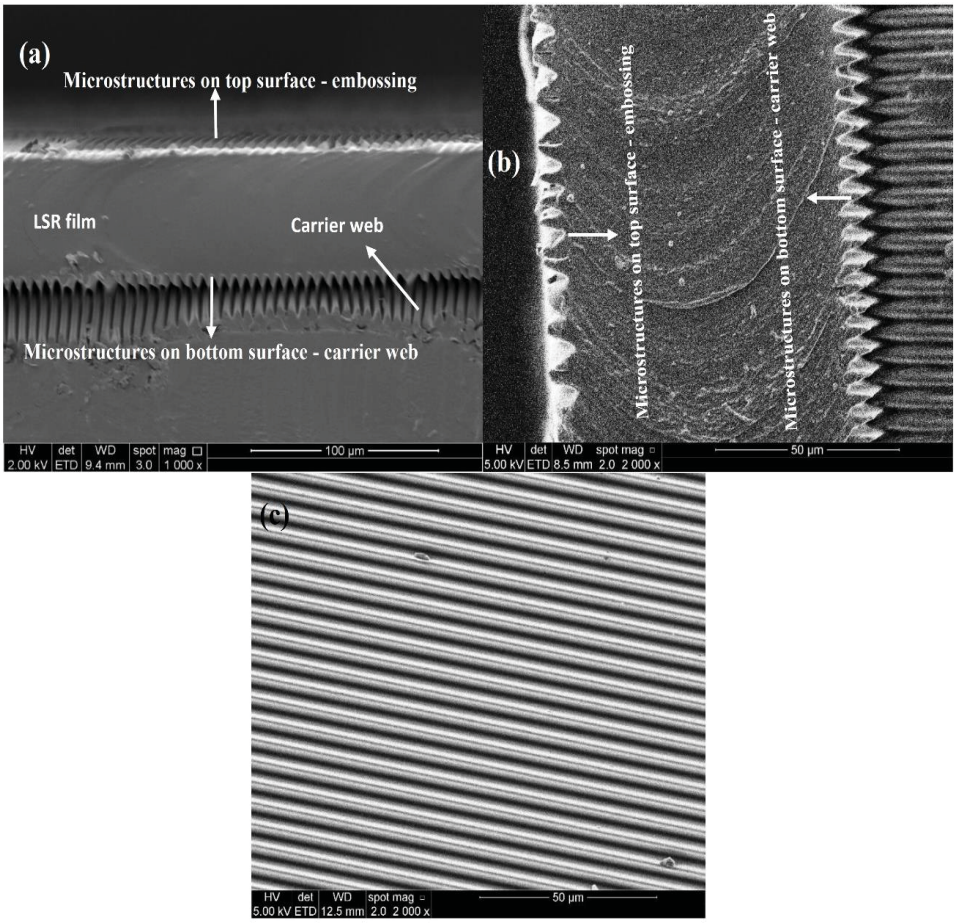

Figure 5.5: **a)** SEM image of the cross-section morphology of XLR630 films (1000 x magnification) **b)** SEM image of cross-section (2000 x magnification) and **c)** SEM image of the film's top surface with corrugations formed by embossing (2000 x magnification)

5.5.Conclusions

Bilaterally microstructured films can be made successfully in a lab with pure and composite LSR systems. The new process is a combination of an embossing method and the existing industrial process used for manufacturing a single microstructured film. The bottom surface of the film receives the microstructure from the carrier web substrate and the top surface from the embossing roll. The embossing conditions are set based on the GPs of the pure and composite LSR systems at 110 ºC, which are determined from a series of time sweeps as 7 s and 4 s, respectively. SEM images confirm that corrugations are made on both sides of the films. Corrugations on the embossed side of the film have exaggerated wave periods, compared to the carrier web side of the film, which can be corrected by refining embossing conditions. The process is quick, easy and economical and can be scaled up for an industry. The new process eliminates the lamination step used in the industry to stick two films together.

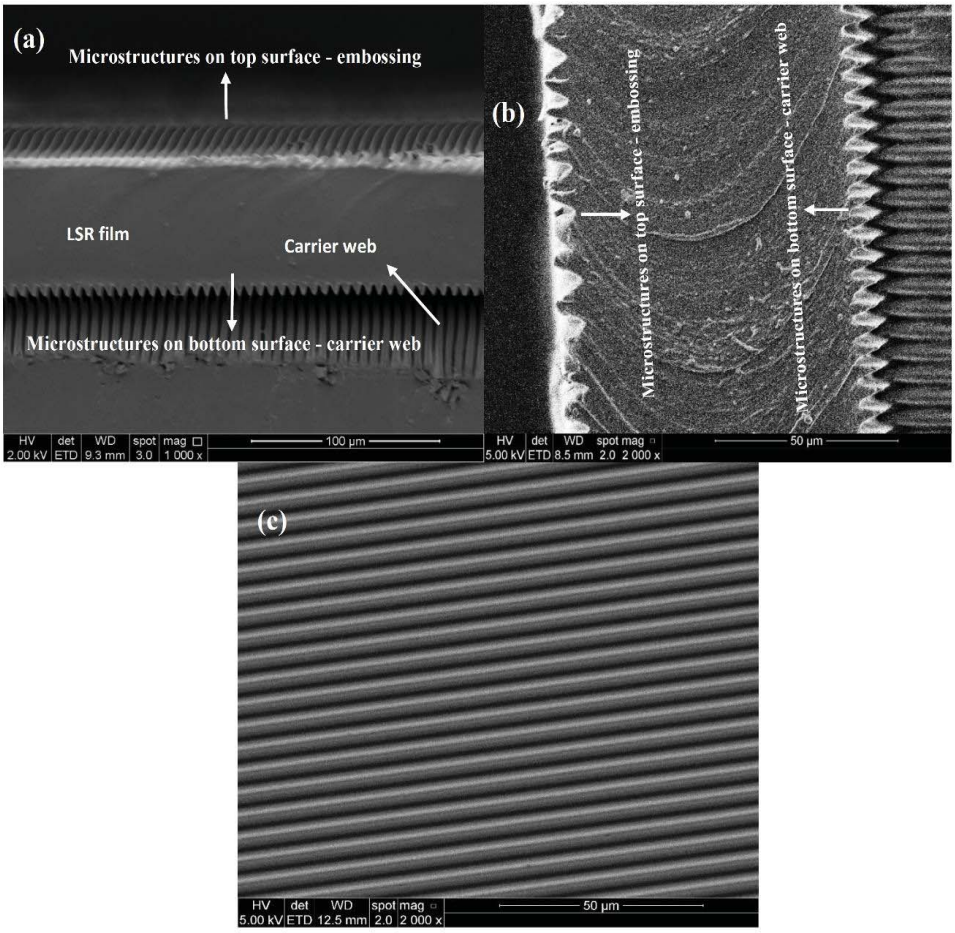

Figure 5.6: **a)** SEM image of the cross-section morphology of XLR630 with TiO_2 films (1000 x magnification) **b)** SEM image of cross-section (2000 x magnification) and **c)** SEM image of the film's top surface with corrugations formed by embossing (2000 x magnification)

6.Conclusions and future work

The conclusions of the research along with some propositions for future work are summarized in this chapter.

6.1.Conclusions

The methods tested in this research for easing the release of thin PDMS films from carrier web substrates are strictly limited by certain process and product constraints. The carrier web substrate is not be replaced or modified chemically. The thickness of the PDMS films has to be ≤ 40 µm. The Young's modulus of the PDMS films coated with metal electrodes has to be ≤ 1 MPa. Any chemical modification of the PDMS films to ease their release, such as adding resins or grafting low surface energy functionalities should not degrade the breakdown strength, dielectric permittivity, Young's modulus or tear strength of the films.

A release agent to be used in the process should fulfil certain requirements. The release agent should reduce the interfacial adhesive forces between the film and substrate. It should be chemically inert and should not degrade the film properties like breakdown strength, Young's modulus and dielectric permittivity. The release agent has to be non-toxic and safe to use. It can be a water based system or a very low viscosity silicone oil. The release agent has to be easy to apply to any surface configuration i.e. with a low viscosity. It should form a complete and uniform film on the carrier web surface. It should dry quickly to reduce the production time. The release agent should produce a film thin enough to conform to the substrate's corrugation detail. The release agent should not accumulate and build-up on the substrate and should be easy to wash off. The release agent should be insoluble in the silicone films and withstand the processing conditions (high curing temperature, shear and other abrasive forces) i.e. remain at the film/substrate interface. Finally, it should be of low cost.

Kendal's thin film peeling model has been used to understand the parameters influencing peel forces. From the simulations of Kendal's model for an elastomer film of thickness 20 µm it is concluded that the adhesive energy/peel force of a thin elastomer film decreases when the Young's modulus of the silicone elastomer increases. The adhesive energy/peel force decreases as the thickness of the films increases and as the peel angle decreases. The experimental results have also shown that the adhesive energy of PDMS films decreases as the Young's modulus increases. Further, it is concluded that perfluoroether allylamide as an additive in small quantities (1 wt. %) is ideal to decrease the surface energy of the PDMS films (19 mJ/m^2 to 8 mJ/m^2). Nonetheless, reduction of surface energy did not decrease the adhesive energy/peel forces as the influence of film's thickness and elastomeric contribution to adhesive energy is much higher than the surface energy contribution. It is concluded that increasing the film thickness and Young's modulus will lower the peel force. Nevertheless, our product constraints do not permit either one to be increased.

When 3 wt. % Belsil resin is compounded with XLR 630 silicone elastomer, the adhesive energy between film and substrate comes down to 10.5 N/m which is a reduction of 50% compared to the films without resin (21 N/m). However, the resin addition method interferes with the Young's modulus and breakdown strength of the films. At 3 wt. % Belsil resin the Young's modulus of the elastomer increases compared to the pure sample and at 1 wt. % and 5 wt. % Belsil resin the modulus of the elastomer decreases. Breakdown strength of the elastomer degrades progressively with increasing resin concentration. Therefore this technique is not suitable.

An aqueous solution of 10 wt. % Polysorbate-20, which is a non-ionic surfactant has been concluded as the release agent which conforms to the above mentioned criteria of a release agent for the current manufacture process at DPP. The 10 wt. % Polysorbate-20 solution does not affect the bulk properties of the films and decreases the adhesive energy from 118 N/m down to 2.8 N/m for LR 3043/50 films. By employing a non-ionic release agent, thin films of thickness ≤ 40 μm and Young's modulus ≤ 1 MPa can be easily peeled from difficult substrates ensuring a smooth, easy and hassle free operation of the DEAP film manufacture process. This technique will also benefit various other thin PDMS film production processes where the substrates are not release friendly. Another significant conclusion from the experiments is that ionic surfactants when used as release agents would interfere with the breakdown strength of the films. Surfactants when used as release agents can percolate into the silicone films in small quantities. In the case of an ionic surfactant, the percolated fraction will get ionized and conduct electricity under the high operating voltages of DEAP transducers or it may lead to premature breakdown of the films. For DEAP film production ionic surfactants are not an option.

Another part of the research is the establishment of hot embossing process as an alternative technique to make the microstructured PDMS films. A step by step procedure for hot embossing addition curing silicone elastomer films has been established as a proof of concept on a lab scale. The process is successful with different types of silicone elastomers with and without fillers. Hot embossing process eliminates the drawbacks of the conventional manufacture process in DPP. Since the corrugation pattern is imprinted directly on films the use of carrier web substrate is eliminated. It is easier to peel a film made on a flat substrate compared to films that are made on a micro corrugated substrate. Also, the carrier web substrates are very expensive. The conventional method requires miles of carrier web for continuous operation in large scale production. With hot embossing technique the use of carrier web is minimized and operating costs can be brought down. In the lab scale, a combination of hot embossing technique with the conventional process has been used to make bilaterally corrugated monolithic films which eliminates the drawbacks of laminated films manufactured in DPP. A nickel stamp with micro corrugations has been successfully used to emboss the silicone elastomers which illustrates the possibility of using a metallic embossing roll. Also, this process can be easily scaled up for mass production. Overall, it is concluded that this technique is ideal for large scale production of thin microstructured PDMS films, not just for DEAP transducers but also for various other industries which produce of microstructured silicone films.

6.2.Future work

In the future work it will be beneficial to explore solutions outside the constraints imposed by the current manufacture process.

A crosslinker that can give a high cross link density and de-crosslink partially in response to temperature or UV could be developed. Such a crosslinker will give films with high Young's modulus which can be peeled easily and once peeled the film can soften due to some de-crosslinking. Furthermore, surface modification of carrier webs by chemical or physical methods to ease the release could be performed. A fluoro resin can be blended with the methyl acrylate resin with which the corrugations on the carrier web are made (Refer to section 1.2.2. for carrier web description.) Such a fluoro resin will make the carrier web surface more release friendly. In addition, different types of inorganic fillers which do not degrade the film properties of concern can be blended in the silicone elastomer matrix and their effect on peel forces could be tested.

Also, other non-ionic surfactants and low viscosity silicone oils could be tested as release agents. Silicone resins other than Belsil can be compounded with silicone elastomers and their effects on the peel forces along with the properties of concern can be tested. For hot embossing process, an embossing roll made of metal with micro corrugations engraved on the metal should be made and tested. An embossing roll with different micro patterns other than corrugation lines can be used in the hot embossing process to examine how effectively the different patterns can be replicated. Finally, a pilot scale plant for manufacturing corrugated films with hot embossing process could be developed to facilitate the implementation of the process on industrial scale.

7. References

1. Bar-Cohen, Y. 'Electroactive Polymer (EAP) Actuators as Artificial Muscles-Reality, Potential and Challenges.' SPIE Press, PM136, 2nd Edition, ISBN 9780819452979 (2004)
2. Bar-Cohen, Y., Xue, T., Joffe, B., Lih, S.S., Shahinpoor, M., Simpson, J., Smith, J. and Willis, P. 'Electroactive polymers (EAP) low mass muscle actuators.' Smart Structured Mater., San Diego, California, USA: Proc. of SPIE, 3041: 697 (2007)
3. Muzaffer, Y. O. and Mavroidis, C. 'Nonlinear force control of dielectric electroactive polymer actuators.' Electroactive Polymer Actuators and Devices (EAPAD) San Diego, California, USA: Proc. of SPIE, 76422C:1-8 (2010)
4. Carpi, F. and De Rossi, D. 'Dielectric elastomer cylindrical actuators: Electromechanical modelling and experimental evaluation.' Materials Science & Engineering C, 24: 555-562, (2004)
5. Pelrine, R., Kornbluh, R., Pei, Q. and Joseph, J. 'High-speed electrically actuated elastomers with strain greater than 100%.' Science, 287 (5454): 836-839 (2000)
6. Carpi, F., De Rossi, D., Kornbluh, R., Pelrine, R. and Sommer-Larsen, P. 'Dielectric elastomers as electromechanical transducers: Fundamentals, materials, devices, models and applications of an emerging electroactive polymer technology.' Elsevier Amsterdam (2008)
7. Madden, J.D. 'Artificial muscle technology: physical principles and naval prospects.' IEEE, Journal of Oceanic Engineering, 29(3): 706-728 (2004)
8. R. Kornbluh, R. Pelrine, Q. Pei, S. Oh, and J. Joseph, "Ultrahigh strain response of field-actuated elastomeric polymers," in Proc. SPIE Smart Structure and Materials 2000: Elect Electroactive Polymer Actuators and Devices, vol. 3987, 2000, pp. 51–64.
9. Kim, K.J. and Tadokoro, S. 'Electroactive Polymers for Robotic Applications.' Chapter 2. Dielectric Elastomers for Artificial Muscles, 36-37, ISBN: 978-1-84628-371-0, Springer-Verlag, London, (2007)
10. Baughman, R.H. 'Playing nature's game with artificial muscles.' Science, 308(5718): 63-65 (2005)
11. Brochu, P. and Pei, Q. 'Advances in dielectric elastomers for actuators and artificial muscles.' Macromolecular. Rapid Communications, 31(1): 10-36 (2010)
12. Heim, J., Pelrine, R., Kornbluh, R. and Eckerle, J.S. 'Electroactive polymer rotary motors.' Patent publication no. US6806621 B2 (2004)
13. Huang, L., Zhang, Z., Andersen, M.A.E. and Sarban, R. 'High voltage bidirectional flyback converter driving DEAP actuator for automotive applications' IEEE, Vehicle Power and Propulsion Conference (VPPC), 204-208, 13917739 (2013)
14. Kim, K.J. and Tadokoro, S. 'Electroactive polymers for robotic applications: Artificial muscles and sensors' Chapter 3. Robotic Applications of Artificial Muscle Actuators, ISBN: 978-1-84628-371-0; 49-52, Springer-Verlag, London (2007)
15. Kiil, H.E. and Benslimane, M. 'Scalable industrial manufacturing of DEAP.' Electroactive Polymer Actuators and Devices (EAPAD) San Diego, California, USA: Proc. of SPIE, 72870R:1-10 (2009)
16. Benslimane, M., Kiil, H.E. and Tryson, M.J. 'Electromechanical properties of novel large strain PolyPower film and laminate components for DEAP actuator and sensor applications.' Electroactive Polymer Actuators and Devices (EAPAD) San Diego, California, USA: Proc. of SPIE, 764231:1-11 (2010)

17. Tryson, M. and Kiil, H.E. 'Dielectric electroactive polymers: Development of an industry.' Electroactive Polymer Actuators and Devices (EAPAD) San Diego, California, USA: Proc. of SPIE, 76421X:1-9 (2010)
18. Benslimane, M. and Gravesen, P. 'Position sensor comprising elastomeric material.' Patent grant no. 7104146 (2005)
19. Benslimane, M. and Gravesen, P. 'Dielectric actuator or sensor structure and method of making it.' Patent grant no. 7573064 (2005)
20. Benslimane, M. and Gravesen, P. 'Multilayer composite and a method of making such.' Patent grant no. 7548015 (2007)
21. Benslimane, M. and Gravesen, P. 'Dielectric actuator or sensor structure and method of making it.' Patent grant no.7785905 (2008)
22. Tryson, M., Benslimane, M., Kiil, H.E. and Zumbrum, M. 'Transducer comprising a composite material and method of making such a composite material.' Patent grant no. 8421316 (2011)
23. http://www.polypower.com/Technology/Overview/PolyPower+DEAP+Technology/PolyPower+DEAP+Characteristics.htm (Accessed on May 2 2014)
24. Stritzke, B. 'Custom Molding of Thermoset Elastomers.' ISBN: 978-3-446-41964-3: 132-141, Carl Hanser Verlag, London (2009)
25. Delebecq, E., Ganachaud, F. 'Looking over liquid silicone rubbers: (1) network topology vs chemical formulations.' ACS Appl. Mater. Interfaces, 4 (7): 3340-3352 (2012)
26. Delebecq, E., Hermeline, N., Flers, A., Ganachaud. F. 'Looking over liquid silicone rubbers: (2) mechanical properties vs network topology.' ACS Appl. Mater. Interfaces, 4 (7): 3353-3363 (2012)
27. Bejenariu, A.B., Yu, L. and Skov, A.L. 'Low moduli elastomers with low viscous dissipation.' Soft Matter, 8(14): 3917-3923 (2012)
28. Larsen, A.L., Hansen, K., Sommer-Larsen, P., Hassager, O., Bach, A., Ndoni, S., and Jørgensen, M. 'Elastic properties of nonstoichiometric reacted PDMS networks.' Macromolecules, 36(26): 10063-10070 (2003)
29. Skov, A.L., Bejenariu, A.G., Bøgelund, J., Benslimane, M. and Egede, A.D. 'Influence of micro- and nanofillers on electromechanical performance of silicone EAPs.' Electroactive Polymer Actuators and Devices (EAPAD) San Diego, California, USA, Proc. of SPIE, 83400M:1-10 (2012)
30. Fröhlich, J., Niedermeier, W., Luginsland, H.D. 'The effect of filler-filler and filler-elastomer interaction on rubber reinforcement.' Composites: Part A, 36(4): 449-460 (2005)
31. Vudayagiri, S., Junker, M.D. and Skov, A.L. 'Factors affecting surface and release properties of thin polydimethylsiloxane films.' Polymer Journal, 45(8): 871-878 (2013)
32. Kendall, K. 'Thin-film peeling-the elastic term.' Journal of Physics D: Applied Physics, 8(13): 1449-1452 (1975)
33. Kuo, A.C.M. 'Poly (dimethylsiloxane). Polymer Data Handbook.' 411–435, Oxford University Press, Oxford (1999)
34. Wallash, A.J. and Levit, L. 'Electrical breakdown and ESD phenomena for devices with nanometer-to-micron gaps.' Reliability, testing, and characterization of MEMS/MOEMS II San Diego, California, USA: Proc. of SPIE, 4980: 87-96 (2003)
35. Yu, L., Vudayagiri, S., Zakaria, S. B., Benslimane, M. Y. and Skov, A. L. 'Filled liquid silicone rubbers: Possibilities and challenges.' Electroactive Polymer Actuators and Devices (EAPAD) San Diego, California, USA, Proc. of SPIE, 90560S:1-9 (2014)
36. Zakaria, S. B., Morshuis, P. H. F., Yahia, B. M., Gernaey, K. and Skov, A. L. 'The electrical

breakdown of thin dielectric elastomers: thermal effects.' Electroactive Polymer Actuators and Devices (EAPAD) San Diego, California, USA, Proc. of SPIE, 90562V:1-11 (2014)
37. http://www.artificialmuscle.com/technology.php (Accessed on May 2 2014)
38. http://www.vivitouch.com/company.html (Accessed on May 2 2014)
39. http://www.smela.umd.edu/polymer-actuators/dea.html (Accessed on May 2 2014)
40. http://www.smela.umd.edu/polymer-actuators/micro-devices.html (Accessed on May 2 2014)
41. http://www.emk.tu-darmstadt.de/en/mems/research/electroactive-polymers/ (Accessed on May 2 2014)
42. http://www.emk.tu-darmstadt.de/en/mems/research/electroactive-polymers/tactile-displays/ (Accessed on May 2 2014)
43. Holger, M., Hausa, H., Kauerb, M. and Schlaak, H.F. 'Tactile feedback to the palm using arbitrarily shaped DEA.' Electroactive Polymer Actuators and Devices (EAPAD) San Diego, California, USA: Proc. of SPIE, 90563C: 1-8 (2014)
44. http://www.emk.tu-darmstadt.de/en/mems/research/electroactive-polymers/peristaltische-pumpe/ (Accessed on May 2 2014)
45. Gattia, D., Tropeaa, C. and Schlaak, H.F. 'Dynamic performance of silicone dielectric elastomer actuators with bi-stable buckled beams.' Electroactive Polymer Actuators and Devices (EAPAD) San Diego, California, USA: Proc. of SPIE, 905638: 1-12 (2014)
46. Foerster, F. and Schlaak, H.F. 'Optimized deformation behavior of a dielectric elastomer generator' Electroactive Polymer Actuators and Devices (EAPAD) San Diego, California, USA, Proc. of SPIE, 905637: 1-11 (2014)
47. http://lmts.epfl.ch/page-37017.html ((Accessed on July 14 2014))
48. http://lmts.epfl.ch/cms/lang/en/pid/105963 ((Accessed on July 14 2014))
49. http://lmts.epfl.ch/cms/site/lmts/lang/en/EAPmotor (Accessed on July 14 2014)
50. Poulin, A., Rosset, S. and Shea, H. 'Toward compression of small cell population: Harnessing stress in passive regions of dielectric elastomer actuators.' Electroactive Polymer Actuators and Devices (EAPAD) San Diego, California, USA, Proc. of SPIE, 90561Q: 1-9 (2014)
51. Rosset, S., Araromi, O.A., Shintake, J. and Shea, H.R. 'Model and design of dielectric elastomer minimum energy structures.' Smart Materials and Structures, doi:10.1088/0964-1726/23/8/085021 (2014)
52. https://unidirectory.auckland.ac.nz/profile/i-anderson (Accessed on July 20 2014)
53. Loa, H.C., Gisby, T.A., Calius, E.P. and Anderson, I.A. 'Transferring electrical energy between two dielectric elastomer actuators.' Sensors and Actuators A, 212: 123-126 (2014)
54. http://www.seas.ucla.edu/ms/faculty1/qibing_pei.html (Accessed on July 20 2014)
55. Ha, M.S., Yuan, W., Pei, Q., Pelrine, R. and Stanford, S. 'Interpenetrating Polymer Networks for High-Performance Electro elastomer Artificial Muscles.' Advanced Materials, 18: 887-891 (2006)
56. http://www.seas.harvard.edu/directory/suo (Accessed on July 20 2014)
57. Lu, T., Foo, C.C., Huang, J., Zhu, J. and Suo, Z. 'Highly deformable actuators made of dielectric elastomers clamped by rigid rings.' Journal of Applied Physics, 115: 184105-1-6 (2014)
58. http://www.sems.qmul.ac.uk/staff/?f.carpi (Accessed on July 20 2014)
59. Galantini, F., Carpi, F. and Gallone, G. 'Effects of plasticization of a soft silicone for dielectric elastomer actuation.' Smart Materials and Structures, 22(10): 104020 (2013)
60. http://www.bris.ac.uk/engineering/people/jonathan-m-rossiter/overview.html (Accessed on July 20 2014)

61. Sareh, S., Rossiter, J., Conn, A., Drescher, K. and Goldstein, R.E. 'Swimming like algae: biomimetic soft artificial cilia.' Journal of the Royal Society Interface, 10(78): 20120666 (2013)
62. http://www.empa.ch/plugin/template/empa/357/*/---/l=/uacc=kov(Accessed on July 20 2014)
63. Weissa, F.M., Zhao, X., Thalmann P., Deyhle, H., Urwyler, P., Kovacs, G. and Müller, B. 'Measuring the bending of asymmetric planar EAP structures.' Electroactive Polymer Actuators and Devices (EAPAD) San Diego, California, USA, Proc. of SPIE, 86871X: 1-6 (2013)
64. Wache, R., McCarthy, D.N., Risse, S. and Kofod, G. 'Rotary Motion Achieved by New Torsional Dielectric Elastomer Actuators Design.' Mechatronics, IEEE/ASME Transactions, 99: 1-3 (2014)
65. Vudayagiri, S. and Skov, A.L. 'Methods to ease the release of thin polydimethylsiloxane films from difficult substrates.' Polymers for Advanced Technology, 25(3): 249-257 (2014)
66. Mannsfeld, S.C.B., Tee, B.C-K., Stoltenberg, R.M., Chen, C.V.H-H., Barman, S., Muir, B.V.O., Sokolov, A.N., Reese, C. and Bao, Z. 'Highly sensitive flexible pressure sensors with microstructured rubber dielectric layers.' Nature Materials, 9: 859-864 (2010)
67. Kim, K., Park, S., Lee, J.B., Manohara, H., Desta, Y., Murphy, M. and Ahn, C.H. 'Rapid replication of polymeric and metallic high aspect ratio microstructures using PDMS and LIGA technology.' Microsystem Technologies, 9: 5-10 (2002)
68. Karlsson, J.M., Haraldsson, T., Carlborg, C.F., Hansson, J., Russom, A. and Wijngaart, W.V. 'Fabrication and transfer of fragile 3D PDMS microstructures.' Journal of Micromechanical Microengineering, 22(8): 1-9 (2012)
69. Hu, J., Li, L., Lin, H., Zhang, P., Zhou, W. and Ma, Z. 'Flexible integrated photonics: where materials, mechanics and optics meet.' Optical Materials Express, 3(9): 1313-1331 (2013)
70. Vudayagiri, S., Yu, L., Hassouneh, S.S. and Skov, A.L. 'Hot embossing of microstructures on addition curing polydimethylsiloxane films.' Journal of Elastomers and Plastics, doi: 10.1177/0095244313483642 (2013)
71. Vudayagiri, S., Yu, L. and Skov, A.L. 'Techniques for hot embossing microstructures on liquid silicone rubbers with fillers.' Journal of Elastomers and Plastics, doi: 10.1177/0095244314526743 (2014)
72. Pritykin, L.M., 'Calculation of the surface energy of homo- and copolymers from the cohesion parameters and refractometric characterisics of the respective monomers.' Journal of colloid and Interface Science, 112(2): 539-543 (1986)
73. Lautrup, B. 'Physics of Continuous Matter. 2nd edn. Exotic and Everyday Phenomena in the Macroscopic World.' ISBN: 9781420077001,CRC Press, New York, (2011)
74. Thouless, M.D., Yang, Q.D. and Arbor, A. 'A Parametric Study of the Peel Test. Internatonal Journal of Adhesion & Adhesives.' 28, 176-184 (2008)
75. Jouwersma, C. 'Notes: On the Theory of Peeling.' Journal of Polymer Science, XLV (145): 253-255 (1960)
76. Newby, B.Z. and Chaudhury, M.K. 'Friction in Adhesion.' Langmuir, 7463 (16): 4865-4872 (1998)
77. Kendall,K. 'Thin-film peeling-the elastic term.' Journal of Physics D: Applied Physics, 8(13): 1449-452 (1975)
78. Koberstein, J.T., Duch, D.E., Hu, W., Lenk, T.J., Bhatia, R., Brown, H.R., Lingelser, J.P. and Gallot, Y. 'Creating Smart Polymer Surfaces with Selective Adhesion Properties.' Journal of Adhesion, 66, 229-249 (1998)

79. Thanawala, S.K. and Chaudhury, M.K. 'Surface Modification of Silicone Elastomer Using Perfluorinated Ether.' Nature, 16(32): 1256-1260 (2000)
80. Bejenariu, A.G., Boll, M., Lotz, M.R., Vraa, C. and Skov, A.L. 'New elastomeric silicone based networks applicable as electroactive systems.' Electroactive Polymer Actuators and Devices (EAPAD) San Diego, California, USA, Proc. of SPIE, 79762V: 1-8 (2011)
81. Chambon, F. and Winter, H.H. 'Linear Viscoelasticity at the Gel Point of a Crosslinking PDMS with Imbalanced Stoichiometry.' Journal of Rheology, 31(8): 683-97 (1987)
82. Winter, H.H. 'Can the Gel Point of a crosslinking polymer be detected by the G'-G" Crossover?' Polymer Engineering and Science, 27(22): 1698-702 (1987)
83. Frankær, S.M.G., Jensen, M.K., Bejenariu, A.G., and Skov, A.L. 'Investigation of the properties of fully reacted unstoichiometric polydimethylsiloxane networks and their extracted network fractions.' Rheologica Acta, 51(6): 559-67 (2012)
84. Fowkes, F.M. 'Attractive Forces at Interfaces. The Interface Symposium-5.Industrial and Engineering Chemistry.' 56(12): 40-52 (1964)
85. Morrison, F.A. 'Understanding Rheology' ISBN13: 9780195141665, Oxford University Press, Oxford (2001)
86. Vogt, W. W. and Evans, R. D. 'Poisson's Ratio and Related Properties for Compounded Rubber.' Industrial & Engineering Chemistry, 15(10): 1015-1018 (1923)
87. Johnson, K.L., Kendall, K. and Roberts, A.D. 'Surface Energy and the Contact of Elastic Solids. Proceedings of the Royal Society A: Mathematical, Physical and Engineering Sciences.' 324(1558): 301-313 (1971)
88. Madsen, F.B., Dimitrov, I., Daugaard, A.E., Hvilsted, S. and Skov, A.L., 'Novel Cros-linkers for PDMS networks for controlled and well distributed grafting of functionalities by click chemistry.' Polymer Chemistry, 4, 1700-1707 (2013)
89. Huibers, P.D.T., Lobanov, V.S., Katritzky, A.R., Shah, D.O. and Karelson,M. 'Prediction of Critical Micelle Concentration Using a Quantitative Structure-Property Relationship Approach.1. Nonionic Surfactants.' Langmuir, 12, 1462-1470 (1996)
90. Chang, H.C., Hwang, B.J., Lin, Y.Y., Chen, L.J. and Lin, S.Y. 'Measurement of critical micelle concentration of nonionic surfactant solutions using impedance spectroscopy technique.' Rev.Sci.Instrum. American Institute of Physics, 69(6): 2514-2520 (1998)
91. Ananthapadmanabhan, K.P., Goddard, E.D., Turro, N.J. and Kuo, P.L. 'Fluorescence Probes for Critical Micelle Concentration.' Langmuir,1, 352-355 (1985)
92. Dominguez, A., Fernandez, A., Gonzalez, N., Iglesias, E. and Montenegro, L. 'Determination of Critical Micelle Concentration of Some Surfactants by Three Techniques.' Journal of Chemical Education, 74(10): 1227-1231 (1997)
93. Mittal, K.L., 'Determination of CMC of Polysorbate-20 in aqueous solution by surface tension method.' Journal of Pharmaceutical Sciences, 61(8): 1334-1335 (1972)
94. Hait, K.S. and Moulik, S.P. 'Determination of critical micelle concentration (CMC) of nonionic surfactants by donor–acceptor interaction with iodine and correlation of CMC with Hydrophile–Lipophile balance and other parameters of the surfactants.' Journal of surfactants and detergents, 4(3): 303-309 (2001)
95. Bautista, F.L., Sanz, R.M., Molina, C.M., Gonzalez, N. and Sanchez, D. 'Effect of different non-ionic surfactants on the biodegradation of PAHs by diverse aerobic bacteria.' 14th International Biodeterioration and Biodegradation Symposium, 63(7): 913-922, (2009)

96. Elworthy, P.H. 'The critical micelle concentration of Cetomacrogol 1000' Research Papers, 293-299 (1960)
97. Skov, A.L., Vudayagiri, S. and Benslimane, M. 'Novel silicone elastomer formulations for DEAPs' Electroactive Polymer Actuators and Devices (EAPAD) San Diego, California, USA, Proc. of SPIE 86871I, doi:10.1117/12.2009465 (2013)
98. Benslimane, M.Y., Kill, H.E and Tryson, M.J. 'Dielectric electro-active polymer push actuators: performance and challenges.' Polymer International, 59(3): 415-421 (2010)
99. Sommer-Larsen, P. and Larsen, A.L. 'Materials for dielectric actuators.' Electroactive Polymer Actuators and Devices (EAPAD) San Diego, California, USA, Proc. of SPIE, 5385, 68-77 (2004)
100. López-Díaz, D. and Velázquez, M.M. 'Variation of the critical micelle concentration with surfactant structure: A simple method to analyze the role of attractive-repulsive forces on micellar association.' The Chemical Educator, 12(5): (2007)
101. Zeigler, J.M. and Fearon, F.W.G. 'Silicon-Based polymer Science.' Advances in Chemistry 224 Chapter 10 (181-199), American Chemical Society, ISBN13:9780841215467, (1990)
102. Mayer,H. 'New Silicones for solvent-free silicone resin paints and primers.' Farbe + Lack, ISSN 0014-7699, 97(10): 867-870 (1991)
103. Li, H.J., Zhang, A.Q., Hu, Y., Sui, L., Qian, D.J., and Chen, M. 'Large-scale synthesis and self-organization of silver nanoparticles with Tween 80 as a reductant and stabilizer.' Nano Express, 7(612): 1-13 (2012)
104. Shrinivas, C. K., Adinath, M.W., Jyotsna, T.W. and Momin, S.A. 'Comparative Analysis of the Properties of Tween-20, Tween-60, Tween-80, Arlacel-60, and Arlacel-80.' Journal of Dispersion Science and Technology, 28: 477-484 (2007)
105. Worgull, M. 'Hot Embossing: Theory and Technology of Microreplication.' Institute for Microstructure technology, Karlsruhe, Germany, ISBN:978-0-8155-1579-1, (2009)
106. Kolew, A., Münch, D., Sikora, K. and Worgull, M. 'Hot embossing of micro and sub-micro structured inserts for polymer replication.' Microsystem Technologies, 17 (4):609-18 (2010)
107. Katoh, T., Tokuno, R., Zhang, Y., Abe, M., Akita, K. and Akamatsu, M. 'Micro injection molding for mass production using LIGA mold inserts.' Microsystem Technologies, 14 (9-11):1507-14 (2008)
108. Larsen, A.L., Hansen, K., Larsen, S.P., Hassager, O., Bach, A., Ndoni, S. and Jørgensen, M. 'Elastic Properties of Nonstoichiometric Reacted PDMS Networks.' Macromolecules, 36(26): 10063-70 (2003)
109. Bejenariu, A.G., Rasmussen, H.K., Skov, A.L., Hassager, O. and Frankaer, S.M. 'Large amplitude oscillatory extension of soft polymeric networks.' Rheologica Acta, 49(8): 807-14 (2010)
110. Venkatraman, S.K. and Winter, H.H. 'Finite shear strain behavior of a crosslinking polydimethylsiloxane near its gel point. 'Rheologica Acta, 29(5): 423-32 (1990)
111. Lewis N, Stein J, Gao Y, Colborn RE and Hutchins G, 'Platinum catalysts used in the silicones industry.' Platinum Metals Review, 41(2): 66-75 (1997)
112. Yu, L. and Skov, A.L. 'Monolithic growth of partly cured polydimethylsiloxane thin film layers.' Polymer Journal, 46(2): 123-129 (2014)
113. Yu, L., Daugaard, A.E. and Skov, A.L. 'Adhesion between polydimethylsiloxane layers by cross-linking.' Advances in Science and Technology, 79: 47-52 (2013)

8. Symbols and abbreviations

DEAP	dielectric electroactive polymer
GP	gel point
PDMS	polydimethylsiloxane
PFE	perfluoroether allylamide
HTV	high temperature vulcanisable
RTV	room temperature vulcanisable
LSR	liquid silicone rubber
DPP	Danfoss Polypower A/S
UV	ultra violet
HCR	high consistency rubbers
EAP	electroactive polymer
SMA	shape memory alloys
EAC	Electroactive ceramics
PETE	polyethylene terephthalate
CMC	critical micelle concentration
LVE	linear viscoelastic
SEM	scanning electron microscope
R	adhesive energy
F	peel force
μ	micron
d	thickness
ɵ	peel angle
C	capacitance
ε_r	relative permittivity
ε_o	permittivity of free space
A	area
t	thickness
p	compressive stress
s_z	thickness strain
Y, E	Young's modulus
V	applied voltage
C_o	initial capacitance
λ	material strain
b	width of film
Δc	unit of length
G'	storage modulus
G''	loss modulus
ω	frequency
t_{97}	time taken to reach 97 % curing
σ_L	surface tension of liquid
σ_L^D	dispersive component of liquid surface tension
σ_L^P	polar component of liquid surface tension

σ_S^D	dispersive component of solid surface tension
σ_S^P	polar component of solid surface tension
σ_S	surface tension of solid surface
G	shear modulus
υ	Poisson ratio
r	stoichiometric imbalance
f	reactive functional groups
M_{PDMS}	molecular weight of PDMS
m_{PDMS}	mass of PDMS
$M_{crosslinker}$	molecular weight of crosslinker
$m_{crosslinker}$	mass of crosslinker
Pt	platinum
Ni	nickel
V	vanadium
phr	parts per hundred rubber
tan δ	G''/G'
psi	pounds per inch^2 (1 psi = 6.9 kPa)
rpm	rotations per minute

Appendix I

Factors affecting the surface and release properties of thin polydimethylsiloxane films

Polymer Journal (2012)

Polymer Journal (2012), 1–8

www.nature.com/pj

ORIGINAL ARTICLE

Factors affecting the surface and release properties of thin polydimethylsiloxane films

Sindhu Vudayagiri[1], Michael Daniel Junker[2] and Anne Ladegaard Skov[1]

Polydimethylsiloxane (PDMS) elastomers are commonly used as dielectric electroactive polymers (DEAPs). DEAP films are used in making actuators, generators and sensors. In the large-scale manufacture of DEAP films, the release of films from the substrate (carrier web) induces some defects and prestrain in the films, which affects the overall performance of the films. The current research is directed toward investigating factors affecting the peel force and release of thin, corrugated PDMS films used as DEAP films. It has been shown that doping the PDMS films with small quantities of perfluoroether allylamide ($F(CFCF_3CF_2O)_7CFCF_3CONHCH_2CH=CH_2$) lowers the surface energy, which could facilitate release. This idea is further investigated, and the resultant change in the film performance is evaluated. The relationship between the adhesive energy, surface energy, Young's modulus and peel force of the films is also analyzed.
Polymer Journal (2012) **0,** 000–000. doi:10.1038/pj.2012.227

Keywords: carrier web; DEAP; elastomers; PDMS; release; surface energy

INTRODUCTION

In the large-scale manufacture of dielectric electroactive polymer (DEAP) films, the polydimethylsiloxane (PDMS) elastomer mixture is applied to the substrate (carrier web) and then peeled off the substrate after the elastomer has cured completely.[1] The process of release from the substrate is not as smooth as desired, and the process induces considerable prestrain and defects in the film, which affects the performance of the films as actuators. To ease the process of release, release agents in the form of sprays or liquids cannot always be used. Modifying or replacing the web for the processing of the microstructured films is not possible at present because of the commercial unavailability of such products in the large quantities required for the continuous process of producing microcorrugated DEAP films.

The surface energy of PDMS is 19–21 mJ m^{-2} [2] and contact angle with water is 110° (Supplementary Figure S1), which explains its inert nature toward many chemical species and its poor adhesion to many substrates. Through the addition of suitable surface-active block copolymers, it has been shown that the surface energy can be decreased further or that the film can be made selectively nonadhesive to a particular substrate.[3] A polymeric additive with a lower surface energy than its host matrix is known to adsorb preferentially at the free surface and consequently decrease the adhesion of that surface toward a particular substrate.[3] The substrate on which the PDMS films are made is a polyethylene terephthalate coated with microscale corrugations of methyl acrylate. This is the substrate used in the large-scale industrial manufacture of DEAP films.[1]

Surface tension, peeling and release

The molecules on a free surface of the film will have lesser binding energy than those molecules in the bulk. This missing (negative) binding energy can be viewed as a positive energy added to the free surface. External forces must perform positive work against internal surface forces to increase the area of a surface. These internal surface forces are called surface tension, which is defined as the normal force per unit area.[4] Surface tension is present at all surfaces and interfaces. The surface energy density associated with an interface between a solid or liquid and a gas is always positive because of the missing negative binding energy of surface molecules. Interfaces between solids and liquids or between solids and solids are not required to have positive interfacial energy density. The sign depends on the strength of the cohesive forces holding molecules of a material together compared with the strength of the adhesive forces between the opposing molecules of the interfacing materials. If the interfacial energy between two liquids is negative, then a large amount of energy can be released by mixing them, and hence, the liquids get mixed instead of staying separate. Immiscible liquids such as oil and water have a positive interfacial energy density, which makes them seek a minimum interfacial area.[4]

The peel force required to peel a film from a substrate is a complex function of geometry, the mechanical properties of the film and the substrate, the thickness of the film, the interfacial cohesive properties and the friction between the surfaces. A detailed study and analysis of the peel test and the factors that govern the peel force has been presented by Thouless *et al.*[5]

[1]Department of Chemical and Biochemical Engineering, The Danish Polymer Centre (DPC), Technical University of Denmark, Kongens Lyngby, Denmark and [2]Danfoss PolyPower A/S, Nordborg, Denmark
Correspondence: Dr AL Skov, Chemical and Biochemical Engineering, The Danish Polymer Centre (DPC), Technical University of Denmark, Søltofts Plads, Building 227, Kongens Lyngby 2800 Denmark.
E-mail: al@kt.dtu.dk
Received 28 August 2012; revised 30 October 2012; accepted 1 November 2012

There are many theories to determine the peel force,[5,6] adhesive fracture energy or the interfacial adhesion[7] when a film is being peeled from a substrate. The thin-film peeling theory developed by Kendall,[8] which explains the peeling of a thin elastomer film from a rigid substrate, will be used to analyze the peeling in this context.

Consider an elastomer film of thickness d that is being peeled from a rigid substrate at a peel angle θ with a force F (Figure 1). The elastomer has a Young's modulus E. The adhesive energy between the film and the glass substrate is R. Consider a unit length Δc of the film being peeled from the substrate between the points A and B.[8] The width of the film at any given point is b. The three contributions to the energy changes involved in the peeling process are

(1) Surface energy due to the creation of new surfaces $[-bR\Delta c]$.
(2) Potential energy due to the movement of the applied force $[F(1-\cos\theta)]$.
(3) Elastic energy due to the extension of the film in the direction of the applied force $[F^2\Delta c/2bdE]$.

Adding up these contributions and assuming energy conservation, the following equation is obtained:[8]

$$-bR\Delta c + F(1-\cos\theta)\Delta c + \frac{F^2\Delta c}{2bdE} = 0 \qquad (1)$$

In our case, the corrugations on the surface of the carrier web make the release process all the more difficult because they increase the surface area, meaning a larger force is needed to peel the film.

From Equation (1), the adhesive energy R can be calculated. R is different from the surface energy, work of adhesion or any thermodynamic quantity, and R gives an estimate of the adhesive force between the substrate and the film. If the R between the substrate and the elastomeric film is high, then the force F required to peel the film will also be high. The smaller the peel angle, the smaller the potential energy contribution will be. Because the standard peel tests are performed at $\theta = \pi/2$ or $= \pi$, the peel angle will not be modified. The elastomeric contribution to peel is governed by E, which is a material property. The surface energy contribution to peel force can be lowered if the surface energy can be decreased. This should preferably be done without affecting the bulk properties of the material (mechanical and dielectric) properties.

To decrease the surface energy of the PDMS, it will be modified with small quantities of a perfluoroether additive that contains low-energy trifluoromethyl (CF_3) groups.[9] These low-energy CF_3 groups will migrate to the two surfaces of the silicone film and will segregate. Because of the high density of the CF_3 groups in the perfluoroether, it is possible to obtain a silicone surface with very low surface energy simply by adding very small quantities of perfluoroether. Perfluoroether allylamide ($F(CFCF_3CF_2O)_7CFCF_3CONHCH_2CH=CH_2$, PFE) added to curing PDMS (0.3–1.5 weight%) lowered the surface energy of PDMS from 19 to 8 mJ m^{-2}.[9] The PFE molecules added to the PDMS are chemically bonded to the silicone network by the platinum-catalyzed hydrosilation reaction.[9] The PDMS films were doped with 1% PFE (that is, 1% of the mass of PDMS), and the films were examined to determine whether they yield favorable results.

To investigate the influence of PFE on the mechanical properties, the linear rheological properties of the pure PDMS and PDMS doped with PFE will be examined. Furthermore, to investigate the changes induced on the surface of the films by the PFE, contact-angle measurements and peel tests on these surfaces have been performed. Dielectric permittivity tests are also conducted to investigate the influence of PFE on permittivity because an increase in the dielectric permittivity would be an advantage for DEAP films and would make it possible to address additional issues beyond process-related problems.[10]

The allyl groups ($-CH=CH_2$) of PFE react with the hydride groups (–Si–H) of the crosslinker (methyl hydrogen siloxane) and compete with PDMS in the hydrosilation reaction. To ensure proper bonding of PFE to the silicone network and complete crosslinking of PDMS, sufficient crosslinker has to be added to the reaction mixture. The effects of the additional crosslinker and platinum catalyst in the reaction mixture are also investigated. Hence, various compositions of crosslinker and catalyst are used in the reaction mixture.

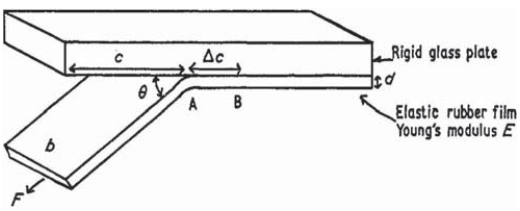

Figure 1 Peeling an elastomer film from a rigid substrate.[8]

EXPERIMENTAL PROCEDURE

Materials

The PDMS elastomer, oil and inhibitor used for the following set of experiments are: (1) Elastosil RT-625 (a commercially available RTV silicone); (2) Powersil Fluid TR50; and (3) Inhibitor PT 88, respectively, obtained from Wacker Chemie AG (München, Germany). The PFE (KDP-4645) was supplied by DuPont Krytox Performance Lubricants (Wilmington, DE, USA).

Carrier web. The carrier webs on which the release property of PDMS film were tested are made of a temperature-stabilized polyethylene terephthalate band (0.2 mm) coated with methyl acrylate UV resin. The surface of the carrier web has microscale corrugations (Figure 2). There are two types of carrier webs used at Danfoss PolyPower A/S (Nordborg, Denmark), depending on whether the corrugation lines are along the length of the web (down-web) or perpendicular to the length of the web (cross-web). In addition, there are two types of carrier webs defined by the wave depth and period. One has a depth of 5 μm and a period of 10 μm (30% web) and is capable of stretching to approximately 35% strain, and the other has both a depth and a period of 7 μm and is capable of stretching up to approximately 80% strain (100% web).[1,11] The carrier web has negligible strain under the present process conditions, and the peel dynamics are not affected.

Instrumentation and specifications

Rheological experiments. Rheological measurements (time sweep and frequency sweep) on the silicone networks were performed with a controlled-stress rheometer AR-2000 (TA Instruments, New Castle, DE, USA).

Contact angle. Contact-angle experiments are performed using the Contact-Angle system (OCA Data Physics, Stuttgart, Germany). The probe liquids are water and hexadecane (product no. H0255) from Sigma-Aldrich (St Louis, MO, USA).

Peel test. Peel tests were performed in Danfoss PolyPower A/S using the Zwick/Roell (Zmart.pro, Ulm, Germany) material tester.

Dielectric permittivity. The dielectric permittivity tests on the samples were performed using a Novocontrol Alpha-A (Novocontrol Technologies GmbH & Co. KG, Hundsangen, Germany), a high-performance frequency analyzer.

Procedure

Preparing the addition-curing PDMS mixture and films. Elastosil RT-625 is supplied as premixes A and B. Premix A is a mixture of vinyl-terminated PDMS and crosslinker, while premix B is a mixture of vinyl-terminated PDMS and catalyst among other components such as fillers. Premixes A and B were mixed in the prescribed proportions (9:1) using the speed mixer DAC 150FVZ-K (Synergy Devices Ltd, Buckinghamshire, UK) for 2 min at 1000 r.p.m. Similarly, samples containing Elastosil RT-625 (9:1), 1% PFE (of the mass of Elastosil RT-625), 15% oil (of the mass of Elastosil RT-625) and 0.8% inhibitor (of the mass of Elastosil RT-625) were also mixed.

Another set of samples was made with Elastosil RT-625, in which A and B are mixed in the ratio 10:1, so that the resultant mixture contains more crosslinker. The amount of PFE added to this mixture was also 1 w/w%. The crosslinker percentage was increased in the second set of samples so that the PFE would have sufficient crosslinker to react with. Oil (15%) and inhibitor (0.8%) were also added to some elastomer samples of this set to investigate the influence of these constituents as well.

To examine the effects of additional catalyst, a new set of samples was made, in which Elastosil RT-625 A and B were mixed in the ratio 9:1.1. PFE (1%), oil (15%) and inhibitor (0.8%) were also added to this set of samples.

Mixing the premixes A and B of Elastosil RT-625 resulted in the hydrosilation reaction of the vinyl-terminated polydimethylsiloxane (PDMS) ($-CH=CH_2$) with the hydride crosslinker ($-Si-H$) in the presence of the platinum catalyst, resulting in a PDMS network. PFE also reacts with the crosslinker when it is present in the mixture (Figure 3). In total, 18 samples were made with varying the composition (Table 1) to investigate the effects of PFE, additional crosslinker and oil on the silicone films. The segregation of PFE in the surface is the same in the film–air interface and the film–substrate interface. The PFE migrates to the surfaces/interfaces of the PDMS film uniformly. Fourier transform infrared spectroscopy curves showing the peaks with the same intensity for PFE on both the interfaces of the PDMS film are presented inSupplementary Figures S2–5.

Rheological tests. To investigate the effects of PFE, additional crosslinker and catalyst on the mechanical properties of Elastosil RT-625, rheological tests were performed.

Time sweep. Time sweeps of 18 samples (Table 1) were performed at 2% strain, at temperatures of 23 and 80 °C and at a frequency of 1 Hz. The applied strain (2%) was designed to be within the linear regimen of the material. Samples with the inhibitor were cured at 80 °C because the inhibitor inhibits curing at room temperature. Samples without the inhibitor were cured at 23 °C.

Frequency sweep. Mechanical characterization (frequency sweeps) of the 18 samples was performed by making LVE measurements. Films with a thickness of 1 mm (1000 μm) were prepared with the 18 sample mixtures. After complete curing, the films were cut to make 25 mm diameter discs. LVE measurements on these samples were performed from a frequency of 100–0.001 Hz with 2% strain (which we ensured was within the linear regimen of the material based on an initial strain sweep) using the 25 mm aluminum parallel plate geometry at 25 °C. The normal force applied by the aluminum disc on the sample was 5–10 N.

Contact-angle tests. As described above, addition-curing mixtures were prepared with the 18 different compositions. Films with a thickness of 1 mm were made on a flat substrate. Once fully cured, the contact angles of the films were tested.

Advancing and receding contact-angle experiments were performed on the 18 samples using water as the probe liquid. Static contact-angle measurements were made with hexadecane as the probe liquid. Because hexadecane swells the

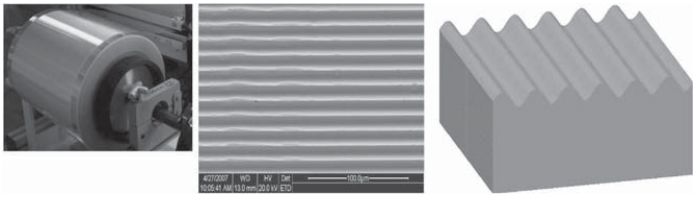

Figure 2 The microscale corrugations on the carrier web.[1] A full color version of this figure is available at *Polymer Journal* online.

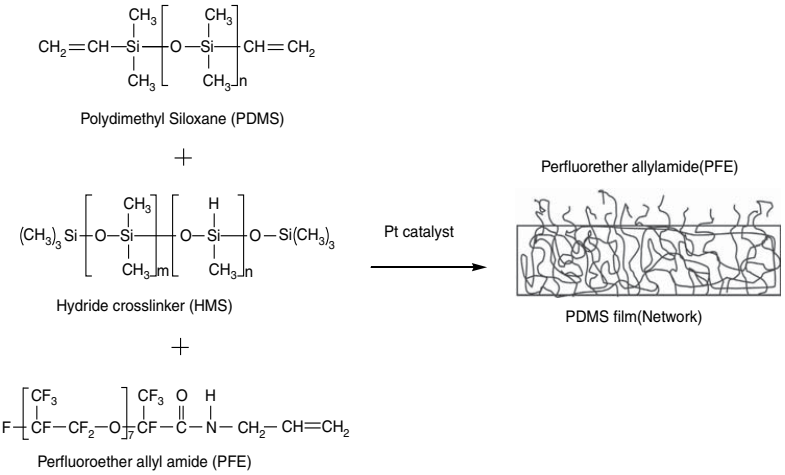

Figure 3 Modification of the polydimethylsiloxane (PDMS) network with perfluoroether allylamide (PFE) (hydrosilation reaction).[9]

Table 1 Composition of the 18 samples and their properties

Sample no.	Elastosil (A:B)	PFE (ww %$^{-1}$)	Inhibitor (ww%$^{-1}$)	Oil (ww%$^{-1}$)	Temperature (°C)	GP (min)	t_{97}(min)	G′(ω → 0) (MPa)	E = 3G (MPa)	Contact angle with n-hexadecane	Surface energy (mN m^{-1})	Max. peel force 'F' (N mm^{-1})	Average peel force (N mm^{-1})	Adhesive energy 'R' (N m^{-1})
1	9:1	—	—	—	23	65.8	780	0.19	0.57	32.5	23.3	0.015	0.007	16.1
2	9:1.1	—	—	—	23	53.9	317	0.06	0.18	28.2	24.3	0.017	0.009	27.0
3	9:1	1	—	—	23	50.5	406	0.06	0.18	55.0	17.0	0.018	0.008	34.2
4	9:1.1	1	—	—	23	54.7	789	0.05	0.15	60.1	15.1	0.016	0.009	32.3
5	9:1	1	0.8	15	80	5.2	52.2	0.05	0.15	57.0	16.4	0.014	0.009	28.0
6	9:1.1	1	0.8	15	80	4.4	67.8	0.03	0.09	63.8	14.3	0.023	0.014	73.9
7	9:1	1	0.8	—	80	4.4	19.8	0.06	0.18	61.0	15.1	0.019	0.013	37.8
8	9:1	1	—	15	23	77.3	1012	0.025	0.08	55.2	16.9	0.011	0.007	39.7
9	9:1.1	1	0.8	—	80	5.5	42.6	0.05	0.15	56.3	16.5	0.018	0.010	41.4
10	9:1.1	1	—	15	23	80.3	826	0.09	0.28	52.5	17.8	0.012	0.007	15.4
11	9:1	—	0.8	15	80	4.7	37.5	0.04	0.12	28.7	24.2	0.012	0.006	20.9
12	9:1.1	—	0.8	15	80	3.4	30.3	0.034	0.10	44.0	20.3	0.022	0.013	61.7
13	10:1	—	—	—	23	45.9	454	0.04	0.12	47.8	19.4	0.016	0.010	26.9
14	10:1	1	—	—	23	51.5	1246	0.09	0.27	42.2	20.8	0.016	0.008	19.2
15	10:1	1	0.8	15	80	7.9	87.5	0.04	0.12	53.9	17.4	0.013	0.009	29.6
16	10:1	1	0.8		80	7.2	50.8	0.074	0.22	56.9	16.4	0.018	0.011	27.3
17	10:1	1	—	15	23	62	679	0.03	0.09	49.0	18.9	0.012	0.008	36.0
18	10:1	—	0.8	15	80	6.9	61	0.05	0.15	30.3	23.9	0.012	0.009	21.4

Abbreviation: GP, gel point.

surface of the PDMS films, the contact-angle measurements were made within 5–10 s of the drop coming into contact with the film.

Peel tests. Peel tests were performed on the 18 samples to estimate the peel force and the adhesive force. Films with a thickness of 100 μm were made on the 30% down-web with the addition-curing mixtures using a 3540 bird film applicator (Elcometer, Aalen, Germany). The dimensions of the samples were $30 \times 30\,mm^2$. Once the films were fully cured on the carrier web, they were tested for peel force with a peel angle of 90°. A peel curve was obtained from plotting the peel force versus the length of sample peeled.

Dielectric permittivity. For the permittivity tests, films with a thickness of 1 mm were made from the 18 addition-curing mixtures, and once fully cured, discs with a diameter of 25 mm were cut from the films. They were then tested for their dielectric permittivity.

RESULTS AND DISCUSSION

Rheological tests

Time sweeps. The time sweeps of samples 6 and 12 are shown in Figure 4; these samples show the greatest deviation because they contain the highest (1%) and lowest (0%) amounts of PFE, respectively. After the onset of the hydrosilation reaction, the PDMS network approaches chemical gelation. A crosslinking polymeric system is said to reach its gel point at a critical extent of the crosslinking reaction at which either the weight-average molecular weight diverges to infinity (infinite sample size) or the first macromolecular cluster extends across the entire sample (finite sample size).[12,13] The gel point that is at the crossover between G' and G'' is an important processing parameter for DEAP materials; for more details, see Bejenariu *et al.*[10] Chambon and Winter[12] and Winter.[13] The addition of PFE to the Elastosil RT-625 does not modify the gel point significantly. From the results, it can be concluded that the addition of 1 w/w% PFE does not lead to any changes in the process conditions for the RTV rubber, which is very favorable for the process.

Frequency sweeps. The frequency sweeps of samples 6 and 12 are compared in Figure 5. Again, these are the samples showing the most deviation because they contain 1 and 0% PFE, respectively. From the frequency sweeps (Figure 5), it is evident that the storage modulus G' of pure Elastosil RT-625 film is not greatly influenced by the addition of PFE. The addition of PFE lowers the elastic modulus by a few percent, which is within the experimental uncertainty of the measurements, but the increase in G'' with the addition of PFE confirms that there is a small but still fairly insignificant decrease in the elasticity of the material with PFE. The deviation in G'' is much clearer because the magnitude of G'' is dominated by the very small sol fraction. In contrast, G' is dominated by the elastically active material.[14]

In Table 1, the elastic moduli of all the samples G' ($\omega \to 0$) and other process-related properties, such as the time for the material to obtain 97% of its final strength (t_{97}) and the crossover point of G' and G'', are tabulated. The t_{97} is also an important parameter for many processing considerations because it may be overly expensive to wait for the last 3% of reaction, which proceeds very slowly, and in the case of fairly stoichiometric networks, does not influence the elasticity significantly.

Contact-angle and surface energy

Advancing and receding water drop. Advancing and receding water contact-angle experiments were performed on the 18 samples. The Elastosil RT-625 samples without PFE had an average water contact angle of 110°, which is characteristic of PDMS.[2] Samples with 1 w w%$^{-1}$ PFE had an average water contact angle of 115°. The results/experimental data from the contact-angle tests are presented in Supplementary Figure S1.

Static contact angle with n-hexadecane. The static contact angles measured with *n*-hexadecane are tabulated in Table 1.

Fowkes' method to calculate the surface energy:[15]

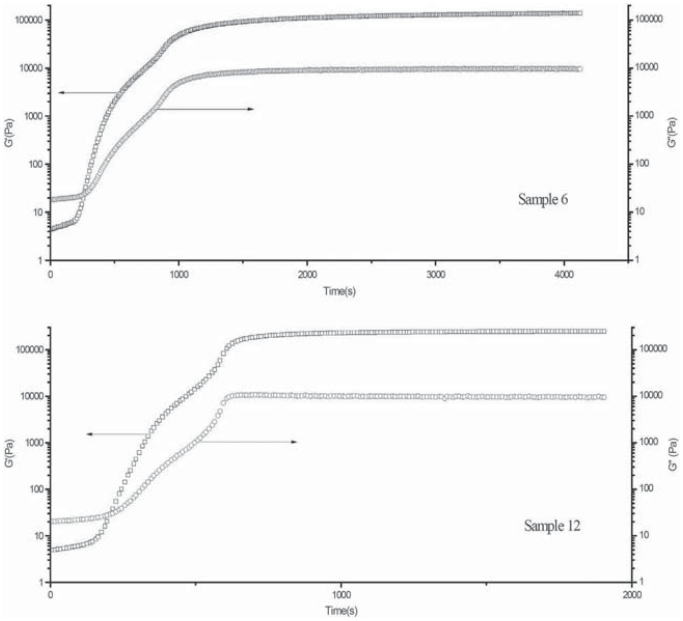

Figure 4 Curing profiles of sample 6 (Elastosil (9:1.1) + oil (15%) + inhibitor (0.8%) + perfluoroether allylamide (PFE) (1%)) and sample 12 (Elastosil (9:1.1) + oil (15%) + inhibitor (0.8%)) at 80 °C. A full color version of this figure is available at *Polymer Journal* online.

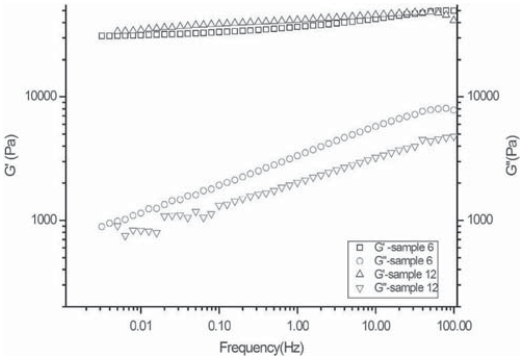

Figure 5 Frequency sweeps of sample 6 (Elastosil (9:1.1) + oil (15%) + inhibitor (0.8%) + perfluoroether allylamide (PFE) (1%)) and sample 12 (Elastosil (9:1.1) + oil (15%) + inhibitor (0.8%)) at 23 °C. A full color version of this figure is available at *Polymer Journal* online.

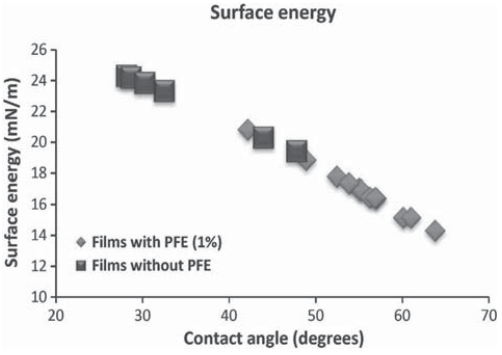

Figure 6 Surface energies calculated using Fowke's method. A full color version of this figure is available at *Polymer Journal* online.

According to the Fowkes' method, the surface energy of a solid surface (S) can be calculated using the contact angle of a liquid (L) using a simple formula:

$$\frac{\sigma_L(cos\theta+1)}{2}=\sqrt{\sigma_S^P}\sqrt{\sigma_L^P}+\sqrt{\sigma_S^D}\sqrt{\sigma_L^D} \quad (2)$$

where $\sigma_L=\sigma_L^D+\sigma_L^P$, σ is the surface energy (surface tension), P denotes the polar component of the surface tension and D is the dispersive component of the surface tension.

When we use a liquid whose polar component is zero, the surface tension of the liquid will then be $\sigma_L=\sigma_L^D$. Hence, Equation (2) will become

$$\sigma_S^D=\frac{\sigma_L(cos\theta+1)^2}{4} \quad (3)$$

Thus, using the contact angles of a polar liquid, such as water, and a nonpolar liquid, such as *n*-hexadecane, one can estimate the surface energy of a solid using Equations (2) and (3). The results are tabulated in Table 1. The samples doped with PFE have a markedly lower surface energy than the pure Elastosil RT-625 samples (Figure 6).

Figure 6 shows a comparison of the surface energy with the contact angle of *n*-hexadecane. Films with PFE have a higher contact angle with *n*-hexadecane and a lower surface energy compared with the films without PFE. However, samples 12, 13, 14 and 17 (20.3, 19.4, 20.8 and 18.9 mN m^{-1}, respectively) have almost similar surface energy values; samples 14 and 17 contain PFE, and samples 12 and 13 do not contain PFE.

Peel tests

A peel curve obtained from the peel test of sample 3 is shown in Figure 7. The peel force F (N mm^{-1}), which is the force used in peeling a width of 1 mm of the sample, is plotted against the length of the sample that is being peeled. From the peel curve, we see that F increases to a maximum value and then falls to a low constant value. From examining the F values of the samples, it is observed that samples 6 and 12 with 15% oil and 0.8% inhibitor have the maximum F values. Samples 5, 8, 10, 11, 15, 17 and 18, all of which contained 15% oil, have low F values compared with the average of 0.0157 N mm^{-1}. In contrast, samples 7, 9 and 16, which contain 0.8% inhibitor (without oil), had higher F values than the average of 0.0157 N mm^{-1}. The presence of oil in the addition curing mixtures certainly makes the release easier because it acts like a release agent. The values of the maximum and constant peel force of all samples are tabulated in Table 1.

In Figure 8, the surface energy and the F of the samples are plotted. It is observed that the samples with a low surface energy and those with a high surface energy both have similar patterns with F. The reduction of surface energy of the samples did not reduce or affect their F. Because the carrier web is very thick and rigid, the stretching of the web is never observed during the experiments.

Calculation of adhesive force 'R'. Using the peel Equation (4), the adhesive energy R is calculated [8]

$$E\left(\frac{F}{b}\right)^2\frac{1}{2dE}+\left(\frac{F}{b}\right)(1-\cos\theta)-R=0 \quad (4)$$

$$E=2G(1+\upsilon)\prime \quad (5)$$

where G is the static shear modulus and υ is the Poisson ratio.

F is obtained from the peel tests, and E is calculated from Equation (5). The value of G $(G=G'(\omega\rightarrow 0))$[16] is obtained from the frequency sweeps (Table 1) of the rheological tests and the Poisson ratio (υ) for silicone elastomers (rubber), which was taken as 0.5. The maximum value of F is used for all calculations to estimate the maximum R between the film and the substrate during the processing. A comparison of samples 2 and 12 clearly shows that as E increased, R decreased. (Sample 2 has $F=0.016$ N mm^{-1}, $E=0.18$ MPa and the calculated $R=27$ N m^{-1}. Sample 12 has $F=0.022$ N mm^{-1}, $E=0.10$ MPa and the calculated $R=61.7$ N m^{-1}.)

From Figures 9 and 10, one can understand the relationship between E, R and F. From Figure 9, it is observed that as F increased, the value of R also increased. To lower the peel force, the adhesive energy needs to be lowered. From Figure 10, it is observed that R and E are inversely related, in accordance with Equation (1). As the E value of the samples increased, their R value decreased, thus making their release easier. Although the surface energy, F and R at the interface are related through the action of surface forces, the relationship is not obvious.[17] The relationship between F, R, E and release can be understood further from the theory proposed by Johnson *et al.*[17] Every surface has a surface energy resulting from the action of surface forces. When two surfaces are in intimate contact, these surface forces act as attractive (adhesive) forces. The strength of the attractive (adhesive) force between two surfaces depends on the contact surface area.[17] Interfacial gaps due to surface asperities or dust particles will strongly influence the adhesion between the surfaces because the attractive forces decrease rapidly with increasing separation.[17] Materials with a low elastic modulus will even out easily against a substrate and make very good contact. Therefore, they are strongly adhered to the substrate.[17] Hence, to peel the film off, one needs to overcome the adhesive forces and apply a high F. To make the release easier, the contact at the interface needs to be reduced to prevent the surfaces from adhering strongly. That is what release agents such as oils and surfactants do, namely, reducing the strength of the contact to ease the release of a surface from another surface. In contrast, materials with a high Young's modulus will not flatten out against another surface and cannot make intimate contact and hence experience a lower adhesive force.

Dielectric permittivity

In Figure 11, the dielectric permittivity $(\varepsilon=\varepsilon^{\dagger\prime}+i\varepsilon'')$ of samples 1, 3, 5, 13, 14 and 15 is shown. The dielectric constant is essential

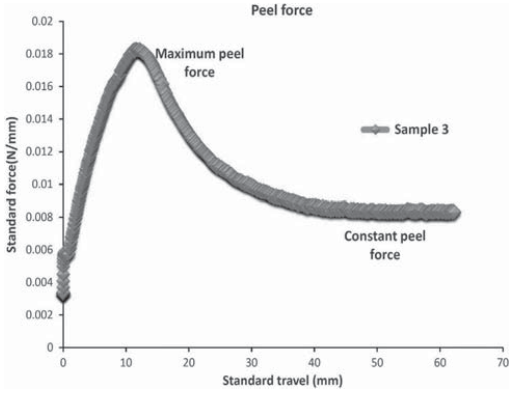

Figure 7 Typical peel curve. A full color version of this figure is available at *Polymer Journal* online.

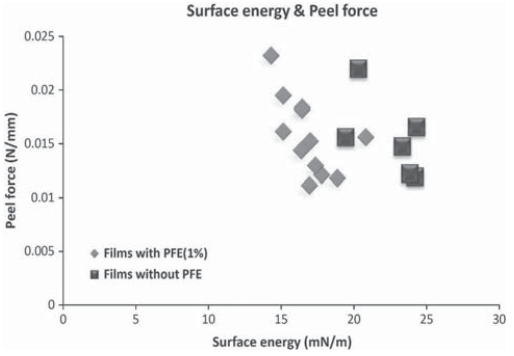

Figure 8 Comparison of the surface energies of the samples with peel force F. A full color version of this figure is available at *Polymer Journal* online.

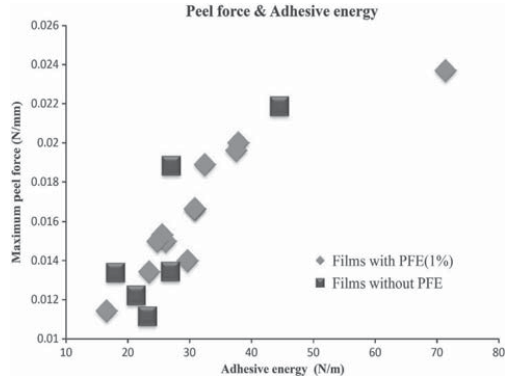

Figure 9 Relationship between the adhesive energy *R* and the peel force *F*. A full color version of this figure is available at *Polymer Journal* online.

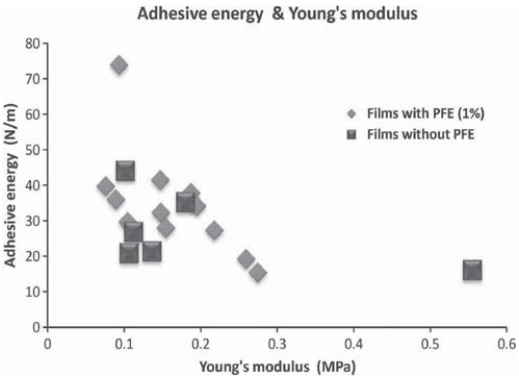

Figure 10 Relationship between the adhesive energy *R* and Young's modulus *E*. A full color version of this figure is available at *Polymer Journal* online.

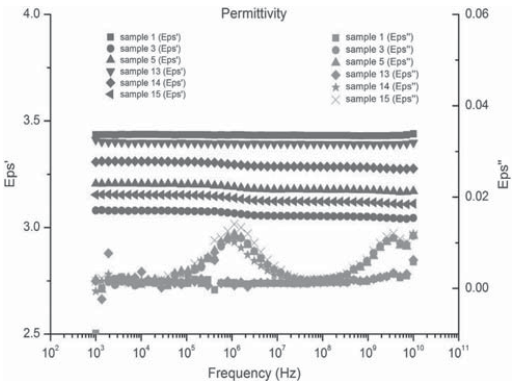

Figure 11 Dielectric permittivity test ($Eps' = \varepsilon'$ and $Eps'' = \varepsilon''$). A full color version of this figure is available at *Polymer Journal* online.

information when designing capacitors or, in our case, an actuator, which operates according to the same principle as a capacitor.

The permittivity (ε) value of PDMS films used in our experiment is usually approximately 3.2.[10] The tests conducted confirmed that the ε values of the samples were not greatly influenced by PFE addition and were well within the allowed limits. The variation in ε was in the range of 3.1–3.4 (Figure 11). In addition, the low variation in permittivity values can be attributed to the addition of oil and inhibitor.

CONCLUSIONS

PDMS was doped with 1% PFE to lower the surface energy, and as expected, the surface energy was lowered. The addition of PFE to the Elastosil RT-625 did not greatly influence the storage modulus G', as observed from the time sweeps. The dielectric permittivity of the samples was also not modified by the addition of PFE. Elastosil RT-625 doped with PFE has a high contact angle in the advancing drop. When the drop is receding, the surface behaves more hydrophilic than the pure Elastosil RT-625 films. This can be due to the presence of high-energy moieties near the surface. The amide groups immediately beneath the surface are highly polar and hence become exposed when water (polar liquid) comes into contact with the surface.[9]

Although the surface energy decreased with the addition of PFE, the peel force values did not decrease. The reason for this is that the elastic contribution to the peel force is markedly higher than the potential and the surface energy contribution. For the investigated elastomer films, the Young's moduli are low, which causes the films to easily smooth out over surfaces and make good contact. This contact increases the adhesive forces, making the release difficult. The samples with a low Young's modulus have a higher adhesive energy between the film and the substrate than those with a higher Young's modulus. Therefore, tuning the elasticity of the networks is actually the easiest path for decreasing the release problems of thin silicon films when other solutions such as using a release agent are not an option.

ACKNOWLEDGEMENTS

We gratefully acknowledge the financial support from the Danish National Advanced Technology Foundation.

1 Yoseph, B. C. & Wallmersperger, T. (Eds). SPIE press. Proc. SPIE 7287, Electroactive Polymer Actuators and Devices (EAPAD) 2009, 72870R (06 April 2009); doi:10.1117/12.815741 San Diego, CA | March 08, 2009.
2 Kuo, A. C. M. *Poly (Dimethylsiloxane). Polymer Data Handbook* 411–435 (Oxford University Press, Oxford, 1999).
3 Koberstein, J. T., Duch, D. E., Hu, W., Lenk, T. J., Bhatia, R., Brown, H. R., Lingelser, J. P. & Gallot, Y. Creating smart polymer surfaces with selective adhesion properties. *J. Adhes.* **66,** 229–249 (1998).
4 Lautrup, B. *Physics of Continuous Matter.* 2nd edn. Exotic and Everyday Phenomena in the Macroscopic World. ISBN: 9781420077001 (CRC Press, New York, 2011).
5 Thouless, M. D., Yang, Q. D. & Arbor, A. A parametric study of the peel test. *Int. J. Adhes. Adhes.* **28,** 176–184 (2008).
6 Jouwersma, C. Notes: on the Theory of Peeling. *J. Polym. Sci.* **XLV,** 253–255 (1960).
7 Newby, B. Z. & Chaudhury, M. K. Friction in adhesion. *Langmuir.* **7463,** 4865–4872 (1998).
8 Kendall, K. Thin-film peeling—the elastic term. *J. Phys. D* **8,** 1449–1452 (1975).
9 Thanawala, S. K. & Chaudhury, M. K. Surface modification of silicone elastomer using perfluorinated ether. *Nature* **16,** 1256–1260 (2000).
10 Bejenariu, A. G., Boll, M., Lotz, M. R., Vraa, C. & Skov, A. L. New elastomeric silicone based networks applicable as electroactive systems. *Proc. SPIE, Int. Soc. Opt. Eng.* **7976,** 79762V–79762V-8 (2011).
11 Yoseph, B. C. (Ed). SPIE press. Electroactive Polymer Actuators and Devices (EAPAD): 7642. San Diego, CA, USA: Proc. of SPIE, 2010: 764231-1–764231-11.
12 Chambon, F. & Winter, H. H. Linear viscoelasticity at the gel point of a crosslinking PDMS with imbalanced stoichiometry. *J. Rheol.* **31,** 683–697 (1987).

13 Winter, H. H. Can the gel point of a cross-linking polymer be detected by the G'–G'' crossover? *Polym. Eng. Sci.* **27,** 1698–1702 (1987).
14 Frankær, S. M. G., Jensen, M. K., Bejenariu, A. G. & Skov, A. L. Investigation of the properties of fully reacted unstoichiometric polydimethylsiloxane networks and their extracted network fractions. *Rheol. Acta.* **51,** 559–567 (2012).
15 Fowkes, F. M. Attractive forces at interfaces. The Interface Symposium-5. *Ind. Eng. Chem.* **56,** 40–52 (1964).
16 Morrison, F. A. *Understanding Rheology.* ISBN13: 9780195141665. (Oxford University Press, Oxford, 2001).
17 Johnson, K. L., Kendall, K. & Roberts, A. D. Surface energy and the contact of elastic solids. *Proc. R. Soc. A* **324,** 301–313 (1971).

Supplementary Information accompanies the paper on Polymer Journal website (http://www.nature.com/pj)

Appendix II

Methods to ease the release of thin polydimethylsiloxane films from difficult substrates

Polymers for advanced technologies (2013)

polymers advanced technologies

Received: 13 September 2013, Revised: 08 November 2013, Accepted: 08 November 2013, Published online in Wiley Online Library: 18 December 2013

(wileyonlinelibrary.com) DOI: 10.1002/pat.3236

Methods to ease the release of thin polydimethylsiloxane films from difficult substrates

Sindhu Vudayagiri and Anne Ladegaard Skov*

Silicone elastomers are used as dielectric electroactive polymers for making actuators, generators, sensors, and as artificial muscles in medical applications. Current requirements in the actuator manufacturing put a strict limitation on the thickness of the elastomers, such that a maximum permissible thickness is around 25–50 μm. The relatively small Young's modulus for these elastomers is a requirement for actuation capabilities. However, peeling and release of such films during manufacture processes are very difficult. To ease the release of the films, techniques such as the use of release agents like surfactants and detergents, incorporating resins in the silicone matrix and grafting/adding low surface energy functionalities to the silicone elastomer have been tested. The methods used are required not to interfere with the Young's modulus and the dielectric permittivity in a negative way. Polysorbate-20, a non-ionic surfactant, fulfills all requirements and gives the lowest peel forces for the films.

Keywords: dielectric electroactive polymers; release; peel force; surfactants; polydimethylsiloxane films

INTRODUCTION

Dielectric electroactive polymers (DEAPs) are now widely used in different applications where various processing techniques such as spin coating procedures, 3D printing, as well as large-film productions are used to give the required size, shape, and geometry to the elastomer films. The latter process still needs improvement for the realization of fast, reliable production. Danfoss PolyPower A/S has established a large-scale manufacturing process for making DEAP films.[1] The manufacture process involves the coating of elastomer mixture (polydimethylsiloxane [PDMS] + cross-linker + Platinum catalyst) on a carrier web (roll) to make a thin film of thickness 25–50 μm. The carrier web is 20 cm in width and moves at an approximate speed of 2.5 m/min in the roll to roll process. The carrier web has micro-scale corrugation lines on the surface on which the elastomer is coated. The carrier web with the elastomer coating is then heated in an oven to approximately 100°C for 2 min to cure the elastomer mixture.[1] The elastomer cures by hydrosilylation reaction to form an elastomer network (Fig. 1). The cured elastomer film is then peeled from the carrier by a delaminator at a speed of 1 m/min. The micro-structures on the carrier web are imprinted on the film as it cures. The flat surface of the peeled film is transferred to a nonwoven backer with the corrugated surface facing upwards. Electrode material, usually silver, is then deposited on the films by vacuum deposition. The entire manufacture process is performed in a clean room environment in order to minimize defects in the fabricated elastomer films, which may manifest themselves as breakdown voltage failures.[1] The release and peeling of the films from carrier webs in the delaminator may also induce some defects in the film if the peel force is high enough to induce pre-strain. The peeling in a delaminator is much different from that of a lab scale peeling by hand. The speed of the delaminator equipment and force with which the film is peeled have to be optimized to produce films without defects or uncontrollable pre-strain. Reducing the delamination speed, which is already quite low, is not economically viable as the production line needs to operate at a profitable speed. Hence, reducing the peel forces and making release easy are a prime focus. Though PDMS has a surface energy of 19–21 mJ/m,[2] the films made from the silicone systems stick too well to the substrate/carrier web owing to their low Young's modulus and thin geometry.[3] Furthermore, because the surface of the carrier web consists of micro-scale corrugations, the surface area is significantly high requiring high-peel force to remove the PDMS film. Detergents and non-ionic surfactants are tested as release agents such as Akuta®, Polysorbate-20, Triton X-100, Cetomacrogol-1000, and Tergitol®. To reduce the strain induced on the film during the peeling, release agents are good alternatives to minimize the peel force. Non-ionic surfactants are chosen in this case, in order to avoid ionization of the surfactant under electric field because the application of films as actuators requires use of high voltage. Another option for improving the process is of course to reinvent the process such as applying embossing where the elastomer is not cured on the corrugated web[4,5] and thus avoiding release problem. One of possible solution can be the addition of highly cross-linked silicone resins (ex: Belsil® TMS 803), which can be compounded with PDMS. Such resins make the films more

* *Correspondence to: Anne Ladegaard Skov, The Danish Polymer Centre, Department of Chemical and Biochemical Engineering, Technical University of Denmark, 2800 Kgs. Lyngby, Denmark.*
E-mail: al@kt.dtu.dk

S. Vudayagiri, A. L. Skov
The Danish Polymer Centre, Department of Chemical and Biochemical Engineering, Technical University of Denmark, 2800 Kgs. Lyngby, Denmark

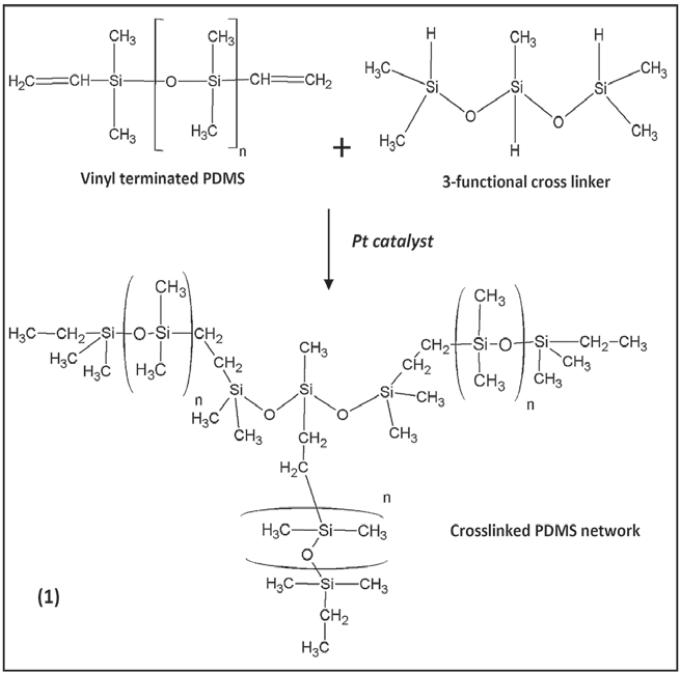

Figure 1. Hydrosilylation reaction.

hydrophobic and less sticky. Finally, when electrode materials with sufficient high conductivity and stretch ability become available, the corrugations will not be required anymore.

Surface energy, surface tension, and interfacial tension

To understand the surface energy of any surface, one should be familiar with the surface physics. Consider the surface of a polymer film. The molecules in the bulk are bound in all directions by the neighboring molecules, whereas the molecules sitting on a free surface of the film will be bound by lesser molecules than those in the bulk as illustrated in Fig. 2(a).[6] The energy with which a molecule is bound to the neighboring molecules is called the binding energy. Because the surface molecules are not bound by as many molecules as those in the bulk, they have less energy binding them than the bulk molecules. This missing (negative) binding energy can be viewed as a positive energy added to the free surface.[6] External forces

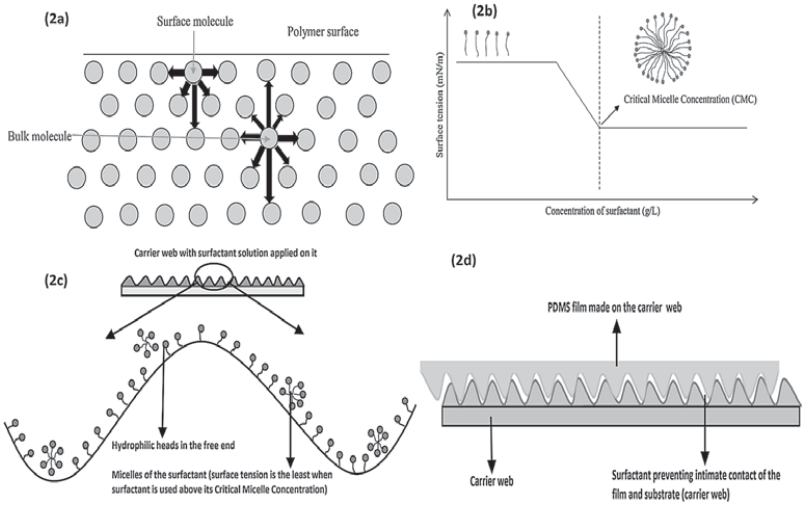

Figure 2. (a) The binding energy of surface and bulk molecules, (b) critical micelle concentration of a surfactant, (c) surfactant on carrier web, and (d) polydimethylsiloxane film on the treated carrier web. This figure is available in color online at wileyonlinelibrary.com/journal/pat

must perform positive work against internal surface forces to increase the area of a surface. These internal surface forces are called surface tension defined as the normal force per unit area.[6] Interfaces between solids and liquids or between solids and solids are not required to have positive interfacial energy density. Even if they have a negative interfacial energy density, they will not mix, but this might lead to adhesion, or the materials will stick too well at the interfaces.[6]

When the strength of the adhesive forces between opposing molecules at the interface is higher, the two materials tend to stick well with each other. The strength of the attractive (adhesive) force between two surfaces depends on the contact surface area.[7] Interfacial gaps due to surface asperities or dust particles will strongly influence the adhesion between the surfaces because the attractive forces decrease rapidly with increasing separation.[7]

Relationship of peel force, Young's modulus, and adhesive force

The PDMS films manufactured for DEAP purposes are approximately 25–50 μm in thickness. These films have a low Young's modulus of approximately 500 kPa. The peel force required to peel such a film from a substrate is a complex function of geometry, the Young's modulus of the film and the substrate, thickness of the film, interfacial cohesive properties, and also the friction between the surfaces. The cohesive/adhesive forces at the film and substrate interface increase as the Young's modulus of the film decreases. Materials with low elastic modulus even out more easily against a substrate and thus make very good contact. Therefore, they strongly adhere to the substrate.[7] As the cohesive forces at the interface increase, the peel force required to peel the film also increases.[3,7] For the processing of thin-corrugated films, the geometry depends strongly on the position where the film is exposed to very different alternating forces.

Addition/grafting of surface-active functionalities

The presence of strong adhesive forces between the films and substrates cannot be avoided in some practical applications which require soft (low Young's modulus) PDMS films. Addition of surface-active block copolymers can make the film selectively non-adhesive or adhesive to a particular substrate[8] and ease the release. When perfluoroether allylamide ($F(CFCF_3CF_2O)_7CFCF_3CONHCH_2CH{=}CH_2$, PFE)[9] is added in small quantities of 0.5–1.5%, the surface energy of the PDMS films decreased from 19 to 8 mJ/m, making the films more hydrophobic. Similarly, grafting functionalities such as bis(trifluoromethyl)phenyl into PDMS network via cross-linkers also made the films more hydrophobic as the water contact angle of PDMS films increased from 110° to 116°.[10] Increasing the hydrophobicity of films will make them poorly adhering to certain substrates and might help ease the release. All these methods of incorporating surface-active functionalities are expensive, and fluoro compounds are not environmentally friendly materials. These methods require advanced chemistry and will increase the price of the elastomer. Furthermore, the migration of the covalently attached surface-active functionalities to the surfaces of the elastomers may be very unfavorable because the deposition of electrodes may become very difficult, and the electrodes may no more be well connected to the elastomer.

Teflon coating on the difficult substrates

The substrates on which the films are made can be treated with polytetrafluoroethylene or Teflon or ceramic non-stick coatings or can be metallized to make the release easy. The substrate in our case has micro-scale corrugation lines (5–7 μm in height and 7–10 μm in period).[1,11] Coating Teflon on a micro-structured surface will interfere with the corrugation pattern, hence, a very thin Teflon coating with 100% coverage is required. Such coatings may not be durable, and one minor defect may destroy the film as the film can be easily torn apart. Also, these coatings are expensive considering the miles of carrier web being used for the manufacture process.

Surfactants

Surfactants are substances that reduce the surface tension of the liquid in which they are dissolved in. Surfactants also reduce the interfacial tension between two liquids. Surfactant molecules have a hydrophilic head and hydrophobic tail. The different types of surfactants are (i) non-ionic, (ii) anionic, (iii) non-ionic, and (iv) zwitterionic (amphoteric).

Surfactants in aqueous solution orient themselves to form micelles, and the concentration at which the micelles appear is called critical micelle concentration, CMC (Fig. 2(b)). At concentrations beyond the CMC, the surface tension attains a constant value. By application of surfactant on the carrier web (Fig. 2(c)), the adhesive forces at the interface between the film and carrier web will be reduced (Fig. 2(d)).[3] By using a surfactant concentration more than CMC, we ensure an effective coverage on the carrier wed and reduction of the interfacial tension (Fig. 2(c)). CMCs can be determined by various methods such as fluorescence spectroscopy, ultraviolet absorption spectroscopy, and the electrical conductivity method to name a few.[12–15]

EXPERIMENTAL

Materials

Detergent and non-ionic surfactants

The detergent tested is Akuta dish washing machine cleaning liquid.

The non-ionic surfactants tested are as follows:

1. Polysorbate-20 (Polyoxyetheylene (20) sorbitan monolaurate) from Sigma-Aldrich, St. Louis, MO, USA. The molecular mass of Polysorbate-20 is 1227.54 g/mol. The CMC of Polysorbate-20 is 0.06 mg/ml.[16]
2. Triton™ X-100 (Polyethyleneglycol tert-octylphenyl ether) from Sigma-Aldrich, St.Louis, MO, USA. The molecular mass of Triton X-100 is 647 g/mol. The CMC of Triton is 0.129–0.582 mg/ml.[17]
3. Tergitol® solution (Nonylphenol Ethoxylate) NP-40s from Sigma-Aldrich, St.Louis, MO, USA. The molecular mass of Tergitol is 1982.47 g/mol. The CMC of tergitol is 0.232 mg/ml.[18]
4. Cetomacrogol-1000 (Polyethylene glycol monocetylether, PO841) from Tokyo Chemical Industrial Co. Ltd., Kita-ku, Tokyo, Japan. The molecular mass of cetomacrogol is 1123.5 g/mol. The CMC of cetomacrogol is 0.0063 mg/ml.[19]

Figure 3(a)–(d) show the chemical structures of the surfactants used.

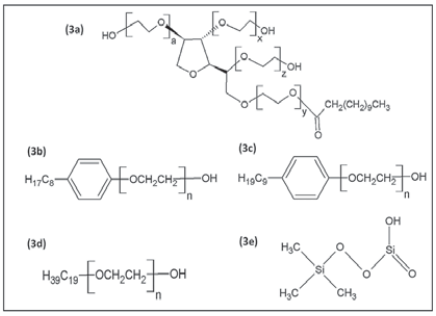

Figure 3. (a) Polysorbate-20, (b) Triton X-100, (c) Tergitol NP40, (d) Cetomacrogol-1000, and (e) Belsil TMS 803.

Silicone networks

1. Elastosil® *RT 625* (Room temperature vulcanizable silicone), Powersil Fluid TR50, and Inhibitor PT 88, respectively, were obtained from Wacker Chemie AG, Germany. Elastosil is supplied as two parts, part A is a mixture of vinyl terminated PDMS and cross-linker while Premix B is a mixture of vinyl terminated PDMS and catalyst among other components such as fillers. The mixing ratio of Elastosil is 9:1. The oil added is 15%, and inhibitor is 0.8% by mass of the elastomer mixture.
2. Elastosil® *LR 3043/50* (Liquid Silicone Rubber [LSR or LR]) was obtained from Wacker Chemie AG, Germany. OS-20 (an ozone-safe volatile methylsiloxane fluid) was obtained from Dow Corning®, USA. Elastosil is supplied as two parts, A and B. The part A has PDMS and platinum catalyst, and part B has the PDMS cross-linker. The mixing ratio of Elastosil A, B, and OS-20 is 5:5:7 by mass.
3. POWERSIL® XLR® 630 A/B (a low viscosity LSR) and Belsil® TMS 803, a resin, were both obtained from Wacker Chemie AG, Germany. XLR630 is supplied as two parts, A and B. The part A has PDMS and platinum catalyst, and part B has the PDMS cross-linker. The mixing ratio of parts A and B is 1:1. Belsil TMS 803 is an MQ type silicone resin commonly known as trimethylsiloxysilicate (Fig. 3(e)). It is a white powder with a particle size of 10 μm. It is also mixed in a mass ratio of 1%, 3%, and 5% with XLR 630 mixture.

Carrier web

The substrate on which the films are made is called carrier web. The carrier webs are made of temperature stabilized polyethylene terephthalate band (0.2 mm) coated with methyl acrylate ultraviolet resin. The surface of the carrier web has micro-scale corrugations (Figs 4(a)–(c)). There are two types of carrier webs used at Danfoss PolyPower A/S (Nordborg, DK) depending on whether the corrugation lines are along the length of the web (down-web) or perpendicular to the length of the web (cross-web). Also, there are two types of carrier webs defined by wave depth and period of corrugations: (i) 30% web which has corrugations of depth of 5 μm and a period of 10 μm. The films made on this carrier web are capable of stretching to about 35% strain without the destruction of the metallic electrodes. (ii) 100% web which has both depth and a period of 7 μm. The films made on this carrier web are capable of stretching up to about 80% strain without the destruction of the metallic electrodes.[1,11]

Instrumentation and specifications

Rheological tests

Rheological measurements (frequency sweep) on the silicone films were performed with a controlled stress rheometer AR-2000 (TA instruments, USA).

Peel test

Peel tests were performed using a Zwick/Roell (Zmart.pro, Germany) material tester.

Break down test

Electrical break down tests were performed in Danfoss Polypower A/S on an in-house built device based on international standards (IEC 60243-1 [1998] and IEC 60243-2 [2001]).

Procedure

Preparing the addition curing mixtures and films

Three formulations, namely an RT (room temperature vulcanizing) and two LR (liquid rubber), were tested to compare a relatively soft RT with relatively hard LR formulations.

Elastosil RT 625 is supplied as premixes A and B. Premixes A and B are mixed in the prescribed proportions (9:1) along with inhibitor (0.8%) and silicone oil (15%) using the speed mixer DAC 150FVZ (Hauschild Co., Germany) for 2 min at 1000 rpm. The recipe is commonly used in the industry for making films for actuator application.

Elastosil LR 3043/50 is also supplied as premixes A and B. Premixes A and B along with OS-20 solvent in the ratio (5:5:7) are mixed uniformly using a speed mixer DAC 150 FVZ (Hauschild Co., Germany) for 5 min at 2000 rpm. The LR requires

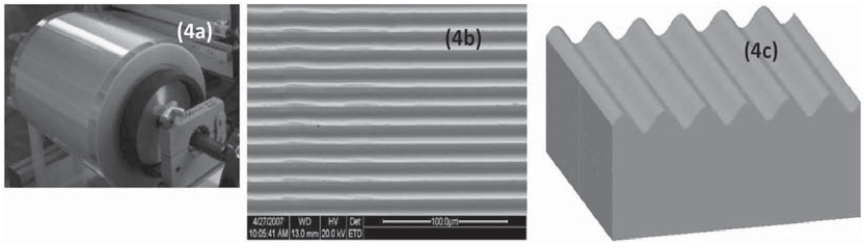

Figure 4. (a) Carrier web as a roll, (b) under the microscope, and (c) 3D schematic of the cross-sectional view of corrugations.[1] This figure is available in color online at wileyonlinelibrary.com/journal/pat

solvent for making it coatable. The LR is not mixed with oil to make it a relatively hard elastomer.

XLR 630 is supplied as premixes A and B. They are mixed in the ratio of 1:1 along with Belsil resin (1%, 3%, and 5%) using the speed mixer DAC 150FVZ (Hauschild Co., Germany) for 2 min at 1000 rpm.

Mixing the premixes A and B of the formulations will result in the hydrosilation reaction of the vinyl terminated polydimethylsiloxane (–CH=CH_2) with the hydride cross-linker (–Si–H) in the presence of the platinum catalyst, resulting in a PDMS network.[20] The XLR is not mixed with oil as well.

The mixtures thus made are coated on the carrier web using a 3540 bird film applicator, (Elcometer, Germany) with 100-μm blade. The webs used for the tests are 100% down carrier webs. Films are cured in the oven for 2 min at 100°C.

Coating carrier web with surfactant

The carrier web is coated with the detergent/surfactant solutions with a soft paper. Pure surfactants are very viscous fluids, and they accumulate on the films as shown in Figs 5(a) and (b). Therefore, the surfactants are diluted with de-ionized water with varying concentrations. Akuta is not a viscous detergent and was tested without any further dilution. The films made on carrier webs coated with 10–20% surfactant solutions do not show much accumulation of surfactants (Figs 5(c) and (d)). Hence, only 10% and 20% surfactant solutions were tested as release agents. The webs coated with surfactant solutions are then dried in the oven for 2 min at 80–100°C. Elastomer mixtures are then coated on these treated webs.

Rheological tests

Linear viscoelastic measurements on the cured silicone films of thickness 1000 μm (made on 1 mm thick frames) and 25 mm diameter are performed from a frequency of 100–0.001 Hz with 2% strain (which is ensured to be within the linear regime of the material based on an initial strain sweep) using the 25 mm aluminum parallel plate geometry at 25°C. The normal force applied by the aluminum disc on the sample is 5–10 N.

Peel tests

The elastomer films made on the surfactant-treated carrier webs were cured in oven at 100°C. The dimensions of the samples used for peel tests are 30 × 30 mm. Once the films are fully cured on the carrier web, they are tested for peel force with a peel angle of 90°. A peel curve is obtained from plotting the peel force versus the length of the sample peeled.

The peel force required to peel an elastomer film from a hard substrate is a complex function of geometry, the mechanical properties of the film and the substrate, thickness of the film, interfacial cohesive properties, and also the friction between the surfaces.[3] Thin-film peeling theory by Kendall[21] is used to calculate the adhesive force R between the rigid substrate and the film.

$$-bR\Delta c + F(1 - cos\theta)\Delta c + \frac{F^2\Delta c}{2bdE} = 0 \qquad (1)$$

The three contributions to the energy changes involved in the peeling process are

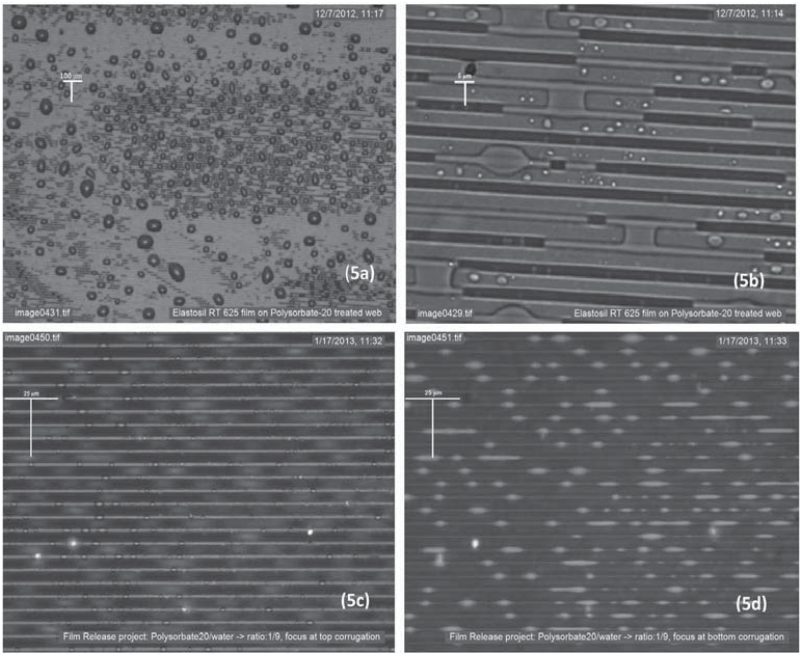

Figure 5. (a), (b) Elastosil RT 625 films made on carrier webs treated with pure Polysorbate-20 solution showing surfactant accumulation in the corrugations. and (c), (d) Elastosil RT 625 films made on carrier webs treated with 10% Polysorbate-20 solution showing reduced surfactant accumulation in the corrugations. This figure is available in color online at wileyonlinelibrary.com/journal/pat

1. Surface energy – due to creation of new surfaces [-$bR\Delta c$]
2. Potential energy – due to the movement of the applied force [$F(1\text{-}cos\theta)$]
3. Elastic energy – due to extension of the film in the direction of the applied force $\left[\frac{F^2\Delta c}{2bdE}\right]$

Here, Δc is a unit length of the film being peeled from the carrier web between the points A and B. The width of the film at any given point is b. The thickness of elastomer film being peeled is d and peeled from a rigid substrate at a peel angle θ with a peel force F. The elastomer has a Young's modulus E. The Young's modulus E of the films can be calculated from the following relations:

$$E = 2G(1+\upsilon)' \tag{2}$$

$$G = G'(\omega \rightarrow 0) \tag{3}$$

The value of G ($G = G'(\omega \rightarrow 0)$)[22] is obtained from the frequency sweeps of the rheological tests. The Poisson ratio (υ) for silicone elastomer, a rubber taken as 0.5.

The maximum F from peel tests is used for all calculations in order to estimate the maximum R between the film and the substrate during the processing.

Dielectric break down tests

The silicone films are made on surfactant treated 100% down carrier webs using a 3540 bird film applicator with 100-μm blade (Elcometer, Germany). The films made on treated webs will have the surfactant on their surfaces. It is necessary to test the influence of these surfactants on the break down strength of the films. The film thicknesses are measured with microscopy of cross-sectional cuts, and the distance between the spherical electrodes is set accordingly with a micrometer stage and gauge. An indent of less than 5% of sample thickness is added to ensure that the spheres were in contact with the sample. The polymer film (30–70 μm) is slid between the two spherical electrodes (radius of 20 mm) as shown in Fig. 6(a), and a stepwise increasing voltage is applied (50–100 V/step) at a rate of 100 V/s. The average breakdown value is found using the Weibull distribution.[23] Each sample is subjected to 10 breakdown measurements, and an average of these values is indicated as the breakdown strength of the sample.

RESULTS AND DISCUSSIONS

Rheological tests

The E values calculated with G′ at the lowest frequency ($\omega \rightarrow 0$) are as follows: (i) Elastosil LR3043/50 is 536 kPa; (ii) Elastosil RT625 is 107 kPa; (iii) XLR 630 with 1% Belsil is 2550 kPa; (iv) XLR 630 with 3% Belsil is 5860 kPa; and (v) XLR 630 with 5% Belsil is 3630 kPa.

Dielectric breakdown

The use of any release agent or technique for easing the release should not lead to a decrease in the dielectric breakdown of the films. Akuta decreased the breakdown strength of the films (Fig. 6(b)) from 82 to 73 V/μm, which is a significant reduction leading to an overall reduction of figure of merit by 20.7%.[24] The Akuta detergent has sodium/potassium cumenesulfonate, which are zwitterionic surfactants with Na^+/K^+

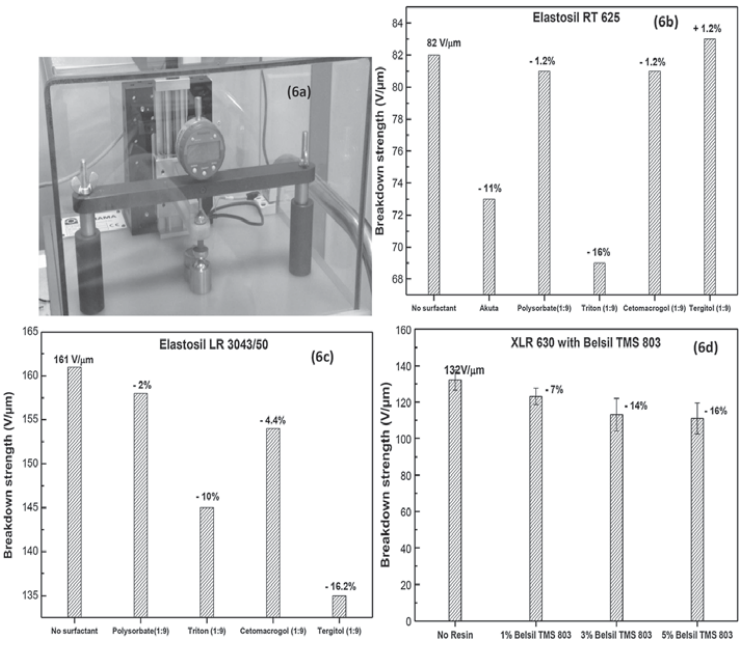

Figure 6. (a) An electrical breakdown test being performed, (b) effect of surfactants on breakdown strength of Elastosil RT 625, (c) effect of surfactants on breakdown strength of Elastosil LR 3043/50 films, and (d) effect of Belsil TMS 803 on breakdown strength. This figure is available in color online at wileyonlinelibrary.com/journal/pat

Table 1. Peel forces and adhesive forces of the polydimethylsiloxane films with various surfactants as release agents

S No.	Surfactant	% of surfactant in aqueous solution	Material	Sample thickness (μm)	Sample width (mm)	Max. peel force (N)	$E = G'(\omega \rightarrow 0)$ (k Pa)	Adhesive energy '*R*'(N/m)
1	Polysorbate-20	0	Elastosil RT 625	58	30	0.33	106	20.9
			Elastosil LR 3043/50	41.7	30	1.6	536	116.4
		2.5	Elastosil RT 625	—	30	—	106	—
			Elastosil LR 3043/50	53	30	1.23	536	70.6
		5	Elastosil RT 625	—	30	—	106	—
			Elastosil LR 3043/50	46	30	1.2	536	70.4
		7.5	Elastosil RT 625	—	30	—	106	—
			Elastosil LR 3043/50	74.5	30	0.74	536	32.5
		10	Elastosil RT 625	52.7	30	0.22	106	12.2
			Elastosil LR 3043/50	52.7	30	0.08	536	2.8
		20	Elastosil RT 625	70	30	0.28	106	15.2
			Elastosil LR 3043/50	23.1	30	0.31	536	14.6
2	Cetomacrogol	0	Elastosil RT 625	58	30	0.33	106	20.9
			Elastosil LR 3043/50	41.7	30	1.6	536	116.4
		10	Elastosil RT 625	50.1	30	0.21	106	11.2
			Elastosil LR 3043/50	40	30	0.71	536	36.8
		20	Elastosil RT 625	38.8	30	0.20	106	11.5
			Elastosil LR 3043/50	44.2	30	0.54	536	24.9
3	Tergitol	0	Elastosil RT 625	58	30	0.33	106	20.9
			Elastosil LR 3043/50	41.7	30	1.6	536	116.4
		10	Elastosil RT 625	54.1	30	0.3	106	18.8
			Elastosil LR 3043/50	54.6	30	0.81	536	39.6
		20	Elastosil RT 625	42.1	30	0.27	106	18.2
			Elastosil LR 3043/50	24.5	30	0.79	536	52.9
4	Triton X-100	0	Elastosil RT 625	58	30	0.33	106	20.9
			Elastosil LR 3043/50	41.7	30	1.6	536	116.4
		10	Elastosil RT 625	90.9	30	0.25	106	11.7
			Elastosil LR 3043/50	41.1	30	0.76	536	39.5
		20	Elastosil RT 625	52.4	30	0.14	106	6.4
			Elastosil LR 3043/50	42.3	30	0.54	536	25.2

and O^- in the hydrophilic head. The detergent adsorbs into the PDMS films. The surfactants and salts in Akuta get ionized/charged under electric field. Because the detergent percolates into the films (network), they make the films conductive as the surfactants get ionized and conduct electricity under high voltage.[25] Also, Akuta had a corrosive effect on films as it is observed that the films became sticky over a period, which makes them unusable. Such conductive films cannot be used for making actuators. Hence, usage of Akuta as a release agent was discarded. In further experiments only non-ionic surfactant solutions were tested. Non-ionic surfactants do not have conducting ions. For both Elastosil RT 625 and LR 3043/50 films, Polysorbate-20 shows the least influence on breakdown strength, compared with other surfactants (Figs 6(b) and (c)). Figure 6(d) shows that the addition of resin depreciates the breakdown strength of the XLR 630 films, the maximum depreciation being 16% for 5% resin. The error bars mark the difference in the measurements between two identical samples

Peel tests

The peel test results and calculated adhesive force values are tabulated in Table 1.

Akuta reduced the *R* between RT 625 film and carrier web from 20.9 to 14.9 N/m, but because Akuta lowered the breakdown strength of the films, its further use was however discarded. The results with non-ionic surfactants are plotted in Figs 7(a) and (b). The *R* values of XLR 630 film with varying percentages of Belsil resin are in Fig. 7(c). For RT 625 films, the value of *R* is reduced from 21 N/m to a lowest of 6.3 N/m with Triton X-100 (20% solution). RT 625 films show lower *R* values (20 N/m) than LR 3043/50 films overall. The low *R* values of RT 625 films can be attributed to the presence of 15% oil in the formulations, which was a trend observed in the work by Vudayagiri *et al*.[3] The 2.5%, 5%, and 7.5% Polysorbate-20 solutions gave very high *R* values for Elastosil LR 3043/50 films as the surfactant content is too low and does not reduce the *R* effectively. For LR 3043/50 films, the value of *R* is reduced from 116.4 N/m to a lowest of 2.8 N/m with Polysorbate-20 (10% solution), which is a decrease of more than 4000%. For XLR630 films, the value of adhesive force (*R*) reduced from 20.7 N/m to a lowest of 10.5 N/m with 3% with Belsil resin. From Fig. 7(c), it is seen that as Young's modulus of the films increase, their peel/adhesive force decreases.[3] Belsil TMS 803 is a trimethylsiloxy silicate MQ type resin,[26] which when compounded with PDMS networks makes them more hydrophobic (Fig. 7(d)). The resins can be incorporated with the reactive Si-H or Si-Vinyl groups so that they can bond with the elastomer matrix via the hydrosilylation reaction.[27] At 3% resin, the cross-linking density is optimum, and a high Young's modulus is attained by the cured elastomer as seen from Fig. 7(c). When the resin is increased to 5%, the Young's modulus decreases, which could be attributed to Belsil interfering negatively with the cross-linking of the elastomer matrix.

Polysorbate-20 (10% solution) is the optimum surfactant to be used as a release agent as it gave low peel forces and had negligible effect on the dielectric breakdown strength of the films. Polysorbate-20 caused the blackening of the silver electrode that is sputtered on it. Initially, the color change suggested oxidation of the silver electrode. On the contrary, Polysorbate-20

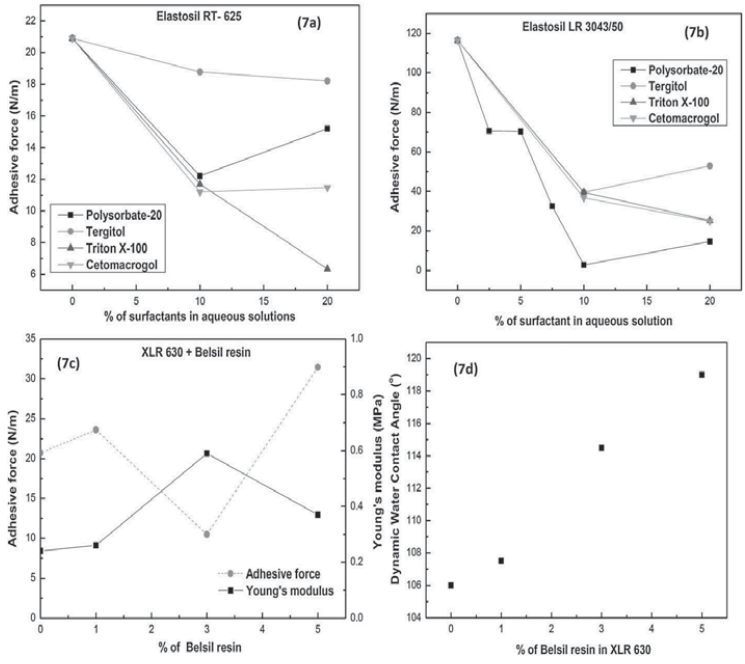

Figure 7. (a) Adhesive forces between Elastosil RT 625 film and the carrier web coated with various surfactants, (b) adhesive forces between Elastosil LR3043/50 film and the carrier web coated with various surfactants, (c) adhesive forces between XLR 630 film with varying concentrations of Belsil resin and the carrier web, and (d) effect of Belsil TMS 803 on the XLR 630 water contact angle. This figure is available in color online at wileyonlinelibrary.com/journal/pat

is a reducing agent and undergoes self-oxidation. Polysorbate-20 and 80 are used as reducing agents to reduce silver salts to silver metal nanoparticles.[28] The possibility of silver metal getting oxidized by Polysorbate-20 is therefore excluded and Polysorbate-20 may rather work as protective sacrificial layer. Polysorbate-20 is obtained from Sigma-Aldrich Corporation, St. Louis, MO, USA for 397 DKK/kg. The amount of Polysorbate-20 required is 3.5 g/m^2 of the surface area of carrier web (real surface area, including corrugations), which translates to 1.4 DKK/m^2. The calculations are made considering a 50% wastage of the surfactant, because there is wastage during the application and evaporation process. The use of Polysorbate-20 is therefore a cheap and environmentally friendly alternative as opposed to fluorinated elastomers and liners. In comparison to Belsil resin, Polysorbate-20 is a cheaper alternative, and it does not interfere with the cross-linking reaction.

CONCLUSIONS

The Akuta detergent reduced the peel forces to 14.9 N/m, but it had a corrosive effect on the films and decreased the breakdown strength of the films. It is therefore not suitable to be a release agent.

The Belsil resin at 3% concentration reduced the peel forces to 10.5 N/m and had a negative influence on the breakdown strength of the XLR630 films. Hence, this method will compromise the quality of the DEAP films.

The adhesive force between the film and the carrier web is the lowest (2.8 N/m) with the Polysorbate-20: water (1:9) formulation. Also, Polysorbate-20 does not interfere with the breakdown of the films unlike Akuta or Belsil resin. Using Polysorbate-20 solution is the best and the most economical method for easy release of very thin polydimethylsiloxane films from microstructured carrier webs in the current manufacturing process set up.

ACKNOWLEDGEMENTS

The authors gratefully acknowledge the financial support from the Danish National Advanced Technology Foundation and the technical support from Michael Daniel Junker, Process Engineer, Danfoss Polypower A/S.

REFERENCES

[1] H. Kiil, M. Y. Benslimane, *Proc. of SPIE, San Diego, California, USA*. **2009**, *7287*, 72870R–1–72870R–10.
[2] A. C. M. Kuo, *Poly (dimethylsiloxane) Polymer Data Handbook*, Oxford University Press, New York, NY, USA, **1999**, 411–435.
[3] S. Vudayagiri, M. D. Junker, A. L. Skov, *Polymer J.* **2013**, *45*(8), 871–878.
[4] S. Vudayagiri, L. Yu, S. S. Hassouneh, A. L. Skov, *Journal of Elastomers and Plastics* **2013**, DOI: 10.1177/0095244313483642.
[5] S. Vudayagiri, L. Yu, S. S. Hassouneh, A. L. Skov, *Proc. SPIE 8687, EAPAD* **2013**, 86870S. DOI:10.1117/12.2009469.
[6] B. Lautrup, *Physics of Continuous Matter' Second Edition: Exotic and Everyday Phenomena in the Macroscopic World*. CRC Press, Boca Raton, Florida, USA, **2011**.
[7] K. L. Johnson, K. Kendall, A. D. Roberts, *Proc. Math. Phys. Eng. Sci.* **1971**, *324*(1558), 301–313.
[8] J. T. Koberstein, D. E. Duch, W. Hu, T. J. Lenk, R. Bhatia, H. R. Brown, J. P. Lingelser, Y. Gallot, *J. Adhes.* **1998**, *66*, 229–249.
[9] S. K. Thanawala, M. K. Chaudhury, *Nature* **2000**, *16*(32), 1256–1260.
[10] F. B. Madsen, I. Dimitrov, A. E. Daugaard, S. Hvilsted, A. L. Skov, *Polym. Chem.* **2013**, *4*, 1700–1707.
[11] M. Benslimane, H. Kiil, M. J. Tryson, *EAPAD* **2010**, 764231, 1–11.
[12] P. D. T. Huibers, V. S. Lobanov, A. R. Katritzky, D. O. Shah, M. Karelson, *Langmuir* **1996**, *12*, 1462–1470.
[13] H. C. Chang, B. J. Hwang, Y. Y. Lin, L. J. Chen, S. Y. Lin, *Rev. Sci. Instrum. Am. Inst. Phys.* **1998**, *69*(6), 2514–2520.
[14] K. P. Ananthapadmanabhan, E. D. Goddard, N. J. Turro, P. L. Kuo, *Langmuir* **1985**; *1*, 352–355.
[15] A. Dominguez, A. Fernandez, N. Gonzalez, E. Iglesias, L. Montenegro, *J. Chem. Educ.* **1997**, *74*(10), 1227–1231.
[16] K. L. Mittal, *J. Pharmaceut. Sci.* **1972**, *61*(8), 1334–1335.
[17] K. S. Hait, S. P. Moulik, *JSD* **2001**, *4*(3), 303–309.
[18] F. L. Bautista, R. M. Sanz, C. M. Molina, N. Gonzalez, D. Sanchez, *IBBS-14* **2009**, *63*(7), 913–922.
[19] P. H. Elworthy, Research Papers **1960**, 293–299.
[20] A. L. Skov, S. Vudayagiri, M. Benslimane, Proc. of SPIE 8687, EAPAD 86871I **2013**, DOI:10.1117/12.2009465.
[21] K. Kendall, *J. Phys. D Appl. Phys.* **1975**, *8*(13), 1449–1452.
[22] F. A. Morrison, *Understanding Rheology*, Oxford University Press, New York, NY, USA, **2001**, 152–166.
[23] M. Y. Benslimane, H. E. Kill, M. J. Tryson, *Polymer Int.* **2010**, *59*(3), 415–421.
[24] P. Sommer-Larsen, A. L. Larsen, *Proc. of SPIE*, **2004**, *5385*, 68–77.
[25] D. López-Díaz, M. M. Velázquez, *Chem. Educat.* **2007**, *12*, 5.
[26] J. M. Zeigler, F. W. G. Fearon, *Silicon-Based polymer Science: Advances in Chemistry*. American Chemical Society, Washington DC, USA, **1990**, 181–199.
[27] H. Mayer, Farbe + Lack **1991**; ISSN 0014-7699, 97(10): 867-870.
[28] H. J. Li, A. Q. Zhang, Y. Hu, L. Sui, D. J. Qian, M. Chen, *Nano Express* **2012**, *7*(612), 1–13.

Appendix III

Hot embossing of microstructures on addition curing polydimethylsiloxane films

Journal of elastomer and plastics (2014)

Journal of Elastomers and Plastics
http://jep.sagepub.com/

Hot embossing of microstructures on addition curing polydimethylsiloxane films

Sindhu Vudayagiri, Liyun Yu, Suzan Sager Hassouneh and Anne Ladegaard Skov

Journal of Elastomers and Plastics 2014 46: 623 originally published online 11 April 2013
DOI: 10.1177/0095244313483642

The online version of this article can be found at:
http://jep.sagepub.com/content/46/7/623

Published by:
SAGE
http://www.sagepublications.com

>> Version of Record - Sep 19, 2014

OnlineFirst Version of Record - Apr 11, 2013

Article

JOURNAL OF ELASTOMERS & PLASTICS

Journal of Elastomers & Plastics
2014, Vol. 46(7) 623–643

DOI: 10.1177/0095244313483642
jep.sagepub.com
SAGE

Hot embossing of microstructures on addition curing polydimethylsiloxane films

Sindhu Vudayagiri, Liyun Yu, Suzan Sager Hassouneh and Anne Ladegaard Skov

Abstract

The aim of this research work is to establish a hot embossing process for addition curing vinyl-terminated polydimethylsiloxane (PDMS), which are thermosetting elastomers, based on the existing and widely applied technology for thermoplasts. To our knowledge, no known technologies or processes are commercially available for embossing microstructures and submicron structures on elastomers like silicones in large scale production of films. The predominantly used technologies to make microscale components for microfluidic devices and microstructures on PDMS elastomer is (a) reaction injection molding, (b) ultraviolet lithography, and (c) photolithography. We focus on hot embossing as it is one of the simplest, most cost-effective, and time-saving methods for replicating structures for thermoplasts. Addition curing silicones are shown to possess the ability to capture and retain an imprint made on it, 10–15 min after the gel point at room temperature. This property is exploited in the hot embossing technology.

Keywords

Embossing, PDMS, carrier web, corrugations, elastomer, DEAP

Introduction

In the large scale manufacture of dielectric electroactive polymers (DEAPs) by Danfoss Polypower A/S (Nordborg, Denmark), the surface of the polydimethylsiloxane (PDMS) elastomer films are imparted with microscale corrugation lines (Figure 1), which enhance the performance of the films as actuators and generators due to the directional

The Danish Polymer Centre, Department of Chemical and Biochemical Engineering, DTU, Lyngby, Denmark

Corresponding author:
Anne Ladegaard Skov, The Danish Polymer Centre, Department of Chemical and Biochemical Engineering, DTU, Kgs Lyngby 2800, Denmark.
Email: al@kt.dtu.dk

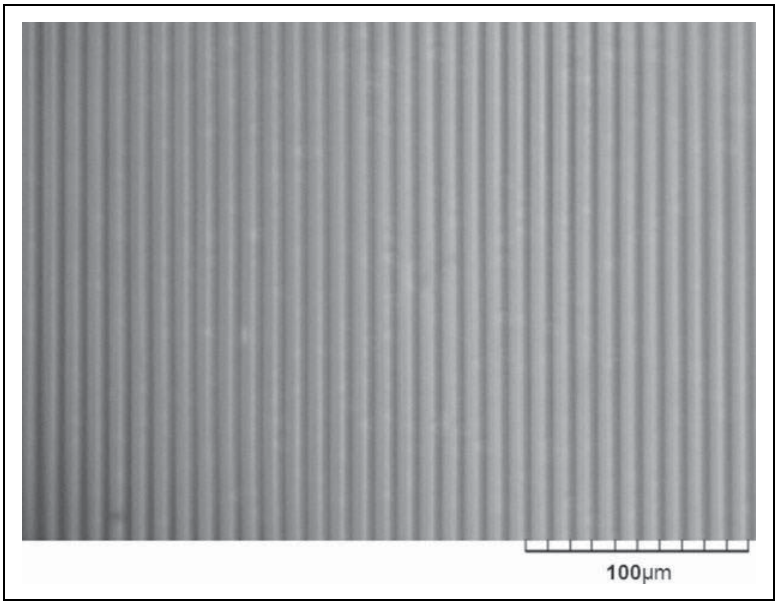

Figure 1. Microscopic image of elastomer film with corrugation lines obtained from the traditional coating process at Danfoss PolyPower A/S. The period of corrugation peaks is 10 μm and the depth is 5 μm, but other aspect ratios are also produced depending on specific requirements.

anisotropy (Figure 2) caused by the thick corrugation lines and it furthermore allows for high strains of the metallic electrodes.[1,2] The films are currently made on a specially designed carrier web that imparts the corrugated structure on to the films. The elastomer mixture is applied on the carrier web, and it is left to cure on the web. The cured elastomer film is then peeled off the web to allow for the deposition of electrodes. The process of releasing the elastomer film from carrier web is not smooth and induces defects and prestrain in the film. Also, this process is expensive, as it requires miles of carrier web to make the films. Therefore, an alternative process to make thin, corrugated elastomer films is required to make the DEAP technology economically competitive with other actuator, generator, and sensor technologies.

Replication of components and structures in macro, micro, submicron, and nanoscale is not new to the polymer industry. Mass fabrication of a lot of components and products in the consumer industry has been made possible by replication technologies. Replication of macroscale components and structures has been carried out for many years with well-established processes like (a) injection molding; (b) injection compression molding, (c) compression molding, (d) thermoforming, and (e) blow molding or extrusion process for a variety of thermoplasts and thermosets.[3,4] A large varieties of polymers can be processed with these methods, comprising a wide range of thermal and mechanical properties. All these methods are highly automated and optimized. With the already established macroscopic replication process, microscale replications can also be performed.[3]

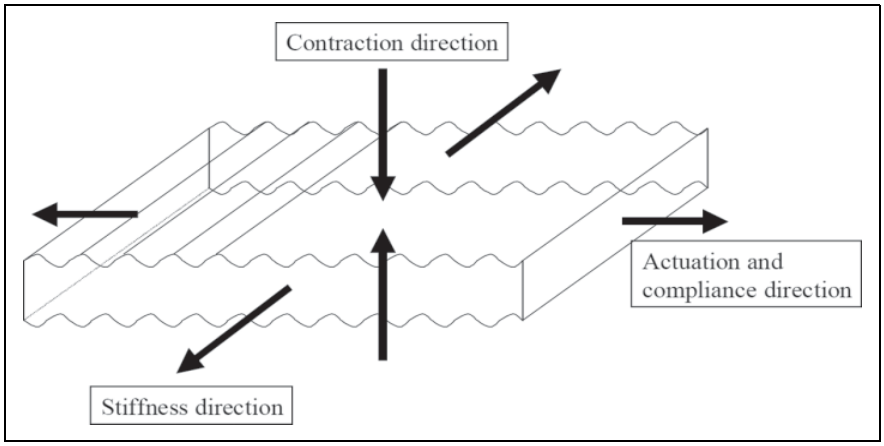

Figure 2. Schematic illustration of a dielectric electroactive polymer actuator film with corrugations showing the direction of actuation.[6]

For replication of microstructures in thermoplasts, thermosets, and ultraviolet (UV)-curable polymers, the processes used are (a) micro reaction injection molding, (b) micro injection molding, (c) micro injection compression molding, (d) micro hot embossing, (e) micro thermoforming, and (f) nanoimprint lithography. The reaction injection molding process technology is available for a few elastomers apart from the thermosets and thermoplasts. It is being used to process some elastomers like liquid silicone rubbers (LSRs)—two component pumpable silicone materials that are mixed and rapidly heat cured to form elastomeric components. In this process, LSR is injected into the mixer at the prescribed amounts and mixed, which are then injected into the mold under pressure, where the mix cures (at elevated temperatures) and gives the product of required shape and structure. Hot embossing and micro/nanoprinting undergo constant development depending on the requirements, materials, and constraints of a particular product.[3,5] Limitations such as structure size, molding area, complexity of structures, material properties, and process times make the processes even more complex.

The hot embossing process that is usually used in industries for thermoplasts is shown in Figure 3. The polymer in the form of a thin film is heated up to the melting range by conduction. Then the film is compressed to fill the microcavities of the mold and then the polymer film is cooled and demolded. The force applied on the film into the mold is optimized, regulated, and controlled. This serves as an inspiration for the following experiments of embossing microstructures on the PDMS films.

Experimental

Materials

The silicone networks used for the hot embossing process are as follows.

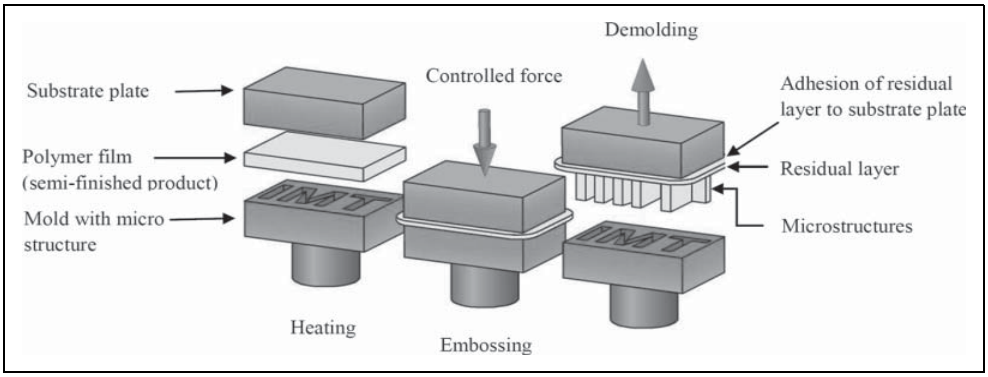

Figure 3. Schematic representation of a typical hot embossing process for thermoplasts.[4]

1. DMS V35 (vinyl terminated PDMS) (M_w = 49,500 g/mol) from Gelest Inc. (Morrisville, PA, USA); cross-linker, tetrakis(dimethylsiloxy)silane (SIT7278.0) (M_w = 328 g/mol) for platinum (Pt) cure of a two-component room temperature vulcanizing silicone from Gelest Inc.; catalyst, platinum cyclovinylmethyl–siloxane complex (511) was supplied by Hanse Chemie AG (AG,Geesthacht, Germany).
2. Elastosil-RT625®; silicone oil (Powersil® fluid TR 50); and inhibitor (Pt 88) was obtained from Wacker Chemie AG (München, Germany). Elastosil-RT625 is supplied as premix A and B. Elastosil A contains the cross-linker and Elastosil B contains the Pt catalyst.
3. Silastic LC-50-2004®; and OS-20, an ozone-safe volatile methylsiloxane fluid, were obtained from Dow Corning (Midland, MI, USA). It is supplied as a two-part system and Silastic A contains the catalyst and Silastic B contains the cross-linker.

Instrumentation and specifications

GP determination. Rheological measurements to estimate the gel point (GP) of the silicone networks were performed with an AR-2000 rheometer (TA instruments, New Castle, DE, USA).

Carrier web. The carrier web with microscale corrugations was supplied by Danfoss Polypower A/S. The carrier webs are made of temperature-stabilized polyethylene terephthalate (PETE) band (0.2 mm) coated with methyl acrylate UV resin. The surface of the carrier web has microscale corrugations (Figure 4). There are two types of carrier webs used at Danfoss depending on whether the corrugation lines are along the length of the web (down-web) or perpendicular to the length of the web (cross-web). Also, there are two types of carrier webs defined by wave depth and period of corrugations; 1) 30% web which has corrugations of depth of 5 μm and a period of 10 μm. The films made on this carrier web are capable of stretching to about 35% strain. 2) 100% web which has both depth and period of 7 μm. The films made on this carrier web is capable of stretching up to about 80% strain.[1,6]

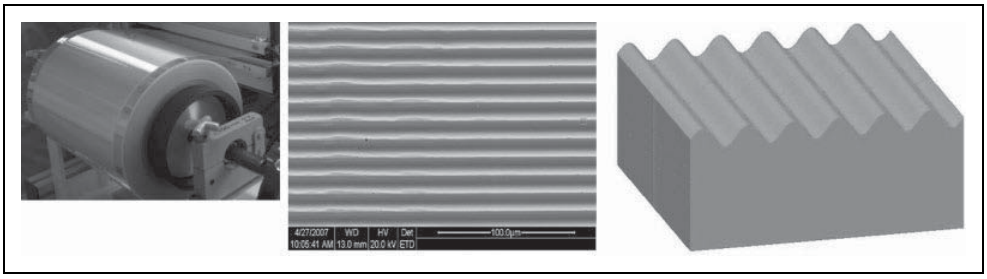

Figure 4. Picture of the carrier web roll (left). Microscopic image of corrugation pattern on carrier web (center). Schematic cross sectional view of carrier web (right).[2]

Aluminum roller. Initially, an embossing roller made of polyvinyl chloride (PVC) was used for embossing. A sheet of the carrier web with microstructure was fixed to the roller, which would impart the structure to the semicured films. However, this roller could not be heated and hence embossing with a PVC roll was not possible. Later, an aluminum roller was employed as it could be heated (Figure 5). Since the roller was operated with hands, the force on the roller could not be controlled and it varied with every operation. The weight of the aluminum roller is 3 kg to which an additional human pressure is also added. So the exact pressure is unknown and dependent on the operator.

Gravure lab coater. In order to completely control the pressure and speed of the embossing, an offset Gravure lab coater, 24″ wide, Model#E-BC12POG3 (Euclid Coating Systems Inc., Bay City, MI, USA) was used for embossing (Figure 6). The diameter of the rolls is 6″. With this instrument, the force applied and the speed of the roller can be regulated. The coater is modified to suit the embossing process. Two infrared lamps are placed one each above the top roller and below the bottom roller to heat them up to a desired temperature. The upper roller of the coater was fixed with a 30% down carrier web. The period of corrugation peaks are 10 μm and the depth is 5 μm.

Procedure

There are five steps in the embossing procedure. An overview of the steps involved is shown in Figure 7.

Preparation of the elastomer mixture. The procedure for making the addition curable PDMS network is different for each material used. In the following section, the details of the different recipes are given.

DMS V35. Two premixes A and B are made by mixing half of the required amount of DMS V35 with the cross-linker and the other half of DMS V35 with the Pt catalyst separately using a Speed mixer DAC 150FVZ-K (Synergy Devices Ltd, UK).[7] The two parts are stored separately to avoid curing and are not mixed until the films have to be made.[7] When premixes A and B are mixed in the ratio 1:1 using a speed mixer (2 min; 2000 r/min), the three components PDMS, catalyst, and cross-linker should be

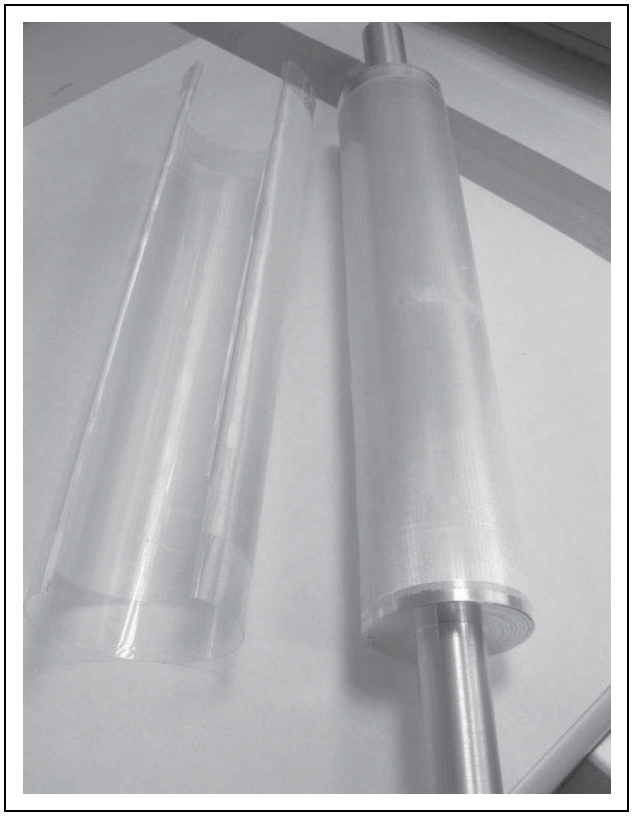

Figure 5. Aluminum embossing roller with a piece of the carrier web ready to be fixed.

homogeneously distributed and the hydrosilation reaction proceeds uniformly. The reaction is exothermic in nature and will proceed in the room temperature at a low rate. The premixes are made such that in the final mixture, the ratio of the number of hydride groups in cross-linker (four hydrides per molecule) is equal to the number of vinyl groups in V35 (two vinyl groups per molecule). The stoichiometric imbalance (r) is calculated from equation (1) and for the applied mixture $r = 1$.[7] However, usually slightly higher values of r give the strongest networks.[8] The cross-linking reaction taking place between the reactive groups of the linear vinyl-terminated PDMS and four functional cross-linkers (i.e., vinyl (–CH=CH_2) and hydride (–Si–H)) are presented in Figure 8.

$$r = \frac{f}{2} \times \frac{M_{\mathrm{PDMS}}}{M_{\mathrm{cross-linker}}} \times \frac{m_{\mathrm{cross-linker}}}{m_{\mathrm{PDMS}}} \tag{1}$$

where f is the functionality of the cross-linker, M_{PDMS} is the molecular weight of PDMS, $M_{\mathrm{cross-linker}}$ is the molecular weight of cross-linker, $m_{\mathrm{cross-linker}}$ is the mass of cross-linker in our mixture, and m_{PDMS} is the mass of PDMS polymer in our mixture.

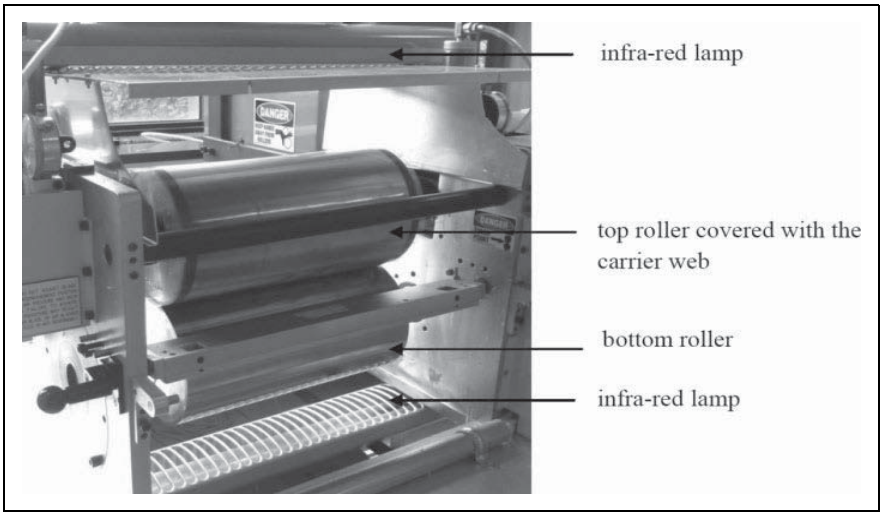

Figure 6. Offset gravure lab coater used for embossing.

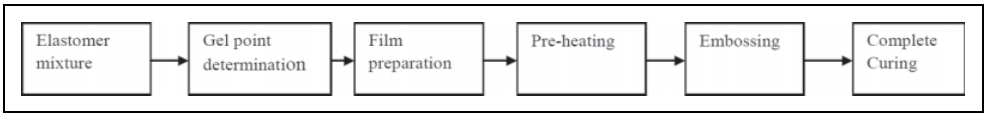

Figure 7. Schematic illustration of the embossing process.

Elastosil-RT625. Elastosil-RT625 is a RTV silicone supplied as premixes A and B, which is recommended to be mixed in the ratio 9:1, to form the addition curing mixture. The speed mixer is used to make a uniform mixture (2 min at 2000 r/min).

Silastic LC-50-2004. Silastic LC-50-2004, an LSR, is supplied as premixes A and B and is mixed in the ratio 1:1 using the speed mixer (2 min at 2000 r/min). The solvent OS-20 is mixed with Silastic in different proportions to reduce the viscosity and thereby ease the processing and initial coating of the films.

Rheological measurements. The GP of the silicone network should be investigated before proceeding to the embossing process. The time and temperature required to reach GP determines the preheating conditions of the embossing process. The linear viscoelastic measurements during the cross-linking of the stoichiometrically-balanced samples (a) DMS V35 ($r = 1$, Pt = 1.6 ppm), (b) Elastosil (A:B::9:1) + 15 wt% silicone oil + 0.8 wt% inhibitor, and (c) Silastic (A:B::1:1) + 10 wt% of OS-20, at temperatures 80, 60, and 40°C are performed at a controlled strain mode with 2% strain, which is within the linear regime of the material based on an initial strain sweep test and in a frequency range from 100 to 0.01 Hz.

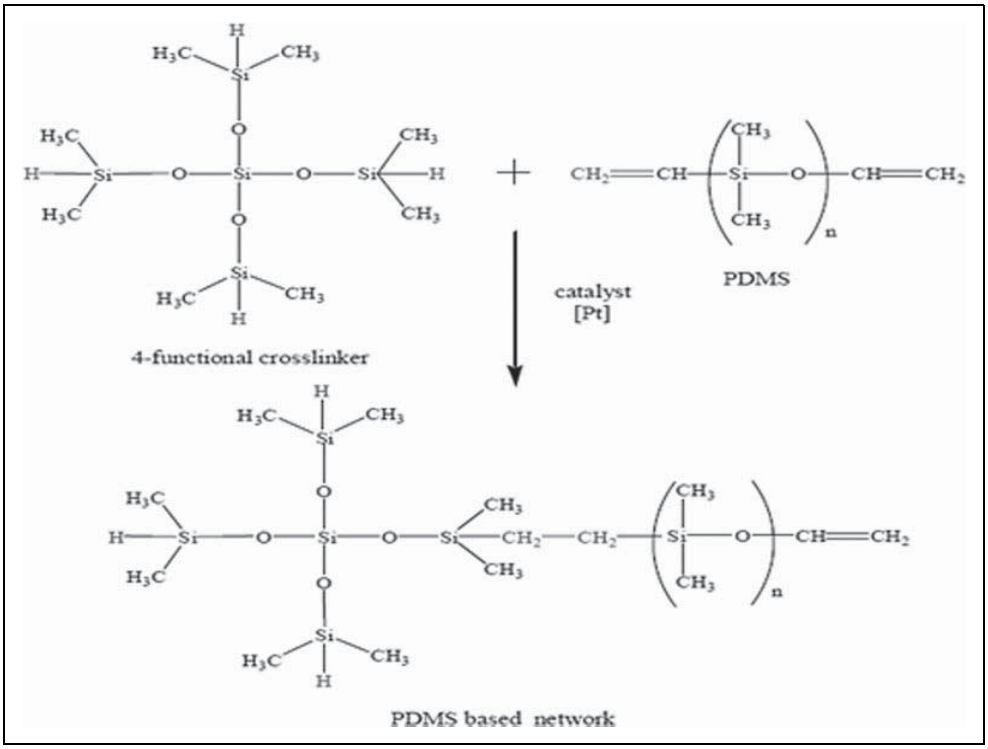

Figure 8. The cross-linking reaction between polydimethylsiloxane and four-functional cross-linker.

Film preparation. Once the elastomer mixtures are ready, films of different thickness are made using 3540 bird film applicator (Elcometer, Germany; 50 and 100 μm) and steel frame (500 μm) on a PETE substrate.

Preheating the film. The films made on the PETE substrate are preheated prior to the embossing till the addition curing proceeds to the GP. The time and temperature for preheating is fixed based on the GP estimated by rheological experiments. Preheating the films in oven rendered films with fully cured surfaces, since free surfaces cured faster than the bulk of the film. Such films cannot be embossed. Therefore, preheating in an oven was ruled out. In contrast, a hot plate heats up the film from the bottom, and thereby the film cures from below and the free surface for embossing is still around the GP. The hot plate used is an C-MAG HS 7 IKAMAG® (IKA, Germany). It was found that homogenous heat transfer was not possible with a hot plate, as the substrate did not have good contact with hot plate. Later, the films on the PETE substrate were pre-heated on a hot steel roll with a smooth surface that gave sufficient contact area and hence large and homogeneous heat transfer. Hot steel roll was therefore used for pre-heating the films.

Embossing

With aluminum roller. The films that are partly cured by preheating are immediately embossed with the aluminum roller that is covered with the carrier web with microscale corrugation lines (Figure 9). The aluminum roller is also heated in the oven prior to embossing. The force applied on the film by the roller imprints the corrugations lines on the film and the temperature of the roller ensures that the film cures and retains the microstructure. The temperature of the embossing roll again depends on the material used.

With gravure lab coater. The films that are partly cured by preheating on a steel roller (Figure 10) are immediately embossed using the gravure lab coater. The top roll of the coater is covered with the 30% down carrier web and hence the top roll acts as the embosser. Both the top and bottom rolls are heated using infrared lamps to a preferred temperature. The temperature of embossing depends on the type of silicone network used. The speed of the rollers and the pressure between the rollers (pressure on the film) is adjusted to give the best results.

Complete curing. The films that are embossed are left to cure completely upon heating in an oven. The temperature and time of curing depends on the material used.

GP, developing elasticity, and onset of embossing

After the onset of the hydrosilation reaction, the PDMS network approaches chemical gelation, which is a phenomenon by which the cross-linking polymeric material undergoes a phase transition from liquid to solid state.[9] A cross-linking polymeric system is said to reach its GP at a critical extent of the cross-linking reaction at which either the weight average molecular weight diverges to infinity (infinite sample size) or the first macromolecular cluster extends across the entire sample (finite sample size).[9,10] Thus at the GP, a thermosetting polymer system is transformed from a viscoelastic liquid to a viscoelastic solid by the introduction of chemical cross-links creating a three-dimensional network. There is a dispute as to whether the GP occurs at the cross-point of the storage and loss moduli G′ and G″ in a linear viscoelastic diagram.[10–12] There is one class of polymer only for which the GP coincides with the crossover point. These are the polymers that have a power law relaxation upon reaching the GP ($G(t) \sim t^{-n}$), with a specific exponent value $n = 1/2$.[12] Stoichiometrically balanced polymer networks or networks with excess cross-linker at temperatures much higher than their glass transition temperature show such behavior and hence have a GP that coincides with the crossover point of G′ and G″.[12] Though power law relaxation is the norm for polymers at GP, not all of them have the exponent value of $n = 1/2$. The polymers that have an exponent value $n \neq 1/2$ will have a crossover point either before the actual GP ($n < 1/2$) or after the actual GP ($n > 1/2$). So, the crossover point cannot be used to detect the GP in such cases.[12]

Since we study the linear viscoelastic model of a stoichiometrically balanced V35 system, where gelation is caused by end-linking reaction of primary chains, the GP occurs at the crossover point of the storage (G′) and loss moduli (G″). In case of the

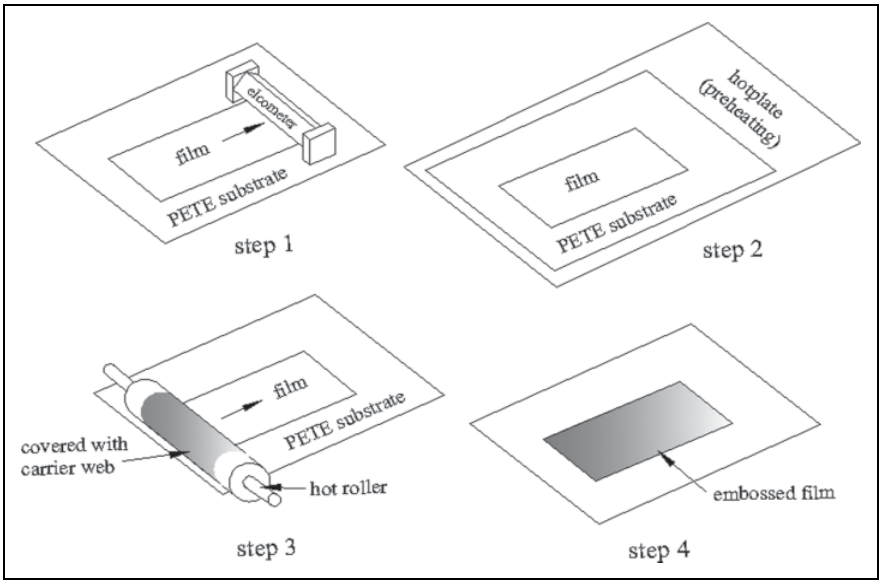

Figure 9. Schematic representation of the hot embossing process with the aluminum roller.

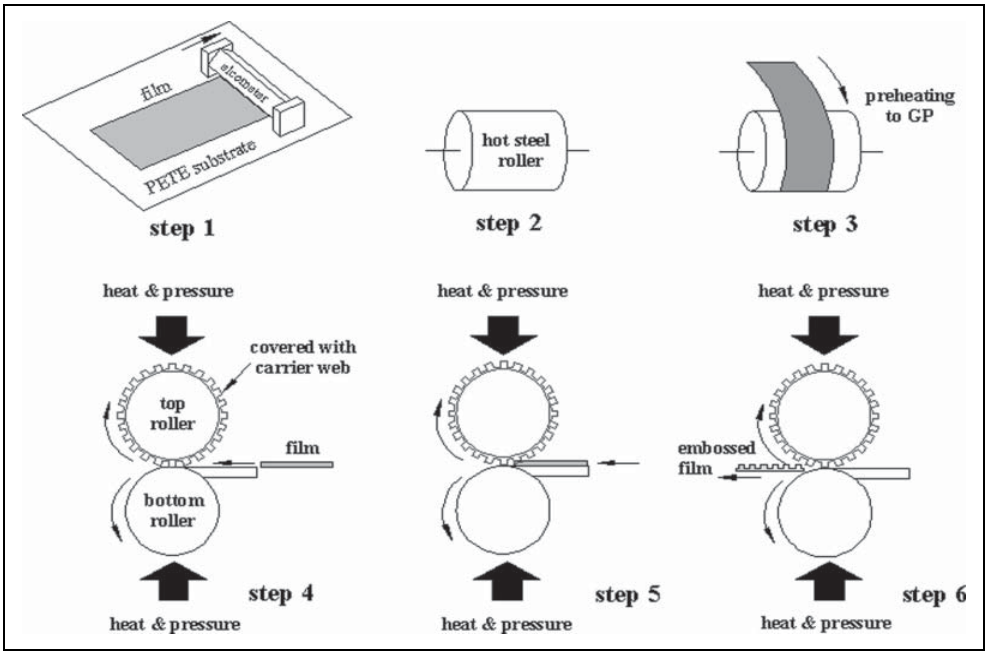

Figure 10. Schematic representation of hot embossing process with the gravure lab coater.

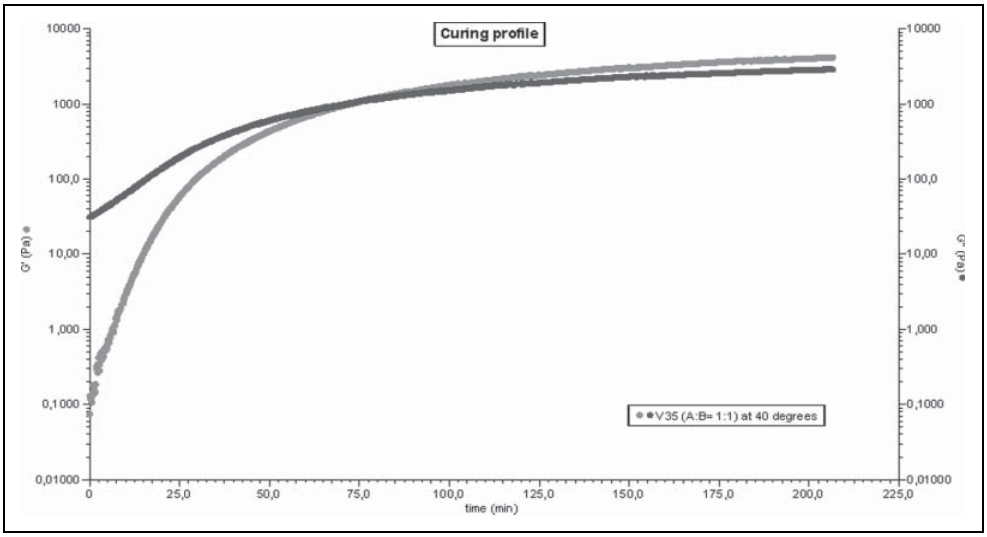

Figure 11. Curing profile of DMS V35 at 40°C, gel point is at 74.7 min.

commercial RTV silicone Elastosil RT-625 and the commercial LSR Silastic LC-50-2004, the crossover of G′ and G″ will be used as the GP, assuming that they are stoichiometrically balanced. Beyond the GP, the elasticity increases steadily with increasing cross-linking density. Knowledge of the GP is essential to design the embossing experiments. The higher the temperature, the quicker is the transition from viscoelastic liquid to solid and the less time required to reach the GP. The embossing should be started at the GP in hot embossing because the hydrosilation reaction is much faster at high temperatures and the window for embossing at GP is reduced to a few seconds. At room temperature, the reaction rates are much slower and there is a space of 10–15 min after the GP, at which embossing can be done.

The curing profile of V35 at 40°C is shown in Figure 11. The system does not contain fillers, so the crossover is very clear as $G' << G''$ in the beginning of the curing process. The same behavior is observed at 60 and 80°C as well with the increase in reaction speed being the only difference.

The curing profile for Elastosil at 80°C is shown in Figure 12. The crossover happens early in the curing process due to the presence of reinforcing particles in the commercial mixture. Curing profiles for Silastic at 80 and 40°C can be seen in Figures 13 and 14, respectively. At 80°C, Silastic shows similar curing behavior as Elastosil. For the Silastic at 40°C, there are three cross-points, which are completely reproducible crossovers. First cross-point is 10 min, second is 69 min, and third is 265 min. The three cross-points are likely to arise due to the competing effect of reaction and solvent evaporation. The Silastic is highly viscous and just a small extent of reaction causes G′ to increase. The first two crossovers are due to these competing phenomena and the third crossover is regarded as the true GP, which is further supported by $\partial G'/\mathrm{d}t$ being strongest at this point. Table 1

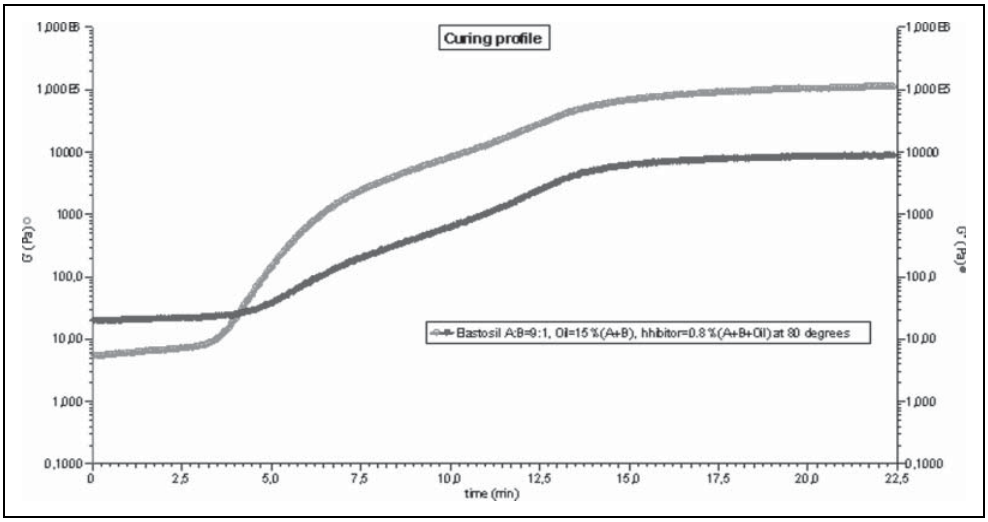

Figure 12. Curing profile of Elastosil at 80°C, gel point is at 4.0 min.

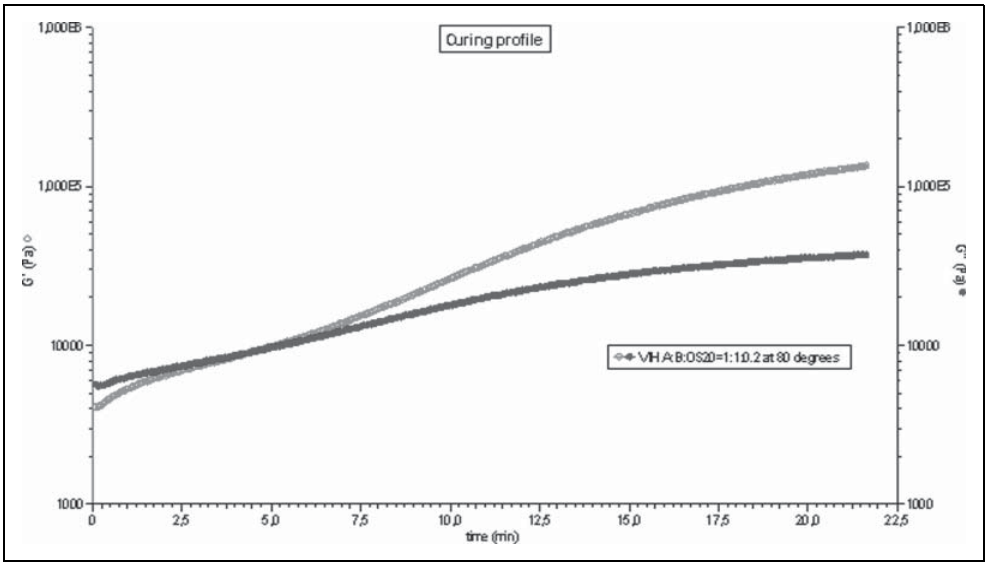

Figure 13. Curing profile of Silastic at 80°C, gel point is at 4.5 min.

shows the GPs of the three materials at 40, 60, and 80°C. Figure 15 shows the storage and loss moduli G′ and G″ of V35, Elastosil and Silastic films as a function of the applied frequency at 23°C. Silastic film has the highest modulus, which means it is harder than the other two films, with V35 being the softest.

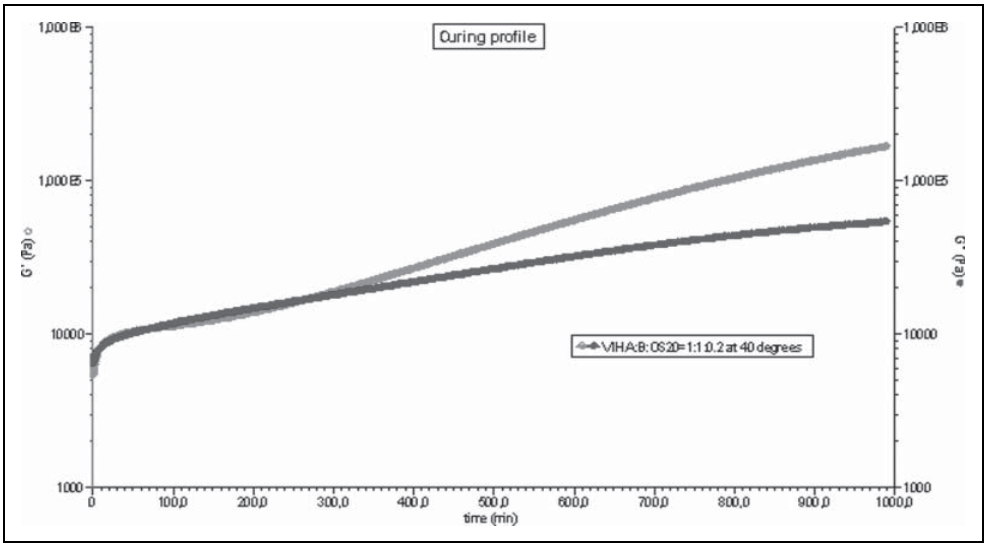

Figure 14. Curing profile of Silastic at 40°C, gel point is at 265 min.

Table 1. Gel points of V35, Elastosil and Silastic.

Temperature (°C)	V35 (min)	Elastosil (min)	Silastic (min)
40	74.7	192	10.3 (first), 69.1 (second), and 265 (third)
60	16	30.2	5.9
80	15.8	4.0	4.5

Requirements for the embossing process

After many trials and errors of the embossing process, the most required conditions of embossing process can be established as given in Figure 16

Results and discussion

Conditions of embossing process

The PVC embossing roller failed to work as it could not be heated. The optimum conditions for embossing were investigated using two methods: (a) aluminum roller and (b) Euclid coater. At 80°C, both Elastosil and Silastic have a GP around 4 min (Table 1). V35 has a GP around 16 min at 80°C. Thus, to emboss the mixtures at 80°C, the film still needs 5 min (for Elastosil and Silastic) and 16 min (for V35) to develop sufficient elasticity. To further decrease this development time, the temperature is increased. When preheated at 110°C approximately 5–15 seconds is sufficient for Elastosil, Silastic, and V35 to reach the GP and embossing can be carried out on the films.

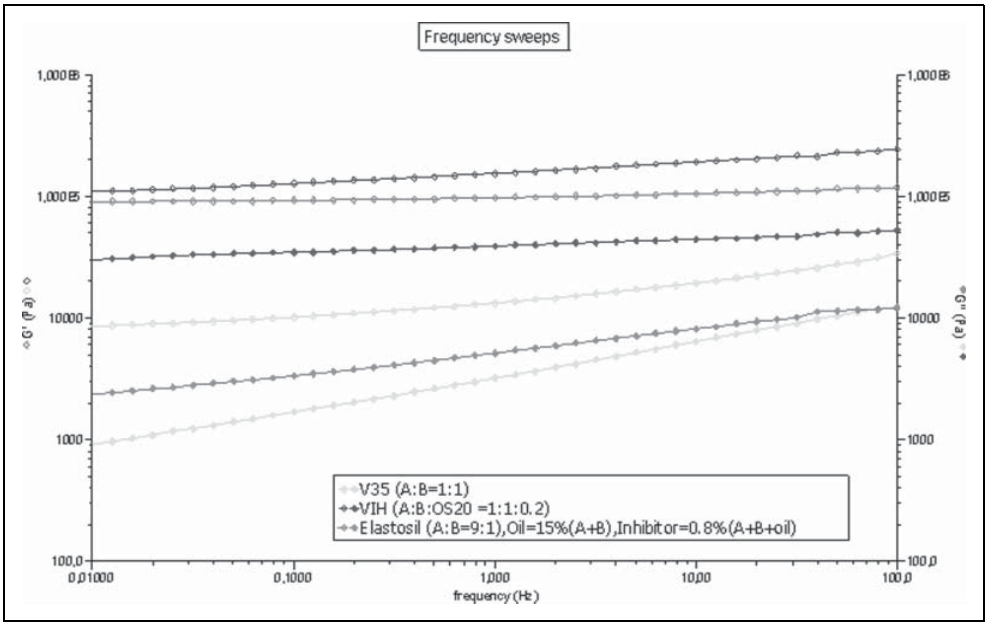

Figure 15. Comparison of the frequency sweeps of V35, Elastosil, and Silastic at 23°C.

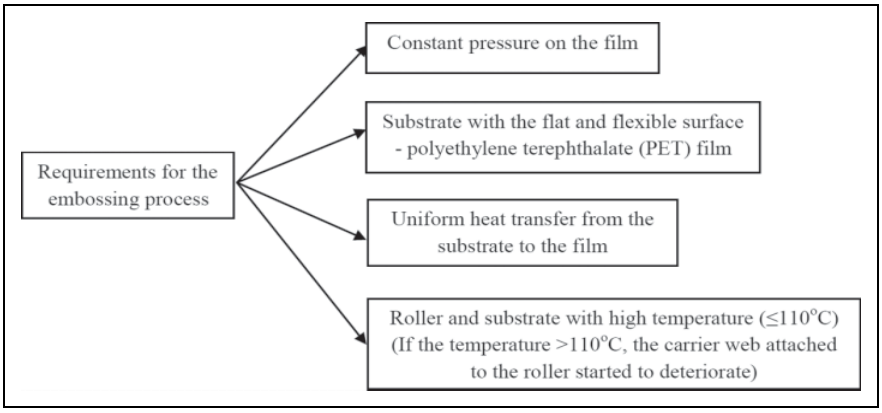

Figure 16. Requirements for the embossing process.

Roller method. The V35 film of 500 μm thickness embossed with aluminum roller at 110°C (15 s to GP) gave the best embossing. The Elastosil film of 100 μm thickness embossed with aluminum roller at 110°C (5 s to GP) gave the best embossing. For the Silastic film of 50 μm thickness embossed with aluminum roller at 110°C (10 s to GP) gave the best embossing. The results are tabulated in Table 2.

Table 2. Optimal conditions of embossing process by aluminum roller for V35, Elastosil and Silastic films.

Material	Thickness of the film (μm)	Preheating temperature (°C) and time (s)
V35	500	Roller (110, 15)
Elastosil	100	Roller (110, 5)
Silastic LC-50-2004	50	Roller (110, 10)

Euclid coater method. The V35 film of 500 μm thickness embossed with coater at 110°C (15 s to GP) with a pressure of 30 lbf/in^2 and roller speed (appendix 1) of 1.4 r/min (0.0112 m/s) gave the best results. Elastosil film of 100 μm thickness embossed with coater at 110°C (5 s to GP) with a pressure of 25 lbf/in^2 and roller speed of 1.4 r/min gave the best results. Silastic film of 100 μm thickness embossed with coater at 110°C (10–12 s to GP) with a pressure of 20 lbf/in^2 and roller speed of 1.4 r/min gave the best embossing. Table 3 briefs these conditions. Figures 17 to 19 show the microscopic pictures of the embossed V35, Elastosil, and Silastic films with the best embossing results. Figure 17 shows the microscopic images of embossed V35 film of thickness 500 μm. It was embossed with a 30% piece of down carrier web (period ~10 μm and height ~4 μm). The V35 film measured a period of ~12.5 μm and a height of ~2.9 μm. This indicated that when the V35 film was peeled off, it did not recover its original shape, as it was highly viscoelastic. Assuming a 25% strain from the period differences, one would expect reduction in height down to 3 μm. Even after waiting for long enough time, it did not recover its original shape.

Figure 18 shows the microscopic images of embossed Elastosil film of thickness 100 μm. It was embossed with a 30% piece of down carrier web (period ~10 μm and height ~4 μm). The Elastosil film was measured a period of ~9.8 μm and a height of ~3.5 μm, which is ~80% of carrier web dimensions.

Figure 19 shows the microscopic images of embossed Silastic film of thickness 100 μm. It was embossed with a 30% piece of down carrier web (period ~10 μm and height ~4 μm). The Silastic film measured a period of ~10 μm and a height of ~4 μm, which is ~100% of carrier web dimensions. The results are tabulated in Table 3.

Time-window for hot embossing

There are two vital factors for designing the embossing experiments

1. Time to reach GP
2. The time window (around GP) at which the embossing can be performed.

As the temperature of preheating and embossing increases (40, 60, and 80°C), the time taken to reach the GP and the time window for embossing decreases. At 80°C, the time available for embossing is still around a few min after GP. To quicken the embossing process, time sweeps of the samples are performed at 110°C. At 110°C, the time to reach GP and the time window for embossing is around a few seconds. For industrial processes, smaller time windows are preferred, as the production is quicker. In Figure 20, the time

Table 3. Results of embossing process by euclid coater for V35, Elastosil and Silastic films.

No.	Material	Preheated on	Preheat temperature (°C) (time of films (s))	Film (μm)	Roller speed (r/min)	Roller pressure (lbf/in^2)	Comments
1	V35	Steel roller	110 (15)	500	1.40	30	Films were at GP and were embossed fully.
2	Elastosil	Steel roller	110 (3)	100	1.40	25	Film did not reach GP and it stuck to the roller while embossing.
3	Elastosil	Steel roller	110 (5)	100	1.40	25	Films were at GP and were embossed fully.
4	Silastic	Hot plate	150 (10)	100	1.40	20	The methyl-acrylate coating (the layer carrying the microstructure) on carrier web bonded with Silastic, and came off with the film.
5	Silastic	Hot plate	110 (10)	100	1.40	20	Film did not reach GP and it stuck to the roller while embossing.
6	Silastic	Steel roller	110 (10)	100	1.40	20	Films were at GP and were embossed fully.
7	Silastic	Steel roller	110 (10)	100	1.40	25	Film did not reach GP and it stuck to the roller while embossing. “Island formation” (Figure 22) was seen
7	Silastic	Steel roller	110 (10)	100	1.85	20	Corrugation is not deep enough on the embossed film.
8	Silastic	Steel roller	110 (10)	100	1.85	30	Due to high embossing pressure, film partly stuck on the web though it was at GP.

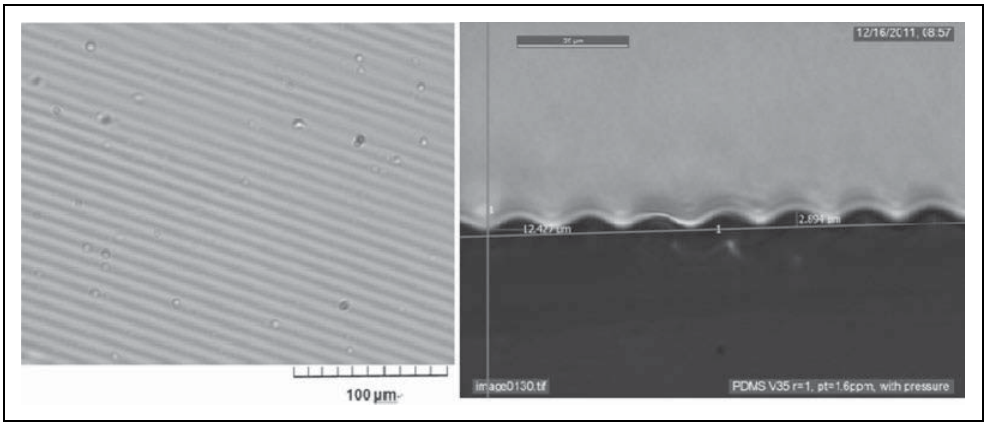

Figure 17. Microscopic images of embossed V35 film (No. 1 in Table 3).

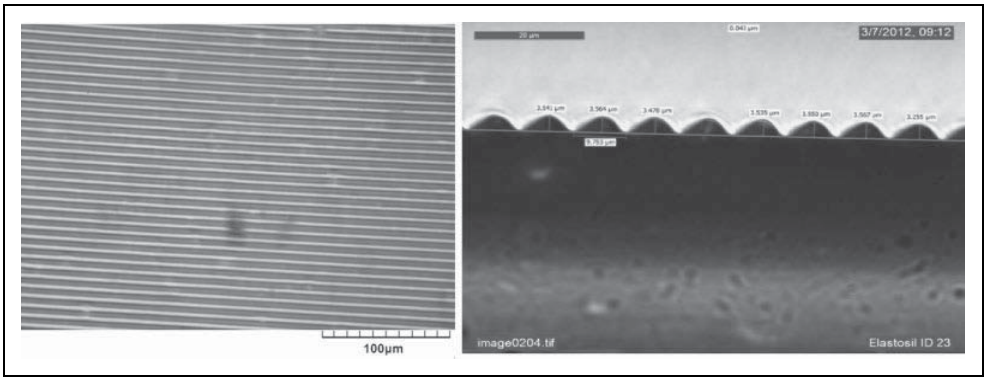

Figure 18. Microscopic images of embossed Elastosil film (No. 3 in Table 3).

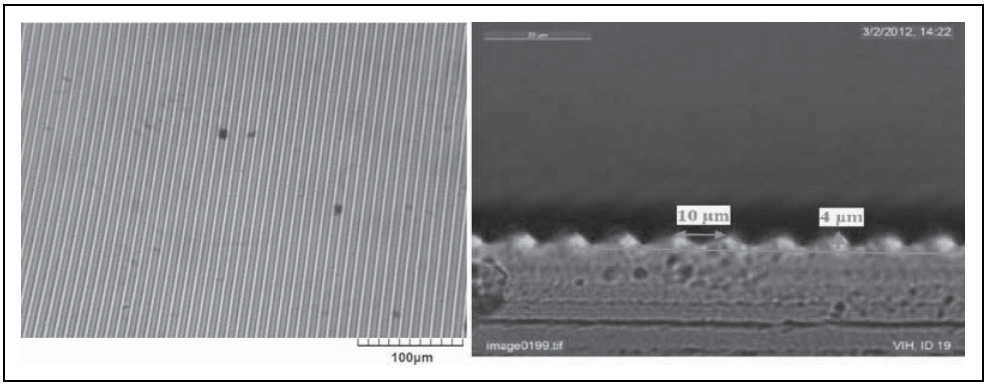

Figure 19. Microscopic images of embossed Silastic film (No. 6 in Table 3).

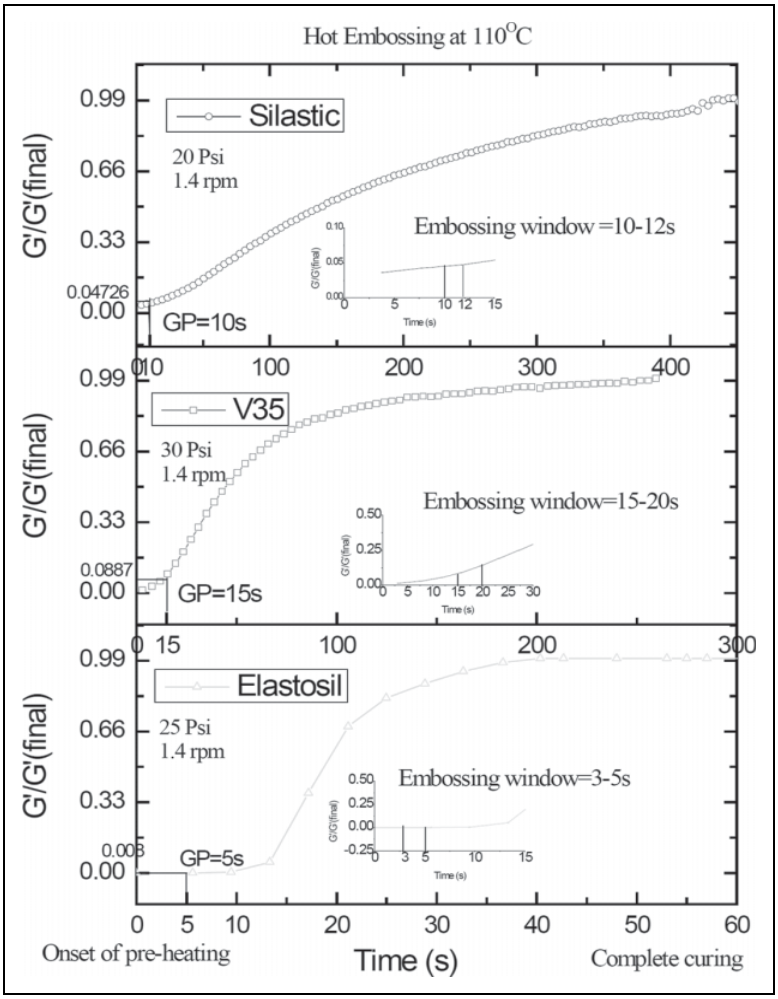

Figure 20. Time window for embossing at 110°C.

window of the embossing process, using the Euclid gravure lab coater for all three materials at 110°C is shown. The entire process of preheating, embossing and complete curing takes less than 60 s. Figure 20 shows a plot of G′/G′ (final) against the time at which preheating is started, followed by embossing. The ratio G′/G′ (final) is used instead of G′, in order to make the data comparable (Table 4). The pressure used varies with the material and is indicated in Figure 20 and the speed of the roller is 1.4 r/min. In Figure 21, the process window for embossing Elastosil RT-625 is shown.

Problems with embossing

Preheating the polymer film made on the substrate is a very important step in the embossing process. The film needs to be preheated uniformly. To ensure uniform

Table 4. G′/G′(final) and GP at 110°C.

Material	GP (s)	G′(at GP)/G′(final)	G′(initial)/G′(final)	G′(final) (Pa)
V35	15	0.089	0.013935	9049
Elastosil	5	0.0008	0.000056	213,500
Silastic	10	0.047	0.0102	44,570

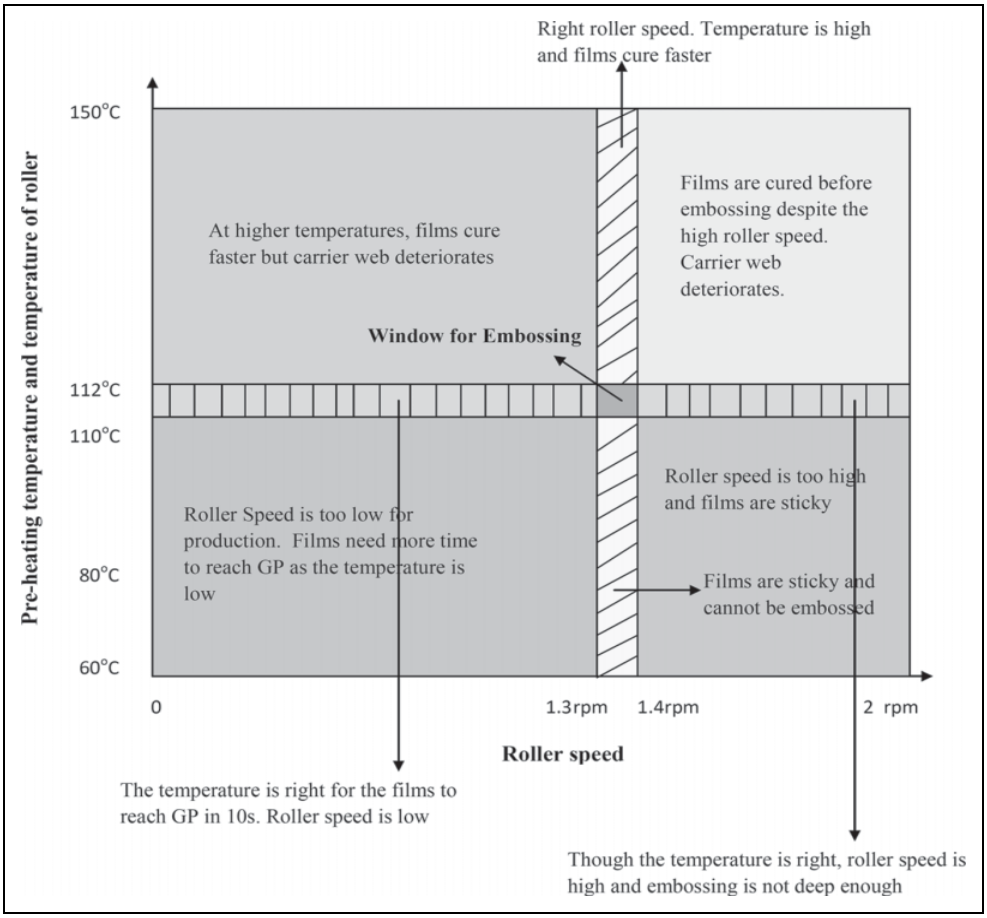

Figure 21. Process window for embossing Elastosil RT-625 at 25 lbf/in^2 roller pressure, pre-heated for 5s.

heating, the film needs to be in good contact with the hot plate. The surface of the hot plate has to be very smooth and should be made of a metal, which is a very good conductor and dissipater of heat like steel, copper, or aluminum. If the film is not heated uniformly, three cases can happen.

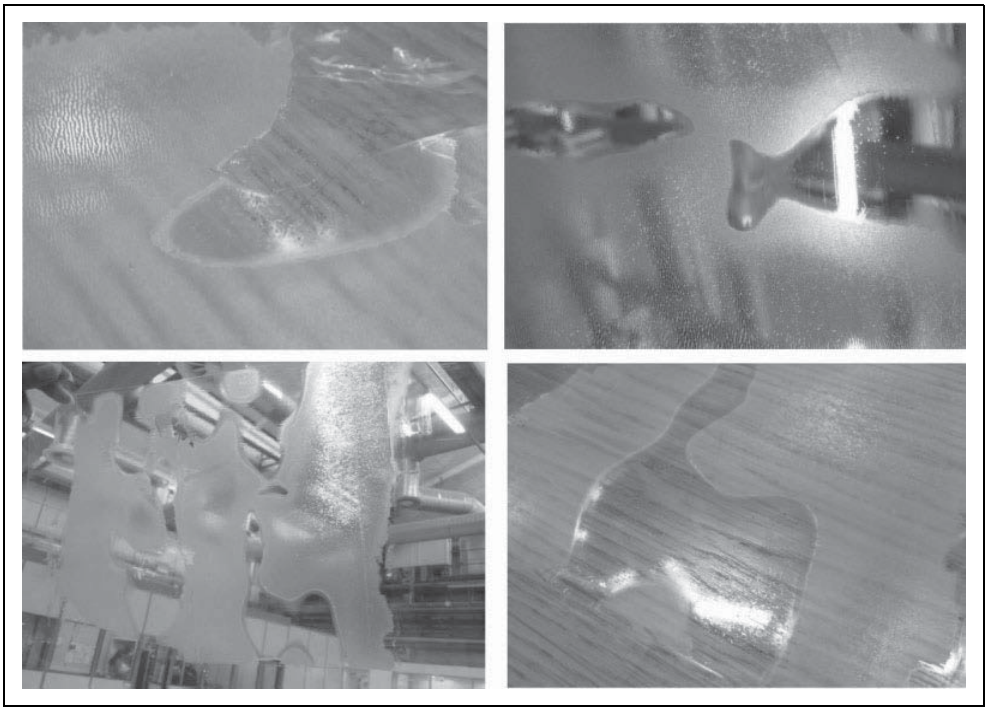

Figure 22. Island formation during embossing process due to nonuniform heating.

1. Regions of the film that are not in contact with hot plate will not reach the GP;
2. regions of the film that are in good contact would reach the GP; or
3. some regions of film would have cured completely due to prolonged preheating.

The uncured parts of the film stuck to the embossing roller and the fully cured regions of the film did not have any embossing on them as they have hardened fully. The regions that are at GPs would have embossing. This results in island-like structures on the film (as seen in Figure 22).

Conclusions

Hot embossing of silicone elastomer is very different and is difficult from embossing thermoplasts. The PDMS elastomer cures and hardens by hydrosilation reaction unlike the thermoplasts, which can be melted and hardened by heating and cooling, respectively.

Determining the GP of the silicone network is the main criteria to design the embossing experiment. Hot embossing is the most cost-effective, simple, and a quick method for imprinting microstructures on addition curing PDMS.

Hot embossing of microscale corrugation lines on addition curing vinyl-terminated polydimethylsiloxane films was successfully performed and the step-by-step embossing

process has been established. The embossing was shown to be possible for systems, with and without fillers with Young's modulus ranging from 27 to 640 kPa, which indicates a great versatility of the process. It can be performed in batch or a continuous process. It is also shown that a given embossing setup could be used for several materials by altering the preheating conditions, pressure, and speed of the rollers.

Appendix 1

Diameter of roller = 6 in.
Circumference of roller = πd = 18.84 in.
Speed of roller = 1.4 r/min = 26.4 in./min = 67 cm/min = 0.0112 m/s.

Funding

The authors gratefully acknowledge the financial support from the Danish National Advanced Technology Foundation.

References

1. Benslimane MY, Kiil H and Tryson MJ. Dielectric electro-active polymer push actuators: performance and challenges. *Polym Int* 2010; 59(3): 415–421.
2. Kiil H and Benslimane M. Scalable industrial manufacturing of DEAP. In: Proceedings of SPIE, San Diego, California, 6 April 2009, Paper no. 72870R-1-72870R-10.
3. Worgull M. *Hot embossing: theory and technology of microreplication*. Karlsruhe, Germany: Institute for Microstructure technology, 2009. ISBN:978-0-8155-1579-1.
4. Kolew A, Münch D, Sikora K and Worgull M. Hot embossing of micro and sub-micro structured inserts for polymer replication. *Microsys Technol* 2010; 17(4): 609–618.
5. Katoh T, Tokuno R, Zhang Y, Abe M, Akita K and Akamatsu M. Micro injection molding for mass production using LIGA mold inserts. *Microsy Technol* 2008; 14(9–11): 1507–1514.
6. Benslimane M, Kiil H and Tryson MJ. Electro-mechanical properties of novel large strain polypower film and laminate components for DEAP actuator and sensor applications. In: *Conference on electroactive polymer actuators and devices (EAPAD)*, San Diego, CA, 7 March 2010, paper no. 7642, 764231, pp. 1–11. USA: Proceedings of SPIE.
7. Larsen AL, Hansen K, Hassager O, Bach A, Ndoni S and Jørgensen M. Elastic properties of nonstoichiometric reacted PDMS networks. *Macromolecules* 2004; 36(26): 10063–10070.
8. Bejenariu AG, Rasmussen HK, Skov AL, Hassager O and Frankaer SM. Large amplitude oscillatory extension of soft polymeric networks. *Rheol Acta* 2010; 49(8): 807–814.
9. Venkatraman SK and Winter HH. Finite shear strain behavior of a crosslinking polydimethylsiloxane near its gel point. *Rheol Acta* 1990; 29(5): 423–432.
10. Chambon F and Winter HH. Linear viscoelasticity at the gel point of a crosslinking PDMS with imbalanced stoichiometry. *J Rheol* 1987; 31(8): 683–697.
11. Frankær SMG, Jensen MK, Bejenariu AG and Skov AL. Investigation of the properties of fully reacted unstoichiometric polydimethylsiloxane networks and their extracted network fractions. *Rheol Acta* 2012; 51(6): 559–567.
12. Winter HH. Can the gel point of a cross-linking polymer be detected by the G′–G″ crossover? *Polym Eng Sci* 1987; 27(22): 1698–1702.

Appendix IV

Techniques for hot embossing microstructures on liquid silicone rubbers with fillers

Journal of elastomer and plastics (2014)

Journal of Elastomers and Plastics
http://jep.sagepub.com/

Techniques for hot embossing microstructures on liquid silicone rubbers with fillers

Sindhu Vudayagiri, Liyun Yu and Anne Ladegaard Skov

Journal of Elastomers and Plastics published online 19 March 2014
DOI: 10.1177/0095244314526743

The online version of this article can be found at:
http://jep.sagepub.com/content/early/2014/03/18/0095244314526743

Published by:
SAGE
http://www.sagepublications.com

Article

JOURNAL OF ELASTOMERS & PLASTICS

Journal of Elastomers & Plastics
1–13

DOI: 10.1177/0095244314526743
jep.sagepub.com
SAGE

Techniques for hot embossing microstructures on liquid silicone rubbers with fillers

Sindhu Vudayagiri, Liyun Yu and Anne Ladegaard Skov

Abstract

Embossing is an established process for the thermoplastic elastomers but not yet for the thermosetting elastomers. It has already been shown that hot embossing is a viable technology for imprinting microstructures in addition to curing thin silicone films at their gel point. It is one of the simplest, most cost-effective, and time-saving methods for replicating microstructures. In the present study, films made from liquid silicone rubber (LSR) formulations containing fillers are hot embossed under modified operating conditions. The use of such relatively hard silicone elastomers shows the versatility of this method that has been established for softer silicone elastomers. Also, as a proof of concept, a microstructured metal (nickel (Ni)) plate is used as an embosser for the films successfully. The ideal condition for hot embossing the LSR formulation (XLR 630 with titanium dioxide fillers) with a Ni embosser is 110°C preheating for 15–35 s, embossed with 2 bar pressure, and postheating for complete curing at 110°C for 3 min showing that the process is extremely fast.

Keywords

Hot embossing, liquid silicone rubber (LSR) with fillers, DEAP transducer, microscale corrugations

Introduction

A transducer is a device that converts a signal from one form of energy to another form of energy. Dielectric electroactive polymer (DEAP) transducers respond to an electrical

The Danish Polymer Centre, Department of Chemical and Biochemical Engineering, Technical University of Denmark, Lyngby, Denmark

Corresponding author:
Anne Ladegaard Skov, The Danish Polymer Centre, Department of Chemical and Biochemical Engineering, Technical University of Denmark, 2800 Kgs Lyngby, Denmark.
Email: al@kt.dtu.dk

field applied by changing its size and shape (Figure 1(a)).[1] The working principle resembles a capacitor with variable capacitance since the elastomer stretches. The elastomer has compliant electrodes that are sputtered on the film's microstructured surface. The purpose of microscale corrugations on the thin films is to protect the metallic electrode from high strains endured by the elastomer when used as actuators, since the local strain on the corrugations are very small compared with the overall strain. The corrugations also enable controlled actuation in a particular direction. (Figure 1(b))

In the large-scale manufacture of DEAPs by Danfoss Polypower A/S (Denmark), the films are made on a specially designed carrier web (Figure 2) that imparts the corrugated structure to the films. There are two types of carrier webs used at Danfoss depending on whether the corrugation lines are along the length of the web (down-web) or perpendicular to the length of the web (cross-web). Also, there are two types of carrier webs defined by the wave depth and period. One that has a depth of 5 μm and a period of 10 μm and such films easily strain 35% with no electrode breakage. Another that has both depth and period of 7 μm and such films work up to about 80% strain without electrode damage.[1,2]

The liquid silicone rubber (LSR) mixture (polydimethyl siloxane (PDMS) + catalyst + cross-linker + solvent + fillers) is applied on the carrier web to make a thin film. The mixture is left to cure by the hydrosilylation reaction directly on the web at elevated temperature in an oven at 110°C for 2 min.[2] The cured elastomer film has the microcorrugations transferred onto it from the carrier web (Figure 2). After curing, it is peeled off the web using delamination equipment and transferred onto another carrier/conveyor belt (without corrugations) to allow for the deposition of metallic electrodes on the corrugated side of the film. The process of releasing the thin elastomer film from the carrier web is not smooth and induces defects and prestrain in the film.[2,3] The performance equation (equation (1)) of the DEAP actuator films indicates that thinner films require smaller voltage to actuate the films and thereby improve their performance as actuators.[4]

$$\rho = \varepsilon\varepsilon_0\left(\frac{V}{d}\right)^2 \tag{1}$$

where ρ is the compressive stress, ε is the relative dielectric constant, $\varepsilon_0 = 8.85 \times 10^{-12}$ F m^{-1} is the permittivity of free space, V is the applied voltage, and d is the thickness of the film.

A novel process should therefore enable the production of thinner films in a fast and efficient process. In the current process, as the films get thinner, processing and handling become very complicated. On delaminating the thinner films, the peel force usually exceeds their tear strength with the result that the films are torn apart. The corrugations on the films contribute to further problems during delamination as they significantly increase the surface area of the film and therefore the delamination becomes more difficult. Such failures in the continuous production process lead to plant shut down. The

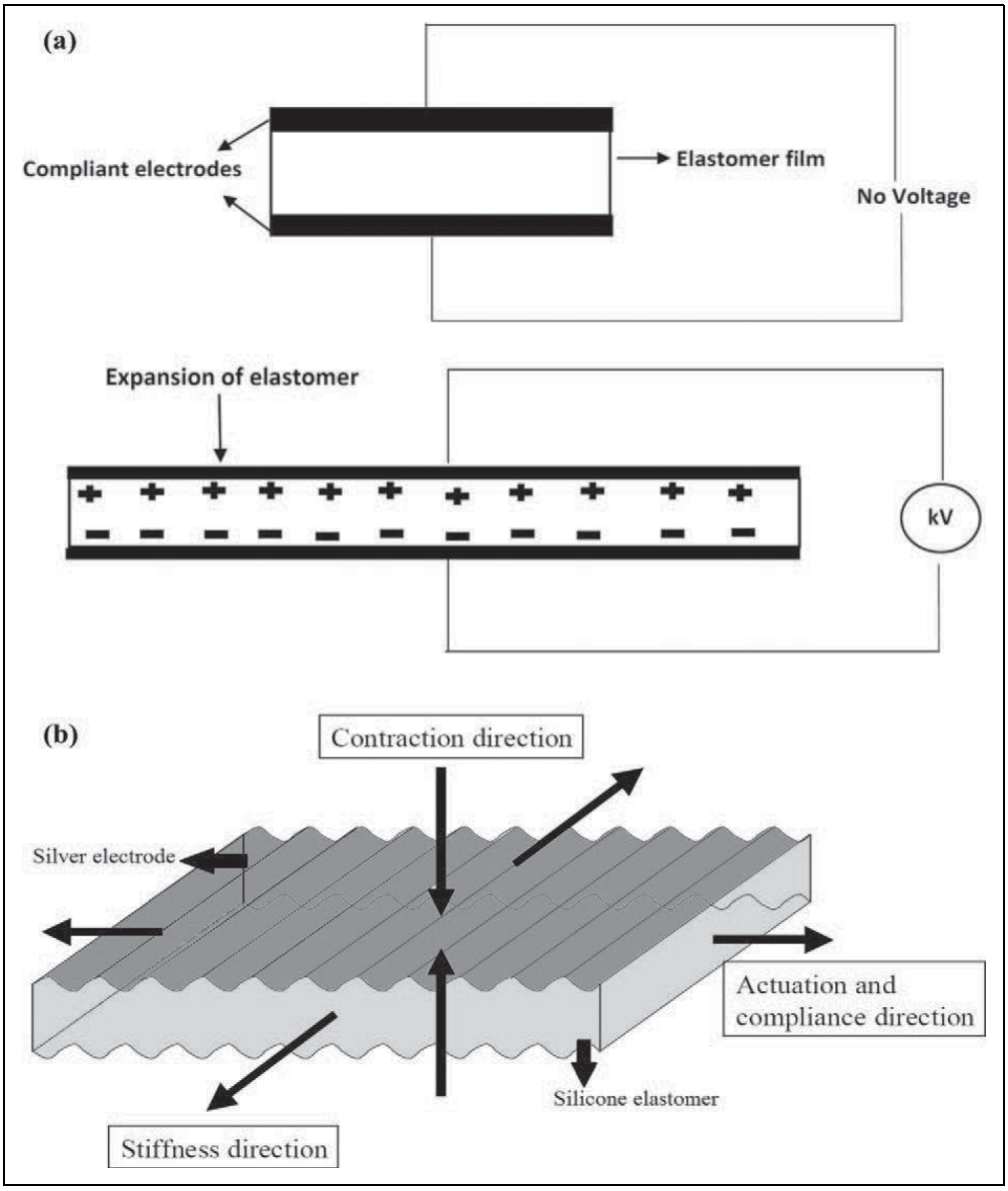

Figure 1. (a) General working principle of a dielectric electroactive polymer transducer with no corrugations and (b): corrugated elastomer film with compliant electrodes actuating under high voltage.[1]

delamination step is the limiting step in this process that does not currently allow for producing very thin films. Innovative processing techniques for producing thin (20–40 μm) PDMS films with microscale patterns are necessary for their efficient application as

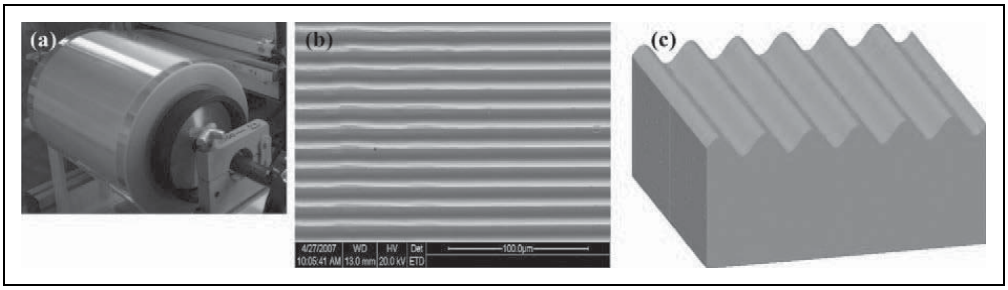

Figure 2. (a) Carrier web roller, (b) microscopic image of corrugation pattern on carrier web, and (c) schematic cross-sectional view of carrier web.[2]

DEAP transducers that are required in large quantities for making wind and wave power generation equipment.[5] The current technology has limitations as it is very likely to induce prestrain in the films during the delamination step and the carrier web is very expensive. Although the carrier web is recycled, the life time of the carrier web is not long enough to make the process economic. Furthermore, the common carrier webs that stick too well to the films are not stable at high temperatures for extended periods of time and have seam lines breaking the corrugation pattern.[6]

Processing techniques should be easy, economic, fast, and should not induce any defects in the thin films. The performance of the film as transducer material depends on the excellence and precision of the production-processing techniques.[7] An alternative method called the hot embossing for producing thin corrugated films was formulated by Vudayagiri et al. (Figure 3).[6]

In this method, a thin coating of the addition curing PDMS mixture is applied on a flat polyethylene terephthalate (PETE) substrate, which is 0.2 mm thick. The thin elastomer coating is preheated on a hot steel roller at 110°C for 10–15 s until the mixture approaches gel point (GP).[6] The film that is precured to the GP is now run through the embossing roll that is running at a speed of 1.4 r min^{-1} with a pressure of 25 psi between the rolls (Figure 3). The surface of embossing roll has the corrugations and the rolls are at a temperature of 100°C. The film runs through the rolls and comes out embossed. In the hot embossing method, there is no delamination step; hence, the danger of tearing apart the films is eliminated. The contact time of the embossing roll and the preheated film is very short such that adhesion is not established between the two. The high temperature of the embossing roll helps the elastomer film reach complete curing. This method was successful with both (1) room temperature vulcanizable rubber (RTV) and (2) LSR.

A piece of carrier web was rolled around the embossing roll to give the corrugation pattern to the roll. For the large-scale industrial hot embossing process, an embossing roll with engraved corrugation pattern is required. The roll needs to be made in a material that can conduct heat and should not inhibit the curing of the PDMS mixture.

Two modifications are now introduced to the above hot embossing process: (1) a nickel (Ni) embosser and (2) LSR with fillers.

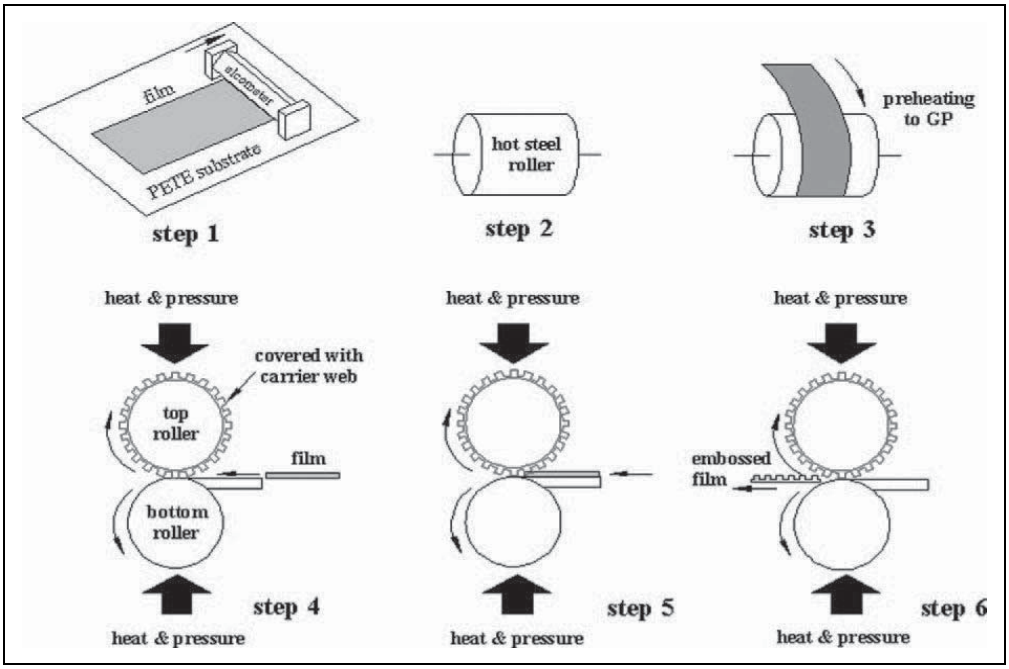

Figure 3. Schematic representation of the hot embossing process with the gravure lab coater.[6]

Ni embosser

The primary focus is to make a mold with engraved corrugation pattern on it. The corrugation pattern on the carrier web is transferred on to a Ni plate by sputtering a thin layer of metal on carrier web and then plated with Ni electrochemically. It has been verified that the structures have been transferred to Ni by visual inspection (light diffraction on surface) and confocal microscopy as shown in Figure 4(a). The plate is made of a Ni–vanadium (V) alloy (93% Ni, 7% V). The thickness of the plate is 237 μm (Figure 4(b)). The Ni plate does not inhibit the addition curing of the films. Films cured on Ni plate as shown in Figure 5 prove that Ni plate does not inhibit the curing of the elastomer films. The microstructured Ni plate, as shown in Figure 4(b), is then used as the embosser. Hot embossing with Ni plate is performed on a simple device that can press under controlled pressure.

LSR with fillers

LSR formulations with different proportions of the filler titanium dioxide (TiO_2) will be embossed, unlike the previous method where pure RTV silicones and LSRs were embossed. LSRs are low-viscosity silicone rubbers (low-molecular-weight) that is pourable or self-leveling in consistency with a viscosity of 300,000 to 1,000,000 cps.[8] They are based on platinum curing that offer curing time of a few seconds. When combined with fillers, the viscosity of the LSR mixtures increases further.[8] Producing thin films

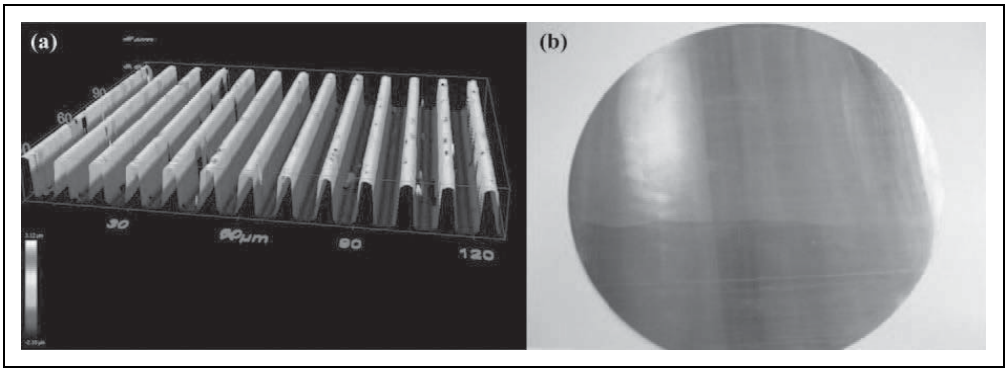

Figure 4. (a) Confocal microscopic image of the corrugated Ni plate and (b) Ni plate (thickness = 237 μm) with microstructure (corrugation: period = 10 μm, depth = 5 μm) used for embossing. Ni: nickel.

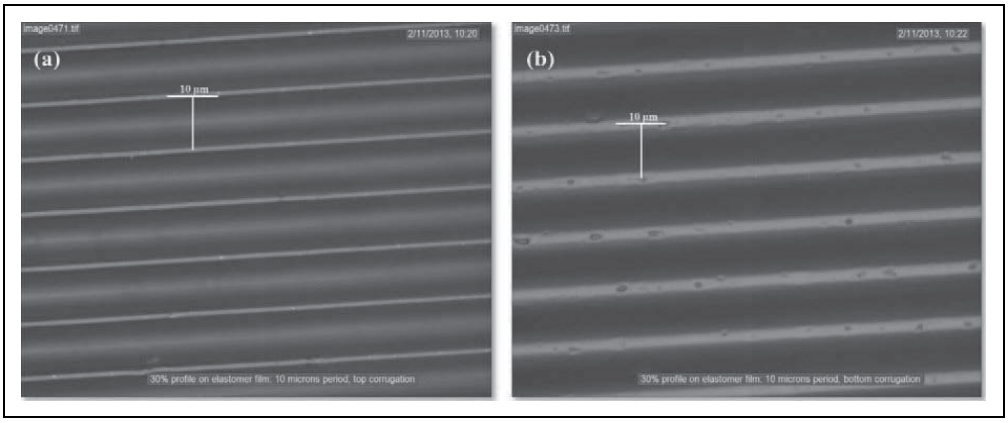

Figure 5. (a) Microstructures replicated on the silicone film cured on Ni plate focus on top surface and (b) focus on bottom surface. Ni: nickel.

(20–40 μm) with highly viscous mixtures is difficult as it is hard to spread the viscous mixtures. In order to prevent the mixtures from getting too viscous and to disperse the fillers efficiently a solvent (OS20) is also used in LSR formulation. Viscosity studies are performed on various formulations in order to examine whether LSR formulations have viscosities permissible by the existing manufacturing constraints.

Experimental

Materials

Low-viscosity extra LSR POWERSIL® XLR® 630 A/B was obtained from Wacker Chemie AG (Germany). XLR630 is supplied as two parts: A and B. The part A contains

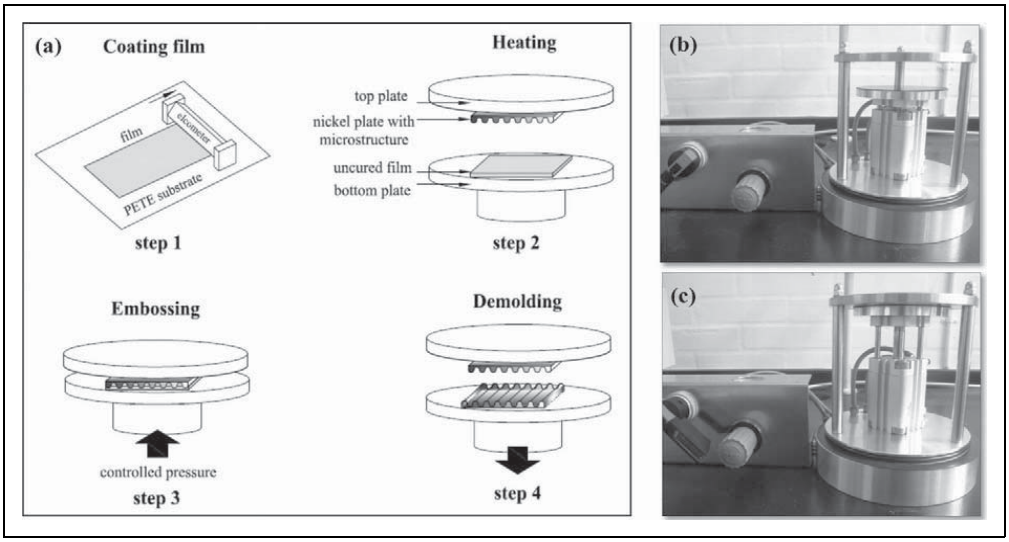

Figure 6. (a) Schematic representation of hot embossing process with the corrugated Ni plate, (b) pressure instrument used for embossing release, and (c) pressurization. Ni: nickel.

PDMS and platinum catalyst, while part B contains PDMS and cross-linker. The mixing ratio of parts A and B is 1:1.

Hydrophobic rutile TiO_2 (Hombitec RM130F) was obtained from Sachtleben Chemie Gmbh (Germany). The primary particle size is 15 nm.

OS20 solvent (an ozone-safe volatile methylsiloxane fluid) was obtained from Dow Corning (Midland. Michigan, USA).

Procedure

There are four steps in the embossing procedure. An overview of the steps involved in the particular embossing scheme used here is shown in Figure 6.

Coating film. Varying amounts (0, 5, 10, and 15wt%) of TiO_2 nanoparticles are mixed into the XLR630 part A and B with solvent OS20 using a speed mixer (DAC 150FVZ, Hauschild Co., Germany) at 3500 r min^{-1} for 2 min. The mixing is ensured to be homogenous by adding sufficient solvent to allow for higher mobility of the particle/silicone mixtures. The formulations of LSR mixtures are listed in Table 1. The uniform mixtures are cast on a temperature-stabilized PETE substrate with a thin film applicator 3540 bird film applicator (Elcometer, Germany; see step 1 in Figure 6(a)).

Preheating. The films made on the PETE substrate are preheated prior to the embossing such that the addition curing elastomer proceeds to the GP, which characterizes the state when a three-dimensional network of cross-linked molecules is formed, namely the transition from a viscoelastic liquid to a viscoelastic solid.[9,10] The time and temperature for

Table 1. Formulations of LSR mixtures.

No.	XLR 630 A:XLR630 B:TiO_2: OS20[a]
1	50%:50%:0%:0 (pph)
2	47.5%:47.5%:5%:10 (pph)
3	45%:45%:10%:15 (pph)
4	42.5%:42.5%:15%:20 (pph)

LSR: liquid silicone rubber; TiO_2: titanium dioxide; XLR: extra liquid silicone rubber.
[a]Amounts of XLR 630 and TiO_2 are in mass ratio, OS20 in parts per hundred.

preheating is fixed based on the GP estimated by rheological experiments.[6] A hot plate heats up the film from the bottom, and thereby, the film cures from below and the free surface for embossing is still around the GP (see step 2 in Figure 6(a)).

Embossing. The films that are partly cured by preheating are immediately embossed using the Ni plate with microscale corrugation lines. The Ni plate is also heated prior to embossing so that it is around 100°C at the time of embossing. The force applied on the film by the plate imprints the corrugation lines on the film, and the temperature of the plate ensures that the film cures and retains the microstructure. The property of the silicone elastomers to retain an imprint made on it at the GP enables the embossing of microstructures. The applied force between the Ni plate and film is adjusted by the pressure meter (Figure 6(b) and (c); see step 3 in Figure 6(a))

Demolding. The film that is embossed is left to cure completely in the oven at 100°C for 2 min and then is demolded from Ni plate by reducing the pneumatic pressure as shown in step 4 of Figure 6(a). The demolding step is not as tedious as the delamination process. When the film is delaminated as in the conventional process, it is subjected to high peel forces. In demolding step, the film has the support of the substrate when the Ni embosser is detached and also their contact time is less to develop any credible adhesive force between the cured film and the Ni plate. In the continuous embossing roll method, there is no demolding/delaminating step, as the film simply moves out continuously from in-between the rolls (Figure 3). The contact time is very short between the embosser and film and complete wetting of the surface does not happen.

Characterization

Rheological measurements. The rheological measurements on the cross-linking behavior were carried out in an inert nitrogen atmosphere using a strain-controlled shear rheometer (AR 2000, Rheology Division, TA instruments, New castle, Delaware, USA) set to a controlled strain mode with 2% strain, which was ensured to be within the linear regime of the material based on an initial strain sweep test.

Time-resolved dynamic mechanical experiments of the LSR mixtures were performed at a constant frequency of 1 Hz applying parallel plate geometry of 25 mm in diameter and a gap of 0.5–1 mm at 60 and 80°C.

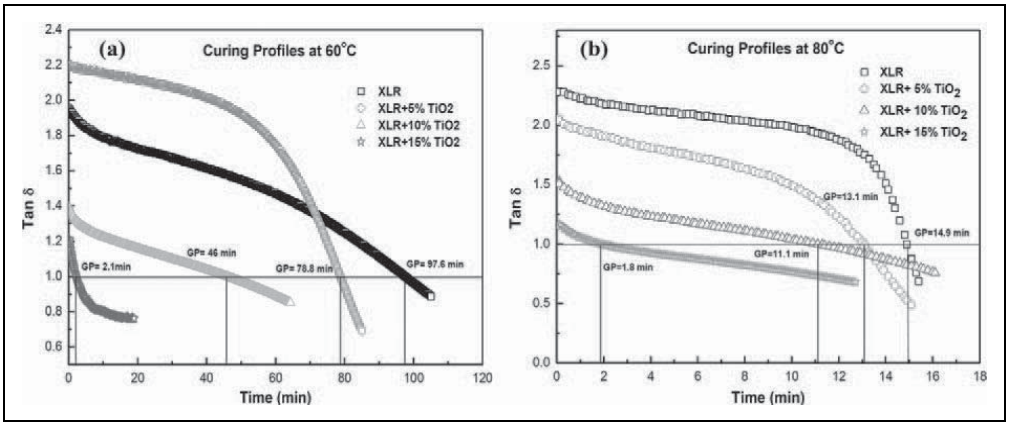

Figure 7. (a) Curing profiles of LSR mixtures at 60°C and (b) curing profiles of LSR mixtures at 80°C. LSR: liquid silicone rubber.

The linear viscoelastic (LVE) data of the LSR films were measured with parallel plate geometry of 25 mm in diameter at 23°C. The LVE diagrams were obtained from frequency sweeps from 100 to 0.01 Hz.

The viscosities of mixtures were tested by the flow sweep of AR2000 with the shear rate from 10^{-2} s^{-1} to 100 s^{-1} at 23°C using a parallel plate geometry of 25 mm in diameter.

Microscopy investigation. Optical characterization of the embossed film was performed using an optical microscope (Leica DMLB, Germany) connected to a Highlight 2000 from Olympus (Tokyo, Japan).

Results and discussions

Curing profiles

The curing profiles of LSR mixtures at 60 and 80°C are shown in Figure 7. The cross-point of storage modulus G' and loss modulus G'' is used as the GP.[6,11] For simplicity, a plot of tan $\delta = G''/G'$ is shown in Figure 7, and the points at which tan δ reaches the value of 1 indicates the GP (cross-point of G' and G''). The GP may not be reached at tan $\delta = 1$ for filled systems but the measure of tan $\delta = 1$ still gives the optimal conditions for embossing. Since the platinum-catalyzed hydrosilylation reaction rate increases with temperature, the time to reach GP decreases with the increase of temperate (60–80°C).[12] The time to reach GP defined as tan $\delta = 1$ also decreases with increasing the filler amount (0–15 wt%) due to hardening effect of the fillers. The curing profiles at 110°C are not presented here as the cross-point (tan $\delta = 1$) occurs within a few seconds (15–40 s). The GPs of the mixtures at 110°C, and the conditions for embossing are presented in Table 2.

Table 2. Embossing conditions of LSR films.

No.	XLR 630 A:B:TiO_2:OS20[a]	Preheat temperature (°C)	Preheat time/time to reach GP (s)	Pressure (bar)
1	50%:50%:0%:0 (pph)	110	35	2
2	47.5%:47.5%:5%:10 (pph)	110	30	2
3	45%:45%:10%:15 (pph)	110	22	2
4	42.5%:42.5%:15%:20 (pph)	110	15	2

LSR: liquid silicone rubber; TiO_2: titanium dioxide; GP: gel point; XLR: extra liquid silicone rubber.
[a]Amounts of XLR 630 and TiO_2 are in mass ratio, OS20 in parts per hundred.

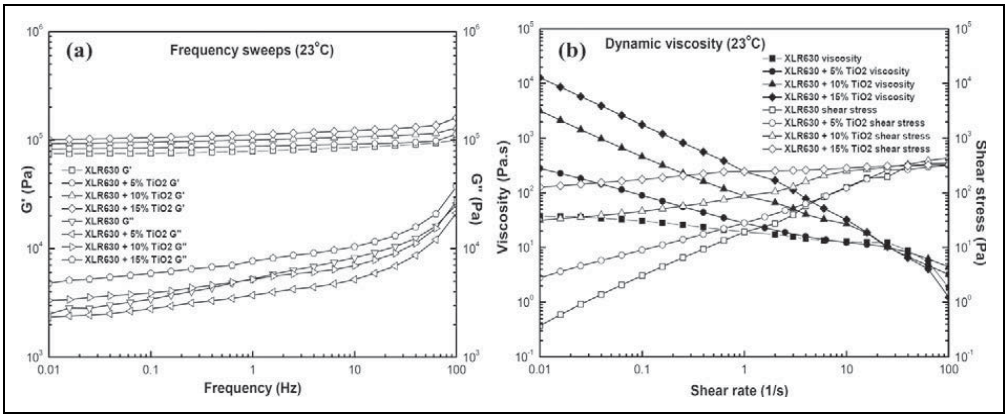

Figure 8. (a): Storage modulus (G') and loss modulus (G'') of LSR films at 23°C and (b) dynamic viscosity curves of the LSR mixtures at 23°C. LSR: liquid silicone rubber.

Elasticity

For any material, the elastic modulus (G') may be defined as the ratio of stress to strain, wherein the strain produced by the stress is small. Therefore, the ''softer'' a material, the smaller its modulus will be. For cross-linkable materials, an increase in the modulus is also a measure of the increased cross-linking of the materials.[13] Figure 8(a) shows the dynamic moduli (G' and G'') of the LSR films with TiO_2 nanoparticles as a function of the applied frequency at 23°C. The G' value increases with increasing filler concentration of the mixtures and so does the G'' value, which indicates that the inorganic filler leads to the enhancement of the plasticity with reduction of elasticity.

Dynamic viscosity

The dynamic viscosity curves of LSR formulations are shown in Figure 8(b). The addition of fillers reinforces the mixture viscosity that results in an increase of the elastic modulus. It is seen that XLR 630 (20 pph OS20) with 15% TiO_2 has the highest viscosity of 10,000 Pa·s (0.01 s^{-1}), which is well below the permissible limit. A viscosity below

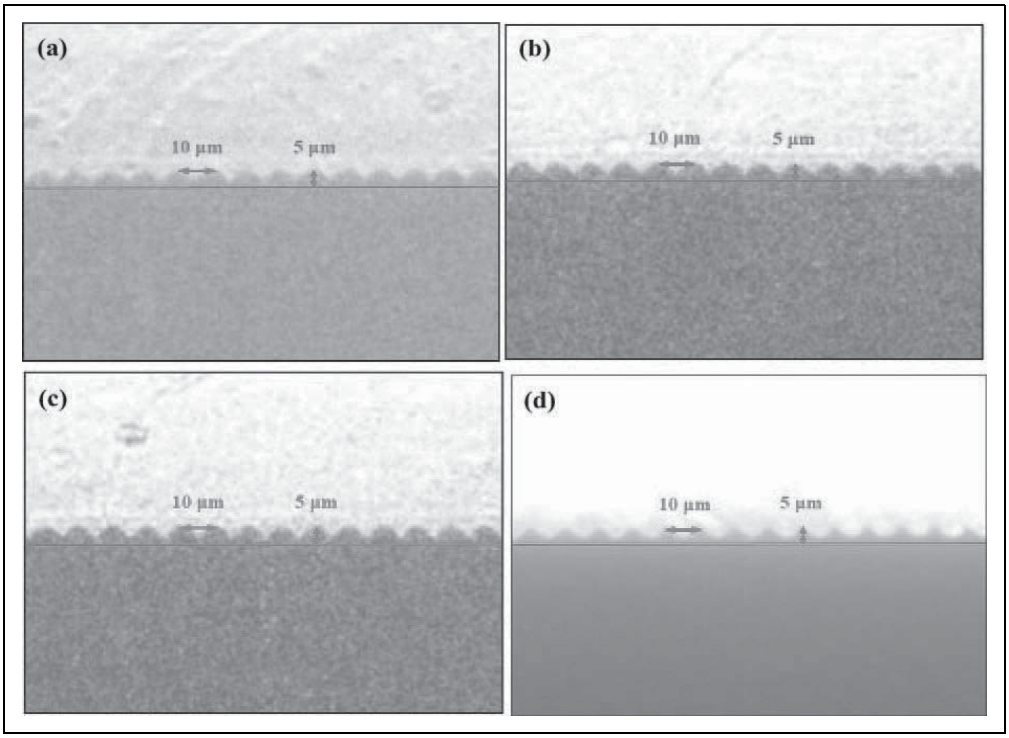

Figure 9. (a) Cross-sectional morphologies of the embossed films, XLR630, (b) XLR630 + 5% TiO_2, (c) XLR630 + 10% TiO_2, and (d) XLR630 + 15% TiO_2. TiO_2: titanium dioxide; XLR: extra liquid silicone rubber.

40,000 Pa·s is preferred in the film manufacture process in order to minimize the energy expenditure on mixing the formulations and spreading them on substrates to make films.

Microstructure

The microscopic images of cross section and surface for the LSR films embossed by the Ni plate are shown in Figures 9 and 10. The embossing conditions are listed in Table 2. The corrugation morphologies are the same as the microstructure on the Ni plate (Figure 4(b)), which means that the films are fully replicated.

Conclusions

Hot embossing using a Ni plate embosser has been employed successfully to imprint microstructures on thin addition curing LSR films with varying amounts of fillers. The technique is successful for all types of silicone elastomer formulations. This further asserts that the process is very suitable for large-scale industrial manufacture. It is envisioned that when the corrugated Ni plate when rolled onto a roller a continuous roll to

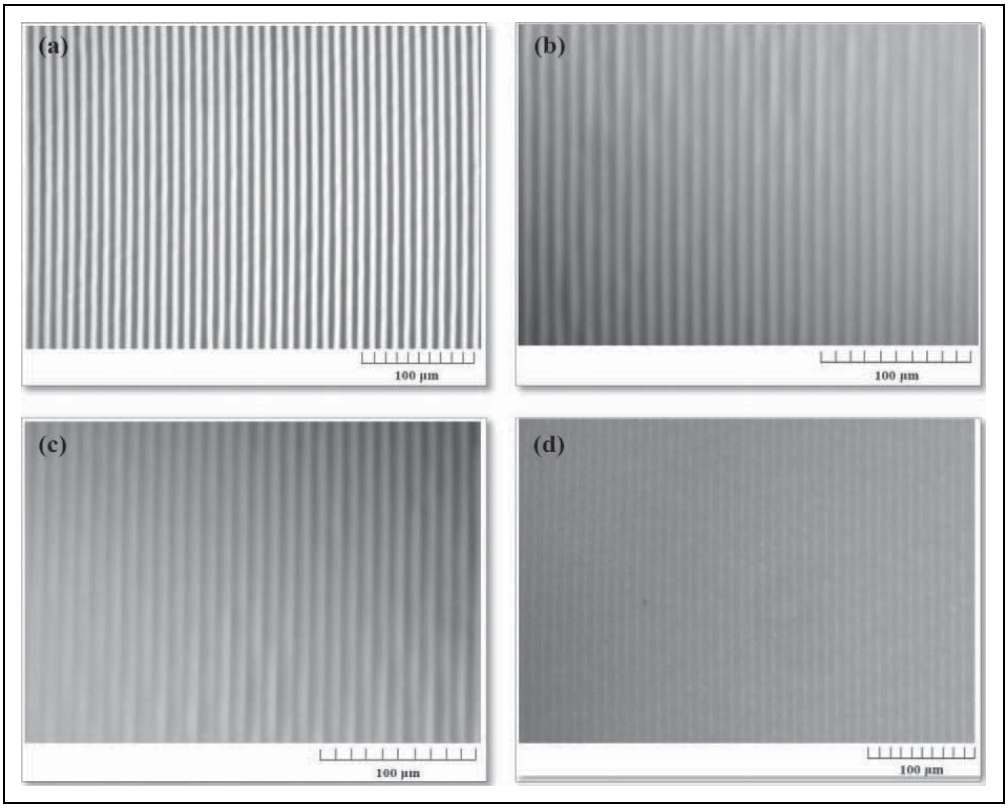

Figure 10. (a) Surface morphologies of the embossed films, XLR630, 1(b) XLR630 + 5% TiO_2, (c) XLR630 + 10% TiO_2, and (d) XLR630 + 15% TiO_2. TiO_2: titanium dioxide; XLR: extra liquid silicone rubber.

roll embossing process can be developed. Thus, a process without carrier web can be established by eliminating release issues and making the process very economic.

Acknowledgment

The authors thank Claus Højgård Nielsen, Process Specialist, DTU Danchip, Denmark, for the technical assistance in making the embossed nickel plate.

Funding

The authors gratefully acknowledge the financial support from the Danish National Advanced Technology Foundation.

References

1. Benslimane M, Kiil HE and Tryson MJ. Electromechanical properties of novel large strain poly power film and laminate components for DEAP actuator and sensor applications. In:

Proceedings of SPIE on electroactive polymer actuators and devices (EAPAD)(ed Y Bar-Cohen), San Diego, California, March 2010, paper no. 764231, pp. 1–11. California, CA: SPIE.
2. Kiil HE and Benslimane M. Scalable industrial manufacturing of DEAP. In: *Proceedings of SPIE on electroactive polymer actuators and devices (EAPAD)(ed Y Bar-Cohen)*, San Diego, California, March 2009, paper no. 72870R, pp. 1–10. California, CA: SPIE.
3. Vudayagiri S, Junker MD and Skov AL. Factors affecting surface and release properties of thin polydimethylsiloxane films. *Polym J* 2013; 45(8): 871–878.
4. Pelrine R, Kornbluh R, Pei Q, et al. High-speed electrically actuated elastomers with strain greater than 100%. *Science* 2000; 287(5454): 836–839.
5. Koh SJA, Keplinger C, Li T, et al. Dielectric elastomer generators: how much energy can be converted? *IEEE/ASME Trans Mechatron* 2011; 16(1): 33–41.
6. Vudayagiri S, Yu LY, Hassouneh SS, et al. Hot embossing of microstructures on addition curing polydimethylsiloxane films. *J Elastom Plast*. Epub ahead of print 11 April 2013. doi: 10.1177/0095244313483642.
7. Benslimane MY, Kill HE and Tryson MJ. Dielectric electro-active polymer push actuators: performance and challenges. *Polym Int* 2010; 59(3): 415–421.
8. Stritzke B. *Custom molding of thermoset elastomers—a comprehensive approach to materials, mold design, and processing*. ISBN: 978-3-446-41964-3, Cincinnati, OH, USA: Hanser Publications, 2009, pp. 132–141.
9. Winter HH and Chambon F. Analysis of linear viscoelasticity of a cross-linking polymer at the gel point. *J Rheol* 1986; 30: 367–382.
10. Chambon and Winter HH. Linear viscoelasticity at the gel point of a crosslinking PDMS with imbalanced stoichiometry. *J Rheol* 1987; 31(8): 683–697.
11. Winter HH. Can the gel point of a cross-linking polymer be detected by the G′-G″ crossover? *Polym Eng Sci* 1987; 27(22): 1698–1702.
12. Lewis N, Stein J, Gao Y, et al. Platinum catalysts used in the silicones industry. *Platinum Metal Rev* 1997; 41(2): 66–75.
13. Ramesh K, Tock RW, Narayan RS, et al. Property evaluation of silicone elastomers used in tension-adhesion joints. *J Mater Sci Lett* 1995; 14: 964–967.

Appendix V

Bilaterally microstructured thin polydimethylsiloxane film production

Accepted by Polymer-Plastics Technology and Engineering

Bilaterally microstructured thin polydimethylsiloxane film production

Sindhu Vudayagiri[1], Liyun Yu[1], Suzan Sager Hassouneh[1], Ulrik Hansen[2], Anne Ladegaard Skov[1]*

[1]The Danish Polymer Centre, Department of Chemical and Biochemical Engineering, *Technical University of Denmark, 2800 Kgs. Lyngby, Denmark*
[2]*Danfoss PolyPower A/S, 6430 Nordborg, Denmark*
* Corresponding author. Tel.: +45 45252825; fax: +45 45882258.
E-mail address: al@kt.dtu.dk

Abstract: Thin PDMS films with complex microstructures are used in the manufacturing of dielectric electro active polymer (DEAP) actuators, sensors and generators, to protect the metal electrode from large strains and to assure controlled actuation. The current manufacturing process at Danfoss Polypower produces films with a one-sided microstructured surface only. It would be advantageous to produce a film with both surfaces microstructured, as this increases the film's performance efficiency. The new technique introduced herein produces bilaterally microstructured film by combining an embossing method with the existing manufacturing process. In employing the new technique, films with microstructures on both surfaces are successfully made with two different liquid silicone rubber (LSR) formulations: 1) pure XLR630 and 2) XLR630 with titanium dioxide (TiO_2). The LSR films (~ 70 μm) are cast on a carrier web substrate using a coating blade. The carrier web, which has a sinusoidal corrugation with wave height of 7 μm and a wave period of 7 μm on its surface, imparts corrugations to the bottom surface of the film. The elastomer film on the carrier web is preheated to the gel point, where the elastomer film can retain an imprint made on it. The preheated film at gel point is embossed between the rolls of a gravure lab coater, which corrugates the top surface of the film. The films are then heated, in order to cure completely. For the LSR systems used in this process, the optimum conditions for preheating are 110°C for 4-7 s, while for embossing the temperature is 110°C with 25 psi pressure between the rolls at a speed of 1.4 rpm. Scanning electron microscope (SEM) images confirm the formation of microstructures on both the surfaces of the film.

Keywords: Microstructured PDMS films, liquid silicone rubber, dielectric electroactive polymer, embossing.

1. Introduction:

Dielectric electroactive polymers (DEAPs) change their size and shape when sandwiched between two compliant electrodes and subjected to a high voltage. DEAPs are used for manufacturing actuators, generators and sensors because of their ability to convert electrical energy into mechanical energy and vice versa. Polydimethylsiloxane (PDMS) is a commonly used DEAP material. Corrugated PDMS films are manufactured by Danfoss Polypower in order to make DEAP actuators, sensors and generators [1,2]. The corrugated design protects the compliant metal electrode sputtered on the film from the large strains encountered by the film during actuation. Compliant metal electrodes have advantages such as high conductivity and low electrical losses, and these properties do not deteriorate significantly with strain [2]. The micro patterned surface restricts the film's actuation along the corrugations, allowing it to elongate only in the direction perpendicular to the corrugation lines, as shown in Figure 1 [1,2].

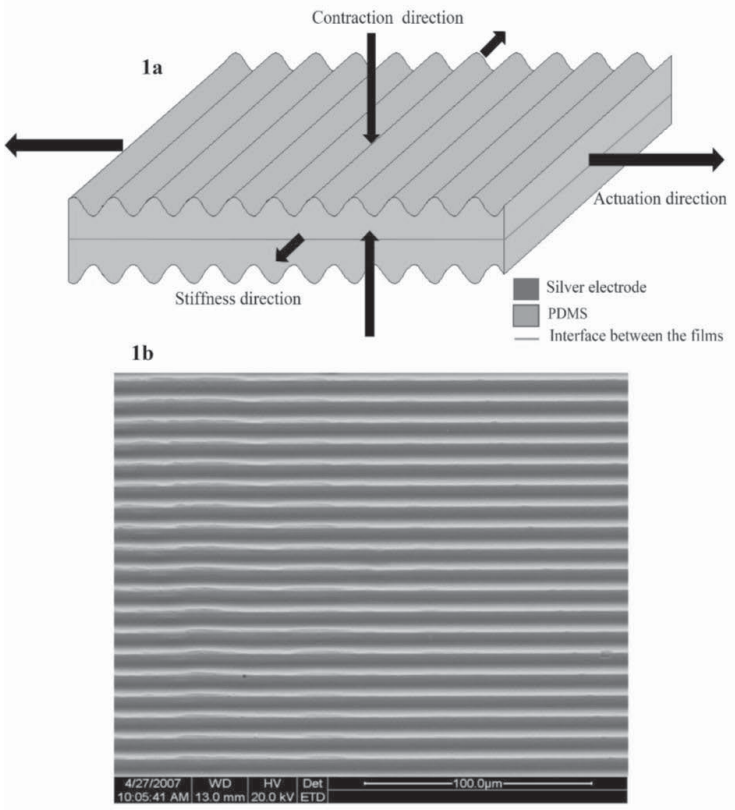

Figure 1: a. Two films adhered to produce a thin film actuator [2],
b. Microscopic image showing corrugations running across the length of carrier web [1]

In the industrial process, corrugated films are manufactured by casting a uniform, thin layer of uncured PDMS elastomer onto the carrier web. [1] The elastomer is then cured on the carrier web surface at 100ºC for 2 minutes. The PDMS elastomer cures by platinum catalyzed hydrosilation reaction. The carrier web acts as a mold and imparts the corrugated structure to the bottom surface of the cured films that are peeled off the carrier web. A schematic of the industrial manufacturing process is shown in Figure 2. The film is then sputtered with silver on the corrugated side. This method allows for making a film with only one microstructured surface. The metallised films are then laminated mechanically in a 'back to back' configuration using a constant load such that the flat sides of the films are in contact.

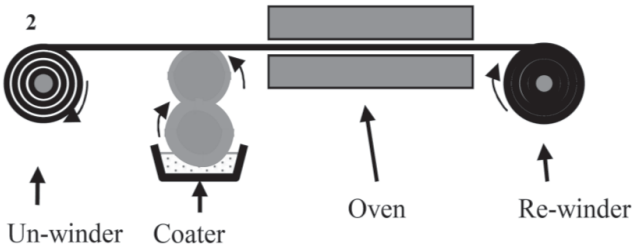

Figure 2: Corrugated thin PDMS film production at Danfoss Polypower A/S [1]

The process of laminating two films has certain drawbacks for two main reasons: 1) it may introduce some defects or air gaps between the films and 2) it doubles the thickness of the dielectric material between the electrodes. The dielectric breakdown strength of air is 3V/μm [3], which is very low compared to the LSR films and the operating voltages of the DEAP laminates [2,4,5]. The air gaps at the interface will thus breakdown easily bringing down the overall dielectric breakdown strength of the laminated film and make them more susceptible to failure. Figure 3 shows a comparison between a laminated film and a monolithic film. In theory, lamination serves to decrease the probability of the thin film actuator to breakdown under high voltage, as it would require two defects at the same spot on both films. However, this advantage would be rendered futile if the lamination process introduced air gaps at the interface. To ensure proper mechanical contact between the films without any air gaps, the flat surfaces of the laminating films are air-plasma treated, and their mechanical strength and breakdown strength is tested. From the studies conducted in our lab, it is established that films laminated by air-plasma treatment showed a decrease in breakdown strength compared to single films of the same thickness, even though they have the same mechanical properties as a single film. Other proposed methods of adhering two PDMS films – using silicone oil and a cross-linker at the interface of two fully cured PDMS films, and adhering two partly cured films – are not suitable for the current manufacturing process [6,7].

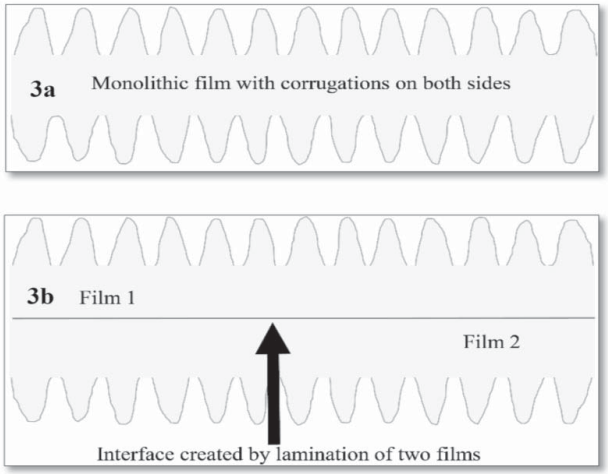

Figure 3: a. Monolithic film, **b**. Laminated film

The actuation of the films increases as film thickness decreases for a given applied voltage. Equations (1) and (2) show that the compressive stress and strain outputs of the DEAP films increase as the thickness of the films decreases [8]:

$$p = \varepsilon_r \varepsilon_0 \left(\frac{V}{d}\right)^2 \quad (1)$$

$$s_z = -\varepsilon_r \varepsilon_0 \frac{(V/d)^2}{Y} \quad (2)$$

where Ɪis compressive stress, is the relative dielectric constant, ₄= 8.85×10^{-12} F/m is the permittivity of free space, V is the applied voltage, d is the thickness of the film, ○is the thickness strain and Y is the Young's modulus.

The thickness of a single film manufactured in the industrial process is ~ 40 μm, making the laminated film thickness ~ 80 μm. [1] As films become thicker, their actuation capacity decreases. The production of thinner films (< 40 μm) is challenged by the release problem in the current manufacturing process [9, 10]. Thin films establish good contact with the carrier web surface due to their low Young's modulus, and often the peel forces required to release these films exceed the tear strength of the films, thus resulting in breakages [9].

The published procedures for manufacturing microstructured thin PDMS films are designed for producing small units, most often with microstructures only on one surface of the PDMS film [11]. Most of the techniques employed for replicating high aspect ratio microstructures on PDMS involve the usage of sacrificial layers, which are either metallic or polymeric [12-14]. Although these methods are highly successful, they are neither suitable for producing a continuous film nor economically viable. A novel, economical, fast, continuous and easy process for making bilaterally microstructured thin PDMS films is therefore necessary to overcome the problems discussed above. In the new method described herein, a combination of an embossing technique with the existing manufacturing process is used. Embossing microstructures on thin PDMS films have been successfully demonstrated with different types of silicone systems, namely room-temperature vulcanisable (RTV) silicone, LSR and LSR composites with additional permittivity-enhancing fillers [15,16].

2. Experimental

2.1. Materials

2.1.1. Elastomer

Low viscosity extra liquid silicone rubber (LSR) POWERSIL® XLR® 630 A/B is obtained from Wacker Chemie AG, Germany. XLR630 is supplied in two parts, namely A and B. Part A contains vinyl terminated PDMS and a platinum catalyst, while part B contains vinyl terminated PDMS and a cross-linker, amongst other inert constituents. The mixing mass ratio for parts A and B is 1:1.

Hydrophobic rutile TiO_2 (Hombitec RM130F) is obtained from Sachtleben Chemie Gmbh, Germany. The primary particle size is 21~25 nm.

OS-20 solvent (an ozone-safe volatile methylsiloxane fluid) is obtained from Dow Corning, USA.

2.1.2. Carrier web

Carrier webs are specially designed substrates which transfers the corrugated microstructure onto the films. They have a sinusoidal corrugation profile. One type of carrier web is defined by a wave depth of 5 μm and a period of 10 μm, which allows for a film strain of 35% with no electrode breakage. Another type of carrier web has a depth and period of 7 μm, and films with this corrugation pattern work well up to about 80% strain without electrode damage. The corrugation lines along the length of the carrier web, are referred to as 'down-web', and when corrugation lines are perpendicular to the length of the web, the pattern is called 'cross-web' [1,2]. For our experiments we use a cross-web with a corrugation of 7 μm period and depth.

2.1.3. Gravure lab coater

In order to completely control the pressure and speed of the embossing procedure, an offset Gravure Lab Coater, 24" wide, Model#E-BC12POG3 (Euclid Coating Systems Inc., USA), is used for embossing the top surface of the films with a microstructure, as shown in Figure 4. The diameter of the rolls is 6". The coater is modified to suit the embossing process. The top roll of the coater is fixed with a cross-web of 7μm corrugation profile, thus making it the embossing roll. To heat the rolls to a desired temperature, infra-red lamps are placed above the top roll and below the bottom roll. Each infra-red lamp has two bulbs. A laser gun thermometer is used to check the temperature of the rolls. When the rolls are heated up to the required temperature, one bulb in each lamp is switched off to maintain the temperature and to prevent the rolls from heating further.

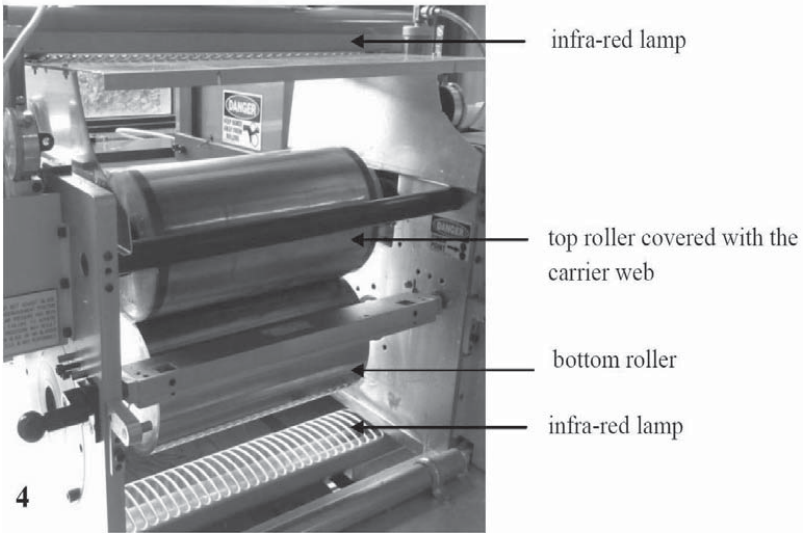

Figure 4: Gravure lab coater modified as an embossing machine

2.2. Procedure

Bilaterally corrugated films of two different elastomer formulations –pure XLR630 and XLR630 with TiO_2 – are made using the new process. An overview of the steps involved is shown in Figure 5.

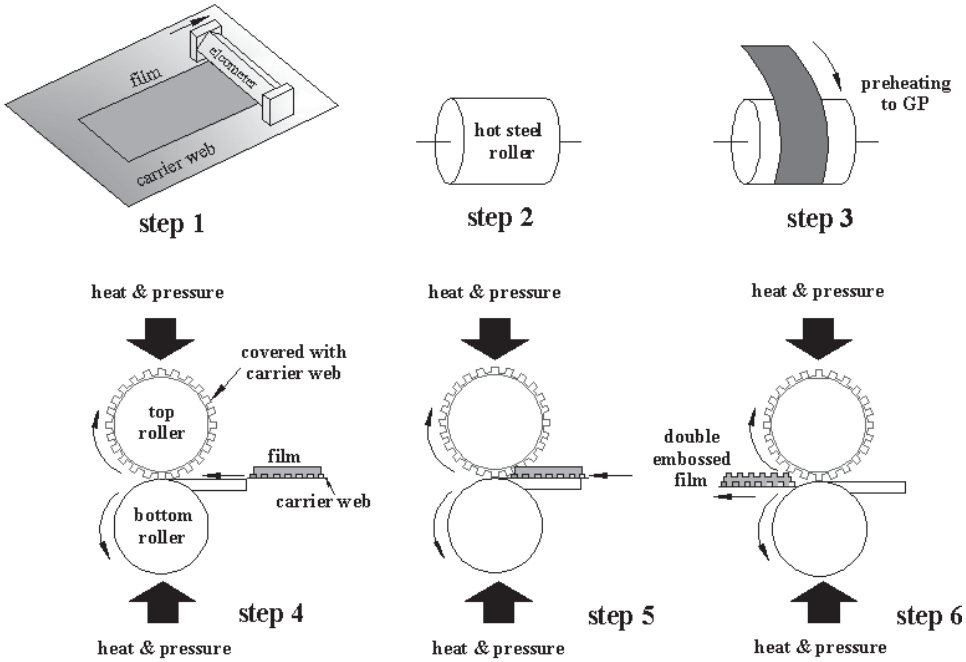

Figure 5: Schematic of the bilaterally microstructured thin film production

2.2.1. Preparing mixtures and films

Formulations for the LSR mixtures, which are listed in Table 1, are mixed using a Speed Mixer (DAC 150FVZ, Hauschild Co., Germany) at 3500 rpm for 2 minutes. In formulation 2, the homogeneity of the TiO_2 particles in the silicone matrix is ensured by adding sufficient solvent. The uniform mixtures are cast onto a carrier web substrate with a 3540 bird film applicator (Elcometer, Germany) to produce a film of thickness ~70 µm (see step 1 in Figure 5).

Table 1: LSR mixture formulations

No.	XLR630 A : XLR630 B : TiO_2 : OS20 * (phr)
1	50% : 50% : 0% : 0 (phr)
2	42% : 42% : 16% : 20 (phr)

*Amounts of XLR630 and TiO_2 are in mass ratio, OS20 in parts per hundred rubber (phr)

2.2.2. Preheating

The elastomer film cast on the carrier web is preheated on a hot steel roll (step 3 in Figure 5) prior to the embossing process, such that the hydrosilylation reaction proceeds to the gel point (GP), which marks the point of transition from a viscoelastic liquid to a viscoelastic solid due to chemical cross-linking and formation of a three dimensional network [17-19]. The time and

temperature for preheating are fixed based on the GP estimated by rheological experiments [15]. The film heats up from the bottom and as a result cures from below, and the free surface for embossing is still around the GP. The bottom surface of the elastomer films takes up the corrugation pattern from the carrier web as it cures.

2.2.3. Embossing

The elastomer film at the GP on the carrier web is embossed by passing it through the rolls of a gravure coater. A piece of the carrier web is wound around the top roll, thus making it the embossing roll. This top roll imprints the corrugation pattern onto the surface of the film, and the temperature of the roll ensures that the film cures and retains the microstructure. Embossing microstructures is possible because of the silicone elastomer's capacity to retain an imprint made on it at the GP during high-temperature curing. The force applied between the rolls is 25 psi and the speed of the rolls is 1.4 rpm (see steps 4, 5 and 6 in Figure 5). The diameter of the roll is 6" and its circumference is therefore 18.84". Thus, the speed of the roll is 1.4 rpm, or 0.0112 m/s.

2.2.4. Post curing

The embossed film is placed in the oven at 100^{o}C for 5 minutes, in order to cure completely. As the thickness of the bilaterally microstructured film (~70 μm) is higher than a single film (~40 μm), peeling away from the carrier web is not as tedious as in the conventional process [13].

2.3. Characterisation

2.3.1. Rheological measurements

Rheological measurements on the cross-linking elastomers are carried out using a strain-controlled shear rheometer (TA instruments Rheology Division, AR 2000, USA) set to a controlled strain mode with 2% strain, which is ensured to be within the linear regime of the material based on an initial strain sweep test. The test is performed at a constant frequency of 1 Hz by applying parallel plate geometry of 25 mm in diameter and a gap of 0.5-1 mm at 60^{o}C and 80^{o}C.

Linear viscoelastic (LVE) data for the LSR films are measured with parallel plate geometry of 25 mm in diameter at 23^{o}C. The LVE diagrams are obtained from frequency sweeps, from 100 Hz to 0.01 Hz.

The viscosities of the mixtures are tested by flow sweep step with the shear rate from 10^{-2} s^{-1} to 100 s^{-1} at 23^{o}C using parallel plate geometry of 25 mm in diameter.

2.3.2. SEM investigation

The morphology of the films is examined with scanning electron microscope (SEM) (FEI Inspect S, USA). The film sample is immersed in liquid nitrogen for a few minutes before cutting, in order to obtain a precise cross-section. The cut sample is deposited on a copper

holder for the investigation of cross-section morphology. All samples are coated with gold under vacuum conditions before testing.

3. Results

3.1. Gel point determination

A vital parameter for designing the embossing experiment is the GP of the elastomer. The GP marks the point at which the PDMS elastomer transitions from a viscoelastic liquid into a viscoelastic solid during the hydrosilylation reaction. For stoichiometrically balanced networks and networks with excess cross-linkers, the GP coincides with the crossover point of storage modulus (G') and loss modulus (G'') in a linear viscoelastic (LVE) diagram [19]. In the case of the filled system – XLR630 with a TiO_2 filler – the GP may not exactly coincide with the crossover point for G' and G''. However it is a good estimate of the optimal time for embossing, since the filled system has similar rheological behaviour at the GP as the unfilled system [16]. For the commercial LSR system, XLR630, the crossover point for G' and G'' in the LVE will be used as its GP, since we are most interested in the physical crossover rather than the true gel point. At room temperature, the time it takes for our LSR systems to reach the GP is three days. As the temperature increases, the time it takes for the LSR systems to reach the GP decreases and the elastomers cure rapidly. Thus, the available time window for embossing at elevated temperatures is reduced to a few seconds, thereby making the process quick and efficient. At 60ºC the GP of XLR630 is 97.6 min, which decreases almost six times by increasing the temperature to 80ºC (Figure 6a). The curing reaction for the filled system proceeds to the GP much faster than pure XLR630. At 60ºC the time taken to reach the GP for the filled system is 3.6 min, which decreases by nine times at 80ºC to a mere 0.4 minutes (Figure 6b). These timescales are still slow for a large-scale manufacturing process to operate at an economical speed. Hence, GPs at 110ºC are determined, though the crossover of G' and G'' could not be represented on an LVE, as the reaction hits the GP within 4-7 s for both systems. The rheometer takes a minimum of 20 s to equilibrate before starting up the measurements, by which time the LSR system on the bottom plate has already cured and the measurements start after the GP. The conditions for embossing are listed in Table 2.

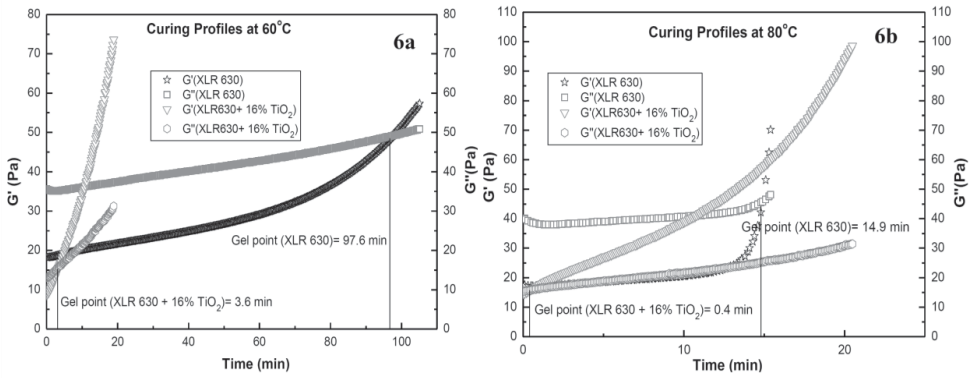

Figure 6: Curing profiles, **a.** Gel point estimation at 60ºC **b.** Gel point estimation at 80ºC

3.2. Modulus and Viscosity

Frequency sweeps of the elastomer mixtures are shown in Figure 7 as a function of the applied frequency at 23°C. The storage modulus (G') and loss modulus (G'') of the composite XLR630 are higher than that of pure XLR630, which indicates that the inorganic filler leads to the enhancement of plasticity along with reduction in elasticity [16].

The viscosity of the elastomer increases with the addition of TiO_2 filler, and the viscosity of the XLR630 with TiO_2 filler is 1.4 kPa·s (0.01 s^{-1}). In order to minimise energy expended while mixing the formulations and spreading them on carrier web to make films, it is preferable to set the viscosity of the elastomers below 40 kPa·s in the manufacturing process and the LSRs used here fall well below this limit [16].

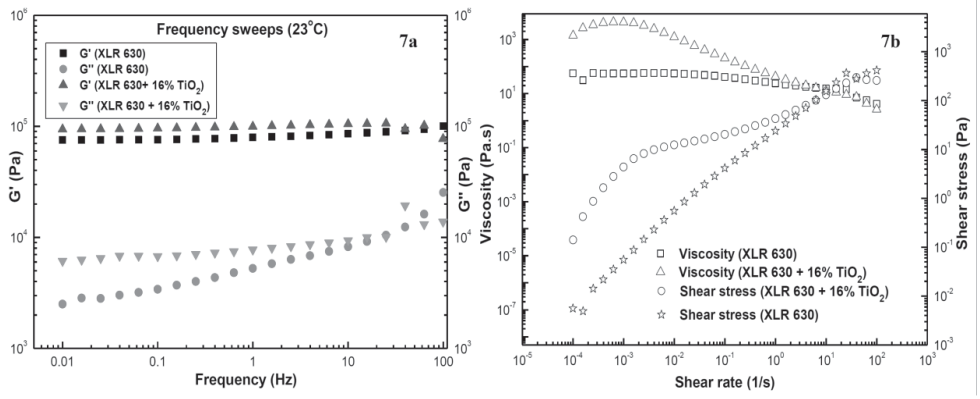

Figure 7: **a**. Storage and loss modulus, **b**. Dynamic viscosity and shear stress of the formulations

Table 2: Conditions for embossing the top surface of the film

Temperature (°C)	Crossover of G' and G'' (GP)		Film thickness (µm)	Pressure (psi)	Roll speed (rpm)
	XLR630	XLR630 + TiO_2 + OS20			
60	97.6 min	3.6 min	70	25	1.4
80	14.9 min	0.4 min	70	25	1.4
110	7 s	4 s	70	25	1.4

3.3. SEM Images

The SEM images in Figure 8 and 9 show the cross-section morphology of the bilaterally microstructured films. Figure 8 shows the XLR630 films and Figure 9 shows the XLR630 with

TiO_2 films. Film thickness is ~70 µm, and no significant deviations in thickness are observed along either the length or the width of the sample. The images confirm the formation of corrugations on both sides of the film. In Figures 8b and 9b it is apparent that the embossed side of the film has corrugations with larger periods than those formed by the carrier web. The wave period on the embossed surface is exaggerated by almost twice the original profile. Furthermore, the embossed side of the film suffers from deformation and the corrugations never recover their original dimensions, perhaps because the LSR mixture is still flowing before complete curing is achieved. This could be corrected by fine-tuning the conditions of the embossing process further. The embossed side of the film also shows an accumulation of dust, which could be prevented by performing the experiment in a clean room facility.

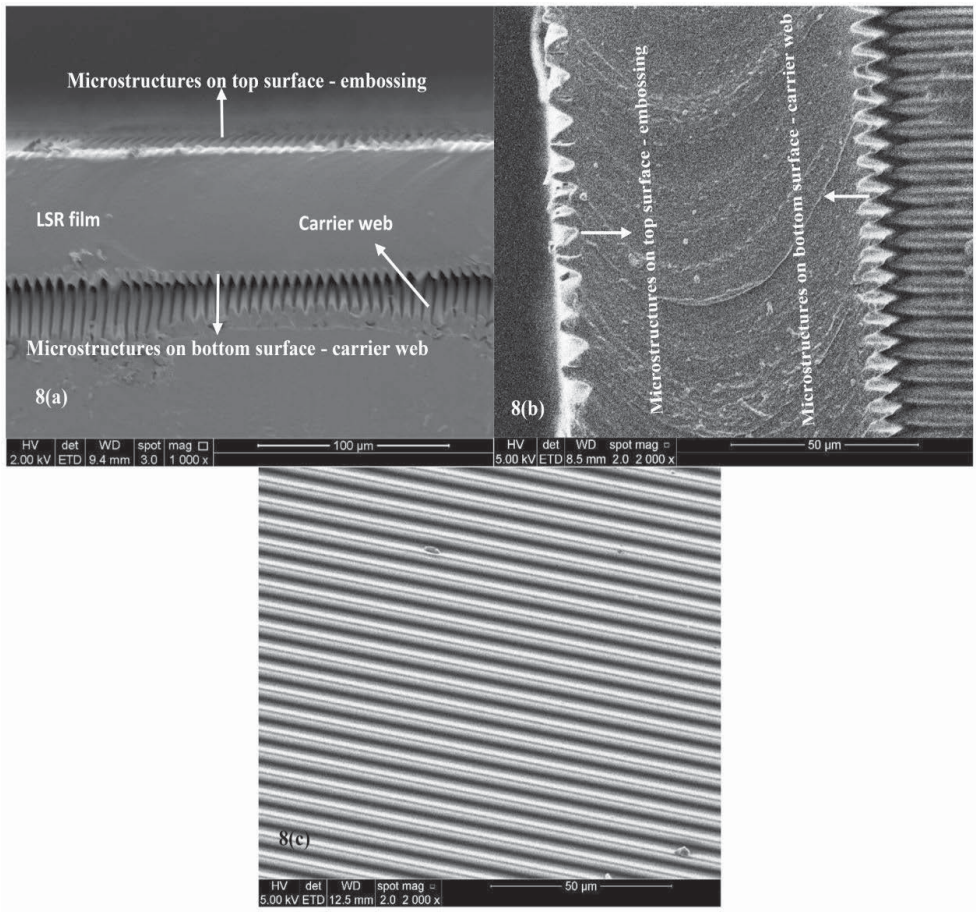

Figure 8: **a**. SEM image of the cross-section morphology of XLR630 films (1000 x magnification) **b**. SEM image of cross-section (2000 x magnification), **c.** SEM image of the film's top surface with corrugations formed by embossing (2000 x magnification)

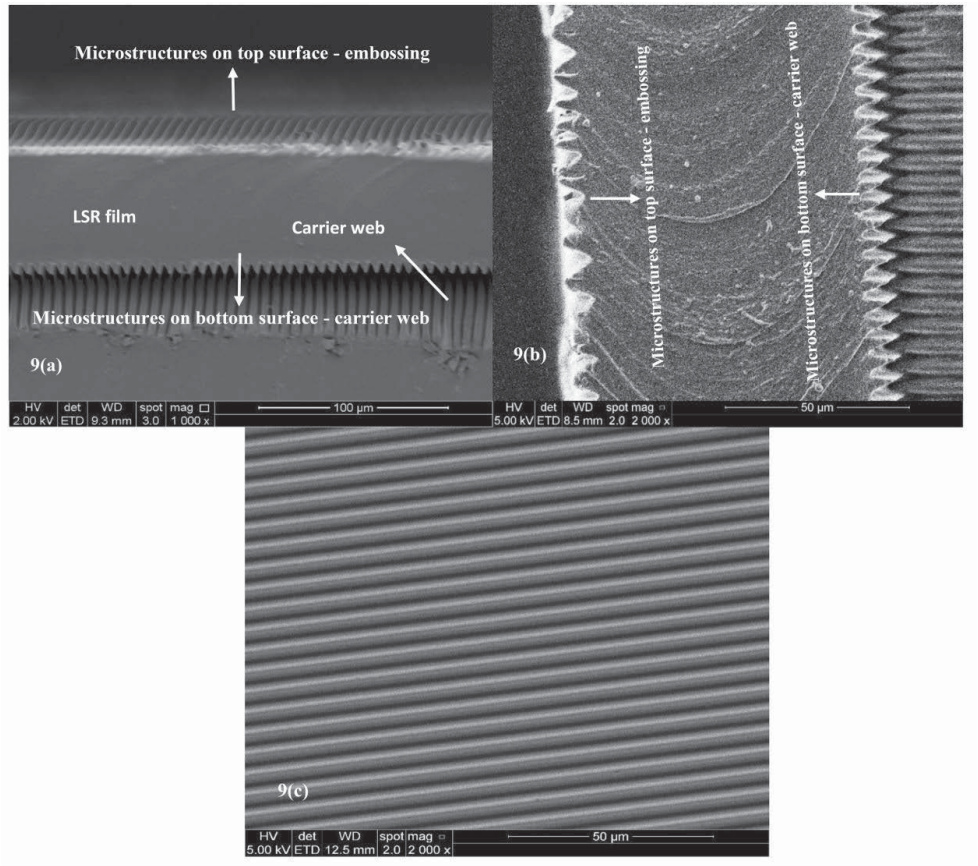

Figure 9: a. SEM image of the cross-section morphology of XLR630 with TiO_2 films (1000 x magnification) **b**. SEM image of cross-section (2000 x magnification), **c**. SEM image of the film's top surface with corrugations formed by embossing (2000 x magnification)

4. Conclusions:

Bilaterally microstructured films can be made successfully in a lab with pure and composite LSR systems. The new process is a combination of an embossing method and the existing industrial process used for manufacturing a single microstructured film. The new process eliminates the lamination step used in the industry to stick two films together. The bottom surface of the film receives the microstructure from the carrier web substrate and the top surface from the embossing roll. The embossing conditions are set based on the gel points of the pure and composite LSR systems at 110ºC, which are determined from a series of time sweeps as 7 s and 4 s, respectively. SEM images confirm that corrugations are made on both sides of the films. Corrugations on the embossed side of the film have exaggerated wave periods, compared to the carrier web side of the film, which can be corrected by refining embossing conditions. The process is quick, easy and economical.

5. Acknowledgment:

The authors gratefully acknowledge the financial support of the Danish National Advanced Technology Foundation.

6. References:

1. Kiil, H.E. and Benslimane, M. 'Scalable industrial manufacturing of DEAP.' In: Electroactive Polymer Actuators and Devices (EAPAD) San Diego, California, USA: Proc. of SPIE, 72870R:1–10 (2009)
2. Benslimane, M., Kiil, H.E. and Tryson, M.J. 'Electromechanical properties of novel large strain PolyPower film and laminate components for DEAP actuator and sensor applications.' In: Electroactive Polymer Actuators and Devices (EAPAD) San Diego, California, USA: Proc. of SPIE, 764231:1–11 (2010)
3. Wallash, A.J. and Levit, L. 'Electrical breakdown and ESD phenomena for devices with nanometer-to-micron gaps.' In: Reliability, Testing, and Characterization of MEMS/MOEMS II San Diego, California, USA: Proc. of SPIE, 4980: 87–96, Editors: Rajeshuni Ramesham, Danelle M. Tanner (2003)
4. Yu, L., Vudayagiri, S., Zakaria, S. B., Benslimane, M. Y. and Skov, A. L. 'Filled liquid silicone rubbers: Possibilities and challenges.' In: Electroactive Polymer Actuators and Devices (EAPAD) San Diego, California, USA: Proc. of SPIE, 90560S:1–9, Editor: Yoseph Bar-Cohen (2014)
5. Zakaria, S. B., Morshuis, P. H. F., Yahia, B. M., Gernaey, K. and Skov, A. L. 'The electrical breakdown of thin dielectric elastomers: thermal effects.' In: Electroactive Polymer Actuators and Devices (EAPAD) San Diego, California, USA: Proc. of SPIE, 90562V:1–11, Editor: Yoseph Bar-Cohen (2014)
6. Yu, L. and Skov, A.L. 'Monolithic growth of partly cured polydimethylsiloxane thin film layers.' Polymer Journal, 46(2): 123–129 (2014)
7. Yu, L., Daugaard, A.E. and Skov, A.L. 'Adhesion between polydimethylsiloxane layers by cross-linking.' Advances in Science and Technology, 79: 47–52 (2013)
8. Pelrine, R., Kornbluh, R., Pei, Q. and Joseph, J. 'High-speed electrically actuated elastomers with strain greater than 100%.' Science, 287 (5454): 836–839 (2000)
9. Vudayagiri, S., Junker, M.D. and Skov, A.L. 'Factors affecting surface and release properties of thin polydimethylsiloxane films.' Polymer Journal, 45(8): 871–878 (2013)
10. Vudayagiri, S. and Skov, A.L. 'Methods to ease the release of thin polydimethylsiloxane films from difficult substrates.' Polymers for Advanced Technology, 25(3): 249–257 (2014)
11. Mannsfeld, S.C.B., Tee, B.C-K., Stoltenberg, R.M., Chen, C.V.H-H., Barman, S., Muir, B.V.O., Sokolov, A.N., Reese, C. and Bao, Z. 'Highly sensitive flexible pressure sensors with microstructured rubber dielectric layers.' Nature Materials, 9: 859–864 (2010)
12. Kim, K., Park, S., Lee, J.B., Manohara, H., Desta, Y., Murphy, M. and Ahn, C.H. 'Rapid replication of polymeric and metallic high aspect ratio microstructures using PDMS and LIGA technology.' Microsystem Technologies, 9: 5–10 (2002)
13. Karlsson, J.M., Haraldsson, T., Carlborg, C.F., Hansson, J., Russom, A. and Wijngaart, W.V. 'Fabrication and transfer of fragile 3D PDMS microstructures.' Journal of Micromechanical Microengineering, 22(8): 1–9 (2012)
14. Hu, J., Li, L., Lin, H., Zhang, P., Zhou, W. and Ma, Z. 'Flexible integrated photonics: where materials, mechanics and optics meet.' Optical Materials Express, 3(9):1313–1331 (2013)

15. Vudayagiri, S., Yu, L., Hassouneh, S.S. and Skov, A.L. 'Hot embossing of microstructures on addition curing polydimethylsiloxane films.' Journal of Elastomers and Plastics, doi: 10.1177/0095244313483642 (2013)
16. Vudayagiri, S., Yu, L. and Skov, A.L. 'Techniques for hot embossing microstructures on liquid silicone rubbers with fillers.' Journal of Elastomers and Plastics, doi: 10.1177/0095244314526743 (2014)
17. Venkatraman, S.K. and Winter, H.H. 'Finite shear strain behavior of a cross-linking polydimethylsiloxane near its gel point.' Rheologica Acta, 29 (5):423–32 (1990)
18. Chambon, F. and Winter, H.H. 'Linear viscoelasticity at the gel point of a cross-linking PDMS with imbalanced stoichiometry.' Journal of Rheology, 31 (8): 683–97 (1987)
19. Winter, H.H. 'Can the gel point of a cross-linking polymer be detected by the G'-G" Crossover?' Polymer Engineering and Science, 27(22): 1698–702 (1987)

The Danish Polymer Centre
Department of Chemical and Biochemical Engineering
Technical University of Denmark
Søltofts Plads, Building 227
DK-2800 Kgs. Lyngby
Denmark

Phone: +45 4525 6801
Web: www.dpc.kt.dtu.dk

ISBN : 978-87-93054-45-5